Hahn, S.L. “Hilbert Transforms.”
The Transforms and Applications Handbook: Second Edition.
Ed. Alexander D. Poularikas
Boca Raton: CRC Press LLC, 2000

7

Hilbert Transforms

Stefan L. Hahn
Warsaw University of Technology

7.0 Foreword

The Hilbert transformations are of widespread interest because they are applied in the theoretical description of many devices and systems and directly implemented in the form of Hilbert analog or digital filters (transformers). Let us quote some important applications of Hilbert transformations:

1. The complex notation of harmonic signals in the form of Euler's equation $\exp(j\omega t) = \cos(\omega t) + j\sin(\omega t)$ has been used in electrical engineering since the 1890s and nowadays is commonly applied in the theoretical description of various, not only electrical systems. This complex notation had been introduced before Hilbert derived his transformations. However, $\sin(\omega t)$ is the Hilbert transform of $\cos(\omega t)$, and the complex signal $\exp(j\omega t)$ is a precursor of a wide class of complex signals called analytic signals.
2. The concept of the analytic signal[11] of the form $\psi(t) = u(t) + jv(t)$, where $v(t)$ is the Hilbert transform of $u(t)$, extends the complex notation to a wide class of signals for which the Fourier transform exists. The notion of the analytic signal is widely used in the theory of signals, circuits, and systems. A device called the Hilbert transformer (or filter), which produces at the output the Hilbert transform of the input signal, finds many applications, especially in modern digital signal processing.
3. The real and imaginary parts of the transmittance of a linear and causal two-port system form a pair of Hilbert transforms. This property finds many applications.

4. Recently 2-D and multidimensional Hilbert transformations have been applied to define 2-D and multidimensional complex signals, opening the door for applications in multidimensional signal processing.[13]

7.1 Basic Definitions

The Hilbert transformation of a one-dimensional real signal (function) $u(t)$ is defined by the integral

$$v(t) = \frac{-1}{\pi} P\int_{-\infty}^{\infty} \frac{u(\eta)}{\eta - t} d\eta = \frac{1}{\pi} P\int_{-\infty}^{\infty} \frac{u(\eta)}{t - \eta} d\eta \tag{7.1.1}$$

and the inverse Hilbert transformation is

$$u(t) = \frac{1}{\pi} P\int_{-\infty}^{\infty} \frac{v(\eta)}{\eta - t} d\eta = \frac{-1}{\pi} P\int_{-\infty}^{\infty} \frac{v(\eta)}{t - \eta} d\eta \tag{7.1.2}$$

where P stands for principal value of the integral. For convenience, two conventions of the sequence of variables in the denominator are given; both have been used in studies. The left-hand formulae will be used in this chapter. The following terminology is applied: the algorithm; that is, the right-hand side of Equations (7.1.1) or (7.1.2), is called "transformation," and the specific result for a given function; that is, the left-hand side of Equations (7.1.1) or (7.1.2), is called the "transform." The above definitions of Hilbert transformations are conveniently written in the convolution notations

$$v(t) = u(t) * \frac{1}{\pi t} \tag{7.1.3}$$

$$u(t) = v(t) * \frac{1}{\pi t} \tag{7.1.4}$$

The integrals in definition (7.1.1) are improper because the integrand goes to infinity for $\eta = t$. Therefore, the integral is defined as the Cauchy Principal Value (sign P) of the form

$$v(t) = \lim_{\substack{\varepsilon \Rightarrow 0 \\ A \Rightarrow \infty}} \frac{-1}{\pi} \left(\int_{-A}^{-\varepsilon} + \int_{\varepsilon}^{A} \frac{u(\eta)}{\eta - t} d\eta \right) \tag{7.1.5}$$

Using numerical integration in the sense of the Cauchy Principal Value with uniform sampling of the integrand, the origin $\eta = 0$ should be positioned exactly at the center of the sampling interval. The limit $\varepsilon \Rightarrow 0$ is substituted by a given value of the sampling interval and the limit $A \Rightarrow \infty$ by a given value of A. The accuracy of the numerical integration increases with smaller sampling intervals and larger values of A.

The Hilbert transformation was originally derived by Hilbert in the frame of the theory of analytic functions. The theory of Hilbert transformations is closely related to Fourier transformation of signals of the form

$$U(\omega) = \int_{-\infty}^{\infty} u(t) e^{-j\omega t} dt\,; \quad \omega = 2\pi f \tag{7.1.6}$$

The complex function $U(\omega)$ is called the Fourier spectrum or Fourier image of the signal $u(t)$ and the variable $f = \omega/2\pi$, the Fourier frequency. The inverse Fourier transformation is

$$u(t) = \int_{-\infty}^{\infty} U(\omega) e^{j\omega t} df \tag{7.1.7}$$

The pair of transforms (7.1.6) and (7.1.7) may be denoted

$$u(t) \overset{F}{\Longleftrightarrow} U(\omega) \tag{7.1.8}$$

called a Fourier pair. Similarly the Hilbert transformations (7.1.1) and (7.1.2) may be denoted

$$u(t) \overset{\mathrm{H}}{\Longleftrightarrow} v(t) \tag{7.1.9}$$

forming a Hilbert pair of functions. Contrary to other transformations, the Hilbert transformation does not change the domain. For example, the function of a time variable t (or of any other variable x) is transformed to a function of the same variable, while the Fourier transformation changes a function of time into a function of frequency.

The Fourier transform (see also Chapter 2) of the kernel of the Hilbert transformation, that is, $\Theta(t) = 1/(\pi t)$ (see Equations [7.1.3] and [7.1.4]) is

$$\Theta(t) = \frac{1}{\pi t} \overset{F}{\Longleftrightarrow} -j\,\mathrm{sgn}(\omega) \tag{7.1.10}$$

with the signum function (distribution) defined as follows:

$$\mathrm{sgn}(\omega) = \begin{cases} +1 & \omega > 0 \\ 0 & \omega = 0 \\ -1 & \omega < 0 \end{cases} \tag{7.1.11}$$

The multiplication to convolution theorem of the Fourier analysis yields the following spectrum of the Hilbert transform

$$v(t) \overset{F}{\Longleftrightarrow} V(\omega) = -j\,\mathrm{sgn}(\omega) U(\omega) \tag{7.1.12}$$

that is, the spectrum of the signal $u(t)$ should be multiplied by the operator $-j\,\mathrm{sgn}(\omega)$ This relation enables the calculation of the Hilbert transform using the inverse Fourier transform of the spectrum defined by Equation (7.1.12); that is, using the following algorithm:

$$u(t) \overset{F}{\Rightarrow} U(\omega) \Rightarrow V(\omega) = -j\,\mathrm{sgn}(\omega) U \overset{F^{-1}}{\Rightarrow} v(t) \tag{7.1.13}$$

where the symbols F and F^{-1} denote the Fourier and inverse Fourier transformations respectively. In practice, the algorithms of DFT (Discrete Fourier Transform) or FFT (Fast Fourier Transform) can be applied (see Section 7.20)

7.2 Analytic Functions Aspect of Hilbert Transformations

The complex signal whose imaginary part is the Hilbert transform of its real part is called the **analytic signal**. The simplest example is the harmonic complex signal given by Euler's formula $\psi(t) = \exp(j\omega t) = \cos(\omega t) + j\sin(\omega t)$. A more general form of the analytic signal was defined in 1946 by Gabor.[11] The term "analytic" is used in the meaning of a complex function $\Psi(z)$ of a complex variable $z = t + j\tau$, which is defined as follows:[39]

Consider a plane with rectangular coordinates (t, τ) (called **C** plane or **C** "space") and take a domain **D** in this plane. If we define a rule connecting to each point in **D** a complex number ψ, we defined a complex function $\psi(z), z \in \mathbf{D}$. This function may be regarded as a complex function of two real variables:

$$\psi(z) = \psi(t, \tau) = u(t, \tau) + j\nu(t, \tau) \tag{7.2.1}$$

in the domain $\mathbf{D} \in \mathbf{R}^2$ ($\mathbf{R}^2$ is Euclidean plane or "space"). The complete derivative of the function $\psi(z)$ has the form

$$d\psi = \frac{\partial\psi}{\partial z}dz + \frac{\partial\psi}{\partial z^*}dz^* \tag{7.2.2}$$

where $z^* = t - j\tau$ is the complex conjugate and the partial derivatives are

$$\frac{\partial\psi}{\partial z} = \frac{1}{2}\left(\frac{\partial\psi}{\partial t} - j\frac{\partial\psi}{\partial\tau}\right); \quad \frac{\partial\psi}{\partial z^*} = \frac{1}{2}\left(\frac{\partial\psi}{\partial t} + j\frac{\partial\psi}{\partial\tau}\right) \tag{7.2.3}$$

The function $\psi(z) = u(t, \tau) + j\nu(t, \tau)$ is called the **analytic function** in the domain **D** if and only if $u(t, \tau)$ and $\nu(t, \tau)$ are **continuously differentiable**. It can be shown that this requirement is satisfied, if $\partial\psi/\partial z^* = 0$. This complex equation may be substituted by two real equations:

$$\frac{\partial u}{\partial t} = \frac{\partial\upsilon}{\partial\tau}; \quad \frac{\partial u}{\partial\tau} = \frac{\partial\upsilon}{\partial t} \tag{7.2.4}$$

called the **Cauchy-Riemann equations**. These equations should be satisfied if the function $\psi(z)$ is analytic in the domain $z \in \mathbf{D}$. For example, the complex function

$$\psi(z) = \frac{1}{\alpha - jz} = u(t, \tau) + j\upsilon(t, \tau) \tag{7.2.5}$$

is analytic because

$$u(t, \tau) = \frac{(\alpha + \tau)}{(\alpha + \tau)^2 + t^2}; \quad \upsilon(t, \tau) = \frac{t}{(\alpha + \tau)^2 + t^2} \tag{7.2.6}$$

and the differentiation

$$\frac{\partial u(t, \tau)}{\partial t} = \frac{\partial\upsilon(t, \tau)}{\partial\tau} = \frac{-2t(\alpha + \tau)}{\left[(\alpha + \tau)^2 + t^2\right]^2} \tag{7.2.7}$$

verifies the Cauchy-Riemann equations.

It was shown by Cauchy that if z_0 is a point inside a closed contour $C \in \mathbf{D}$ such that $\psi(z_0)$ is analytic inside and on C, then (see also Appendix 1)

$$\psi\left(z_0\right) = \frac{1}{2\pi j}\int_C \frac{\psi\left(z\right)}{z - z_0} dz \tag{7.2.8}$$

$$\psi\left(z_0\right) = \frac{1}{2\pi j}\int_C \frac{\psi\left(y + z_0\right)}{y} dy \tag{7.2.9}$$

This is a contour integral in the $(t, j\tau)$ plane. Let us take the contour C in the form shown in Figure 7.2.1. It is a sum of $C_t + C_\varepsilon + C_R$, where C_t is a line parallel to the t axis shifted by ε, C_ε is a half-circle of radius ε and C_R a half-circle of radius R. The analytic signal is defined as a complex function of the real variable t given by the formula

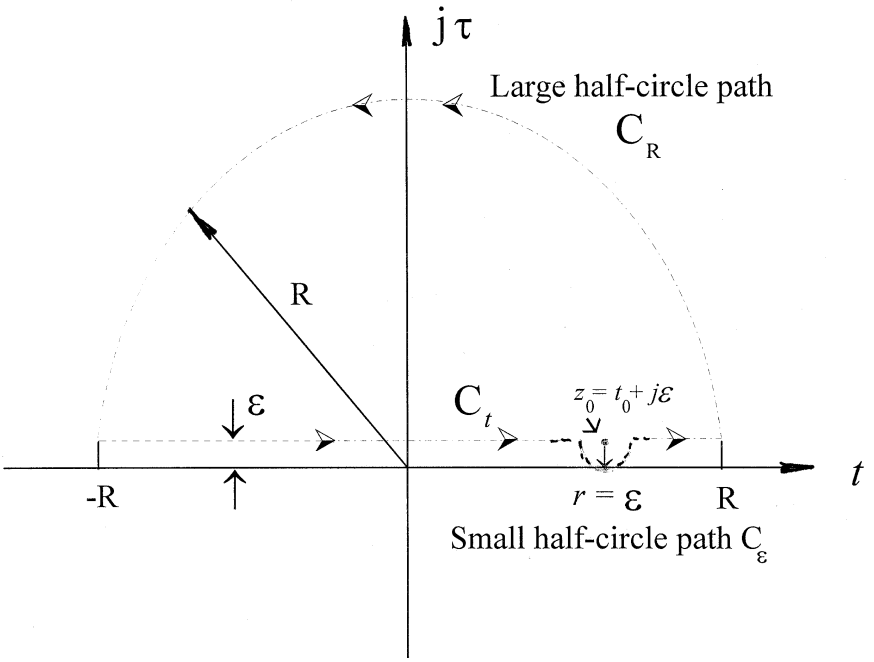

FIGURE 7.2.1 The integration path defining the analytic signal (7.2.10).

$$\psi(t) = u(t, 0_+) + j\upsilon(t, 0_+) \tag{7.2.10}$$

obtained by inserting in the Equation (7.2.1) $\tau = 0_+$, where the subscript + indicates that the path C_t approaches the t axis from the upperside. The Equation (7.2.10) is the result of contour integration along the path of Figure 7.2.1 using the limit $\varepsilon \to 0$, $R \to \infty$. We have

$$\psi\left(t_0, 0_+\right) = \lim_{\varepsilon \to 0, R \to \infty} \frac{1}{2\pi j}\left\{P\int_{-R}^{R} \frac{\psi\left(z\right)}{z - z_0} dz + \int_{C_R} \frac{\psi\left(z\right)}{z - z_0} dz + \int_{C_\varepsilon} \frac{\psi\left(z\right)}{z - z_0} dz\right\} \tag{7.2.11}$$

The symbol P denotes the Cauchy Principal Value; that is

$$P\int_{-R}^{R} = \int_{-R}^{t_0-\varepsilon} + \int_{t_0+\varepsilon}^{R} \tag{7.2.12}$$

For analytic functions the integral along C_R vanishes for $R \to \infty$ and in the limit $\varepsilon \to 0$ the integral along the small half-circle C_ε equals $0.5\,\psi(t_0, 0_+)$ since within the very small circle around t_0 the function $\psi(z)$ $= \psi(t_0, 0_+)$ is a constant and the integral $\int_{C_\varepsilon} \frac{dz}{z - z_0} = \pi$ j. In consequence, the real and imaginary parts of the analytic signal are given by the integrals (a Hilbert pair)

$$v(t) = \frac{-1}{\pi} P\int_{-\infty}^{\infty} \frac{u(\eta, 0)}{\eta - t} d\eta \tag{7.2.13}$$

$$u(t) = \frac{-1}{\pi} P\int_{-\infty}^{\infty} \frac{v(\eta, 0)}{\eta - t} d\eta \tag{7.2.14}$$

where the subscripts t_0 and 0_+ are deleted. The only difference between the above integrals and those defined by Equations (7.1.1) and (7.1.2) consists in notation (deleting zeros in parentheses). Therefore, the real and imaginary parts of the analytic signal

$$\psi(t) = u(t) + jv(t) \tag{7.2.15}$$

form a Hilbert pair of functions. For example, inserting $\tau = 0$ in Equation (7.2.6) yields the Hilbert pair

$$u(t) = \frac{\alpha}{\alpha^2 + t^2} \overset{\mathrm{H}}{\Longleftrightarrow} v(t) = \frac{t}{\alpha^2 + t^2} \tag{7.2.16}$$

The signal $u(t)$ is called the Cauchy signal and $v(t)$ is its Hilbert transform.

A real signal $u(t)$ may be written in terms of analytic signals

$$u(t) = \frac{\psi(t) + \psi^*(t)}{2} \tag{7.2.17}$$

and its Hilbert transform is

$$v(t) = \frac{\psi(t) - \psi^*(t)}{2j} \tag{7.2.18}$$

where $\psi^*(t) = u(t) - jv(t)$ is the conjugate analytic signal. For this signal the Equation (7.2.11) takes the form $\psi(t) = u(t, 0_-) - jv(t, 0_-)$ and the path C is in the lower half of the z plane. Notice, that the above formulae present a generalization of Euler's formulae

$$\cos(\omega t) = \frac{e^{j\omega t} + e^{-j\omega t}}{2} \tag{7.2.19}$$

$$\sin(\omega t) = \frac{e^{j\omega t} - e^{-j\omega t}}{2j} \tag{7.2.20}$$

7.3 Spectral Description of the Hilbert Transformation: One-Sided Spectrum of the Analytic Signal

Any real signal $u(t)$ may be decomposed into a sum

$$u(t) = u_e(t) + u_o(t) \tag{7.3.1}$$

where the **even term** is defined as

$$u_e(t) = \frac{u(t) + u(-t)}{2} \tag{7.3.2}$$

and the **odd term**

$$u_o(t) = \frac{u(t) - u(-t)}{2} \tag{7.3.3}$$

The decomposition is **relative**, i.e., changes with the shift of the origin of the coordinate $t' = t - t_o$. In general, the Fourier image of $u(t)$ defined by Equation (7.1.6) is a complex function

$$U(\omega) = U_{\mathrm{Re}}(\omega) + jU_{\mathrm{Im}}(\omega) \tag{7.3.4}$$

where the real part is given by the cosine transform

$$U_{\mathrm{Re}}(\omega) = \int_{-\infty}^{\infty} u_e(t)\cos(\omega t)dt \tag{7.3.5}$$

and the imaginary part of the sine transform

$$U_{\mathrm{Im}}(\omega) = -\int_{-\infty}^{\infty} u_o(t)\sin(\omega t)dt \tag{7.3.6}$$

The multiplication of the Fourier image by the operator $-j\,\mathrm{sgn}(\omega)$ changes the real part of the spectrum to the imaginary one and vice versa (see Equation [7.1.12]). The spectrum of the Hilbert transform is

$$V(\omega) = V_{\mathrm{Re}}(\omega) + jV_{\mathrm{Im}}(\omega) \tag{7.3.7}$$

where

$$V_{\mathrm{Re}}(\omega) = -j\,\mathrm{sgn}(\omega)[jU_{\mathrm{Im}}(\omega)] = \mathrm{sgn}(\omega)U_{\mathrm{Im}}(\omega) \tag{7.3.8}$$

and

$$V_{\mathrm{Im}}(\omega) = -\mathrm{sgn}(\omega)U_{\mathrm{Re}}(\omega) \tag{7.3.9}$$

Therefore, the Hilbert transformation changes any even term to an odd term and any odd term to an even term. The Hilbert transforms of harmonic functions are

$$H[\cos(\omega t)] = \sin(\omega t) \tag{7.3.10}$$

$$H[\sin(\omega t)] = -\cos(\omega t) \tag{7.3.11}$$

$$H[e^{j\omega t}] = -j\,\mathrm{sgn}(\omega)e^{j\omega t} = \mathrm{sgn}(\omega)\,e^{j(\omega t - 0.5\pi)} \tag{7.3.12}$$

Therefore, the Hilbert transformation changes any cosine term to a sine term and any sine term to a reversed signed cosine term. Because $\sin(\omega t) = \cos(\omega t - 0.5\pi)$ and $-\cos(\omega t) = \sin(\omega t - 0.5\pi)$, the Hilbert transformation in the time domain corresponds to a phase lag by -0.5π (or $-90°$) of all harmonic terms of the Fourier image (spectrum). Using the complex notation of the Fourier transform, the multiplication of the spectral function $U(\omega)$ by the operator $-j\,\mathrm{sgn}(\omega)$ provides a 90° phase lag at all positive frequencies and a 90° phase lead at all negative frequencies. A linear two-port network with a transfer function $H(\omega) = -j\,\mathrm{sgn}(\omega)$ is called an ideal **Hilbert transformer** or filter. Such a filter cannot be exactly realized because of constraints imposed by causality (details in Section 7.2.1).

The Fourier image of the analytic signal

$$\psi(t) = u(t) + jv(t) \tag{7.3.13}$$

is one-sided. We have

$$u(t) \overset{\mathrm{H}}{\Longleftrightarrow} v(t) \quad u(t) \overset{F}{\Longleftrightarrow} U(\omega); \quad v(t) \overset{F}{\Longleftrightarrow} j\,\mathrm{sgn}(\omega)U(\omega). \tag{7.3.14}$$

Therefore,

$$\psi(t) \overset{F}{\Longleftrightarrow} U(\omega) + j\left[-j\,\mathrm{sgn}(\omega)U(\omega)\right] = \left[1 + \mathrm{sgn}(\omega)\right]U(\omega) \tag{7.3.15}$$

where

$$1 + \mathrm{sgn}(\omega) = \begin{cases} 2 & \text{for } \omega > 0 \\ 1 & \text{for } \omega = 0 \\ 0 & \text{for } \omega < 0 \end{cases} \tag{7.3.16}$$

The Fourier image of the analytic signal is doubled at positive frequencies and cancelled at negative frequencies with respect to $U(\omega)$. For the conjugate signal $\psi^*(t) = u(t) - jv(t)$ the Fourier image is doubled at negative frequencies and cancelled at positive frequencies.

Examples

1. Consider the analytic signal $e^{j\omega_0 t} = \cos(\omega_0 t) + j\sin(\omega_0 t)$. We have

$$\cos(\omega_0 t) \overset{H}{\Longleftrightarrow} \sin(\omega_0 t); \quad \omega_0 = 2\pi f_0$$

$$\cos(\omega_0 t) \overset{F}{\Longleftrightarrow} 0.5\left[\delta(f + f_0) + \delta(f - f_0)\right]$$

$$\cos(\omega_0 t) \overset{F}{\Longleftrightarrow} 0.5j\left[\delta(f + f_0) - \delta(f - f_0\right.$$

$$e^{j\omega_0 t} \overset{F}{\Longleftrightarrow} \delta(f - f_0)$$

The spectra are shown in Figure 7.3.1.

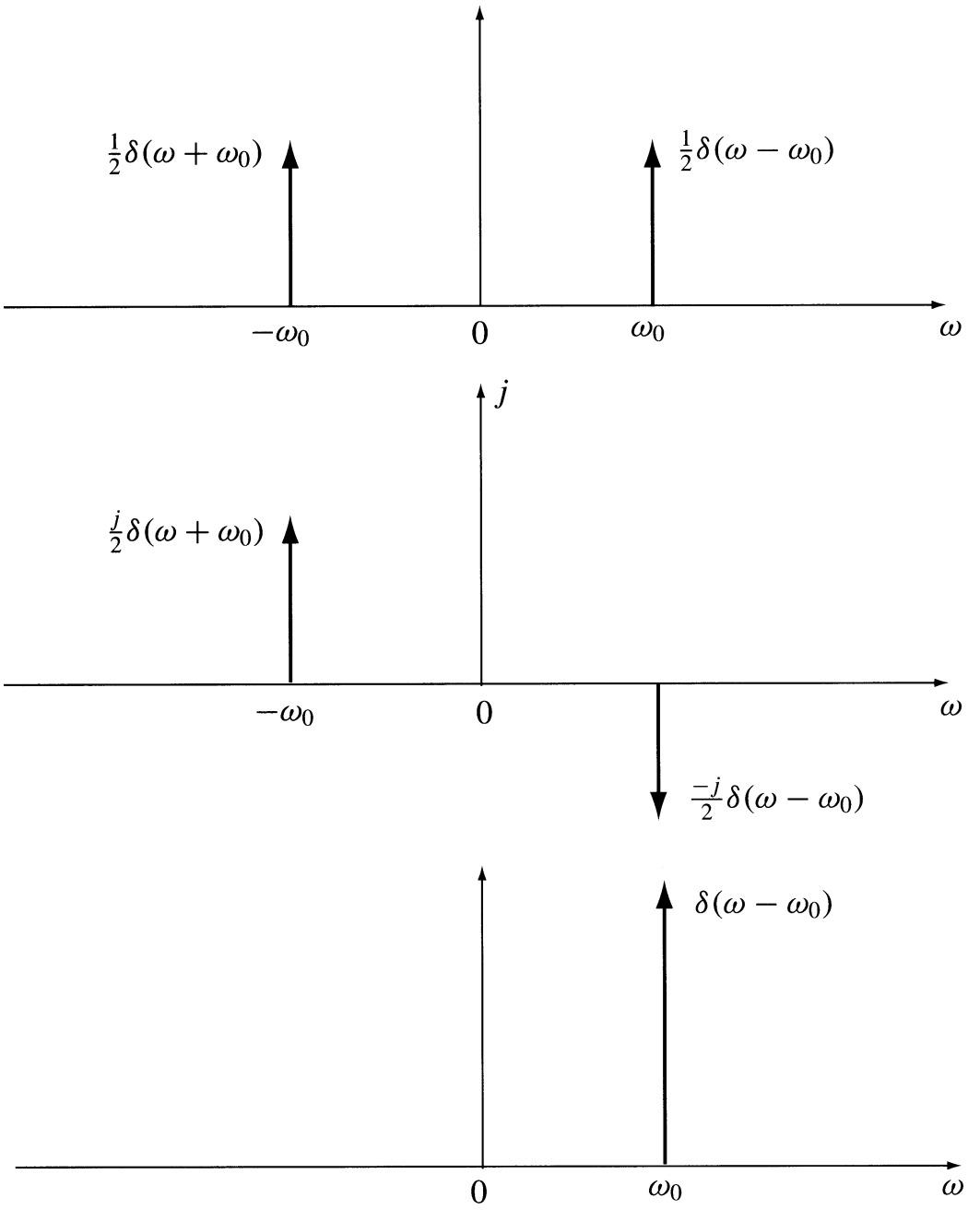

FIGURE 7.3.1 The spectra of $\cos(\omega_0 t)$, $\sin(\omega t_0)$, and of the analytic signal $e^{j\omega_0 t}$.

2. Consider the analytic signal $\psi(t) = \dfrac{1}{1+t^2} + j\,\dfrac{t}{1+t^2}$. We have

$$\frac{1}{1+t^2} \overset{\mathrm{H}}{\Longleftrightarrow} \frac{t}{1+t^2}$$

$$\frac{1}{1+t^2} \overset{F}{\Longleftrightarrow} \pi e^{-|\omega|}; \quad \frac{t}{1+t^2} \overset{F}{\Longleftrightarrow} -j\,\mathrm{sgn}(\omega)\pi e^{|\omega|}$$

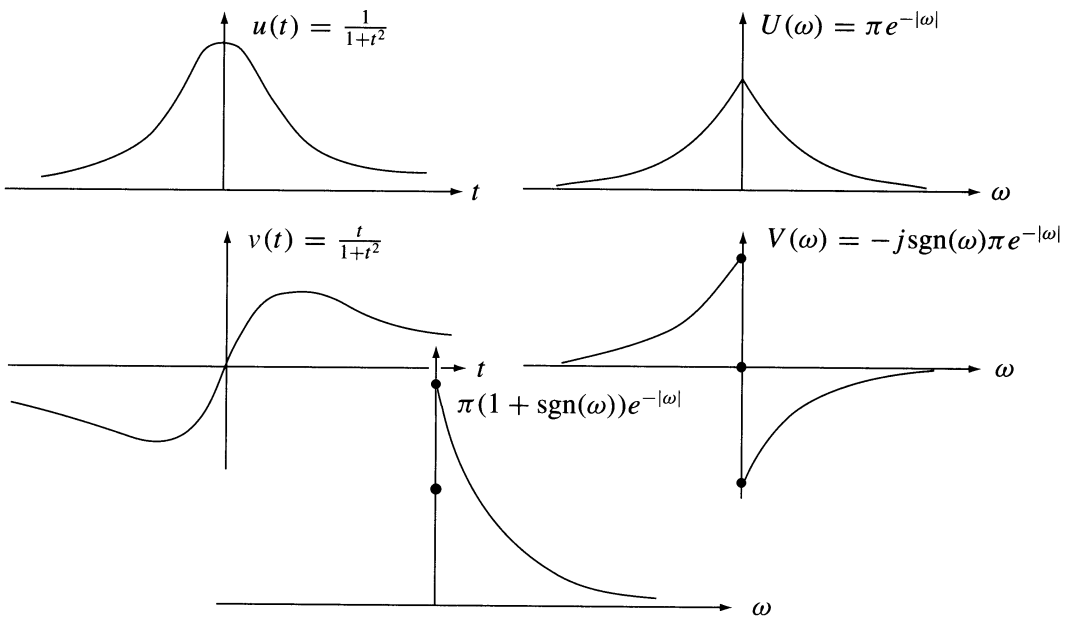

FIGURE 7.3.2 The Cauchy pulse, its Hilbert transform, and the corresponding spectra and the spectrum of the analytic signal $\psi(t) = 1/(1 - jt)$.

$$\psi(t) \overset{F}{\Longleftrightarrow} \left[1 + \mathrm{sgn}(\omega)\right]\pi e^{-|\omega|}$$

The signals and spectra are shown in Figure 7.3.2.

Derivation of Hilbert Transforms Using Hartley Transforms

(See also Chapter 4). Alternatively, the Hilbert transform may be derived using a special Fourier transformation known as Hartley transformation; it is given by the integral

$$U_{\mathrm{Ha}}(\omega) = \int_{-\infty}^{\infty} u(t)\,\mathrm{cas}(\omega t)\,dt\,; \quad \omega = 2\pi f \tag{7.3.17}$$

and the inverse Hartley transformation is

$$u(t) = \int_{-\infty}^{\infty} U_{\mathrm{Ha}}(\omega)\,\mathrm{cas}(\omega t)\,df \tag{7.3.18}$$

where $\mathrm{cas}(\omega t) = \cos(\omega t) + \sin(\omega t)$. The Hartley spectral function was denoted by the index Ha because in this chapter the index H denotes the Hilbert transform. Consider the Hartley pair

$$u(t) \overset{\mathrm{Ha}}{\Longleftrightarrow} U_{\mathrm{Ha}}(\omega) \tag{7.3.19}$$

The Hartley spectral function of the Hilbert transform is

$$V_{\mathrm{Ha}}(\omega) = \mathrm{sgn}(\omega)U_{\mathrm{Ha}}(-\omega) \tag{7.3.20}$$

Therefore, the Hilbert transform is given by the inverse Hartley transformation

$$v(t) = \int_{-\infty}^{\infty} \operatorname{sgn}(\omega) U_{\mathrm{Ha}}(-\omega) \operatorname{cas}(\omega t)\, df \tag{7.3.21}$$

Example

Consider the one-sided square pulse $\Pi_a\,(t-a)$ (see Figure 7.3.3). The Hartley transform of this pulse is

$$U_{\mathrm{Ha}}(\omega) = \int_0^{2a} \left[\cos(\omega t) + \sin(\omega t)\right] dt = 2a\left[\frac{\sin(2\omega a)}{2\omega a} + \frac{\sin^2(\omega a)}{\omega a}\right]$$

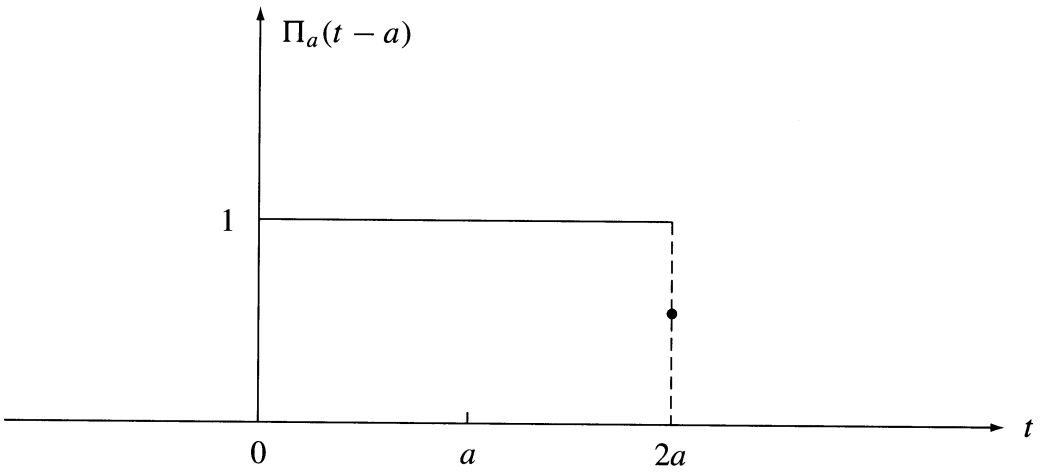

FIGURE 7.3.3 One-sided square pulse.

The spectrum of the Hilbert transform given by Equation (7.3.20) is

$$V_{\mathrm{Ha}}(\omega) = 2a\,\operatorname{sgn}(\omega)\left[\frac{\sin(2\omega a)}{2\omega a} - \frac{\sin^2(\omega a)}{\omega a}\right]$$

The inverse Hartley transformation of this spectrum is

$$\int_{-\infty}^{\infty} 2a\,\operatorname{sgn}(\omega)\left[\frac{\sin(2\omega a)}{2\omega a} - \frac{\sin^2(\omega a)}{\omega a}\right]\left[\cos(\omega t) + \sin(\omega t)\right] df$$

Notice that the integrals of products of opposite symmetry equal zero and the integration yields

$$v(t) = \frac{1}{\pi} \ln\left|\frac{t}{t-2a}\right|$$

(see Equation [7.4.7]).

7.4 Examples of Derivation of Hilbert Transforms

1. The harmonic signal $u(t) = \cos(\omega t)$; $\omega = 2\pi f$, where f is a constant. The Hilbert transform of the periodic cosine signal using the defining integral (7.1.1) is:

$$H\left[\cos\left(\omega t\right)\right] = v\left(t\right) = \frac{-1}{\pi} P\int_{-\infty}^{\infty} \frac{\cos\left(\omega\eta\right)}{\eta - t} d\eta \tag{7.4.1}$$

The change of variable $y = \eta - t$, $dy = d\eta$ yields

$$\begin{aligned} v\left(t\right) &= \frac{-1}{\pi} P\int_{-\infty}^{\infty} \frac{\cos\left[\omega\left(y + t\right)\right]}{y} dy \\ &= \frac{-1}{\pi}\left\{\cos\left(\omega t\right) P\int_{-\infty}^{\infty} \frac{\cos\left(\omega y\right)}{y} dy - \sin\left(\omega t\right) P\int_{-\infty}^{\infty} \frac{\sin\left(\omega y\right)}{y} dy\right\} \end{aligned} \tag{7.4.2}$$

The integrals inside the brackets are

$$P\int_{-\infty}^{\infty} \frac{\cos\left(\omega y\right)}{y} dy = 0\,; \quad P\int_{-\infty}^{\infty} \frac{\sin\left(\omega y\right)}{y} dy = \pi \tag{7.4.3}$$

Therefore, $v(t) = \sin(\omega t)$. The same derivation for the function $u(t) = \sin(\omega t)$ yields $v(t) = -\cos\omega(t)$.

2. The two-sided symmetric unipolar square pulse:

$$u\left(t\right) = \Pi_a\left(t\right) = \begin{cases} 1 & \text{for } \left|t\right| < a \\ 0.5 & \text{for } \left|t\right| = a \\ 0 & \text{for } \left|t\right| > a \end{cases} \tag{7.4.4}$$

The Hilbert transform of this pulse is

$$\begin{aligned} v\left(t\right) = H\left[\Pi_a\left(t\right)\right] &= \frac{-1}{\pi} P\int_{-\infty}^{\infty} \frac{\Pi_a\left(\eta\right)}{\eta - t} d\eta \\ &= \lim_{\varepsilon \Rightarrow 0}\left\{\frac{-1}{\pi}\int_{-a}^{t-\varepsilon} \frac{d\eta}{\eta - t} - \frac{1}{\pi}\int_{t+\varepsilon}^{a} \frac{d\eta}{\eta - t}\right\} \\ &= \lim_{\varepsilon \Rightarrow 0}\left\{-\frac{1}{\pi}\ln\left(\eta - t\right)\Big|_{-a}^{t-\varepsilon} - \frac{1}{\pi}\ln\left(\eta - t\right)\Big|_{t+\varepsilon}^{a}\right\} \end{aligned} \tag{7.4.5}$$

The insertion of the limits of integration yields

$$v\left(t\right) = \frac{1}{\pi}\ln\left|\frac{t + a}{t - a}\right| \tag{7.4.6}$$

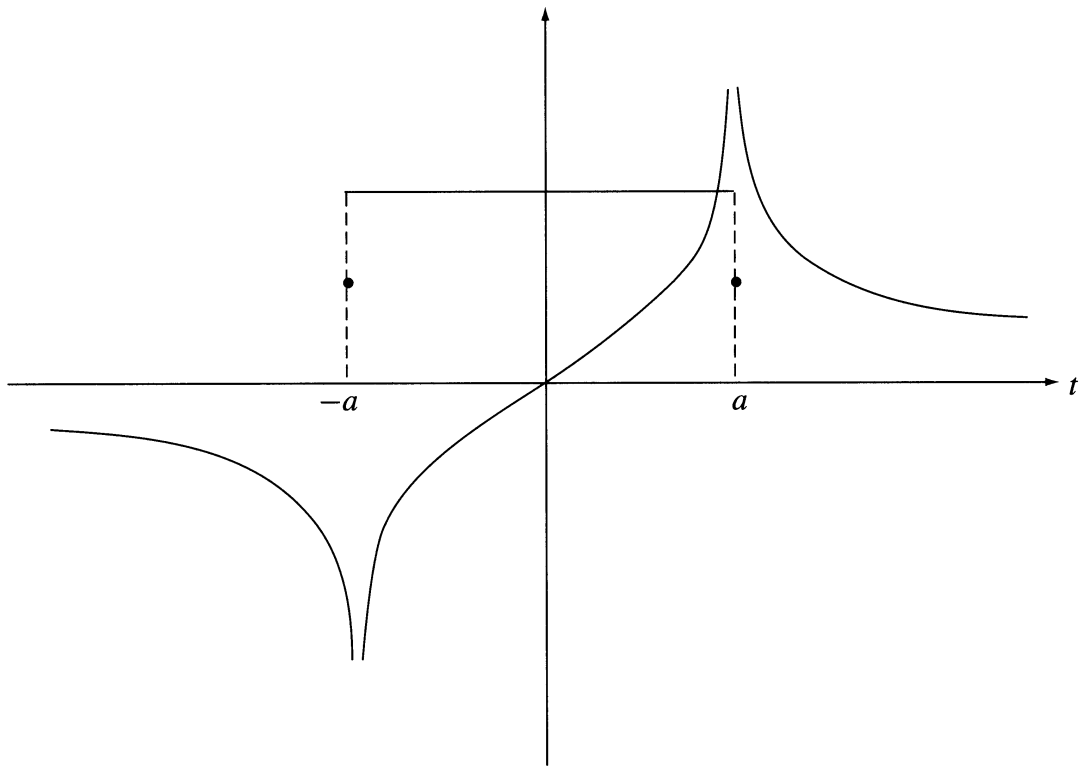

FIGURE 7.4.1 The square pulse $\Pi_a(t)$ and its Hilbert transform.

The square pulse and its Hilbert transform are shown in Figure 7.4.1. Notice that the support of the square pulse is limited within the interval $|t| \le a$, while the support of the Hilbert transform is infinite. This statement applies to all Hilbert transforms of functions of limited support. Of course, the inverse Hilbert transformation of the logarithmic function (7.4.6) restores the square pulse of limited support. The change of variable $t' = t - a$ (time shift of the pulse) yields the Hilbert transform of a one-sided square pulse.

$$H\left[\Pi_a\left(t-a\right)\right] = \frac{1}{\pi}\ln\left|\frac{t}{t-2a}\right| \tag{7.4.7}$$

3. The Hilbert transform of a constant function $u(t) = u_0$ equals zero. This is easily seen from Eq. (7.4.6) at the limit $a \Rightarrow \infty$. The mean value of a function is given by the integral

$$u_0 = \lim_{T\Rightarrow\infty}\frac{1}{T}\int_{-T/2}^{T/2} u\left(t\right)dt \tag{7.4.8}$$

Therefore, the Hilbert transform of a function $u(t) = u_0 + u_1(t)$ is

$$H[u_0 + u_1(t)] = H[u_1(t)] \tag{7.4.9}$$

that is, in electrical terminology the Hilbert transformation cancels the DC term u_0.

4. Consider the Gaussian pulse and its Fourier image

$$e^{-\pi t^2} \overset{F}{\Longleftrightarrow} e^{-\pi f^2}; \quad \omega = 2\pi f \tag{7.4.10}$$

Because for this signal the Hilbert transform defined by the integral (7.1.1) has no closed form, it is convenient to derive the Hilbert transform using the inverse Fourier transformation of the Fourier image (Equation [7.4.10]). This inverse transform has the form

$$v(t) = \int_{-\infty}^{\infty} -j\,\mathrm{sgn}(\omega) e^{-\pi f^2} e^{j\omega t} df \tag{7.4.11}$$

Because the integrand is an odd function, this integral has the simplified form

$$v(t) = 2\int_{0}^{\infty} e^{-\pi f^2} \sin(\omega t) df \tag{7.4.12}$$

This integral has no closed solution and may be represented by a power series defining a function called $Ei(t)$. However, in the days of proliferation of computers it is much simpler to find a numerical solution of this integral. The Gaussian pulse and its Hilbert transform computed using Equation (7.4.12) are shown in Figure 7.4.2.

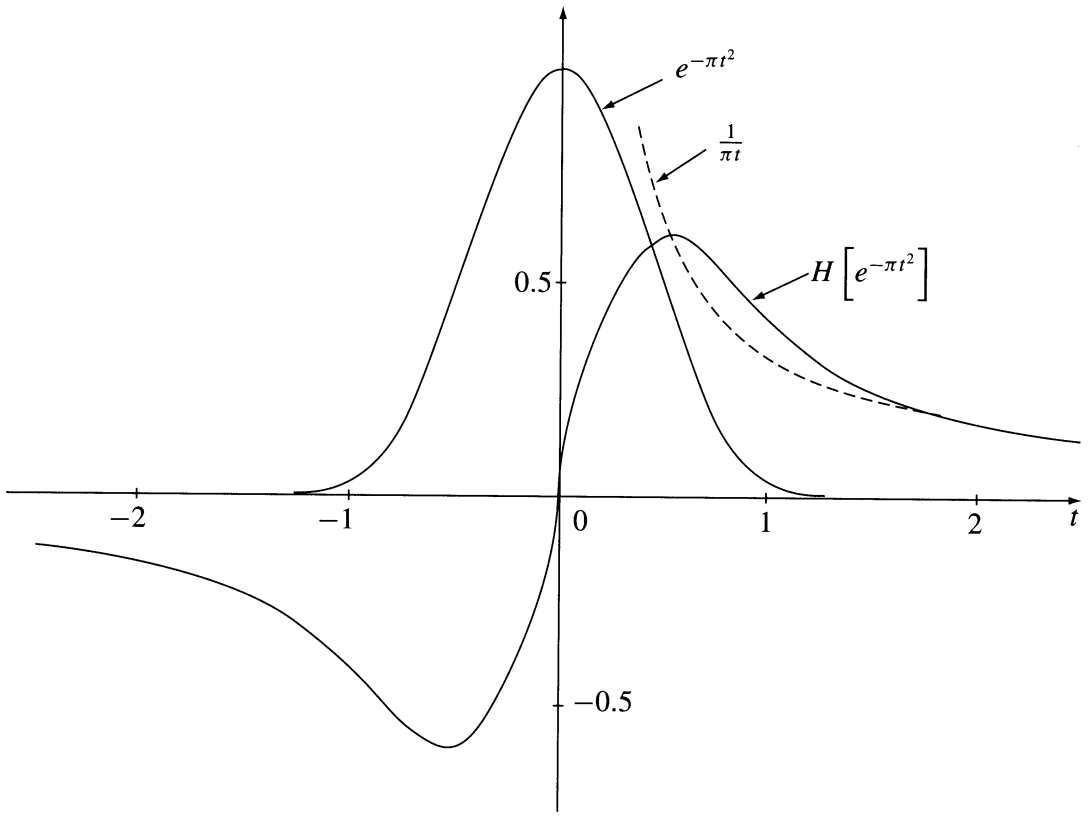

FIGURE 7.4.2 The Gaussian pulse and its Hilbert transform.

7.5 Definition of the Hilbert Transformation by Using a Distribution

It is well known that the concept of the delta function, the unit step, and similar functions extend the class of functions for which the Fourier transform exists. The formal Fourier integral theory restricts the functions to those satisfying Dirichlet's conditions, including the requirement of finite energy (finite value of the integral of the square). The mathematicians eliminated this restriction by introducing the

concept of a distribution, giving a rigorous foundation to the notions of the delta pulse, the signum function, and so forth. The notion of a distribution is not unique, because there exist several definitions. The most accepted theory of a distributions was formulated by Schwartz,[35] who used the concept of a functional. Another useful approach was formulated by Mikusinski[23] who used sequences of approximating functions.

Equation (7.3.15) shows that the Fourier image of analytic signals is one-sided. A good example is the one-sided spectrum given by the doubled unit step $2\ \mathbf{1}(f)$ defined as a distribution in the Fourier frequency domain. This distribution may be decomposed into the even and odd parts:

$$2\ \mathbf{1}(f) = \mathbf{1} + \operatorname{sgn}(f) \tag{7.5.1}$$

where **1** is a constant distribution and $\operatorname{sign}(f)$ is a signum distribution. The inverse Fourier transformation of this unit step is given by the integral

$$\psi_\delta(t) = \int_{-\infty}^{\infty} 2\,\mathbf{1}(f) e^{j\omega t} df\,; \quad \omega = 2\pi f \tag{7.5.2}$$

or by the integral

$$\psi_\delta(t) = 2\int_0^{\infty} e^{j\omega t} df \tag{7.5.3}$$

which defines the complex delta distribution of the form

$$\psi_\delta(t) = \delta(t) + j\,P\frac{1}{\pi t} = F^{-1}\left[2\,\mathbf{1}(f)\right] \tag{7.5.4}$$

with P the Cauchy Principal Value. We observe, that the delta distribution and the kernel of the Hilbert transformation are forming a Hilbert pair

$$\delta(t) \overset{\mathrm{H}}{\Longleftrightarrow} P\frac{1}{\pi t} \tag{7.5.5}$$

where the Fourier images are

$$\delta(f) \overset{F}{\Longleftrightarrow} \mathbf{1}; \quad \Theta(t) = P\frac{1}{\pi t} \overset{F}{\Longleftrightarrow} -j\operatorname{sgn}(\omega) \tag{7.5.6}$$

Therefore, the kernel of the Hilbert transformations (7.1.3) and (7.1.4) denoted by $\Theta(t)$ has been redefined as a distribution in the form of the Hilbert transform of the delta pulse (distribution).

The **analytic signal** (7.2.15) may be defined in the form of a convolution of a given function (or distribution) $u(t)$ with the **complex delta distribution**; that is,

$$\psi(t) = \psi_\delta(t) * u(t) = \left[\delta(t) + jP\frac{1}{\pi t}\right] * u(t) \tag{7.5.7}$$

Indeed, the well-known alternative definition of the delta distribution is

$$u(t) = u(t) * \delta(t) \tag{7.5.8}$$

This is a convolution equation. The application of the theorem about the Hilbert transform of a convolution (see Table 7.7.3) yields the following two alternative forms of $H[u(t)]$:

$$v(t) = u(t) * \frac{1}{\pi t}; \quad v(t) = v(t) * \delta(t) \tag{7.5.9}$$

The complex delta distribution may be defined alternatively using approximating functions. A convenient choice is the Cauchy signal (see Equation [7.2.16]):

$$\psi_\delta(t) = \lim_{\alpha \Rightarrow 0} \left[\frac{\alpha}{\pi(\alpha^2 + t^2)} + j \frac{t}{\pi(\alpha^2 + t^2)} \right] \tag{7.5.10}$$

(see Figure 7.5.1). The division by π is needed to get the integral of the real part equal to 1. In terms of this representation, the distribution $\Theta(t) = 1/\pi t$ equals zero for $t = 0$. The real and imaginary parts of the complex delta distribution, as for any analytic signal, are orthogonal; that is, the integral of their product equals zero

$$P\int_{-\infty}^{\infty} \frac{\delta(t)}{\pi t} dt = 0 \tag{7.5.11}$$

7.6 Hilbert Transforms of Periodic Signals

A real function (signal) $u_p(t)$ is periodic if there is some interval T (the period) for which

$$u_p(t) = u_p(t + kT) \tag{7.6.1}$$

for all t in $(-\infty, \infty)$, where k is an integer $(-\infty, \infty)$. The fundamental frequency is $f = 1/T$ and the fundamental angular frequency is $\omega = 2\pi f = 2\pi/T$. The periodic function may be alternatively defined using a periodic repetition of a so-called **generating function** $u_T(t)$. This repetition is represented by the infinite series

$$u_p(t) = \sum_{k=-\infty}^{\infty} u_T(t - kT) \tag{7.6.2}$$

where the generating function is

$$u_T(t) = \begin{cases} u_p(t) & \text{in the interval } t_0, t_0 + T \\ 0 & \text{otherwise} \end{cases} \tag{7.6.3}$$

Using the well-known shifting property of the convolution of a given function with the delta pulse, the periodic function (7.6.2) may be written in the form

$$u_p(t) = u_T(t) * \sum_{k=-\infty}^{\infty} \delta(t - kT) \tag{7.6.4}$$

that is, the generating function is convolved with the periodic sequence of delta pulses well known from the sampling theory.

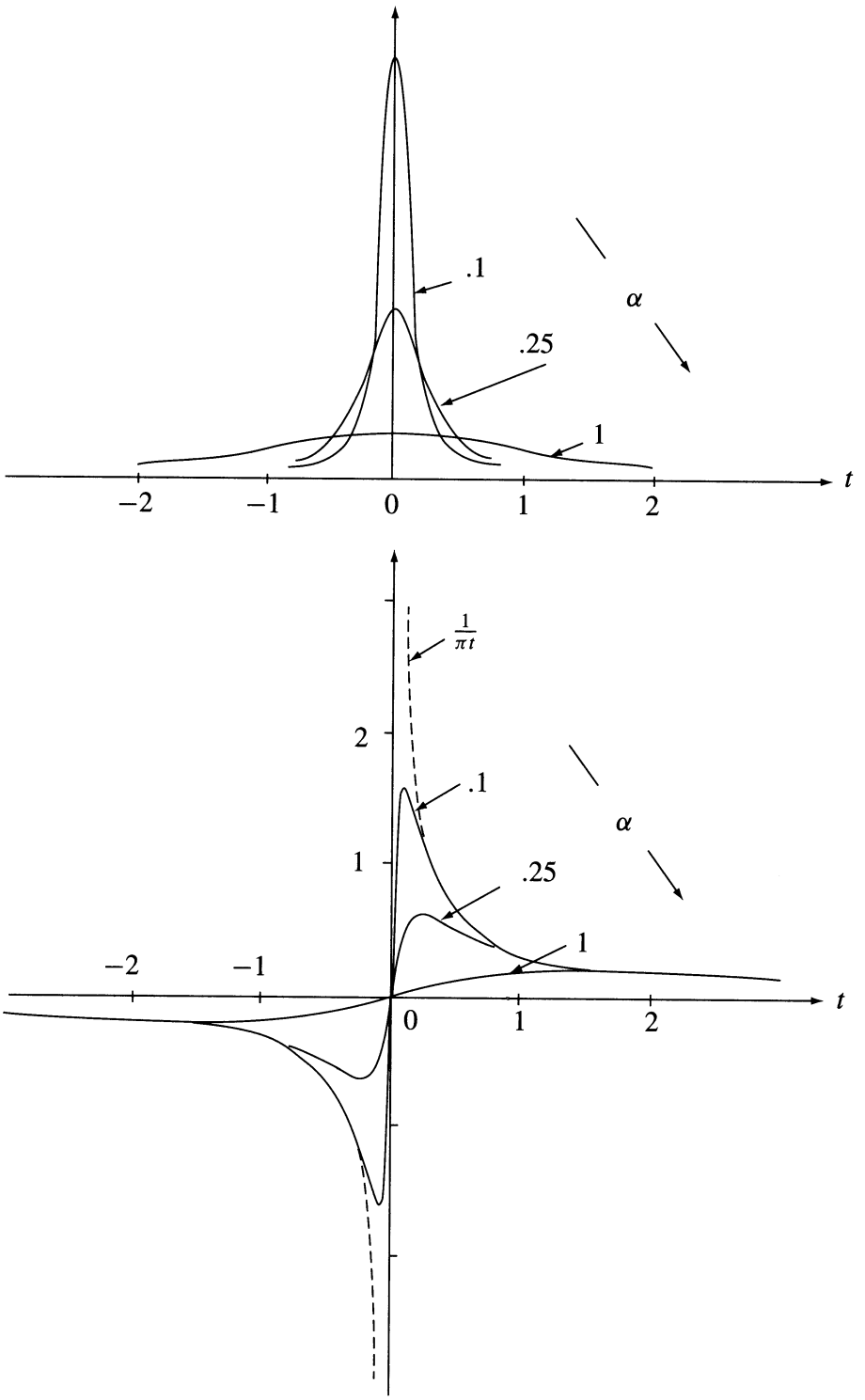

FIGURE 7.5.1 The approximation of the delta pulse $\delta(t)$ and its Hilbert transform $\Theta(t) = 1/(\pi t)$ by Cauchy pulses and its Hilbert transforms (see Figure 7.3.2).

Three different methods of derivation of the Hilbert transform of periodic functions are presented here:

1. A method using Fourier series.
2. Direct derivation in the form of infinite products.
3. The convolution with a cotangent periodic function.

First Method

The periodic function may be expanded into a Fourier series

$$u_p(t) = U_0 + \sum_{n=1}^{\infty} U_n \cos\left(n\omega_0 t + \Phi_n\right); \quad \omega_0 = \frac{2\pi}{T} \tag{7.6.5}$$

The number of terms of this series may be finite or infinite. Because $H[\cos(n\omega t + \Phi)] = \sin(n\omega t + \Phi)$, the Hilbert transform of the periodic function $u_p(t)$ is given by the Fourier series

$$v_p(t) = \sum_{n=1}^{\infty} U_n \sin\left(n\omega_0 t + \Phi_n\right) \tag{7.6.6}$$

Notice the cancellation of the constant term U_0 (in electrical terminology the DC term). If the Fourier series is given using the complex notation

$$u_p(t) = \sum_{n=-\infty}^{\infty} C_n e^{jn\omega_0 t} \tag{7.6.7}$$

where the complex coefficient C_n is given by the integral

$$C_n = \frac{1}{T}\int_{-T/2}^{T/2} u_p(t) e^{-jn\omega_0 t} dt \tag{7.6.8}$$

then the Hilbert transform has the form (see Equation [7.3.12])

$$v_p(t) = \sum_{n=-\infty}^{\infty} -j\,\mathrm{sgn}(n) C_n e^{jn\omega_0 t}; \quad \omega_0 > 0 \tag{7.6.9}$$

Again, the constant term is eliminated (sgn(0) = 0).

Example

Consider the Fourier series of the periodic square wave given by the formula $u_p(t) = \mathrm{sgn}[\cos(\omega t)]$ ($\omega = 2\pi f$ – a constant):

$$u_p(t) = \frac{4}{\pi}\left[\cos(\omega t) - \frac{1}{3}\cos(3\omega t) + \frac{1}{5}\cos(5\omega t) - \frac{1}{7}\cos(7\omega t) + \cdots\right] \tag{7.6.10}$$

The Hilbert transform has the form

$$v_p(t) = \frac{4}{\pi}\left[\sin(\omega t) - \frac{1}{3}\sin(3\omega t) + \frac{1}{5}\sin(5\omega t) - \frac{1}{7}\sin(7\omega t) + \cdots\right] \tag{7.6.11}$$

Figures 7.6.1a/b show the signals represented by the Fourier series (7.6.10) and (7.6.11) truncated at the 5th harmonic and at a much higher harmonic term. We observe the Gibbs peaks for the cosine series. Because in the limit, the energy of the Gibbs peaks equals zero (a zero function), the Gibbs peaks disappear for the sine series.

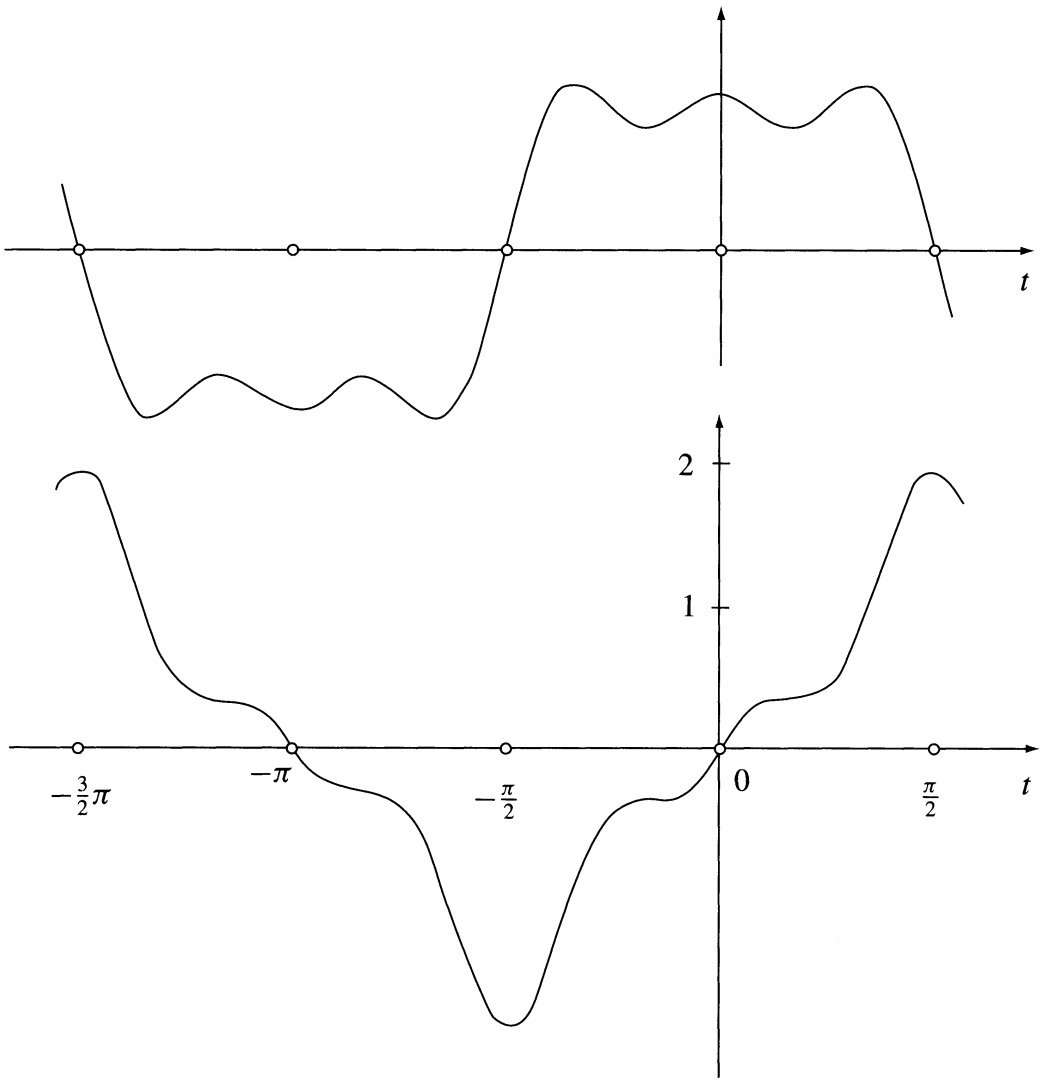

FIGURE 7.6.1a The waveforms given by the truncation of the Fourier series of a square wave at the 5th harmonic number and of the corresponding Hilbert transform.

Second Method

The derivation of the Hilbert transform of a periodic signal directly in the time domain (or any other domain) using the basis integral definition of the Hilbert transformation given by Equation (7.1.1) has the form of the infinite sum of integrals over successive periods. Only one of these integrals includes the pole of the kernel $1/(\pi t)$. For example, the Hilbert transform of the periodic square wave (see Figure 7.6.2a) has the form

$$\upsilon_p(t) = -\frac{1}{\pi}\left\{\cdots\int_{-5b}^{-3b}\frac{d\eta}{\eta - t} - \int_{-3b}^{-b}\frac{d\eta}{\eta - t} + \lim_{\varepsilon \Rightarrow 0}\left[\int_{-b}^{t-\varepsilon}\frac{d\eta}{\eta - t} + \int_{t+\varepsilon}^{b}\frac{d\eta}{n - t}\right] - \int_{b}^{3b}\frac{d\eta}{\eta - t} + \int_{3b}^{5b}\frac{d\eta}{\eta - t} - \cdots\right\} \tag{7.6.12}$$

where $b = T/4$. The result of this integration has the form

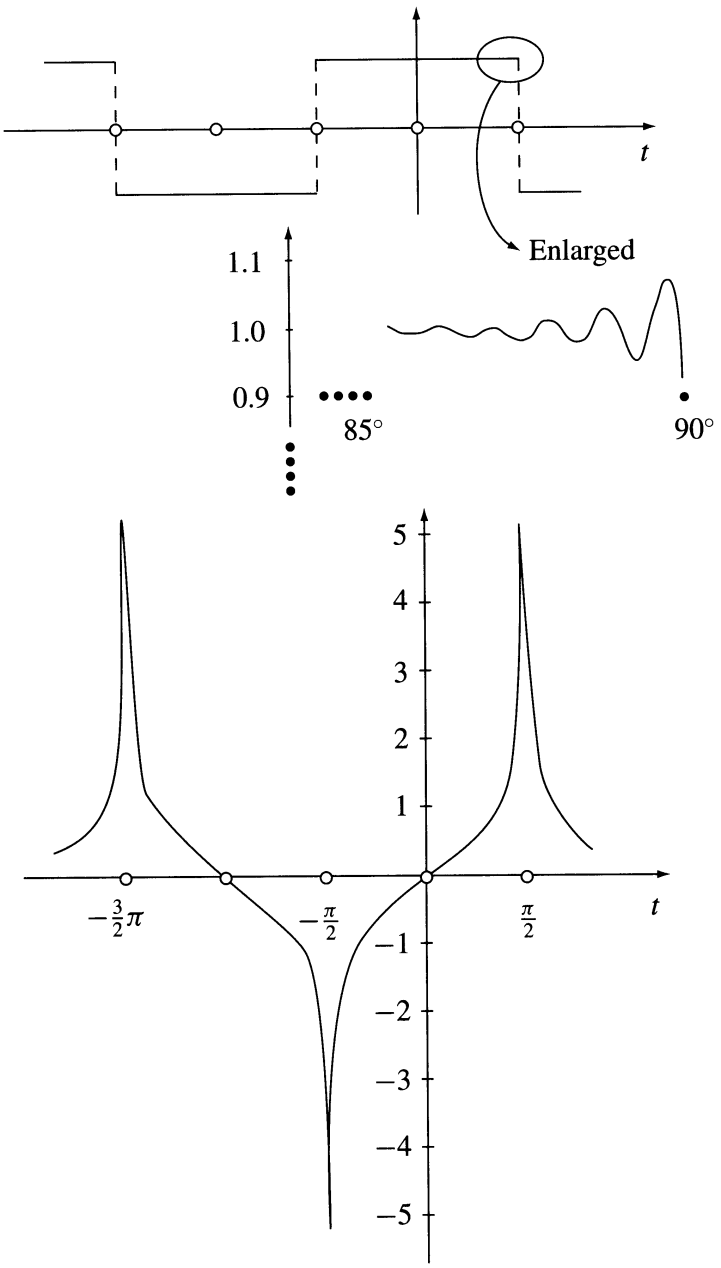

FIGURE 7.6.1b Analogous waveforms by the truncation at a high harmonic number.

$$v_p(t) = \frac{2}{\pi}\left\{\ln\left|\frac{\Pi_{m=1}\left[2m-1-(1)^m x\right]}{\Pi_{m=1}\left[2m-1+(1)^m x\right]}\right|\right\} \tag{7.6.13}$$

where $x = 4t/T$ and $m = 1, 2, 3, \ldots$. The first terms of the infinite products are

$$v_p(t) = \frac{2}{\pi}\ln\left|\frac{(1+x)(3-x)(5+x)(7-x)\cdots}{(1-x)(3+x)(5-x)(7+x)\cdots}\right| \tag{7.6.14}$$

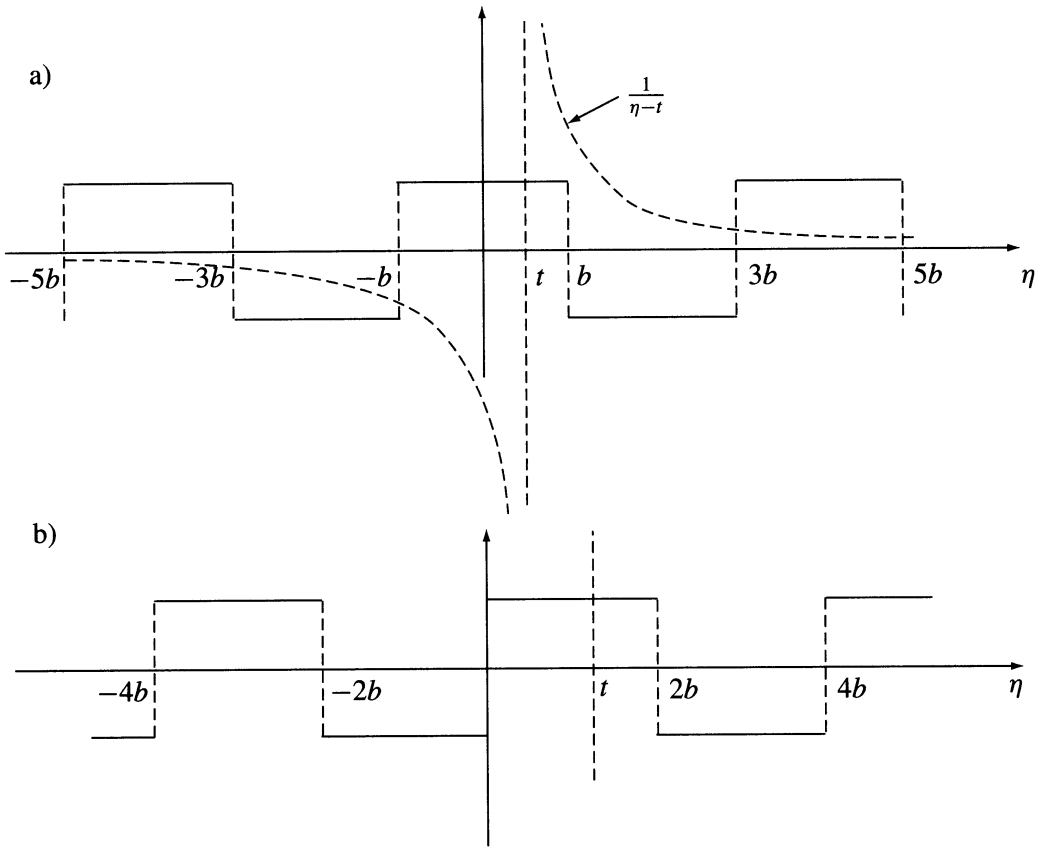

FIGURE 7.6.2 Illustration to the derivation of the Hilbert transform of a square wave.

The infinite products in the above formulas are convergent. Using the numerical evaluation of Equation (7.6.14) we have to truncate the products having the same number of terms in the nominator and denominator. For the odd square wave $u_p(t) = \text{sgn}[\sin(\omega t)]$ (see Figure 7.6.2b), Equation [7.6.14] changes to

$$v_p(t) = \frac{2}{\pi} \ln \left| \frac{y\left(4 - y^2\right)\left(16 - y^2\right)\left(36 - y^2\right)\cdots}{\left(1 - y^2\right)\left(9 - y^2\right)\left(15 - y^2\right)\left(7 - y\right)\cdots} \right|; \quad y = 2x = 2t/T \tag{7.6.15}$$

Notice that the denominator has been truncated so that a half-term of $(49 - y^2) = (7 - y)\ (7 + y)$ is deleted. This is needed to obtain a symmetrical truncation. Using a computer, the quotients in Equations (7.6.14) or (7.6.15) should be calculated using one term of the nominator divided by one term of the denominator. Otherwise there is a danger of entering in the overflow range of the computer ("number too big"). Let us recall that the harmonic functions have a representation in the form of infinite series.

$$\sin(z) = z \prod_{k=1}^{\infty} \left(1 - \frac{z^2}{k^2 \pi^2} \right) \tag{7.6.16}$$

$$\cos(z) = \prod_{k=1}^{\infty} \left(1 - \frac{4z^2}{(2k-1)^2 \pi^2} \right) \tag{7.6.17}$$

Third Method: Cotangent Hilbert Transformations

The cotangent form of the Hilbert transformation of periodic functions may be conveniently derived starting with the convolution equation (7.6.4). The Hilbert transform of a convolution of two functions equals the convolution of the Hilbert transform of one function (arbitrary choice) with the original of the other function (see Table 7.7.3). The Hilbert transform of the delta sampling sequence is

$$\delta_p(t) = \sum_{k=-\infty}^{\infty} \delta(t - kT) \overset{\mathrm{H}}{\Longleftrightarrow} \Theta_p(t) = \frac{1}{T} \sum_{k=-\infty}^{\infty} \cot\left[\frac{\pi}{T}(t - kT)\right] \tag{7.6.18}$$

This Hilbert pair is shown in Figure 7.6.3. The derivation is given at the end of this section. The insertion of this Hilbert transform in the convolution Equation (7.6.4) yields the following form of the Hilbert transform of periodic functions:

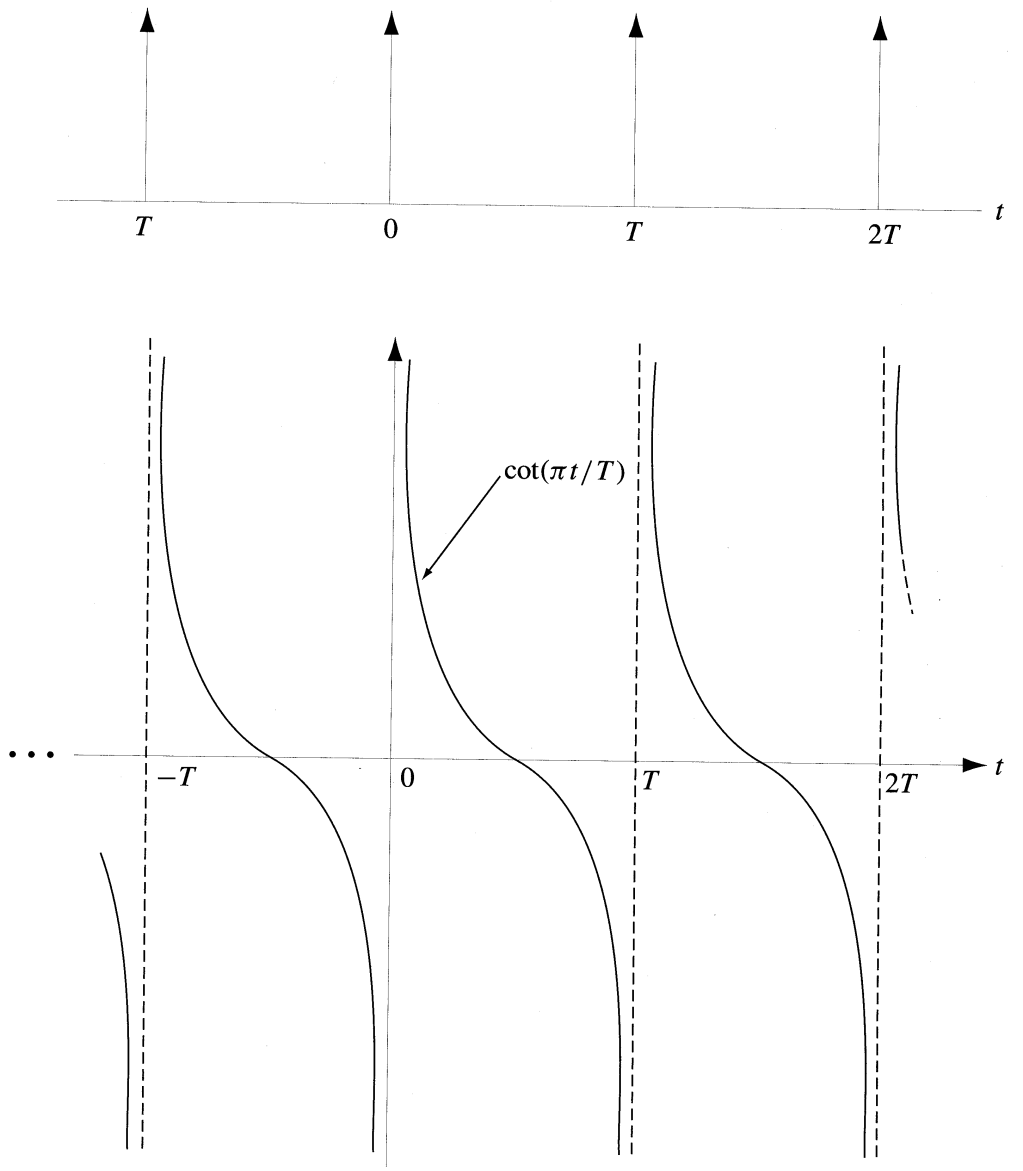

FIGURE 7.6.3 The periodic sequence of delta pulses and its Hilbert transform.

$$v_p(t) = u_T(t) * \frac{1}{T}\sum_{k=-\infty}^{\infty} \cot\left[\frac{\pi}{T}(t - kT)\right] \tag{7.6.19}$$

where $u_T(t)$ is the generating function defined by Equation (7.6.3). Contrary to Fourier series, Equation (7.6.19) has a closed integral form and for many generating functions a closed analytic solution. If the analytic solution does not exist, a numerical evaluation of the convolution yields the desired Hilbert transform.

Example

Consider again the square wave of sgn[cos(ωt)]. The generating function is

$$u_T(t) = \begin{cases} \text{sgn}\left[\cos(\omega t)\right] & \text{for } |t| \le 0.5T; \quad \omega = \dfrac{2\pi}{T} \\ 0 & \text{otherwise} \end{cases} \tag{7.6.20}$$

This generating function equals –1 in the intervals $-T/2$ to $-T/4$ and $T/4$ to $T/2$ and equals 1 in the interval $-T/4$ to $T/4$. The insertion of the integration intervals (Cauchy Principal Value)

$$-\begin{vmatrix} -T/4 \\ -T/2 \end{vmatrix} + \begin{vmatrix} t-\varepsilon \\ -T/4 \end{vmatrix} + \begin{vmatrix} T/4 \\ t+\varepsilon \end{vmatrix} - \begin{vmatrix} T/2 \\ T/4 \end{vmatrix} \tag{7.6.21}$$

into the integral

$$\frac{1}{T}\int \cot\left[\frac{\pi}{T}(\tau - t)\right] d\tau = \frac{1}{\pi}\ln\left|\sin\left[\frac{\pi}{T}(\tau - t)\right]\right| \tag{7.6.22}$$

yields the following form of the Hilbert transform of the square wave

$$v_p(t) = \frac{2}{\pi}\ln\left|\frac{\sin\left[\dfrac{\pi}{T}\left(\dfrac{T}{4} - t\right)\right]}{\sin\left[\dfrac{\pi}{T}\left(\dfrac{T}{4} + t\right)\right]}\right| \tag{7.6.23}$$

Using trigonometric relations, we get the Hilbert pair

$$\text{sgn}\left[\cos(\omega t)\right] \overset{\text{H}}{\Longleftrightarrow} \frac{2}{\pi}\ln\left|\tan(\omega t/2 + \pi/4)\right| \tag{7.6.24}$$

Similarly, it may be shown that

$$\text{sgn}\left[\sin(\omega t)\right] \overset{\text{H}}{\Longleftrightarrow} \frac{2}{\pi}\ln\left|\tan(\omega t/2)\right| \tag{7.6.25}$$

The Hilbert transform of the periodic delta sequence given by Equation (7.6.18) may be derived as follows: We start with the Hilbert pair

$$\delta(t) \overset{\mathrm{H}}{\Longleftrightarrow} \frac{1}{\pi t} \tag{7.6.26}$$

The support of the Hilbert transform $1/(\pi t)$ is infinite. Therefore, in the interval of one period, for example, the interval from 0 to T, there is a summation of successive tails of functions $\Theta_n(t) = 1/[\pi(t - nT)]$, i.e., the generating function of the Hilbert transform of the delta sampling sequence is

$$\Theta_T(t) = \sum_{n=-\infty}^{\infty} \frac{1}{\pi(t - nT)} = \frac{1}{T}\cot(\pi t/T) \tag{7.6.27}$$

that is, the infinite sum converges to the cotangent function. The repetition of this generating function yields the periodic Hilbert transform of the delta sampling sequence of the form

$$\Theta_p(t) = \sum_{k=-\infty}^{\infty} \Theta_T(t - kT) = \frac{1}{T}\sum_{k=-\infty}^{\infty} \cot\left[\frac{\pi}{T}(t - kT)\right] \tag{7.6.28}$$

This sequence also may be written in the convolution form

$$\Theta_p(t) = \frac{1}{T}\cot(\pi t/T) * \sum_{k=-\infty}^{\infty} \delta(t - kT) \tag{7.6.29}$$

The generating function $\Theta_T(t)$ (Equation [7.6.27]) may be alternatively derived using Fourier transforms. The well-known Fourier pair is

$$\sum_{k=-\infty}^{\infty} \delta(t - kT) \overset{F}{\Longleftrightarrow} \frac{1}{T}\sum_{k=-\infty}^{\infty} \delta(f - k/T) \tag{7.6.30}$$

The multiplication of this Fourier image by the operator $-j\,\mathrm{sgn}(f)$ yields the Fourier image of the generating function $\Theta_T(t)$:

$$\Theta_T(t) \overset{F}{\Longleftrightarrow} \frac{1}{T}\sum_{n=-\infty}^{\infty} -j\,\mathrm{sgn}(f)\,\delta(f - n/T) \tag{7.6.31}$$

The inverse Fourier transform of this spectrum yields:

$$\Theta_T(t) = \frac{j}{T}\sum_{n=-\infty}^{\infty} e^{-j2\pi nt/T} - \frac{j}{T}\sum_{n=1}^{\infty} e^{j2\pi n/T} = \frac{2}{T}\sum_{n=1}^{\infty} \sin(2\pi\, nt/T) \tag{7.6.32}$$

The insertion of the relation (in the distribution sense)

$$\sum_{n=1}^{\infty} \sin(nx) = \frac{1}{2}\cot(x/2) \tag{7.6.33}$$

yields $\Theta(t)$ given by the formula (7.6.27). Notice that the derivation of the periodic Hilbert transform $\Theta_p(t)$ involves two summations. The first yields the generating function $\Theta_T(t)$ and the second gives the periodic repetition of this function.

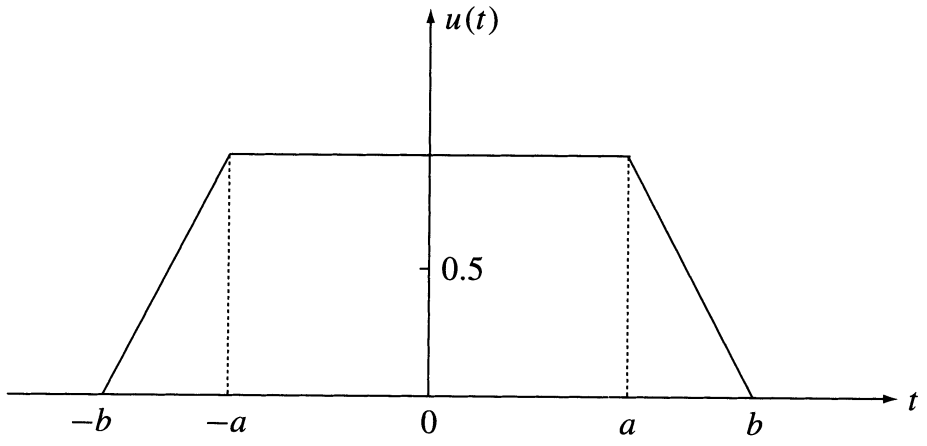

FIGURE 7.7.1 A trapezoidal pulse (see Table 7.7.1, #9.)

7.7 Tables Listing Selected Hilbert Pairs and Properties of Hilbert Transformations

Table 7.7.1 presents the Hilbert transforms of some selected aperiodic signals and the two basic periodic harmonic signals $\cos(\omega t)$ and $\sin(\omega t)$. The Hilbert transforms of selected other periodic signals are listed in Table 7.7.2. The knowledge of the Hilbert transforms listed in these tables and the application of various properties of the Hilbert transformation listed in Table 7.7.3 enables an easy derivation of a large variety of Hilbert transforms. Applications of the properties listed in these tables are given in Sections 7.8 to 7.14, which also include selected derivations and applications of the properties of Hilbert transformations.

7.8 Linearity, Iteration, Autoconvolution, and Energy Equality

The Hilbert transformation is linear and, if a complicated waveform can be decomposed into a sum of simpler waveforms, then the summation of the Hilbert transforms of each term yields the desired transform. For example, the waveform of Figure 7.8.1a may be a decomposed into a sum of two rectangular pulses. Therefore, the Hilbert transform of this waveform is (see Table 7.7.1)

$$\begin{aligned} v(t) &= H\left[\Pi_a(t) + \Pi_b(t)\right] = \hat{\Pi}_a(t) + \hat{\Pi}_b(t) \\ &= \frac{1}{\pi}\left\{\ln\left|\frac{t+a}{t-a}\right| + \ln\left|\frac{t+b}{t-b}\right|\right\} = \frac{1}{\pi}\ln\left|\frac{(t+b)(t+a)}{(t-b)(t-a)}\right| \end{aligned} \tag{7.8.1}$$

Let us derive in a similar way the Hilbert transform of the "ramp" pulse shown in Figure 7.8.1b. We decompose this pulse into a sum of one-sided square pulse and one-sided inverse triangle. The summation of Equation (7.4.7) and No. 8 of Table 7.7.1 yields

TABLE 7.7.1 Selected Useful Hilbert Pairs

Number	Name	$u(t)$	$v(t)$
1	sine	$\sin(\omega t)$	$-\cos(\omega t)$
2	cosine	$\cos(\omega t)$	$\sin(\omega t)$
3	exponential harmonic	$e^{j\omega t}$	$-j\,\mathrm{sgn}(\omega)e^{j\omega t}$
4	square pulse	$\Pi_a(t)$[†]	$\frac{1}{\pi}\ln\left\lvert\frac{t+a}{t-a}\right\rvert$
5	bipolar pulse	$\Pi_a(t)\,\mathrm{sgn}(t)$	$\frac{1}{\pi}\ln\left\lvert 1-(a/t)^2\right\rvert$
6	double triangle	$t\Pi_a(t)\,\mathrm{sgn}(t)$	$\frac{t}{\pi}\ln\left\lvert 1-(a/t)^2\right\rvert$
7	triangle tri(t)	$1-\lvert t/a\rvert;\quad \lvert t\rvert\le a$ $0;\quad \lvert t\rvert > a$	$\frac{-1}{\pi}\left\{\ln\left\lvert\frac{t-a}{t+a}\right\rvert+\frac{t}{a}\ln\left\lvert\frac{t^2}{t^2-a^2}\right\rvert\right\}$
8	one-sided triangle	$\mathbf{1}(t)\,\mathrm{tri}(t)$	$\frac{1}{\pi}\left\{(1-t/a)\ln\left\lvert\frac{t}{t+a}\right\rvert+1\right\}$
9	trapezoid pulse	waveform[‡]	$\frac{-1}{\pi}\left\{\frac{b}{b-a}\ln\left\lvert\frac{(a+t)(b-t)}{(b+t)(a-t)}\right\rvert+\frac{t}{b-a}\ln\left\lvert\frac{a^2-t^2}{b^2-t^2}\right\rvert+\ln\left\lvert\frac{a-t}{a+t}\right\rvert\right\}$
10	Cauchy pulse	$\frac{\alpha}{\alpha^2+t^2};\quad \alpha>0$	$\frac{t}{\alpha^2+t^2}$
11	Gaussian pulse	$e^{-\pi t^2}$	$2\int_0^\infty e^{-\pi f^2}\sin(\omega t)\,df$ $\omega=2\pi f$
12	parabolic pulse	$1-\lvert t/a\rvert^2;\quad \lvert t\rvert\le a$ $0;\quad \lvert t\rvert > a$	$\frac{-1}{\pi}\left\{\left[1-(t/a)^2\right]\ln\left\lvert\frac{t-a}{t+a}\right\rvert-\frac{2t}{a}\right\}$
13	symmetric exponential	$e^{-a\lvert t\rvert}$	$2\int_0^\infty\frac{2a}{a^2+\omega^2}\sin(\omega t)\,df$ or $\frac{-1}{\pi}\{\exp(-a\lvert t\rvert)E(-a\lvert t\rvert)-\exp(a\lvert t\rvert)E(a\lvert t\rvert)\}$ where $E(x)=\int_X^\infty\frac{\exp(-\tau)}{\tau}\,d\tau$
14	antisymmetric exponential	$\mathrm{sgn}(t)e^{-a\lvert t\rvert}$	$-2\int_0^\infty\frac{2\omega}{a^2+\omega^2}\cos(\omega t)\,df$
15	one-sided exponential	$\mathbf{1}(t)e^{-a\lvert t\rvert}$	$2\int_0^\infty\frac{a\sin(\omega t)-\omega\cos(\omega t)}{a^2+\omega^2}\,df$
16	sinc pulse	$\frac{\sin(at)}{at}$	$\frac{\sin^2(at/2)}{(at/2)}=\frac{1-\cos(at)}{at}$
17	video test pulse	$\cos^2(\pi t/2a);\quad \lvert t\rvert\le a$ $0;\quad \lvert t\rvert > a$	$2\int_0^\infty\frac{2a^2}{4a^2-\omega^2}\frac{\sin(\pi\omega/2a)}{\omega}\sin(\omega t)\,df$
18	constant	a	zero

[†]See Figure 7.4.1

[‡]See Figure 7.7.1

$$H\left["\text{ramp}"\right]=H\left[\Pi_{b/2}\left(t-b/2\right)\right]-H\left[1\left(t\right)\text{tri}\left(t\right)\right]$$
$$=\frac{1}{\pi}\left\{\ln\left|\frac{t}{t-b}\right|-\left(1-t/a\right)\ln\left|\frac{t}{t+a}\right|-1\right\} \tag{7.8.2}$$

Iteration

Iteration of the Hilbert transformation two times yields the original signal with the reverse sign, and the iteration four times restores the original signal $u(t)$. In the Fourier frequency domain the n-time iteration

TABLE 7.7.1 Selected Useful Hilbert Pairs (Continued)

Hyperbolic Functions: Approximation by summation of Cauchy signals (see Hilbert pairs 10 and 43)		
Number	$u(t)$	$v(t)$
19	$\tanh(t) = 2\sum_{\eta=0}^{\infty} \frac{t}{(\eta+0.5)^2\pi^2+t^2}$	$-2\pi \sum_{\eta=0}^{\infty} \frac{(\eta+0.5)}{(\eta+0.5)^2\pi^2+t^2}$

Notice the infinite energy of the functions $\tanh(t)$, $\coth(t)$, and $\operatorname{cosech}(t)$.
The part of finite energy of $\tanh(t)$ is:

20	$\operatorname{sgn}(t) - \tanh(t)$;	$\pi\delta(t) + 2\pi \sum_{\eta=0}^{\infty} \frac{(\eta+0.5)}{(\eta+0.5)^2\pi^2+t^2}$
21	$\coth(t) = \frac{1}{t} + 2\sum_{\eta=1}^{\infty} \frac{t}{(\eta\pi)^2+t^2}$;	$-\pi\delta(t) + 2\pi \sum_{\eta=1}^{\infty} \frac{\eta}{(\eta\pi)^2+t^2}$
22	$\operatorname{sech}(t) = -2\pi \sum_{\eta=0}^{\infty}(-1)^{(\eta-1)} \frac{(\eta+0.5)}{(\eta+0.5)^2\pi^2+t^2}$;	$-2\sum_{\eta=0}^{\infty}(-1)^{(\eta-1)} \frac{t}{(\eta+0.5)^2\pi^2+t^2}$
23	$\operatorname{cosech}(t) = \frac{1}{t} - 2\sum_{\eta=1}^{\infty}(-1)^{(\eta-1)} \frac{t}{(\eta\pi)^2+t^2}$;	$-\pi\delta(t) + 2\pi \sum_{\eta=1}^{\infty}(-1)^{(\eta-1)} \frac{\eta}{(\eta\pi)^2+t^2}$
Hyperbolic Functions by inverse Fourier transformation ($\omega = 2\pi f$)		
24	$\operatorname{sgn}(t) - \tanh(at/2)$; $\operatorname{Re} a > 0$;	$2\int_0^{\infty} \left[\frac{2\pi}{a\sinh(\pi\omega/a)} - \frac{2}{\omega}\right] \cos(\omega t)\, df$
25	$\coth(at/2) - \operatorname{sgn}(t)$;	$2\int_0^{\infty} \left[\frac{2\pi}{a}\coth(\pi\omega/a) - \frac{2}{\omega}\right] \cos(\omega t)\, df$
26	$\operatorname{sech}(at/2)$;	$2\int_0^{\infty} \frac{2\pi}{a\cosh(\pi\omega/2a)} \sin(\omega t)\, df$
27	$\operatorname{cosech}(at/2)$;	$-2\int_0^{\infty} \frac{2\pi}{a}\tanh(\pi\omega/2a)\cos(\omega t)\, df$
28	$\operatorname{sech}^2(at/2)$;	$2\int_0^{\infty} \frac{2\pi\omega}{a\sinh(\pi\omega/2a)} \sin(\omega t)\, df$
Delta distribution, $1/\pi t$ distribution and its derivatives		
29	$\delta(t)$	$1/\pi t$
30	$1/\pi t$	$-\delta(t)$
31	$\delta^{(1)}(t)$	$-1/\pi t^2$
32	$1/\pi t^2$	$\delta^{(1)}(t)$
33	$\delta^{(2)}(t)$	$2/\pi t^3$
34	$1/\pi t^3$	$-0.5\delta^{(2)}(t)$
35	$\delta^{(3)}(t)$	$-6/\pi t^4$
36	$1/\pi t^4$	$(1/6)\delta^{(3)}(t)$
37	$u(t)\delta(t)$	$v(t) = (1/\pi t)u(0)$
Equality of convolutions:		
38	$\delta(t) = \delta(t) * \delta(t)$	$\delta(t) = -(1/\pi t) * (1/\pi t)$
39	$\delta^{(1)}(t) = \delta^{(1)}(t) * \delta(t)$	$\delta^{(1)}(t) = (1/\pi t^2) * (1/\pi t)$
40	$\delta^{(2)}(t) = \delta^{(1)}(t) * \delta^{(1)}(t)$	$\delta^{(2)}(t) = -(1/\pi t^2) * (1/\pi t^2)$
41	$\delta^{(3)}(t) = \delta^{(3)}(t) * \delta(t) = \delta^{(2)}(t) * \delta^{(1)}(t)$	$\delta^{(3)}(t) = (6/\pi t^4) * (1/\pi t) = (2/\pi t^3) * (1/\pi t^2)$

TABLE 7.7.1 Selected Useful Hilbert Pairs (Continued)

Approximating functions to the above distributions		
42	$\int \delta(a,t)\,dt = \frac{1}{\pi}\tan^{-1}(t/a)$;	$\int \Theta(a,t)\,dt = \frac{\ln(a^2+t^2)}{2\pi}$
43	$\delta(a,t) = \frac{1}{\pi}\frac{a}{a^2+t^2}$;	$\Theta(a,t) = \frac{1}{\pi}\frac{t}{a^2+t^2}$
44	$\delta^{(1)}(a,t) = \frac{1}{\pi}\frac{-2at}{(a^2+t^2)^2}$;	$\Theta^{(1)}(a,t) = \frac{1}{\pi}\frac{a^2-t^2}{(a^2+t^2)^2}$
45	$\delta^{(2)}(a,t) = \frac{1}{\pi}\frac{6at^2-2a^2}{(a^2+t^2)^3}$;	$\Theta^{(2)}(a,t) = \frac{1}{\pi}\frac{2t^3-6at^2}{(a^2+t^2)^3}$
46	$\delta^{(3)}(a,t) = \frac{1}{\pi}\frac{24a^3t-24at^2}{(a^2+t^2)^4}$;	$\Theta^{(3)}(a,t) = \frac{1}{\pi}\frac{-6t^2+36a^2t^2-6a^4}{(a^2+t^2)^4}$
Trigonometric functions		
47	$\frac{\sin(at)}{t}$	$\frac{1-\cos(at)}{t}$
48	$\frac{\cos(at)}{t}$	$-\pi\delta(t) + \frac{\sin(at)}{t}$
49	$\frac{\sin(at)}{t^2}$	$-\pi a\delta(t) + \frac{1-\cos(at)}{t^2}$
50	$\frac{\cos(at)}{t^2}$	$\pi\delta^{(1)}(t) - \frac{a}{t} + \frac{\sin(at)}{t^2}$
51	$\frac{\sin(at)}{t^3}$	$\pi a\delta^{(1)}(t) - \frac{a^2}{2t} + \frac{1-\cos(at)}{t^3}$
52	$\frac{\cos(at)}{t^3}$	$-\frac{\pi}{2}\delta^{(2)}(t) + \frac{a^2\pi}{2}\delta(t) - \frac{a}{t^2} + \frac{\sin(at)}{t^3}$

TABLE 7.7.2 Selected Useful Hilbert Pairs of Periodic Signals

Number	Name	$u_p(t)$	$v_p(t)$
1	sampling sequence	$\sum_{k=-\infty}^{\infty}\delta(t-kT)$	$\frac{1}{T}\sum_{k=-\infty}^{\infty}\cot[(\pi/T)(t-kT)]$
2	even square wave	$\operatorname{sgn}[\cos(\omega t)]$ $\omega = 2\pi/T$	$(2/\pi)\ln\lvert\tan(\omega t/2+\pi/4)\rvert$
3	odd square wave	$\operatorname{sgn}[\sin(\omega t)]$ $\omega = 2\pi/T$	$(2/\pi)\ln\lvert\tan(\omega t/2)\rvert$
4	squared cosine	$\cos^2(\omega t)$	$0.5\sin(2\omega t)$
5	squared sine	$\sin^2(\omega t)$	$-0.5\sin(2\omega t)$
6	cube cosine	$\cos^3(\omega t)$	$\frac{3}{4}\sin(\omega t) + \frac{1}{4}\sin(3\omega t)$
7	cube sine	$\sin^3(\omega t)$	$-\frac{3}{4}\cos(\omega t) + \frac{1}{4}\cos(3\omega t)$
8		$\cos^4(\omega t)$	$\frac{1}{2}\sin(2\omega t) + \frac{1}{8}\sin(4\omega t)$
9		$\sin^4(\omega t)$	$\frac{-1}{2}\sin(2\omega t) + \frac{1}{8}\sin(4\omega t)$
10		$e^{\pm j\omega t}$	$\mp j\operatorname{sgn}(\omega)e^{\pm j\omega t}$
11	product	$\cos(at+\varphi)\cos(bt+\psi)$ $0 < a < b$; φ, ψ are constants	$\cos(at+\varphi)\sin(bt+\psi)$
12	Fourier series	$U_0 + \sum_{k=1}^{n} U_k\cos(k\omega t + \phi_k)$	$\sum_{k=1}^{n} U_k\sin(k\omega t+\phi_k)$
13	any periodic function	$u_T(t) * \sum_{k=-\infty}^{\infty}\delta(t-kT)i^a$	$u_T(t) * \frac{1}{T}\sum_{k=-\infty}^{\infty}\cot[(\pi/T)(t-kT)]$

[a] $u_T(t)$ is the generating function (see Equation [7.7.3]).

TABLE 7.7.3 Properties of the Hilbert Transformation

Number	Name	Original or Inverse Hilbert Transform	Hilbert Transform
1	notations	$u(t)$ or $H^{-1}[v]$	$v(t)$ or $\hat{u}(t)$ or $H[u]$
2	time domain definitions	$\begin{cases} u(t) = \frac{1}{\pi}\int_{-\infty}^{\infty} \frac{v(\eta)}{\eta - t}\, d\eta \\ u(t) = \frac{-1}{\pi t} * v(t) \end{cases}$ or	$\begin{cases} v(t) = \frac{-1}{\pi}\int_{-\infty}^{\infty} \frac{u(\eta)}{\eta - t}\, d\eta \\ v(t) = \frac{1}{\pi t} * u(t) \end{cases}$
3	change of symmetry	$u(t) = u_{1e}(t) + u_{2o}(t)^*$;	$v(t) = v_{1o}(t) + v_{2e}(t)$
4	Fourier spectra	$u(t) \overset{F}{\Longleftrightarrow} U(\omega) = U_e(\omega) + j\, U_o(\omega)$; $U(\omega) = j\,\mathrm{sgn}(\omega) V(\omega)$;	$v(t) \overset{F}{\Longleftrightarrow} V(\omega) = V_e(\omega) + jV_o(\omega)$ $V(\omega) = -j\,\mathrm{sgn}(\omega) U(\omega)$
	For even functions the Hilbert transform is odd:		
		$U_e(\omega) = 2\int_0^{\infty} u_{1e}(t)\cos(\omega t)\, dt$	$v_o(t) = 2\int_0^{\infty} U_e(\omega)\sin(\omega t)\, df$
	For odd functions the Hilbert transform is even:		
		$U_o(\omega) = -2\int_0^{\infty} u_{2o}(t)\sin(\omega t)\, dt$	$v_e(t) = 2\int_0^{\infty} U_o(\omega)\cos(\omega t)\, df$
5	linearity	$au_1(t) + bu_2(t)$	$av_1(t) + bv_2(t)$
6	scaling and time reversal	$u(at)$; $a > 0$ $u(-at)$	$v(at)$ $-v(-at)$
7	time shift	$u(t - a)$	$v(t - a)$
8	scaling and time shift	$u(bt - a)$	$v(bt - a)$
			Fourier image
9	iteration	$H[u(t)] = v(t)$	$-j\,\mathrm{sgn}(\omega) U(\omega)$
		$H[H[u]] = -u(t)$	$[-j\,\mathrm{sgn}(\omega)]^2\ U(\omega)$
		$H[H[H[u]] = -v(t)$	$[-j\,\mathrm{sgn}(\omega)]^3\ U(\omega)$
		$H[H[H[Hu]]]] = u(t)$	$[-j\,\mathrm{sgn}(\omega)]^4\ U(\omega)$
10	time derivatives	First option	
		$\dot{u}(t) = \frac{-1}{\pi t} * \dot{v}(t)$	$\dot{v}(t) = \frac{1}{\pi t} * \dot{u}(t)$
		Second option	
		$\dot{u}(t) = \left[\frac{d}{dt}(-1/\pi t)\right] * v(t)$	$\dot{v}(t) = \left[\frac{d}{dt}(1/\pi t)\right] * u(t)$
11	convolution	$u_1(t) * u_2(t) =$ $-v_1(t) * v_2(t)$	$u_1(t) * v_2(t) =$ $v_1(t) * u_2(t)$
12	autoconvolution equality	$\int u(\tau)u(t - \tau)\, d\tau = -\int v(\tau)v(t - \tau)\, d\tau$ for $\tau = 0$ energy equality	
13	multiplication by t	$tu(t)$	$tv(t) - \int_{-\infty}^{\infty} u(\tau)\, d\tau$
14	multiplication of signals with non-overlapping spectra	$u_1(t)$ (low pass signal)	$u_2(t)$ (high pass signals)
		$u_1(t)u_2(t)$	$u_1(t)v_2(t)$
15	analytic signal	$\psi(t) = u(t) + jH[u(t)]$	$H[\psi(t)] = -j\psi(t)$

*e = even; o = odd

TABLE 7.7.3 Properties of the Hilbert Transformation (Continued)

16	product of analytic signals	$\psi(t) = \psi_1(t)\psi_2(t)$	$H[\psi(t)] = \psi_1(t)H[\psi_2(t)] = H[\psi_1(t)]\psi_2(t)$
17	nonlinear transformations	$u(x)$	$v(x)$
17a	$x = \frac{c}{bt+a}$	$u_1(t) = u\left[\frac{c}{bt+a}\right]$	$v_1(t) = v\left[\frac{c}{bt+a}\right] - \frac{1}{\pi} P \int_{-\infty}^{\infty} \frac{u(t)}{t}\, dt$
17b	$x = a + \frac{b}{t}$	$u_1(t) = u\left[a + \frac{b}{t}\right]$	$v_1(t) = \frac{b}{a}\left\{v\left[a + \frac{b}{t}\right] - v(a)\right\}$
	Notice that the nonlinear transformation may change the signal $u(t)$ of finite energy to a signal $u_1(t)$ of infinite energy. P is the Cauchy Principal Value.		
18	Asymptotic value as $t \Rightarrow \infty$ for even functions of finite support: $u_e(t) = u_e(-t)$		$\lim_{t\Rightarrow\infty} \lvert v_o(t)\rvert = \frac{1}{\pi t}\int_S u_e(t)\, dt$[a]

[a] S is support of $u_e(t)$

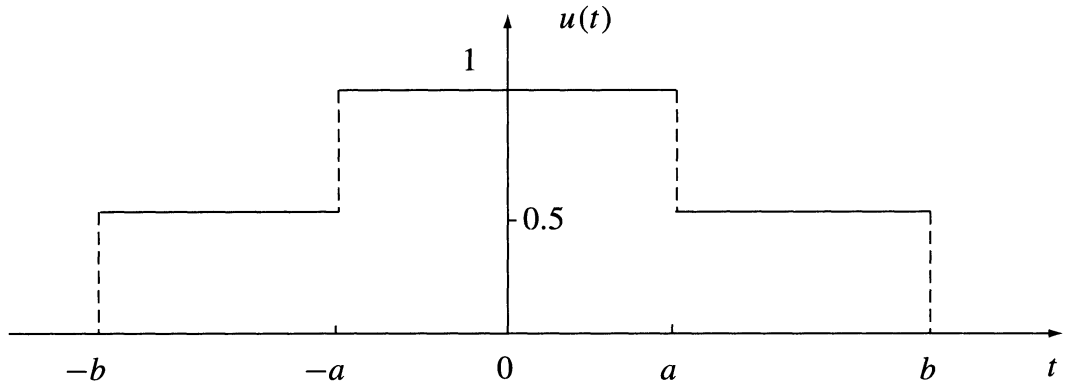

FIGURE 7.8.1a A pulse given by the summation of two square pulses $\Pi_a(t) + \Pi_b(t)$.

is translated to the n-time multiplication by the operator $-j\ \mathrm{sgn}(\omega)$. We have $(-j\ \mathrm{sgn}(\omega))^2 = -1$, $(-j\ \mathrm{sgn}(\omega))^3 = j\ \mathrm{sgn}(\omega)$ and $(-j\ \mathrm{sgn}(\omega))^4 = 1$. In analog or digital signal processing, the Hilbert transform is produced approximately and with a delay. The n-time iteration is implemented using a series connection of Hilbert filters (see Section 7.21) and the time delay increases n-times.

Autoconvolution and Energy Equality

The energy of a real signal $u(t) \overset{F}{\Longleftrightarrow} U(\omega)$ is given by the integrals

$$E_u = \int_{-\infty}^{\infty} u^2(t)dt = \int_{-\infty}^{\infty} \left|U(\omega)\right|^2 df; \quad \omega = 2\pi f \tag{7.8.3}$$

The above equality of the energy defined in the time domain and Fourier frequency domain is called **Parseval's theorem**. The squared magnitude of the Fourier image of the Hilbert transform $v(t) = H[u(t)]$ $\overset{F}{\Longleftrightarrow} V(\omega) = -j\ \mathrm{sgn}(\omega)U(\omega)$ is

$$|V(\omega)|^2 = |-j\ \mathrm{sgn}(\omega)\, U(\omega)|^2 = |U(\omega)|^2 \tag{7.8.4}$$

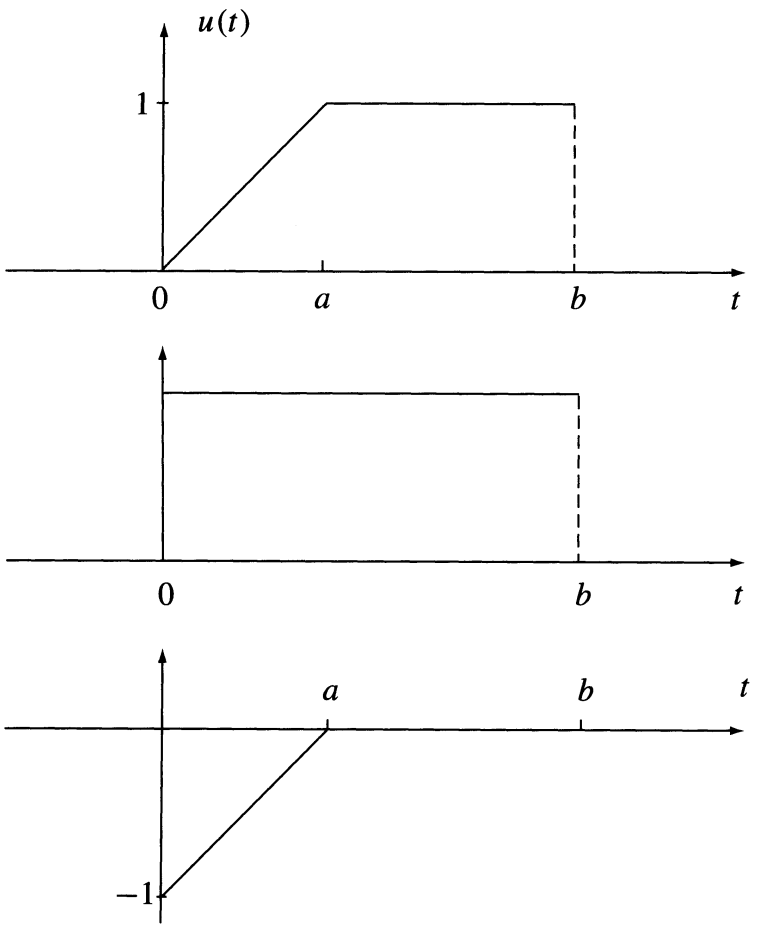

FIGURE 7.8.1b The "ramp" pulse and its decomposition in two pulses.

that is, the energy of the Hilbert transform is given by the integrals

$$E_v = \int_{-\infty}^{\infty} v^2(t)\,dt = \int_{-\infty}^{\infty} \left|U(\omega)\right|^2 df \tag{7.8.5}$$

Therefore, the energies E_u and E_v are equal. This property of a pair of Hilbert transforms may be used to check the algorithms of numerical evaluation of Hilbert transforms. A large discrepancy $\Delta E = E_v - E_u$ indicates a fault in the program. A small discrepancy may be used as a measure of the accuracy. Notice that the Hilbert transformation cancels the mean value of the signal. Therefore, the energy (or the power) of this term is rejected.

The signals forming a Hilbert pair are **orthogonal**; that is, the mutual energy defined by the integral

$$\int_{-\infty}^{\infty} u(t)v(t)\,dt = 0 \tag{7.8.6}$$

equals zero. The **autoconvolution** of the signal $u(t)$ is defined by the integral

$$\rho_{u-u}(t) = u(t) * u(t) = \int_{-\infty}^{\infty} u(t)u(t-\tau)\,d\tau \tag{7.8.7}$$

The autoconvolution equality theorem for a Hilbert pair of signals has the form:

$$\rho_{u-u}(t) = -\rho_{v-v}(t) \tag{7.8.8}$$

that is, the autoconvolutions of $u(t)$ and $v(t)$ have the same waveform and differ only by sign.

Proof

Let us apply the convolution to multiplication theorem of Fourier analysis to both sides of the equality (7.8.8). We get the Fourier pairs

$$\rho_{u-u}(t) = u(t) * u(t) \overset{F}{\Longleftrightarrow} U^2(\omega) \tag{7.8.9}$$

$$\rho_{v-v}(t) = v(t) * v(t) \overset{F}{\Longleftrightarrow} \left[-j\,\mathrm{sgn}(\omega)U(\omega)\right]^2 = -U^2(\omega) \tag{7.8.10}$$

We have shown that the functions $\rho_{u-u}(t)$ and $-\rho_{v-v}(t)$ have the same waveforms because they have equal Fourier transforms.

Examples

1. It is really amazing to observe the result of calculation of the autoconvolutions of some Hilbert pairs. Consider the Hilbert pair $\delta(t) \overset{H}{\Longleftrightarrow} \dfrac{1}{\pi t}$. Because the autoconvolution of the delta pulse is $\delta(t) = \delta(t) * \delta(t)$ (see Section 7.5), the autoconvolution equality yields the surprising result

$$\delta(t) = -\frac{1}{\pi t} * \frac{1}{\pi t} \tag{7.8.11}$$

that is, the autoconvolution of the function (distribution) $\dfrac{1}{\pi t}$ of infinite support yields the delta pulse of a point support. Figure 7.8.2 shows the result of a numerical approximate calculation of the autoconvolution (7.8.11).

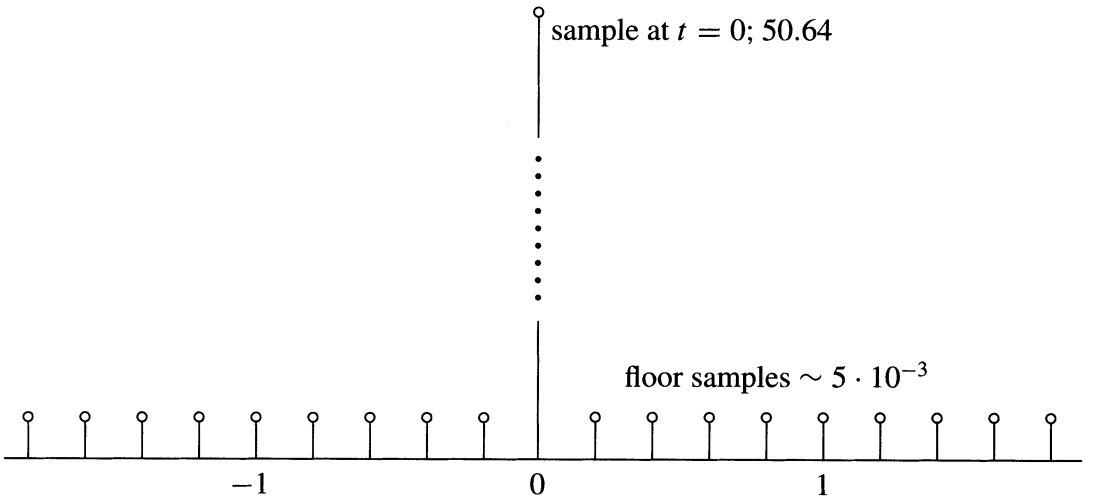

FIGURE 7.8.2 The discrete delta pulse obtained by numerical computing of the autoconvolution $-1/(\pi t) * 1/(\pi t)$.

2. Consider the square pulse and its Hilbert transform

$$\Pi_a(t) \overset{\mathrm{H}}{\Longleftrightarrow} \frac{1}{\pi}\ln\left|\frac{t+a}{t-a}\right| \tag{7.8.12}$$

The waveforms are shown in Figure 7.4.1. The autoconvolution of the square pulse is a tri(t) (triangle) pulse of doubled support (Figure 7.8.3a). Again, the autoconvolution of the logarithmic function of infinite support defined by Equation (7.8.12), which has infinite peaks at points $|t| = a$, yields the triangle pulse of finite support. Indeed, we have

$$tri(t) = -\frac{1}{\pi^2}\left\{\ln\left|\frac{t+a}{t-a}\right| * \ln\left|\frac{t+a}{t-a}\right|\right\} \tag{7.8.13}$$

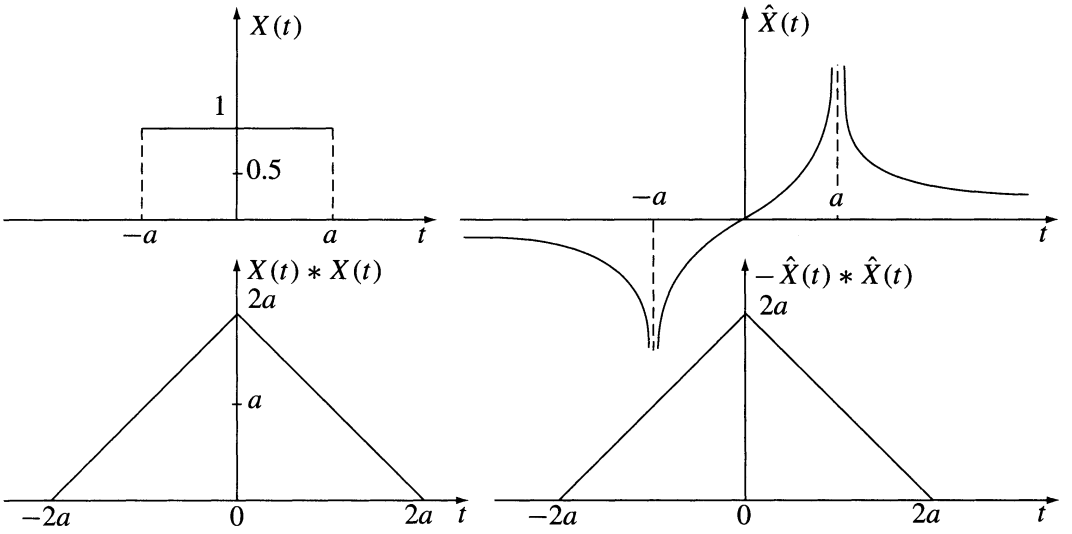

FIGURE 7.8.3a An example of the autoconvolution equality: (left) the square pulse and its autoconvolution; (right) the Hilbert transform of the square pulse and its autoconvolution.

Figure 7.8.3b shows the result of a numerical evaluation of the above autoconvolution.

7.9 Differentiation of Hilbert Pairs

Consider a Hilbert pair $u(t) \overset{\mathrm{H}}{\Longleftrightarrow} v(t)$. Differentiation of both sides gives a new Hilbert pair:

$$\dot{u}(t) \overset{\mathrm{H}}{\Longleftrightarrow} \dot{v}(t) \tag{7.9.1}$$

Therefore, differentiation is a useful tool for creating new Hilbert pairs. Obviously, the operation can be repeated to get the next Hilbert pairs:

$$\frac{d^n u}{dt^n} \overset{\mathrm{H}}{\Longleftrightarrow} \frac{d^n v}{dt^n} \tag{7.9.2}$$

Because the signal $\psi(t) = u(t) + jv(t)$ is an analytic function, in principle all of its derivatives exist.[39]

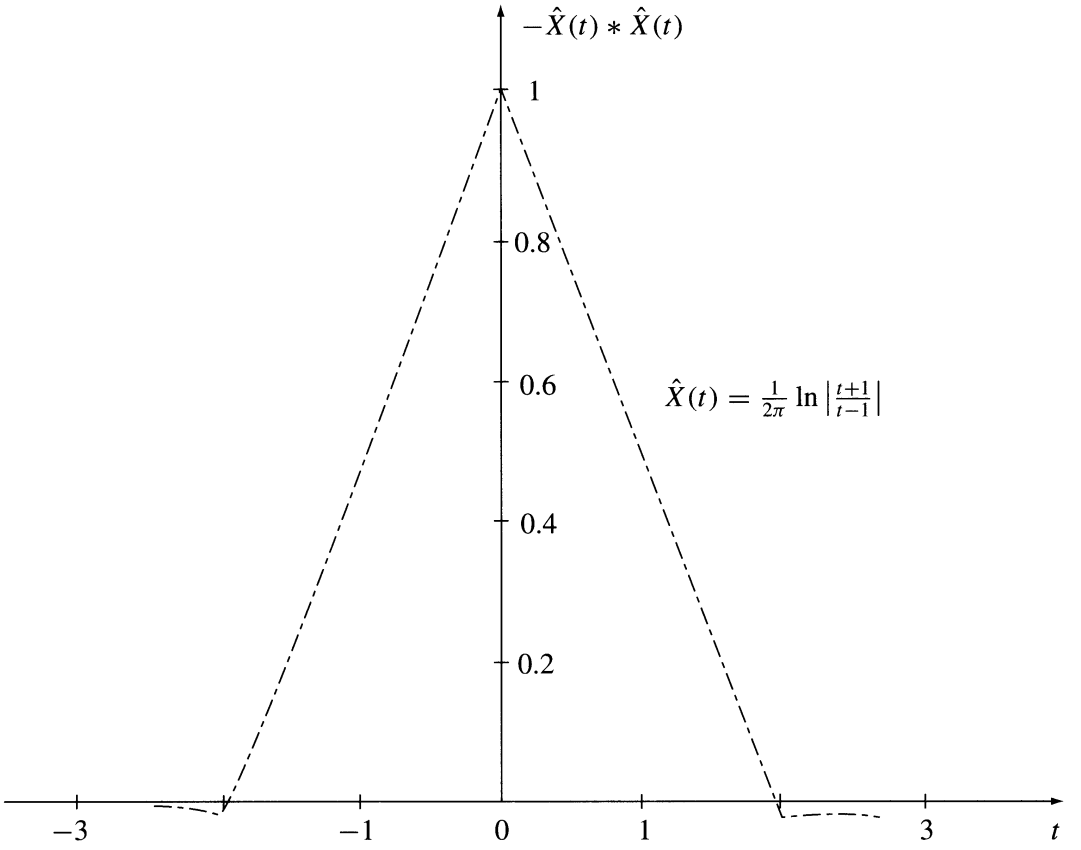

FIGURE 7.8.3b The result of numerical computing of the autoconvolution of the Hilbert transform.

Consider the convolution notation of the Hilbert transformations:

$$u(t) = \frac{-1}{\pi t} * v(t) \overset{\text{H}}{\Longleftrightarrow} v(t) = \frac{1}{\pi t} * u(t) \tag{7.9.3}$$

The derivative of a convolution has **two options**: the convolution of the derivative of the first term with the second term, or the convolution of the first term with the derivative of the second term; i.e., the **first option** has the form

$$\begin{aligned} \dot{u}(t) &= \frac{d}{dt}\left(t/\pi t\right) * v(t) \overset{\text{H}}{\Longleftrightarrow} \dot{v}(t) = \frac{d}{dt}\left(t/\pi t\right) * u(t) \\ &= \left[1/\left(\pi t^2\right)\right] * v(t) \overset{H}{\Longleftrightarrow} \left[-1/\left(\pi t^2\right)\right] * u(t) \end{aligned} \tag{7.9.4}$$

and the **second option** is

$$\dot{u}(t) = -\frac{1}{\pi t} * \dot{v}(t) \overset{\text{H}}{\Longleftrightarrow} \dot{v}(t) = \frac{1}{\pi t} * \dot{u}(t) \tag{7.9.5}$$

Proof

The Hilbert integrals (7.1.1) and (7.1.2) are

$$v(t) = \frac{-1}{\pi} P\int_{-\infty}^{\infty} \frac{u(\eta)}{\eta - t} d\eta; \quad u(t) = \frac{1}{\pi} P\int_{-\infty}^{\infty} \frac{v(\eta)}{\eta - t} d\eta \tag{7.9.6}$$

The differentiation of these integrals with respect to t yields

$$\dot{v}(t) = \frac{1}{\pi} P\int_{-\infty}^{\infty} \frac{u(\eta)}{(\eta - t)^2} d\eta; \quad \dot{u}(t) = \frac{-1}{\pi} P\int_{-\infty}^{\infty} \frac{v(\eta)}{(\eta - t)^2} d\eta \tag{7.9.7}$$

These integrals have in the convolution notation the form (7.9.4). The change of variable $y = \eta - t$ yields the following form of the Hilbert integrals:

$$v(t) = \frac{-1}{\pi} P\int_{-\infty}^{\infty} \frac{u(y+t)}{y} dy; \quad u(t) = \frac{1}{\pi} P\int_{-\infty}^{\infty} \frac{v(y+t)}{y} dy \tag{7.9.8}$$

and the differentiation yields

$$\dot{v}(t) = \frac{-1}{\pi} P\int_{-\infty}^{\infty} \frac{\dot{u}(y+t)}{y} dy; \quad \dot{u}(t) = \frac{1}{\pi} P\int_{-\infty}^{\infty} \frac{\dot{v}(y+t)}{y} dy \tag{7.9.9}$$

These integrals have in the convolution notation the form (7.9.5).

Very illustrative is the same proof in terms of the frequency domain representation:

$$v(t) = \frac{1}{\pi t} * u(t) \overset{F}{\Longleftrightarrow} -j\,\mathrm{sgn}(\omega) U(\omega) \tag{7.9.10}$$

Time domain differentiation corresponds to the multiplication of the Fourier image by the differentiation operator $j\omega$. Therefore,

$$\dot{v}(t) \overset{F}{\Longleftrightarrow} -j\omega\left[-j\,\mathrm{sgn}(\omega) U(\omega)\right] \tag{7.9.11}$$

However, the operator $j\omega$ may be arbitrarily assigned to the first or second factor of the product in parentheses. In the time domain, this arbitrary choice corresponds to the two options of the convolution.

Example 1

Consider the Hilbert pair

$$\delta(t) \overset{\mathrm{H}}{\Longleftrightarrow} \frac{1}{\pi t} \tag{7.9.12}$$

The derivatives are

$$\dot{\delta}(t) \overset{\mathrm{H}}{\Longleftrightarrow} \frac{d}{dt}(1/\pi t) = -\frac{1}{\pi t^2} \tag{7.9.13}$$

The derivative $\dot{\delta}(t)$ and, hence, the function $d/dt\ (1/\pi t)$ are defined in the distribution sense (notation FP $1/(\pi t^2)$, where FP denotes "finite part of").[35] The energy of these signals is infinite.

Example 2

Consider the Hilbert pair

$$u(t) = \frac{1}{1+t^2} \overset{\mathrm{H}}{\Longleftrightarrow} \frac{t}{1+t^2} = v(t) \tag{7.9.14}$$

Let us differentiate n-times both sides of this equation. In this way we find an infinite series of Hilbert transform pairs as shown in Table 7.9.1. The derivations are simpler by using the differentiation of the analytic signal

$$\psi(t) = u(t) + jv(t) = \frac{1}{1-jt} \tag{7.9.15}$$

and determining the real and imaginary parts of the derivatives in the form of Hilbert pairs.

TABLE 7.9.1 Hilbert Transforms of the Derivatives of the Cauchy Signal $u(t) = 1/(1 + t^2)$

n	Signal	Hilbert Transform	Analytic Signal	Energy
	$u^{(n)}$	$v^{(n)}$	$\psi^{(n)}$	
0	$\frac{1}{1+t^2}$	$\frac{t}{1+t^2}$	$\frac{1}{1-jt}$	$\frac{\pi}{2}$
1	$\frac{-2t}{(1+t^2)^2}$	$\frac{1-t^2}{(1+t^2)^2}$	$\frac{j}{(1-jt)^2}$	$\frac{\pi}{4}$
2	$2\frac{3t^2-1}{(1+t^2)^3}$	$2\frac{t^3-3t}{(1+t^2)^3}$	$\frac{-2}{(1-jt)^3}$	$\frac{3\pi}{4}$
3	$-6\frac{4t^3-4t}{(1+t^2)^4}$	$-6\frac{t^4-6t^2+1}{(1+t^2)^4}$	$\frac{-6j}{(1-jt)^4}$	$\frac{45}{8}\pi$
4	$24\frac{5t^4-10t^2+1}{(1+t^2)^5}$	$24\frac{t^5-10t^3+5t}{(1+t^2)^5}$	$\frac{24}{(1-jt)^5}$	$\frac{315}{4}\pi$
.....				
n		$\frac{(-j)^n n!}{(1-jt)^{n+1}}$	*)	

*) Energy $= \int_0^\infty \frac{n!dt}{(1+t^2)^{n+1}} = \frac{(n!)^2 1.3.5.\ldots.(2n-1)}{2.4.6.\ldots.2n}\frac{\pi}{2}$

The waveforms of the first four terms of the Hilbert pairs of Table 7.9.1 are shown in Figures 7.9.1a/b. The energy was normalized to unity by division of the amplitudes by the SQR of energy. The Cauchy pulse may serve as the function approximating the delta pulse (see Equation [7.5.10]). Therefore, the derivatives of the Cauchy-Hilbert pair may serve as the approximating functions defining the derivatives of the complex delta distribution. For example

$$\dot{\delta}(t) = \lim_{\alpha \Rightarrow 0}\left[\frac{1}{\pi}\frac{-2\alpha t}{\left(\alpha^2+t^2\right)^2}\right] \overset{\mathrm{H}}{\Longleftrightarrow} \dot{\Theta}(t) = \lim_{\alpha \Rightarrow 0}\left[\frac{1}{\pi}\frac{\alpha^2-t^2}{\left(\alpha^2+t^2\right)^2}\right] \tag{7.9.16}$$

(see Table 7.7.1, 42 to 46).

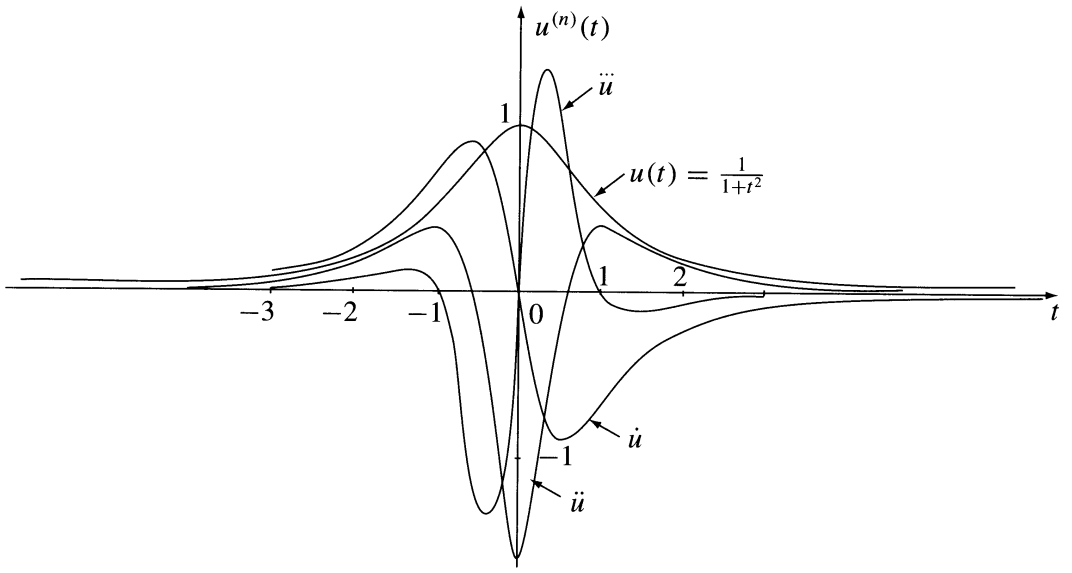

FIGURE 7.9.1a The waveforms of the Cauchy pulse and of its derivatives.

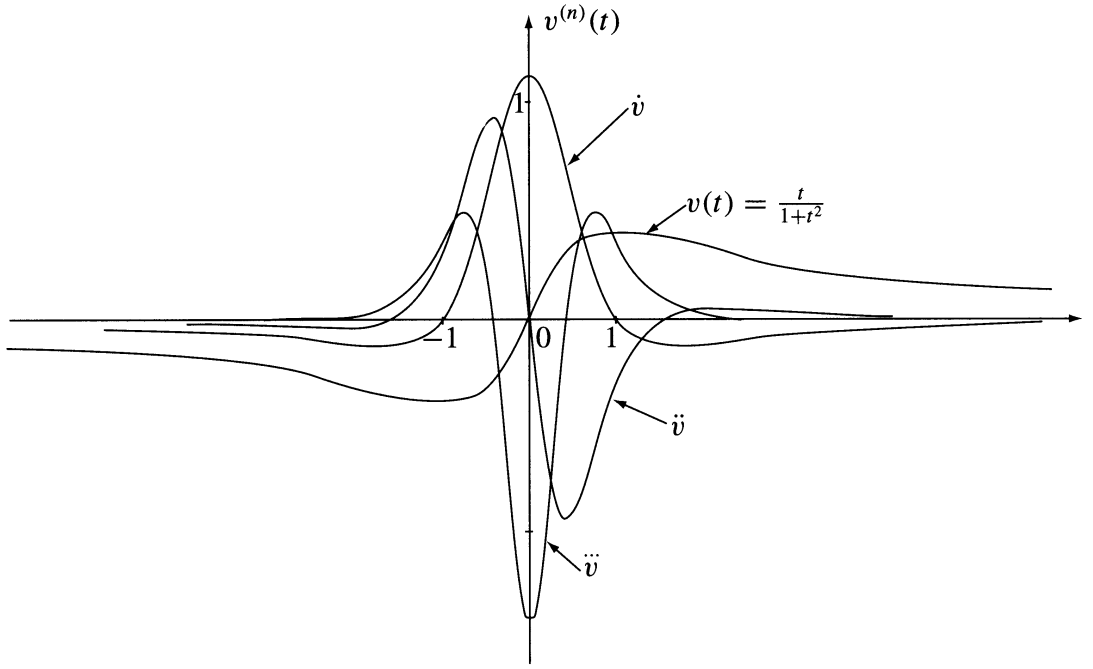

FIGURE 7.9.1b The waveforms of the corresponding Hilbert transforms.

7.10 Differentiation and Multiplication by t: Hilbert Transforms of Hermite Polynomials and Functions

Consider the Gaussian Fourier pair:

$$e^{-t^2} \overset{F}{\Longleftrightarrow} \pi^{0.5} e^{-\pi^2 f^2} \tag{7.10.1}$$

The successive differentiation of the Gaussian pulse $\exp(-t^2)$ generates the n-th order **Hermite polynomial** (see Table 7.10.1). The Hermite polynomials are defined by the formula (see also Chapter 1)

$$\mathrm{H}_n(t) = (-1)^n e^{t^2} \frac{d^n}{dt^n} e^{-t^2} \tag{7.10.2a}$$

$$n = 0, 1, 2, \ldots; \qquad t \in \pm\infty$$

(roman H is used to denote the Hermite polynomial in distinction from the italic H for the Hilbert transform). The Hermite polynomials are also defined by the recursion formula

$$\mathrm{H}_n(t) = 2t\,\mathrm{H}_{n-1}(t) - 2(n-1)\,\mathrm{H}_{n-2}(t); \qquad n = 1, 2, \ldots \tag{7.10.2b}$$

The first terms of the Hermite polynomials weighted by the generating function $\exp(-t^2)$ and their Hilbert transforms are listed in Table 7.10.1. The Hilbert transform of the first term was calculated using the frequency domain method represented by the Hilbert pair (see Table 7.7.1, the Hilbert transform of the Gaussian pulse)

TABLE 7.10.1 Weighted Hermite Polynomials and Their Hilbert Transforms

Notation: $u = \exp(-t^2)$

	Hermite Polynomial	Hilbert Transform	Energy
n	$\mathrm{H}_n u$	$H(\mathrm{H}_n u)$	E
0	$(1)u$	$2\sqrt{\pi}\int_0^\infty \exp(-\pi^2 f^2)\sin(\omega t)\,df$	$\sqrt{\pi/2}$
1	$(2t)u$	$-2\sqrt{\pi}\int_0^\infty \omega\exp(-\pi^2 f^2)\cos(\omega t)\,df$	$\sqrt{\pi/2}$
2	$(4t^2-2)u$	$-2\sqrt{\pi}\int_0^\infty \omega^2\exp(-\pi^2 f^2)\sin(\omega t)\,df$	$3\sqrt{\pi/2}$
3	$(8t^3-12t)u$	$2\sqrt{\pi}\int_0^\infty \omega^3\exp(-\pi^2 f^2)\cos(\omega t)\,df$	$15\sqrt{\pi/2}$
4	$(16t^4-48t^2+12)u$	$2\sqrt{\pi}\int_0^\infty \omega^4\exp(-\pi^2 f^2)\sin(\omega t)\,df$	$105\sqrt{\pi/2}$
5	$(32t^5-160t^3+120t)u$	$-2\sqrt{\pi}\int_0^\infty \omega^5\exp(-\pi^2 f^2)\cos(\omega t)\,df$	$945\sqrt{\pi/2}$
n	$\mathrm{H}_n u =$ $(-1)^n[2t\mathrm{H}_{n-1}(t) - 2(n-1)\mathrm{H}_{n-2}(t)$	$(-1)^n 2\sqrt{\pi}\int_0^\infty \omega^n\exp(-\pi^2 f^2)\sin(\omega t + n\pi/2)\,df$	

Energy $= \int_{-\infty}^{\infty} u^2\mathrm{H}_n^2\,dt = \int_{-\infty}^{\infty}[H(u\mathrm{H}_n)]^2\,dt = 1\times 3\times 5\times\cdots\times|2n-1|\times\sqrt{\pi/2}$

$$e^{-t^2} \overset{\mathrm{H}}{\Longleftrightarrow} 2\pi^{0.5}\int_0^\infty e^{-\pi^2 f^2}\sin(\omega t)\,df; \quad \omega = 2\pi f \tag{7.10.3}$$

The next terms are obtained by calculating the successive time derivatives of both sides of this Hilbert pair. For example, the second term is

$$2te^{-t^2} \overset{\mathrm{H}}{\Longleftrightarrow} -2\pi^{0.5}\int_0^\infty \omega e^{-\pi^2 f^2}\cos(\omega t)\,df \tag{7.10.4}$$

The value of the energy of successive terms is listed in the last column of Table 7.10.1. The waveforms are shown in Figure 7.10.1. Each Hilbert pair in Table 7.10.1 is a pair of orthogonal functions. However, the weighted Hermite polynomials do not form a set of orthogonal functions; that is, the integral of the product

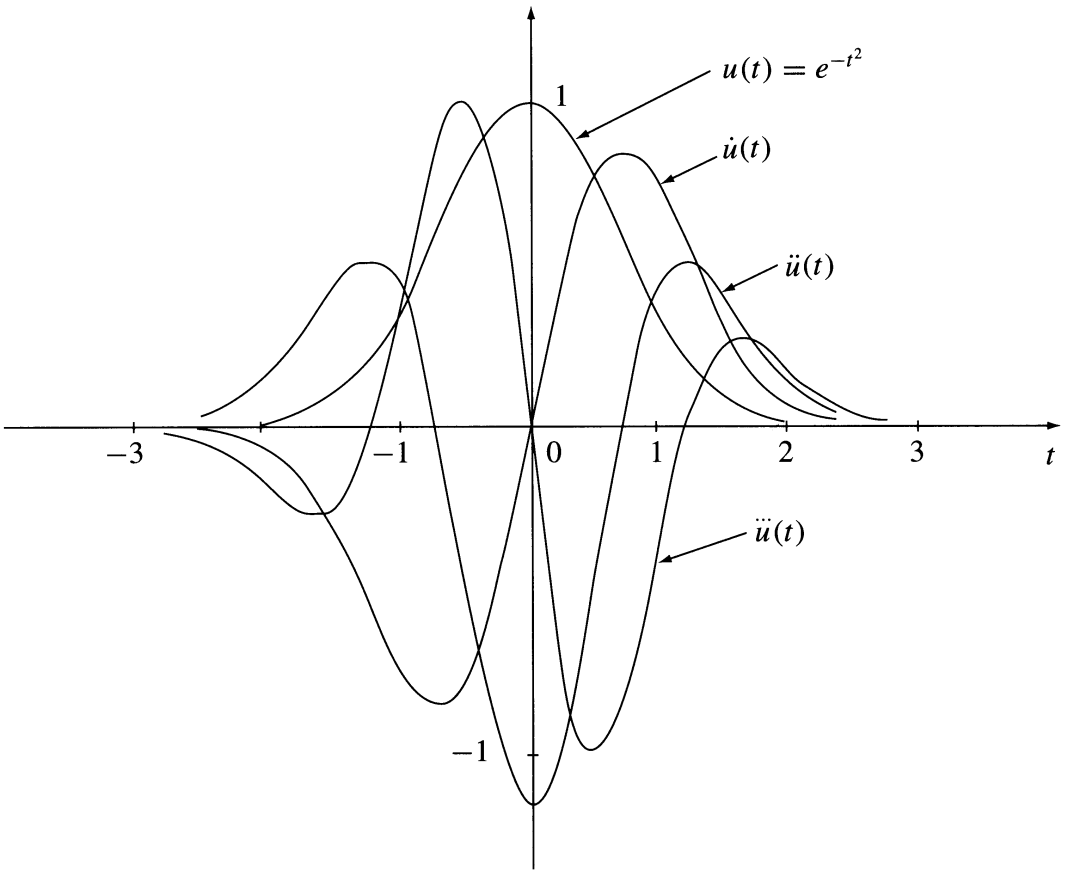

FIGURE 7.10.1a The waveforms of Hermite polynomials.

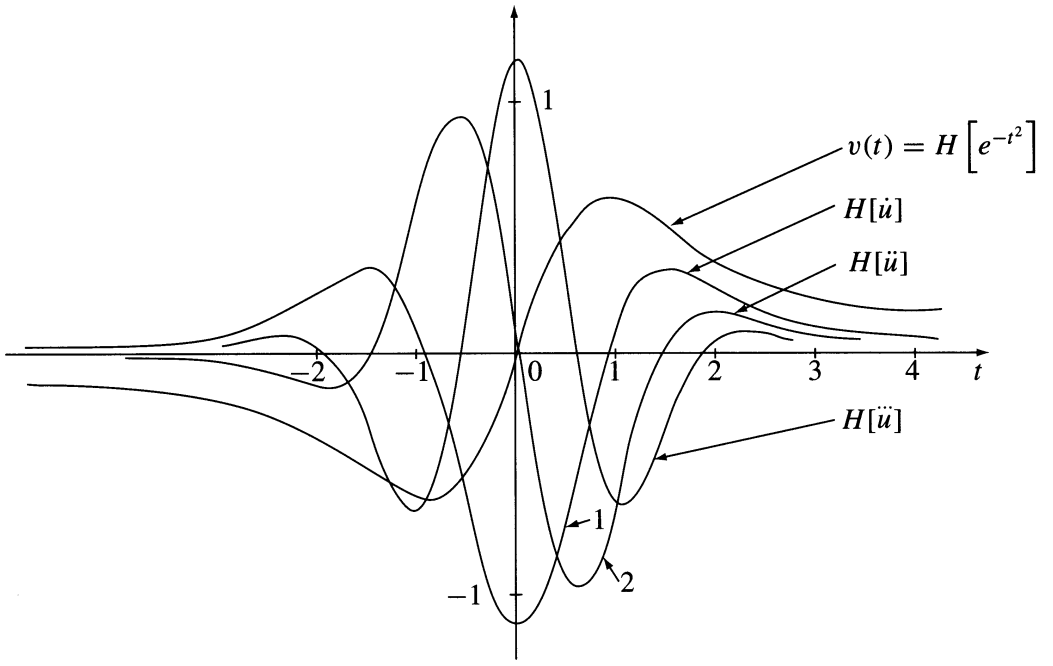

FIGURE 7.10.1b The waveforms of the corresponding Hilbert transforms.

$$\int_{-\infty}^{\infty} e^{-2t^2} H_n(t) H_m(t)\, dt \neq 0 \quad \text{for } n \neq m \tag{7.10.5}$$

differs from zero for $n \neq m$. The Hermite polynomials can be orthogonalized by replacing the weighting function $\exp(-t^2)$ by $\exp(-2t^2)$ because

$$\int_{-\infty}^{\infty} e^{-t^2} H_n(t) H_m(t) = \begin{cases} 0 & \text{for } n \neq m \\ 2^n n! \pi^{0.5} & \text{for } n = m \end{cases} \tag{7.10.6}$$

Therefore, the functions denoted by small italic $h(t)$

$$h_n(t) = \left(2^n n!\right)^{-0.5} \pi^{-0.25} e^{-t^2/2} H_n(t); \quad n = 0, 1\ldots \tag{7.10.7}$$

are forming an orthonormal (energy is equal unity) set of functions called **Hermite functions**. Let us derive the Hilbert transforms of the Hermite functions. Combining the Equations (7.10.2) and (7.10.6) we get the following recurrency:

$$h_n(t) = \left\{\frac{2(n-1)!}{n!}\right\}^{0.5} t h_{n-1}(t) - (n-1)\left\{\frac{(n-2)!}{n!}\right\}^{0.5} h_{n-2}(t) \tag{7.10.8}$$

The Hilbert transforms $H[h_n(t)]$ may be derived using the multiplication by t theorem (see Table 7.7.3):

$$tu(t) \overset{\mathrm{H}}{\Longleftrightarrow} tv(t) - \frac{1}{\pi}\int_{-\infty}^{\infty} u(\tau)\, d\tau \tag{7.10.9}$$

Proof

The formula (7.1.1) yields

$$H\left[tu(t)\right] = -\frac{1}{\pi}\int_{-\infty}^{\infty} \frac{\eta u(\eta)}{\eta - t} d\eta \tag{7.10.10}$$

The insertion of the new variable $y = \eta - t$ gives

$$\begin{aligned} H\left[tu(t)\right] &= -\frac{1}{\pi}\int_{-\infty}^{\infty} \frac{(y+t)u(y+t)}{y} dy \\ &= -\frac{1}{\pi}\int_{-\infty}^{\infty} \frac{tu(y+t)}{y} dy - \frac{1}{\pi}\int_{-\infty}^{\infty} u(y+t) dy \\ &= t H\left[u(t)\right] - \frac{1}{\pi}\int_{-\infty}^{\infty} u(\tau)\, d\tau \end{aligned} \tag{7.10.11}$$

This is exactly the relation (7.10.9). The second term in this equation equals zero for odd functions $u(t)$. The first term in the recurrent formula (7.10.8) has the form of the product $th(t)$ enabling the application of Equation (7.10.9). Therefore, the Hilbert transforms of the Hermite functions $h_n(t)$ have the form:

$$H\left[h_n(t)\right] = \upsilon_n(t) = \left[\frac{2(n-1)!}{n!}\right]^{0.5}\left[t\upsilon_{n-1}(t) - \frac{1}{\pi}\int_{-\infty}^{\infty} u_{n-1}(\tau)d\tau\right] - (n-1)\left[\frac{(n-2)!}{n!}\right]^{0.5}\upsilon_{n-2}(t) \tag{7.10.12}$$

To derive the Hilbert transforms of Hermite functions, we have to derive by any method the first term $v_0(t)$ and then apply the above recurrency. Let us use the frequency domain method. The function $h_0(t)$ and its Fourier image are

$$h_0(t) = \pi^{-0.25}\exp\left(-t^2/2\right) \overset{F}{\Longleftrightarrow} (4\pi)^{0.25}\exp\left[-2(\pi f)^2\right] \tag{7.10.13}$$

By using Equation (7.4.12) we obtain:

$$H\left[h_0(t)\right] = \upsilon_0(t) = 2(4\pi)^{0.25}\int_0^{\infty} e^{-2\pi^2 f^2}\sin(\omega t)df \tag{7.10.14}$$

Introducing the abbreviated notation ($\omega = 2\pi f$)

$$b = \pi^{0.25}, \quad g(t) = \int_0^{\infty} e^{-2\pi^2 f^2}\sin(\omega t)df \tag{7.10.15}$$

we get the form of Equation (7.10.13) used in Table 7.10.2. The next terms υ_1, υ_2, … in this table are derived by using Equation (7.10.11). They are listed using two notations: the recurrent and nonrecurrent. The waveforms of the first four terms of the Hermite functions $h_n(t)$ and their Hilbert transforms are shown in Figures 7.10.2a/b.

7.11 Integration of Analytic Signals

Consider the analytic signal defined by Equation (7.2.15) as a complex function of a real variable t in the form

$$\psi(t) = u(t) + j\,v(t) \tag{7.11.1}$$

This function is integrable in the Riemann sense in the interval $[\alpha, \beta]$ if and only if the functions $u(t)$ and $v(t)$ are integrable; that is,

$$\Phi(t) = \int_{\alpha}^{t}\psi(t)dt = \int_{\substack{\alpha \\ \alpha\le t\le\beta}}^{t} u(t)dt + j\int_{\alpha}^{t}\upsilon(t)dt \tag{7.11.2}$$

Let us define

$$\Phi(t) = U(t) + jV(t) \tag{7.11.3}$$

The functions $U(t)$ and $V(t)$ are forming a Hilbert pair only if $\Phi(z)$ is an analytic function of a complex variable $z = t + j\tau$. Therefore, let us give without a proof the following theorem:

If the function $\psi(z) = u(t, \tau) + j\,v(t, \tau)$ is analytic in a simply connected domain **D**, then the function

TABLE 7.10.2 Hilbert Transforms of Orthonormal Hermite Functions (Energy = 1).

Notations: $h_0(t), h_1(t), \ldots \Rightarrow h_0, h_1, \ldots$; $\quad v_0(t), v_1(t), \ldots \Rightarrow v_0, v_1, \ldots$

$g(t) = \int_0^\infty e^{-2\pi^2 f^2} \sin(2\pi f t)\, df$; $\quad a = \pi^{-0.25} e^{-t^2/2}$; $\quad b = \pi^{0.25}$

Hermite Functions $h_n(t)$	Hilbert Transforms $v_n(t)$
Recurrent Notation	
$h_0 = a$	$v_0 = 2\sqrt{2}bg(t)$
$h_1 = \sqrt{2}th_0$	$v_1 = \sqrt{2}\left[tv_0 \frac{\sqrt{2}b}{\pi}\right]$
$h_2 = th_1 - \sqrt{1/2}h_0$	$v_2 = tv_1 - \sqrt{1/2}v_0$
$h_3 = \sqrt{2/3}\,[th_2 - h_1]$	$v_3 = \sqrt{2/3}\left[tv_2 - \frac{b}{\pi} - v_1\right]$
$h_4 = \sqrt{1/2}th_3 - \sqrt{3/4}h_2$	$v_4 = \sqrt{1/2}tv_3 - \sqrt{3/4}v_2$
$h_5 = \sqrt{2/5}th_4 - \sqrt{4/5}h_3$	$v_5 = \sqrt{2/5}\left[tv_4 - \frac{\sqrt{3}b}{2\pi}\right] - \sqrt{4/5}v_3$
.....	.....
$h_n = \sqrt{\frac{2(n-1)!}{n!}}th_{n-1} +$	$v_n = \sqrt{\frac{2(n-1)!}{n!}}[tv_{n-1} +$
$(n-1)\sqrt{\frac{(n-2)!}{n!}}h_{n-2}$	$-\frac{1}{\pi}\int h_{n-1}(\tau)\,d\tau\ ] - (n-1)\sqrt{\frac{(n-2)!}{n!}}v_{n-2}$
Nonrecurrent Notation	
$h_0 = a1$	$2\sqrt{2}bg(t)$
$h_1 = \sqrt{2}at$	$2b\left[2\,tg(t) - \pi^{-1}\right]$
$h_2 = \frac{a}{\sqrt{8}}\left(4t^2 - 2\right)$	$2b\left[\left(2t^2 - 1\right)g(t) - t\pi^{-1}\right]$
$h_3 = \frac{a}{\sqrt{48}}(8t^3 - 12t)$	$\sqrt{8/3}b\left[\left(2t^3 - 3t\right)g(t) - \frac{t^2}{\pi} + \frac{1}{2\pi}\right]$
$h_4 = \frac{a}{\sqrt{384}}\left(16t^4 - 48t^2 + 12\right)$	$\sqrt{4/3}b\left[\left(2t^4 - 6t^2 + 1.5\right)g(t) - \frac{t^3}{\pi} + \frac{2t}{\pi}\right]$
$h_5 = \frac{a}{\sqrt{3840}}\left(32t^5 - 160t^3 + 120t\right)$	$\sqrt{8/15}b\left[\left(2t^5 - 10t^3 + 7.5t\right)g(t) + -\frac{(t^4 - 4t^2) + 1.75}{\pi}\right]$
.....	.....

$h_n(t) = \frac{a}{\sqrt{2^n n!}}H_n(t)$,

$$H_n(t) = 2tH_{n-1}(t) - 2(n-1)H_{n-2}(t)$$

n	0	1	2	3	4	5	...
$\int_{-\infty}^{\infty} h_n(\tau)\,d\tau$	$\sqrt{2}b$	0	b	0	$\sqrt{3/4}b$	0	...

$$\Phi(z) = \int_{z_0}^{z} \psi(z)dz \tag{7.11.4}$$

is also analytic, and the derivative $\Phi'(z) = \psi(z)$. The integral (7.11.4) is defined as a path integral in the plane (t, τ), and in the domain **D** the integral depends on z and z_0 but not on the particular path Γ connecting them (Figure 7.11.1).[39]

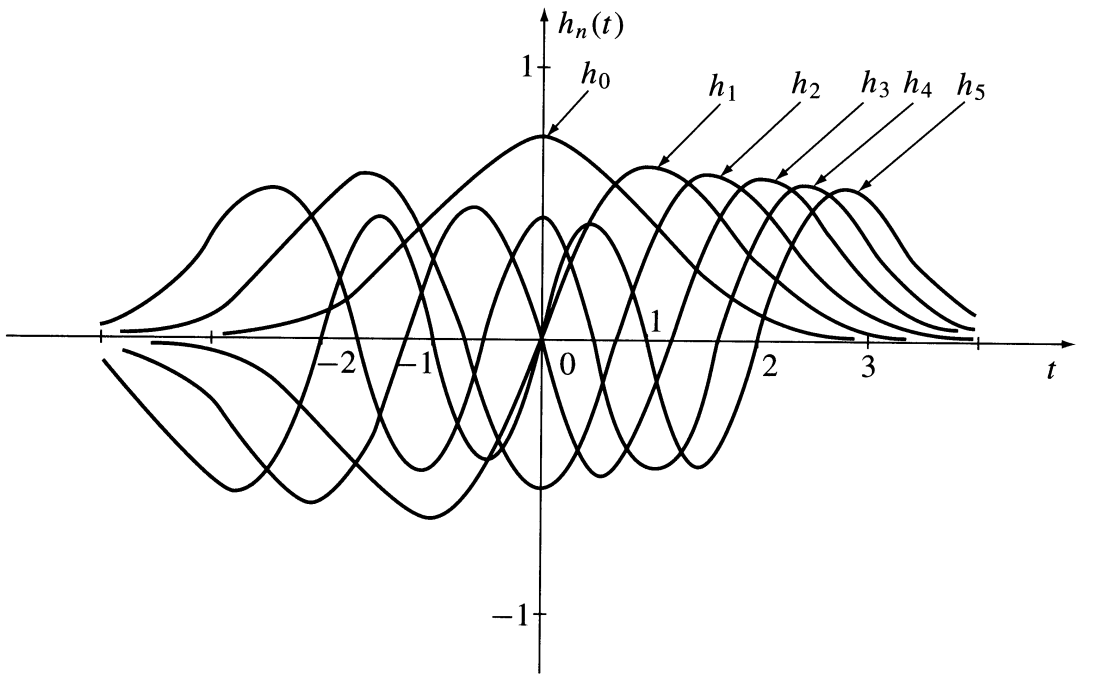

FIGURE 7.10.2a Waveforms of Hermite functions.

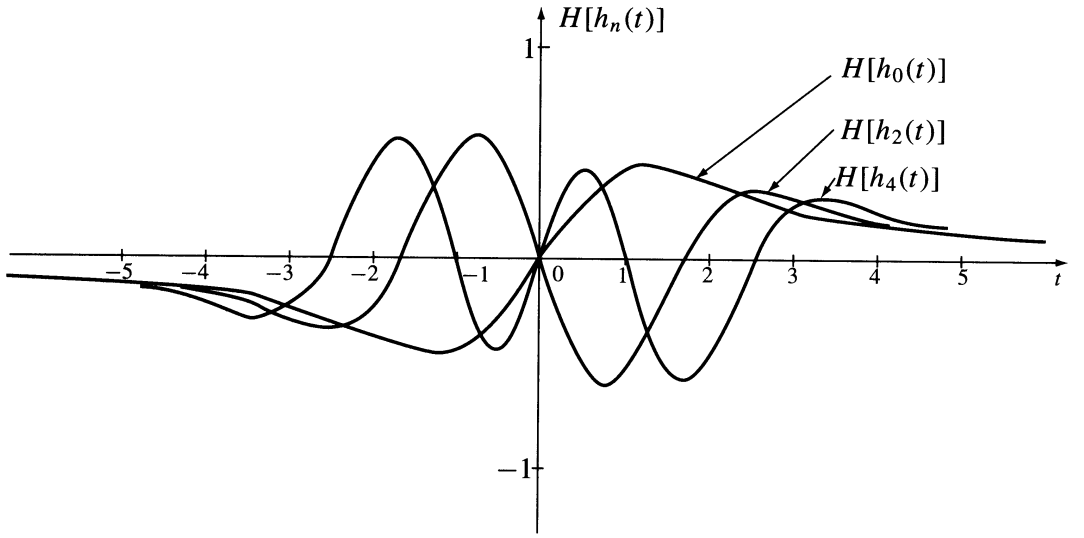

FIGURE 7.10.2b Waveforms of the corresponding Hermite transforms.

If function (7.11.1) is continuous in the interval $[\alpha, \beta]$, then the function defined by the integral

$$\Phi(t) = \int_{\alpha}^{t} \psi(t)dt; \quad \alpha \le t \le \beta \tag{7.11.5}$$

is called the primary function, or antiderivative of $\psi(t)$, and has in the interval $[\alpha, \beta]$ a continuous derivative $\Phi'(t) = \psi(t)$ and the relation holds

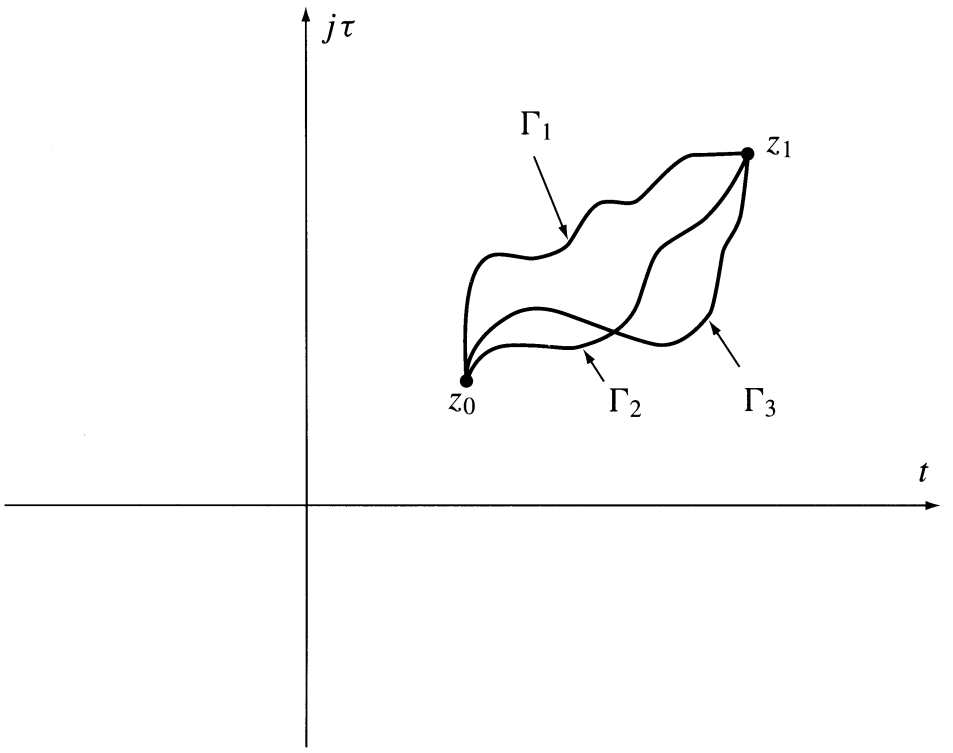

FIGURE 7.11.1 Passes of integration in the complex plane $(t, j\tau)$.

$$\int_{\alpha}^{\beta} \psi(t)dt = \Phi(t)\Big|_{\alpha}^{\beta} = \Phi(\beta) - \Phi(\alpha) \tag{7.11.6}$$

Example

The function e^{jt} has in the interval $(-\infty, \infty)$ the primary function $e^{jt}/j + c$, where c is any complex constant. We have

$$\int_{0}^{\pi/2} e^{jt}dt = \frac{e^{jt}}{j}\Big|_{0}^{\pi/2} = \frac{e^{\pi j/2} - 1}{j} = 1 + j$$

If the analytic function has a representation in the form of a power series:

$$\psi(z) = \sum_{n=0}^{\infty} d_n (z - z_0)^n \tag{7.11.7}$$

its integral must have a power series in the form:

$$\Phi(z) = a + \sum_{n=0}^{\infty} \frac{d_n}{n+1} (z - z_0)^{n+1} \tag{7.11.8}$$

This means that the power series representation can be integrated term-by-term.

Integration in the time domain can be converted by using the Fourier transforms into integration in the frequency domain. For instance, the function $u(t)$ can be integrated using the Fourier pairs

$$u(t) \overset{F}{\Longleftrightarrow} U(\omega) \tag{7.11.9}$$

$$\int_{-\infty}^{t} u(t)dt \overset{F}{\Longleftrightarrow} U(\omega)\left[\frac{\delta(f)}{2} + \frac{1}{j\omega}\right] \tag{7.11.10}$$

$$\omega = 2\pi f$$

The term $[\delta(f)/2]\ U(\omega)$ is equal to $(1/2)\ U(0)$ and the term $1/j\,\omega$ is the well-known integration operator. The same algorithm may be used to integrate the Hilbert transform $v(t)$.

Example

Consider the analytic function of the complex variable $z = t + j\tau$

$$\psi(z) = \frac{1}{\pi}\frac{1}{\alpha - jz} = \frac{1}{\pi}\frac{1}{\alpha + \tau - jt} \tag{7.11.11}$$

where α is a real constant ($\alpha > 0$). We get

$$\psi(z) = \psi(t, \tau) = u(t, \tau) + j\ v(t, \tau) \tag{7.11.12}$$

where

$$u(t, \tau) = \frac{1}{\pi}\frac{\alpha + \tau}{(\alpha + \tau)^2 + t^2} \tag{7.11.13}$$

and

$$v(t, \tau) = \frac{1}{\pi}\frac{t}{(\alpha + \tau)^2 + t^2} \tag{7.11.14}$$

Let us integrate the function (7.11.11) in the interval $[-a, t]$ where $\alpha > 0$ is a real constant. Hence, we find

$$\Phi(z) = \int_{-a}^{t} \frac{1}{\pi}\frac{dz}{\alpha - jz} = \frac{j}{\pi}\mathrm{Ln}(\alpha - jz)\Big|_{-a}^{t} = \frac{j}{\pi}\mathrm{Ln}(\alpha + \tau - jt)\Big|_{-a}^{t} \tag{7.11.15}$$

The insertion of the limits of integration and change of coordinates from rectangular to polar yields

$$\Phi(t, \tau) = \frac{1}{\pi}\left[\tan^{-1}\left(\frac{t}{\alpha + \tau}\right) + \tan^{-1}\left(\frac{a}{\alpha + \tau}\right)\right] + \frac{j}{2\pi}\mathrm{Ln}\left[\frac{(\alpha + \tau)^2 + t^2}{(\alpha + \tau)^2 + a^2}\right] \tag{7.11.16}$$

Because $\arg(\alpha - jz)$ is only determined to within a constant multiple of 2π, the function $(1/\pi)\,\mathrm{Ln}(\alpha - jz)$ is not single valued (Notation Ln instead of ln). The prevent any winding of the integration path around $z = -j\alpha$, let us make a cut extending from the point $z = -j\alpha$ to infinity. Then $\Phi(z)$ is analytic in the remaining part of the z-plane and satisfies the Cauchy-Riemann equation (see also Appendix 1).

Example

Consider a signal represented by the product:

$$u(t) = \mathrm{sgn}(t)\Pi_a(t) \tag{7.11.17}$$

where $\Pi_a(t)$ is defined by Eq. (7.4.4) and $\mathrm{sgn}(t)$ by Eq. (7.1.11). We have the Fourier pair

$$0.5\,\mathrm{sgn}(t)\Pi_a(t) \overset{F}{\Longleftrightarrow} \frac{1-\cos(\omega a)}{j\omega} \tag{7.11.18}$$

The above Fourier spectrum is easy to derive by decomposing $u(t)$ into right-sided and reverse sign left-sided square pulses and adding the spectra of these pulses. In a similar way we can derive the Hilbert transform by adding the two Hilbert transforms defined by Equation (7.4.7). The resulting Hilbert pair is

$$0.5\,\mathrm{sgn}(t)\Pi_a(t) \overset{\mathrm{H}}{\Longleftrightarrow} \frac{1}{2\pi}\ln\left|\frac{t^2}{t^2-a^2}\right| \tag{7.11.19}$$

Let us integrate the signal $u(t)$ by frequency domain integration. We get the spectrum of the primary function using the operator $1/j\omega$:

$$U_p(\omega) = \frac{1}{j\omega}\frac{1-\cos(\omega a)}{j\omega} = \frac{-1+\cos(\omega a)}{\omega^2} \tag{7.11.20}$$

The primary function of $u(t)$ is the inverse Fourier transform of Equation (7.11.20) and has the form of a reverse signed triangle pulse.

$$-\frac{\alpha}{2}\mathrm{tri}(t) \overset{F}{\Longleftrightarrow} \frac{-1+\cos(\omega a)}{\omega^2} \tag{7.11.21}$$

The signal $\mathrm{tri}(t)$ is defined in Table 7.7.1 and its Hilbert transform is

$$-\frac{\alpha}{2}\mathrm{tri}(t) \overset{\mathrm{H}}{\Longleftrightarrow} \frac{1}{2\pi}\left\{a\ln\left|\frac{t-a}{t+a}\right| + \ln\left|\frac{t^2}{t^2-a^2}\right|\right\} \tag{7.11.22}$$

7.12 Multiplication of Signals with Nonoverlapping Spectra

Consider a signal of the form of the product

$$u(t) = f(t)\,g(t) \tag{7.12.1}$$

where $f(t)$ is a low-pass and $g(t)$ a high-pass signal. The Fourier spectra of these signals do not overlap; that is, if

$$f(t) \overset{F}{\Longleftrightarrow} F(\omega) \tag{7.12.2}$$

$$g(t) \overset{F}{\Longleftrightarrow} G(\omega) \tag{7.12.3}$$

then ($\omega = 2\pi f$)

$$|F(f)| = 0 \qquad \text{for } |f| > W \tag{7.12.4}$$

$$|G(f)| = 0 \qquad \text{for } |f| < W \tag{7.12.5}$$

as shown in Figure 7.12.1. In terms of Fourier methods, the Hilbert transform of the product $u(t) = f(t)g(t)$ may be derived using **the multiplication-convolution theorem** of the form (see also Chapter 2)

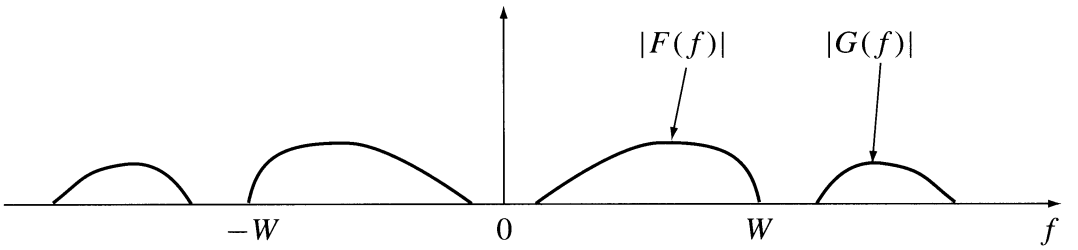

FIGURE 7.12.1 Nonoverlapping Fourier spectra of two signals.

$$f(t)g(t) \overset{F}{\Longleftrightarrow} \int_{-\infty}^{\infty} F(f-u)G(u)du \tag{7.12.6}$$

The multiplication of the spectrum by $-j\,\mathrm{sgn}(f)$ (see Equation (7.1.12)) yields the spectrum of the Hilbert transform

$$H\left[f(t)g(t)\right] \overset{F}{\Longleftrightarrow} -j\,\mathrm{sgn}(f)\int_{-\infty}^{\infty} F(f-u)G(u)du \tag{7.12.7}$$

However, the product $f(t)H[g(t)]$ and its Fourier transform are

$$f(t)H\left[g(t)\right] \overset{F}{\Longleftrightarrow} \int_{-\infty}^{\infty} F(f-u)\left[-j\,\mathrm{sgn}(u)G(u)\right]du \tag{7.12.8}$$

One can show[4] that the right-hand sides of (7.12.7) and (7.12.8) are identical. Therefore, the left-hand sides are identical too, and

$$H[f(t)g(t)] = f(t)H[g(t)] \tag{7.12.9}$$

This equation presents Bedrosian's theorem: Only the high-pass signal in the product of low-pass and high-pass signals gets Hilbert transformed.[4]

Example

Consider a signal in the form of the amplitude-modulated harmonic function:

$$u(t) = A(t)\cos(\Omega t + \Phi); \qquad \Omega = 2\pi F \tag{7.12.10}$$

$$A(t) \overset{F}{\Longleftrightarrow} C_A(f) \tag{7.12.11}$$

and the magnitude of $C_A(f)$ is low-pass limited:

$$|C_A(f)| = 0 \text{ for } f \geq F \tag{7.12.12}$$

By using Bedrosian's theorem, we get

$$v(t) = H[u(t)] = A(t)\sin(\Omega t + \Phi) \tag{7.12.13}$$

Therefore, the amplitude-modulated signal (7.12.10) is a real part of the analytic signal:

$$\Psi(t) = A(t)\, e^{j(\Omega t + \Phi)} \tag{7.12.14}$$

and has a geometrical representation in the form of a phasor of instantaneous amplitude $A(t)$ and rotating with a constant regular velocity Ω. Bedrosian's theorem was extended by Nuttal and Bedrosian[25] to include "frequency-translated" analytic signals. The condition, which applies to vanishing spectra at negative frequencies, can be applied more generally to signals whose Fourier spectra satisfy the condition

$$\begin{aligned} F(\omega) &= F[\Psi_1(t)] = 0, \quad \omega < -a \\ G(\omega) &= F[\Psi_2(t)] = 0, \quad \omega > a \end{aligned} \tag{7.12.15}$$

where a is an arbitrary positive constant. The extension of Bedrosian's theorem for multidimensional signals is given in Section 7.22.

7.13 Multiplication of Analytic Signals

The Hilbert transform of the analytic signal is given by the formula

$$H[\psi(t)] = H[u(t) + jH[u(t)]] = H[u(t)] - ju(t) = -j\psi(t) \tag{7.13.1}$$

where the formula $H[H[u(t)]] = -u(t)$ (iteration) (see Table 7.7.3) has been applied. The Hilbert transform of the product of two analytic signals is given by the formula

$$H[\psi_1(t)\psi_2(t)] = \psi_1(t)H[\psi_2(t)] = \psi_2(t)H[\psi_1(t)] \tag{7.13.2}$$

that is, the Hilbert transformation should be applied to **one term of the product only** (to the first or the second).

Proof

The product of two analytic functions is an analytic function.[39] Therefore, if

$$\psi(t) = \psi_1(t)\psi_2(t) \tag{7.13.3}$$

where $\psi_1(t)$ and $\psi_2(t)$ are analytic signals, then using Equation (7.13.1), we get:

$$H[\psi(t)] = -j\psi(t) = -j\psi_1(t)\psi_2(t) \tag{7.13.4}$$

However, the operator $-j$ may be assigned either to $\psi_1(t)$ or $\psi_2(t)$. The application of Equation (7.13.2) yields two options:

$$H[\psi\ (t)] = H[\psi_1(t)]\psi_2(t); \qquad H[\psi\ ] = \psi_1(t)H[\psi_2(t)] \tag{7.13.5}$$

Let us apply Equations (7.13.1) and (7.13.5) to find the Hilbert transforms of the n-th power of the analytic signal. We get

$$H[\psi^2(t)] = \psi\ (t)H[\psi\ (t)] = -j\psi^2(t) \tag{7.13.6}$$

$$H[\psi^n(t)] = \psi^{n-1}(t)H[\psi\ (t)] = -j\psi^n(t) \tag{7.13.7}$$

Example

Let us find the Hilbert transform of

$$\psi^2(t) = (1 - jt)^{-2} \tag{7.13.8}$$

The application of Equation (7.13.1) gives

$$H[\psi\ (t)] = -j(1 - jt)^{-1} \tag{7.13.9}$$

and Equation (7.13.6) yields

$$H[\psi^2(t)] = (1 - jt)^{-1}\ [-j(1 - jt)^{-1}] = -j(1 - jt)^{-2}$$

Equation (7.13.1) has a generalized form given by the formula

$$H[\psi\ (at)] = -j\ \mathrm{sgn}(a)\psi\ (at) \tag{7.13.10}$$

where a is a real positive or negative constant. The negative sign of a may be interpreted as time reversal. For example, the Hilbert transform of $\exp(j\omega t)$ is

$$H(e^{j\omega t}) = -j\ \mathrm{sgn}(\omega)\, e^{j\omega t}$$

where ω may be positive or negative.

7.14 Hilbert Transforms of Bessel Functions of the First Kind

The Bessel functions (see also Chapter 1) are the solution of the second order Bessel differential equation:

$$z^2\psi''(z) + z\psi'(z) + (z^2 - \lambda^2)\psi\ (z) = 0 \tag{7.14.1}$$

where $\psi(z)$ is a complex function of a complex variable $z = t + j\tau$ and λ is a complex constant. If $\lambda = n$, where n is an integer (0, 1, 2, …), and $z = t$, we get the solution in the form of Bessel functions of the first kind of the order n denoted $J_n(t)$. They find numerous applications in signal and system theory. For example, they are used to calculate the Fourier spectra of frequency modulated signals.

The substitution in Equation (7.14.1) of a solution in the form of a series $J_n(t) = \sum_{m=0}^{\infty} a_m t^m$ gives the power series representation

$$J_n\left(t\right) = \sum_{k=0}^{\infty} \frac{\left(-1\right)^k}{k!\left(n-k\right)!}\left(t/2\right)^{n+2k}; \quad -\infty < t < \infty \tag{7.14.2}$$

The computation of the Bessel functions by means of this power series is inconvenient. Due to the truncation of the series at some value of k, we get divergence for large values of t. It is possible to apply Equation (7.14.2) up to $t < t_1$ and calculate the values for $t > t_1$ using the asymptotic formula

$$J_n(t) = \frac{2}{\pi t}\sin\left(t - \frac{\pi n}{2} + \frac{\pi}{4}\right) + \frac{r(t)}{t\sqrt{t}} \tag{7.14.3}$$

The term $r(t)$ is a limited function for $t \Rightarrow \infty$. However, it is much **easier** to compute the Bessel functions and its Hilbert transforms using **integral forms**, as described below.

Let us start with the periodic complex function $\exp(jt\sin(\varphi))$ and its Hilbert transform. We have a Hilbert pair

$$e^{jt\sin(\varphi)} \overset{\mathrm{H}}{\Longleftrightarrow} H\left[e^{jt\sin(\varphi)}\right] = -j\,\mathrm{sgn}\left[\sin(\varphi)\right]e^{jt\sin(\varphi)} \tag{7.14.4}$$

The Fourier series expansion of the left-hand side is

$$e^{jt\sin(\varphi)} = \sum_{n=-\infty}^{\infty} J_n(t)e^{jn\varphi} \tag{7.14.5}$$

The Bessel functions, i.e., the coefficients of this series, are given by the integral:

$$J_n(t) = \frac{1}{2\pi}\int_{-\pi}^{\pi} e^{j\left(t\sin(\varphi) - n\varphi\right)}d\varphi \tag{7.14.6}$$

The odd-ordered Bessel functions are odd functions of the argument t, while the even-ordered are even functions and

$$J_{-n}(t) = (-1)^n J_n(t) \tag{7.14.7}$$

In fact, the integral of the imaginary part of Equation (7.14.6) equals zero, and due to the evenness of the real part of the integrand, we have

$$J_n(t) = \frac{1}{\pi}\int_0^{\pi} \cos\left[t\sin(\varphi) - n\varphi\right]d\varphi \tag{7.14.8}$$

This formula enables very efficient calculation of Bessel functions $J_n(t)$ using numerical integration. The number of integration steps may be halved using two separate integrals:

$$J_{2n}(t) = \frac{2}{\pi}\int_0^{\pi/2} \cos\left[t\sin(\varphi)\right]\cos(2n\varphi)d\varphi \tag{7.14.9}$$

$$J_{2n+1}(t) = \frac{2}{\pi}\int_0^{\pi 2} \sin\left[t\sin(\varphi)\right]\sin\left[(2n+1)\varphi\right]d\varphi \tag{7.14.10}$$

The real part of the Fourier series (7.14.5) is

$$\cos\left[t\sin(\varphi)\right] = J_0(t) + 2\sum_{n=1}^{\infty} J_{2n}(t)\cos(2n\varphi) \tag{7.14.11}$$

and the imaginary part is

$$\sin\left[t\sin(\varphi)\right] = 2\sum_{n=1}^{\infty} J_{2n-1}(t)\sin\left[(2n-1)\varphi\right] \tag{7.14.12}$$

Inserting $\varphi = \pi/2$ gives the well-known formulae:

$$\cos(t) = J_0(t) - 2J_2(t) + 2J_4(t) - \cdots \tag{7.14.13}$$

$$\sin(t) = 2J_1(t) - 2J_3(t) + \cdots \tag{7.14.14}$$

The following recursion formula is very useful

$$(2n/t)J_n(t) = J_{n-1}(t) + J_{n+1}(t) \tag{7.14.15}$$

The derivative of a Bessel function is also given by the recursion formula

$$2\dot{J}_n(t) = J_{n-1}(t) - J_{n+1}(t) \tag{7.14.16}$$

For example

$$\dot{J}_0(t) = 0.5\left[J_{-1}(t) - J_1(t)\right] = -J_1(t) \tag{7.14.17}$$

(we used Equation (7.14.7)).

The left-hand side of Equation (7.14.4) was expanded in the Fourier series (7.14.5). Similarly, due to the linearity of the Hilbert transformation, the right-hand side may be expanded in the Fourier series

$$H\left[e^{jt\sin\varphi}\right] = -j\,\mathrm{sgn}(\varphi)e^{jt\sin\varphi} = \sum_{n=-\infty}^{\infty} \hat{J}_n(t)e^{jn\varphi} \tag{7.14.18}$$

where $\hat{J}_n(t) = H[J_n(t)]$ are the Hilbert transforms of the Bessel functions. For these functions we have the relation

$$\hat{J}_{-n}(t) = (-1)^{n+1}\hat{J}_n(t) \tag{7.14.19}$$

because the Hilbert transforms of odd functions are even, and vice versa (compared with Equation [7.14.7]). The functions $\hat{J}_n(t)$, i.e., the coefficients of the Fourier series (7.14.18), are given by the integral

$$\hat{J}_n(t) = \frac{1}{2\pi}\int_{-\pi}^{\pi} H\left[e^{j\left[t\sin\varphi - n\varphi\right)}\right]d\varphi \tag{7.14.20}$$

As in Equation (7.14.6), the integral of the imaginary part equals zero and due to the evenness of the real part, we have

$$\hat{J}_n(t) = \frac{1}{\pi}\int_0^{\pi} \sin\left[t\sin\varphi - n\varphi\right]d\varphi \tag{7.14.21}$$

Notice that the integrand is even because it is multiplied by sgn(φ) (see Equation [7.14.18]). As before, using numerical integration, the Hilbert transforms of the Bessel functions can be easily computed. The first five Bessel functions and their Hilbert transforms computed using Equations (7.14.18) and (7.14.21) are shown in Figures 7.14.1a/b.

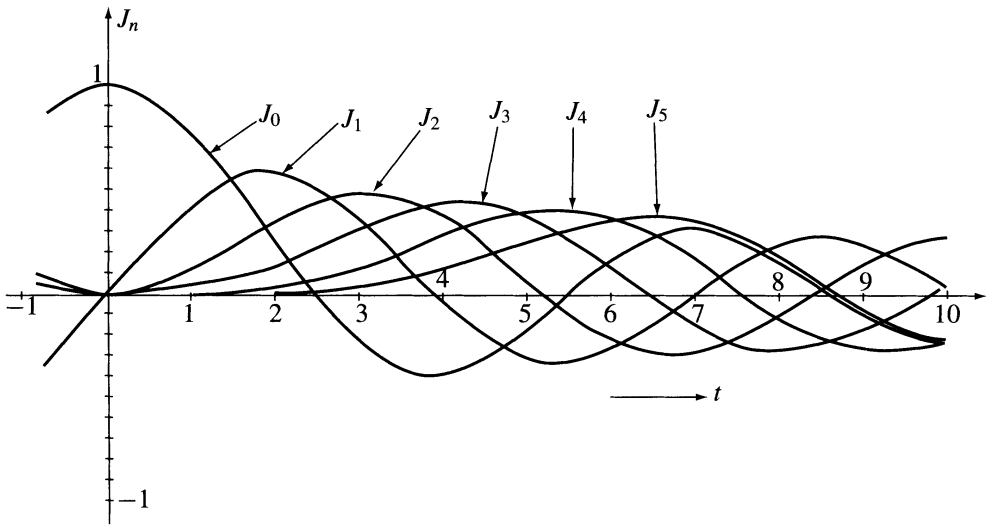

FIGURE 7.1.4.1a Waveforms of the first five Bessel functions $J_n(t)$.

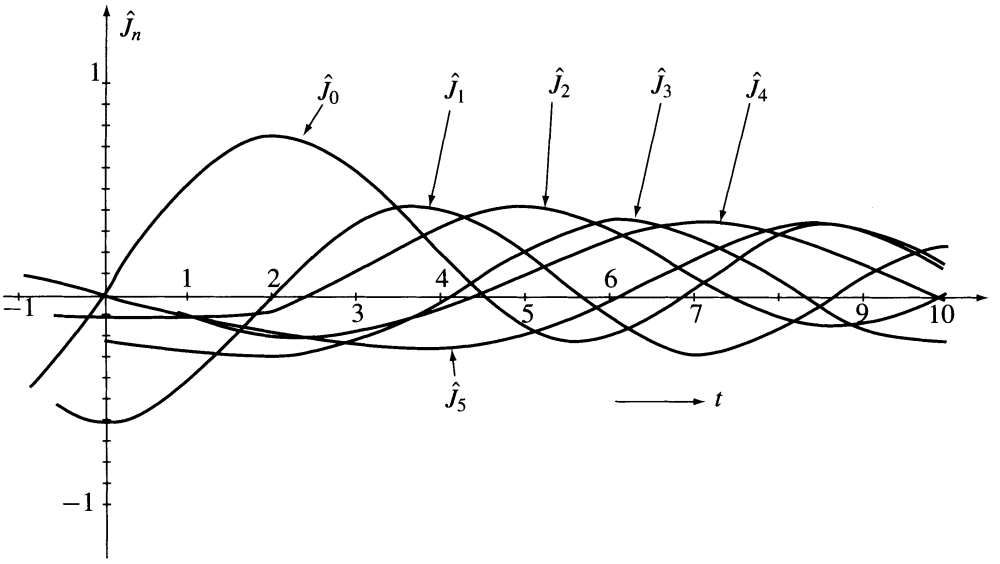

FIGURE 7.14.1b Waveforms of the corresponding Hilbert transforms.

Let us derive the Hilbert transforms of the Bessel functions $J_n(t)$ using Fourier transforms. The Fourier transform of the function $J_0(t)$ is

$$J_0(t) \overset{F}{\Longleftrightarrow} C_0(f) = \begin{cases} \dfrac{2}{\left(1-\omega^2\right)^{0.5}} & \text{for } |\omega| < 1 \\ 0 & \text{for } |\omega| > 1 \end{cases} \tag{7.14.22}$$

Proof

Let us find the inverse transform of this spectrum:

$$J_0(t) = \frac{1}{2\pi}\int_{-1}^{1} \frac{2}{\left(1-\omega^2\right)^{0.5}} \cos(\omega t)\, d\omega = \left\{ \begin{matrix} \omega = \sin(\varphi) \\ d\omega = \cos(\varphi)\, d\varphi \end{matrix} \right\} \tag{7.14.23}$$

$$= \frac{1}{\pi}\int_{0}^{\pi} \cos\left[t \sin\varphi\right] d\varphi$$

(See Equation [7.14.8].) The Fourier transforms of higher-order Bessel functions can be calculated using the recursion formula (7.14.16) and frequency domain differentiation. We have

$$J_{n+1}(t) = J_{n-1}(t) - 2\dot{J}_n(t) \tag{7.14.24}$$

obtaining the following Fourier parts

$$J_0(t) \overset{F}{\Longleftrightarrow} C_0(f) = \frac{2}{\left(1-\omega^2\right)^{0.5}} \tag{7.14.25}$$

$$J_1(t) = -\dot{J}_0(t) \overset{F}{\Longleftrightarrow} -j\omega C_0(f) \tag{7.14.26}$$

$$J_2(t) = -J_0(t) - 2\dot{J}_1(t) \overset{F}{\Longleftrightarrow} C_0(f) - 2j\omega C_1(f) \tag{7.14.27}$$

Successive application of the recurrency gives the Fourier spectra of the Bessel functions $J_n(t)$ tabulated in Table 7.14.1. We find that

$$\dot{J}_n(t) \overset{F}{\Longleftrightarrow} C_n(f) = (-j)^n 2^{n-1} T_n(t) C_0(f) \tag{7.14.28}$$

where $C_0(f)$ is defined by Equation (7.14.25) and $T_n(t)$ is a Tchebycheff polynomial defined by the formula

$$T_n(t) = \cos[n \cos^{-1}(t)]; \quad n = 0, 1, 2, \ldots \tag{7.14.29}$$

A recursion formula can be applied

$$T_{n+1}(t) - 2t\, T_n(t) + T_{n-1}(t) = 0; \quad n = 1, 2, \ldots \tag{7.14.30}$$

TABLE 7.14.1 Fourier and Hilbert Transforms of Bessel Functions of the First Kind

Bessel Function	Fourier Transform	Hilbert Transform
$J_n(t)$	$C_n(f)$	$\hat{J}_n(t) = H[J_n(t)]$
$J_0(t)$	$C_0 = \frac{2}{(1-\omega^2)^{0.5}}; \quad \lvert\omega\rvert < 1$ $= 0; \quad \lvert\omega\rvert > 0$	$\frac{1}{\pi}\int_0^1 C_0(f)\sin(\omega t)\,d\omega$
$J_1(t)$	$C_1 = -j\omega C_0$	$-\frac{1}{\pi}\int_0^1 \lvert C_1(f)\rvert\cos(\omega t)\,d\omega$
$J_2(t)$	$C_2 = -(2\omega^2 - 1)C_0$	$-\frac{1}{\pi}\int_0^1 \lvert C_2(f)\rvert\sin(\omega t)\,d\omega$
$J_3(t)$	$C_3 = j(4\omega^3 - 3\omega)C_0$	$\frac{1}{\pi}\int_0^1 \lvert C_3(f)\rvert\cos(\omega t)\,d\omega$
$J_4(t)$	$C_4 = (8\omega^4 - 8\omega^2 + 1)C_0$	$\frac{1}{\pi}\int_0^1 \lvert C_4(f)\rvert\sin(\omega t)\,d\omega$
$J_5(t)$	$C_5 = -j(16\omega^5 - 20\omega^3 + 5\omega)C_0$	$-\frac{1}{\pi}\int_0^1 \lvert C_5(f)\rvert\cos(\omega t)\,d\omega$
$J_6(t)$	$C_6 = -(32\omega^6 - 48\omega^4 + 18\omega^2 - 1)C_0$	$-\frac{1}{\pi}\int_0^1 \lvert C_6(f)\rvert\sin(\omega t)\,d\omega$
.....	.....	.....
$J_n(t)$	$C_n = (-j)^n 2^{n-1} T_n(\omega)C_0$	$\frac{(-1)^{n/2}}{\pi}\int_0^1 \lvert C_n(f)\rvert\sin(\omega t)\,d\omega$ for $n = 0, 2, 4, \ldots$ $\frac{(-1)^{(n+1)/2}}{\pi}\int_0^1 \lvert C_n(f)\rvert\cos(\omega t)\,d\omega$ for $n = 1, 3, 5, \ldots$

$T_n(\omega) = \cos[n\cos^{-1}(\omega)]$ is the Tchebycheff polynomial

Because we derived the analytical expressions for the Fourier images of the Bessel functions, the use of inverse Fourier transformations enables the evaluation of either the Bessel function $J_n(t)$ or its Hilbert transform $\hat{J}_n(t)$. For example

$$J_0(t) = \frac{1}{\pi}\int_0^1 \frac{2}{(1-\omega^2)^{0.5}}\cos(\omega t)\,d\omega \tag{7.14.31}$$

and the Hilbert transform is

$$\hat{J}_0(t) = H[J_0(t)] = \frac{1}{\pi}\int_0^1 \frac{2}{(1-\omega^2)^{0.5}}\sin(\omega t)\,d\omega \tag{7.14.32}$$

Hence, we have an analytic signal

$$\psi_0(t) = J_0(t) + j\hat{J}_0(t) \tag{7.14.33}$$

Equations (7.14.31) and (7.14.32) may be regarded as alternative definitions of the Bessel functions $J_0(t)$ and $\hat{J}_0(t)$. However, the computation by means of the integrals (7.14.8) and (7.14.9) ($n = 0$) gives much better accuracy with a given number of integration steps.

The expressions for the Fourier images of Bessel functions and their Hilbert transforms derived using these images are listed in Table 7.14.1. If needed, the Fourier spectra enable the derivation of the

coefficients of the power series representation of $J_n(t)$ and $\hat{J}_n(t)$. Starting with the power series for $J_n(t)$ given by Equation (7.14.2), let us derive the power series for $\hat{J}_n(t)$. We start with the expression defining the Taylor series

$$\hat{J}_n(t) = \sum_{n=0}^{\infty} \frac{\hat{J}_n^{(n)}(t=0)}{n!} t^n \tag{7.14.34}$$

The derivatives $\hat{J}_n^{(n)}(t)$ $(t = 0)$ can be obtained by differentiation of the integrand of the integrals listed in Table 7.14.1. By inserting $t = 0$, we obtain

$$\begin{aligned}
\hat{J}_0(0) &= \frac{1}{\pi}\int_0^1 \frac{2d\omega}{\left(1-\omega^2\right)^{0.5}} \sin(0) = 0 \\
\hat{J}_0^{(1)}(0) &= \frac{1}{\pi}\int_0^1 \frac{2\omega d\omega}{\left(1-\omega^2\right)^{0.5}} \cos(0) = \frac{2}{\pi} \\
\hat{J}_0^{(2)}(0) &= -\frac{1}{\pi}\int_0^1 \frac{2\omega^2 d\omega}{\left(1-\omega^2\right)^{0.5}} \sin(0) = 0 \\
\hat{J}_0^{(3)}(0) &= -\frac{1}{\pi}\int_0^1 \frac{2\omega^3 d\omega}{\left(1-\omega^2\right)^{0.5}} \cos(0) = \frac{-4}{3\pi}
\end{aligned} \tag{7.14.35}$$

where (1), (2), … denote the order of the derivative. Continuing the differentiation using Equation (7.14.34), we get the following power series:

$$\hat{J}_0(t) = \frac{2}{\pi}\left[t - \frac{1}{9}t^3 + \frac{1}{225}t^5 - \frac{2}{33075}t^7 + \cdots + \frac{(-1)^{(3+n)/2}\,2^{n-2}}{n!(1.3.5..n)}t^n + \cdots\right] \tag{7.14.36}$$

In the same way one can derive the power series of higher order Hilbert transforms of the Bessel functions.

7.15 Instantaneous Amplitude, Complex Phase, and Complex Frequency of Analytic Signals

Signal theory needs precise definitions of various quantities such as the **instantaneous amplitude**, instantaneous **phase**, and instantaneous **frequency** if a given signal and many other quantities. Let us recall that **neither definition is true or false**. If we define something, we simply propose to make an **agreement** to use a specific name in the sense of the definition. When using this name, for instance, "instantaneous frequency," we should never forget what we have defined. The history of signal theory contains examples of misunderstanding when various authors applied the same name — instantaneous frequency — to different definitions and then tried to discuss which is true or false. Such a discussion

in **meaningless**. Of course, one may discuss which definition has advantages or disadvantages from a specific point of view or whether it is compatible with other definitions or existing knowledge. The notions of the instantaneous amplitude, instantaneous phase, and instantaneous frequency of the analytic signal $\psi(t) = u(t) + j\upsilon(t)$ may be uniquely and conveniently defined introducing the notion of a phasor rotating in the Cartesian (u, υ) plane, as shown in Figure 7.15.1. The change of coordinates from rectangular (u, υ) to polar (A, φ) gives

$$u(t) = A(t)\cos[\varphi(t)] \tag{7.15.1}$$

$$\upsilon(t) = A(t)\sin[\varphi(t)] \tag{7.15.2}$$

$$\psi(t) = A(t)e^{j\varphi(t)} \tag{7.15.3}$$

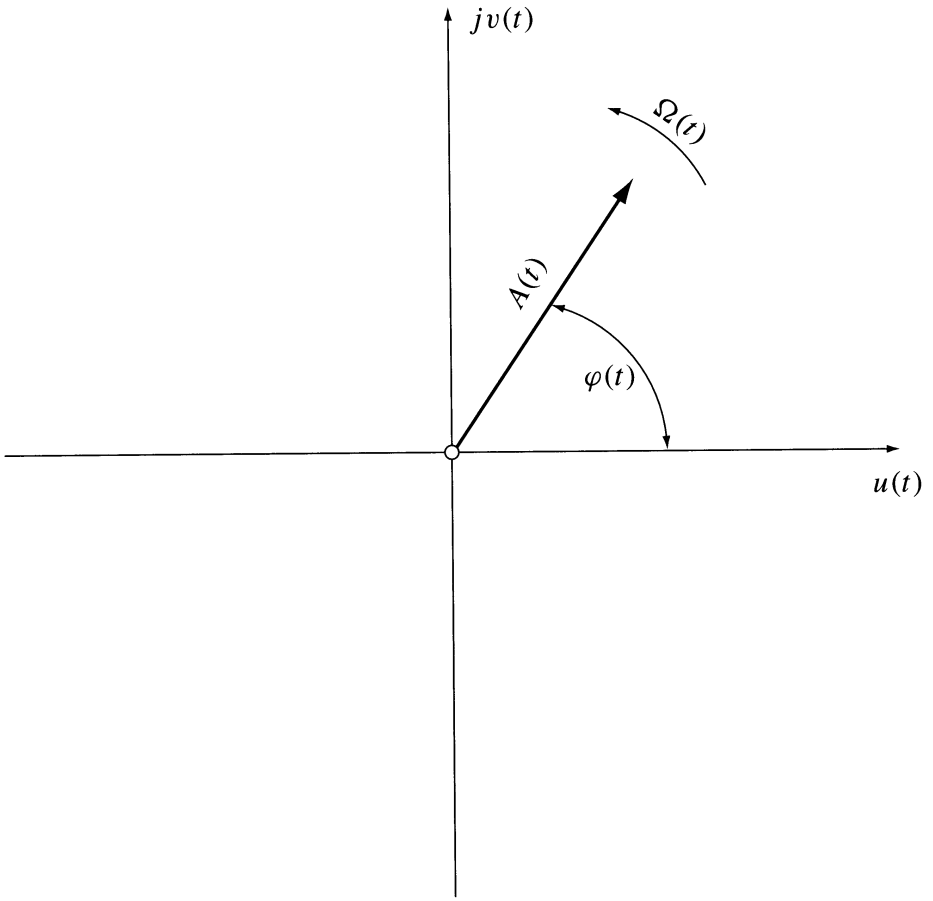

FIGURE 7.15.1 A phasor in the Cartesian (u, v) plane representing the analytic signal $\psi(t) = u(t) + jv(t) = A(t)e^{j\varphi(t)}$.

We define the instantaneous amplitude of the analytic signal equal to the length of the phasor (radius vector) A):

$$A(t) = \sqrt{u^2(t) + \upsilon^2(t)} \tag{7.15.4}$$

and define the instantaneous phase of the analytic signal equal to the instantaneous angle

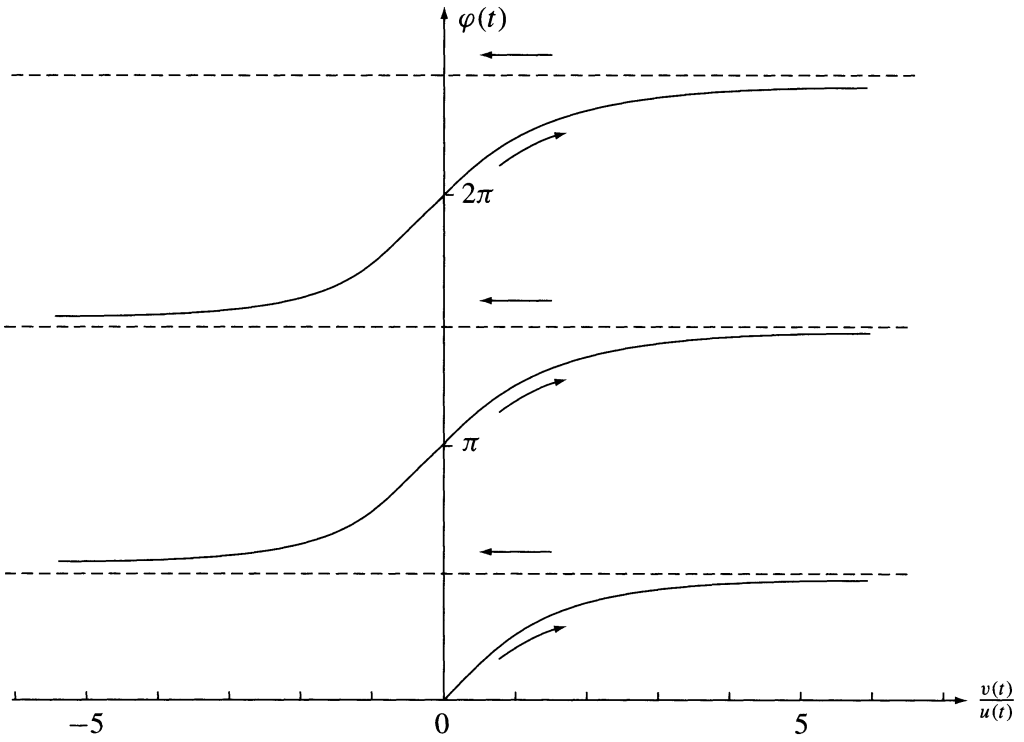

FIGURE 7.15.2 The multibranch function $\varphi(t) = \tan^{-1}[\upsilon(t)/u(t)]$. As time elapses (arrows) they are jumps from one branch to a next branch.

$$\varphi(t) = \mathrm{Tan}^{-1}\frac{\upsilon(t)}{u(t)} \tag{7.15.5}$$

The notation with capital T indicates the multibranch character of the Tan^{-1} function, as shown in Figure 7.15.2. As times elapses, the phasor rotates in the (u, υ) plane and its instantaneous angular speed defines the **instantaneous angular frequency** of the analytic signal given by the time derivative

$$\dot{\varphi}(t) = \Omega(t) = 2\pi F(t) \tag{7.15.6}$$

or

$$\Omega(t) = \frac{d}{dt}\tan^{-1}\frac{\upsilon(t)}{u(t)} = \frac{u(t)\dot{\upsilon}(t) - \upsilon(t)\dot{u}(t)}{u^2(t) + \upsilon^2(t)} \tag{7.15.7}$$

Notice the anticlock direction of rotation for positive angular frequencies. The instantaneous frequency is defined by the formula

$$F(t) = \frac{\Omega(t)}{2\pi} = \frac{1}{2\pi}\dot{\varphi}(t) \tag{7.15.8}$$

Summarizing, using the notion of the analytic signal, we defined the instantaneous amplitude, phase, and frequency. A number of different definitions of the notion of instantaneous amplitude, phase, and

frequency have developed over the years. There are many pairs of functions $A(t)$ and $\varphi(t)$, which inserted into Equation (7.15.1) reconstruct a given signal $u(t)$, for example, functions defining a phasor in the phase plane $\left[u(t), \dot{u}(t)\right]$. But only the analytic signal has the unique feature of having a one-sided Fourier spectrum. Let us recall that a real signal and its Hilbert transform are given in terms of analytic signals by Equations (7.2.17) and (7.2.18) (see Section 7.2). Figure 7.15.3 shows the geometrical representation of these formulae in the form of two phasors of a length 0.5 $A(t)$ and opposite direction of rotation, positive for $\psi(t)$ and negative for $\psi*(t)$. Equation (7.15.5) defines the instantaneous frequency of a signal regardless of the bandwidth. It is sometimes believed that the notion of instantaneous frequency has a physical meaning only for narrow-band signals (high-frequency (HF) modulated signals). However, using adders, multipliers, dividers, Hilbert filters, and differentiators, it is possible to implement a frequency demodulator used for wide-band signals, for example, speech signals, the algorithm defined by Equation (7.15.7). Modern VLSI enables efficient implementation of such frequency demodulators at reasonable cost.

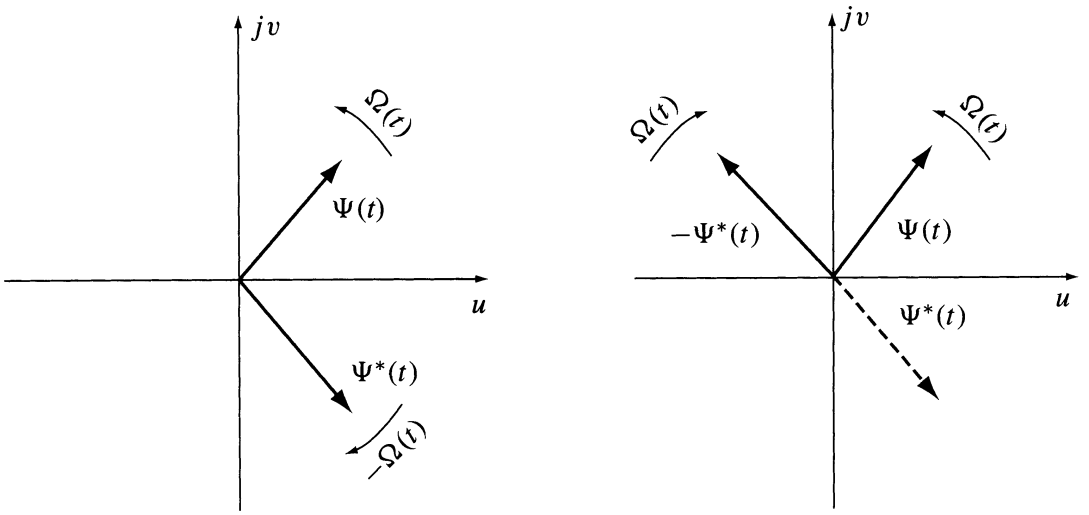

FIGURE 7.15.3 A pair of conjugate phasors representing the Equations (7.2.17) and (7.2.18).

Instantaneous Complex Phase and Complex Frequency

Signal and systems theory widely uses the Laplace transformation of a real signal $u(t)$ of the form

$$U(s) = \int_0^\infty u(t) e^{-st} dt \tag{7.15.9}$$

where

$$s = \alpha + j\omega\,; \qquad \omega = 2\pi f$$

is a time-independent complex frequency (α and ω are real). The exponential kernel e^{-st} has the form of a harmonic wave with an exponentially decaying amplitude; that is, its instantaneous amplitude is

$$A(t) = e^{-\alpha t} \tag{7.15.10}$$

The notion of the complex frequency has been generalized by this author in 1964 defining a complex instantaneous variable frequency using the notion of the analytic signal.[12] It is convenient to define the

instantaneous complex frequency as the time derivative of a complex phase. The instantaneous complex phase of the analytic signal $\psi(t)$ is defined by the formula

$$\Phi_c(t) = \mathrm{Ln}[\psi(t)] \tag{7.15.11}$$

Capital L denotes the multibranch character of the logarithmic function of the complex function $\psi(t)$. The insertion of the polar form of the analytic signal (see Equation [7.15.3]) yields:

$$\Phi_c(t) = \mathrm{Ln}[A(t)] + j\varphi(t) \tag{7.15.12}$$

The instantaneous complex frequency is defined by the derivative

$$s(t) = \dot{\Phi}_c(t) = \frac{\dot{A}(t)}{A(t)} + j\omega(t) \tag{7.15.13}$$

or

$$s(t) = \alpha(t) + j\omega(t) \tag{7.15.14}$$

where

$$\alpha(t) = \frac{\dot{A}(t)}{A(t)} \tag{7.15.15}$$

is the instantaneous radial frequency (a measure of the radial velocity representing the speed of changes of the radius or amplitude of the phasor), and

$$\omega(t) = \dot{\varphi}(t) \tag{7.15.16}$$

is the instantaneous angular frequency. Equation (7.15.15) has the form of a first-order differential equation. The solution of this equation yields the following form of the instantaneous amplitude

$$A(t) = A_0 e^{\int_0^t \alpha(t)dt} \tag{7.15.17}$$

A_0 is the value of the amplitude at the moment $t = 0$. Let us introduce the notation

$$\beta(t) = \int_0^t \alpha(t)dt \tag{7.15.18}$$

Using this notation the complex phase can be written as

$$\Phi_c(t) = \ln A_0 + \beta(t) + j\varphi(t) \tag{7.15.19}$$

or

$$\Phi_c(t) = \ln A_0 + \int_0^t s(t)dt + j\Phi_0 \tag{7.15.20}$$

Φ_0 is the integration constant or the angular position of the phasor at $t = 0$. The introduction of the concept of a complex constant $\psi_0 = A_0 e^{j\Phi_0}$ gives the following form of the analytic signal

$$\Psi(t) = \psi_0 e^{\int_0^t s(t)dt} \tag{7.15.21}$$

Examples

1. Consider the analytic signal given by Equation (7.5.10):

$$\psi_\delta(t) = \underbrace{\frac{\alpha}{\pi(\alpha^2 + t^2)}}_{u(t)} + j\underbrace{\frac{t}{\pi(\alpha^2 + t^2)}}_{v(t)} \tag{7.15.22}$$

The polar form of this signal is

$$\psi_\delta(t) = \underbrace{\frac{1}{\pi\sqrt{\alpha^2 + t^2}}}_{A(t)} \exp\underbrace{\left[j\tan^{-1}(t/\alpha)\right]}_{\varphi(t)} \tag{7.15.23}$$

Therefore, the instantaneous complex phase is

$$\Phi_c(t) = \underbrace{\mathrm{Ln}\left\{\frac{1}{\pi\sqrt{\alpha^2 + t^2}}\right\}}_{\beta(t)} + \underbrace{j\tan^{-1}(t/\alpha)}_{\varphi(t)} \tag{7.15.24}$$

and the instantaneous complex frequency is

$$s(t) = \dot{\Phi}_c(t) = \underbrace{\frac{-t}{\alpha^2 + t^2}}_{\alpha(t)} + j\underbrace{\frac{\alpha}{\alpha^2 + t^2}}_{\omega(t)} \tag{7.15.25}$$

Because in the limit $\alpha \Rightarrow 0$ the signal (7.15.22) approximates the complex delta distribution (see Equation [7.5.4]), the instantaneous complex phase of this distribution is

$$\Phi_{c\delta}(t) = \mathrm{Ln}\underbrace{\frac{1}{\pi|t|}}_{A(t)} + j\underbrace{0.5\pi\,\mathrm{sgn}(t)}_{\varphi(t)} \tag{7.15.26}$$

and the complex frequency is

$$s_\delta(t) = \underbrace{\frac{-1}{t}}_{\alpha(t)} + j\underbrace{\pi\delta(t)}_{\omega(t)} \tag{7.15.27}$$

2. Consider the analytic signal

$$\psi(t) = \underbrace{\frac{\sin(at)}{at}}_{u(t)} + j\underbrace{\frac{\sin^2(0.5at)}{0.5at}}_{v(t)} \tag{7.15.28}$$

where $u(t)$ is the well-known interpolating function of the sampling theory. Equations (7.15.4) and (7.15.5) yield, using trigonometric relations, the polar form of this signal:

$$\psi(t) = \underbrace{\left|\frac{\sin(0.5at)}{0.5at}\right|}_{A(t)} \exp\underbrace{(j\,at/2)}_{\varphi(t)} \tag{7.15.29}$$

Therefore, the instantaneous complex phase is

$$\psi_c(t) = \mathrm{Ln}\underbrace{\left|\frac{\sin(0.5at)}{0.5at}\right|}_{A(t)} + j\,at/2 \tag{7.15.30}$$

and the instantaneous complex frequency

$$s(t) = \frac{a}{2}\cot(0.5at) - \frac{1}{t} + j\frac{a}{2} \tag{7.15.31}$$

In conclusion, the interpolating function may be regarded as a signal of a variable amplitude and a constant angular frequency $\omega = a/2$.

3. The classic complex notation of a frequency or phase modulated signal (Carson and Fry, 1937) has the form[41]

$$\psi(t) = A_0 e^{j\left[\Omega_0 t + \Phi_0 + \varphi(t)\right]}; \quad \Omega_0 = 2\pi F_0 \tag{7.15.32}$$

where $\varphi(t)$ represents the angle modulation. The whole argument of the exponential function $\Phi(t) = \Omega_0 t + \Phi_0 + \varphi(t)$ defines the instantaneous phase and its derivative, the instantaneous frequency

$$F(t) = \frac{1}{2\pi}\frac{d\Phi}{dt} = F_0 + \frac{1}{2\pi}\frac{d\varphi}{dt} \tag{7.15.33}$$

The signal (7.15.32) is represented by a phasor in the plane $(\cos[(\Phi(t)], \sin[\Phi(t)])$, as shown in Figure 7.15.4. These definitions of the instantaneous phase and frequency differ from the definition using the analytic signal that is represented by a phasor in the $(\cos[\Phi(t)], H(\cos[\Phi(t)])$ plane, because $\sin[\Phi(t)]$ is not the Hilbert transform of $\cos[\Phi(t)]$ and the signal (7.15.32) is not an analytic function. However, it may be nearly analytic if the carrier frequency is large. If the spectra of the functions $\cos[\varphi(t)]$ and $\sin[\varphi(t)]$ have a limited low-pass support of a highest frequency $|W| < |F_0|$, then Bedrosian's theorem (see Section 7.12) may be applied and

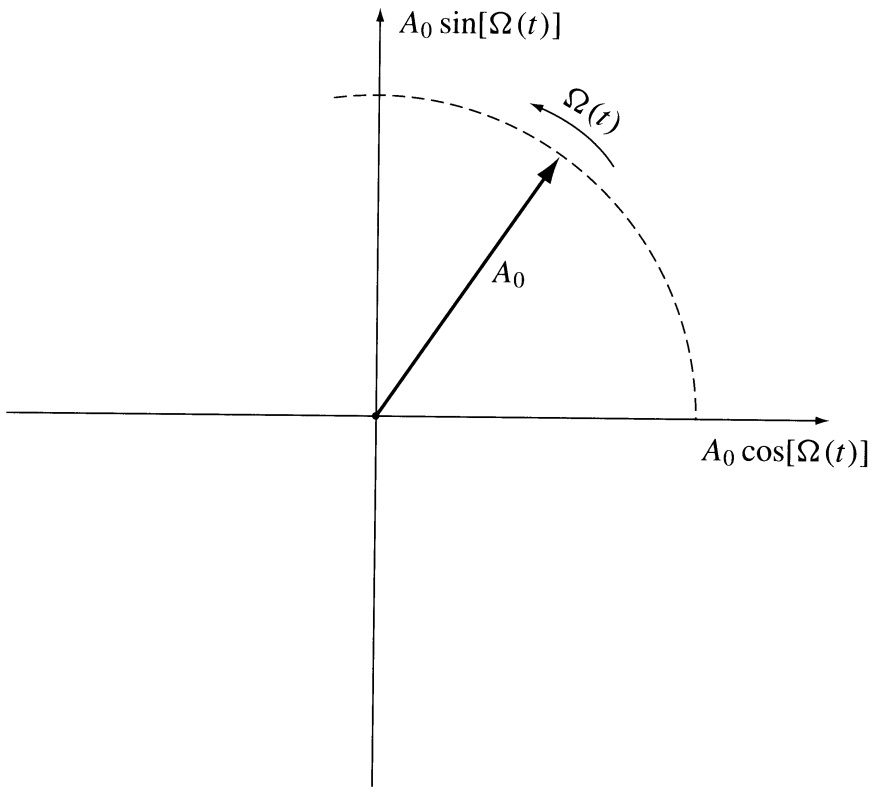

FIGURE 7.15.4 A phasor representing a frequency (or phase) modulated signal.

$$H\left\{\cos\left[\Omega_0 t + \Phi_0 + \varphi(t)\right]\right\} = \cos\left[\varphi(t)\right] H\left[\cos\left(\Omega_0 t + \Phi_0\right)\right] - \sin\left[\varphi(t)\right] H\left[\sin\left(\Omega_0 t + \Phi_0\right)\right] = \sin\left[\Omega_0 t + \Phi_0 + \varphi(t)\right] \tag{7.15.34}$$

In the case of harmonic modulation with $\varphi(t) = \beta \sin(\omega t)$, where β is the modulation index, the spectra of the functions $\cos[\varphi(t)]$ and $\sin[\varphi(t)]$ are given by the Fourier series

$$\cos\left[\beta \sin(\omega t)\right] = J_0(\beta) + 2\sum_{n=1}^{\infty} J_{2n}(\beta)\cos(2n\omega t) \tag{7.15.35}$$

$$\sin\left[\beta \sin(\omega t)\right] = 2\sum_{n=1}^{\infty} J_{2n-1}(\beta)\sin\left[(2n-1)\omega t\right] \tag{7.15.36}$$

and this is not a pair of Hilbert transforms (see Section 7.6). Although the number of terms of the series is infinite, the number of significant terms is limited and for a good approximation Bedrosian's theorem may be applied for large values of F_0. Further comments are given in Reference 25.

7.16 Hilbert Transforms in Modulation Theory

This section is devoted to the theory of analog modulation of a harmonic carrier $u_c(t) = A_0 \cos(2\pi F_0 t + \Phi_0)$ with emphasis on the role of Hilbert transformation, analytic signals, and complex frequencies. The theory of amplitude and angle modulation is mentioned briefly in favor of a more detailed description of the theory of single side-band modulations. The last are conveniently defined using Hilbert transforms. Many modulators are implemented using Hilbert filters, mostly digital filters, because nowadays modulated signals can be conveniently generated digitally and converted into analog signals.

Concept of the Modulation Function of a Harmonic Carrier

The complex notation of signals is widely used in modern modulation theory. The harmonic carrier is written in the form of the analytic signal

$$\psi_c(t) = A_0 e^{j(\Omega_0 t + \Phi_0)} \tag{7.16.1}$$

Analog modulation is the operation of continuous change of one or more of the three parameters of the carrier: the amplitude A_0, the frequency F_0, or the phase Φ_0, resulting in amplitude, frequency, or phase modulation. The complex modulated signal has a convenient representation in the form of a product[3]

$$\psi(t) = \gamma(t)\psi_c(t) = A_0\gamma(t)e^{j(\Omega_0 t + \Phi_0)} \tag{7.16.2}$$

The function $\gamma(t)$ is called the **modulation function**. It is a function of the modulating signal (the message) $x(t)$, that is, $\gamma(t) = \gamma[x(t)]$. Any kind of modulation, for example, amplitude, frequency, or phase modulation, is represented by a specific real or complex modulation function. We shall investigate models of modulating signals for which the Fourier transform exists and is given by the Fourier pair

$$x(t) \overset{F}{\Longleftrightarrow} X(\omega); \quad \omega = 2\pi f \tag{7.16.3}$$

The frequency band containing the terms of the spectrum $X(\omega)$ is called the **baseband**. In general, the modulation function is a nonlinear function of the variable x, and the spectrum of the modulation function differs from $X(\omega)$ and is represented by the Fourier pair:

$$\gamma(t) \overset{F}{\Longleftrightarrow} \Gamma(\omega) \tag{7.16.4}$$

The nonlinear transformations of the spectrum may have a complicated analytic representation. Usually only approximate determination of the spectrum is possible. The approximations are easier to perform if the energy of the modulating signal is nonuniformly distributed and concentrated in the low-frequency part of the baseband, for example, the energy of voice, music, or TV signals. Usually it is possible to find the terms of $\Gamma(\omega)$ for harmonic modulating signals. In special cases, if the modulation function is proportional to the message; that is, $\gamma(t) = mx(t)$ (m is a constant), we have

$$\Gamma(f) = mX(f) \tag{7.16.5}$$

The initial phase of the carrier Φ_0 is of importance only if we deal with two or more modulated carriers of the same frequency, for example, by summation or multiplication of modulated signals. It is convenient to write the modulated signal in the form

$$\psi(t) = A_0 \gamma(t) e^{j\Phi_0} e^{j\Omega_0 t} \tag{7.16.6}$$

and define a **modified modulation function** in the form of the product

$$\gamma_1(t) = \gamma(t) e^{j\Phi_0} \tag{7.16.7}$$

The new Fourier spectrum is

$$\gamma_1(t) \overset{F}{\Longleftrightarrow} \Gamma_1(\omega) = \Gamma(\omega) e^{j\Phi_0} \tag{7.16.8}$$

We observe that the spectra (7.16.4) and (7.16.8) have the same magnitude and differ only by the phase relations. Notice that the spectrum $\Gamma_1(\omega)$ is defined at zero carrier frequency and the spectrum of the modulated signal is obtained by shifting this spectrum from zero to carrier frequency by the Fourier shift operator $e^{j\Omega_0 t}$. This approach enables us to study the spectra of modulated signals at zero carrier frequency.

Examples of modulation functions:

The modulation function for a linear full-carrier AM has the form

$$\gamma(t) = 1 + mx(t); \quad |mx(t)| < 1 \tag{7.16.9}$$

The number 1 represents the carrier term. Therefore, the modulation function for balanced modulation (suppressed carrier) has the simple form

$$\gamma(t) = mx(t) \tag{7.16.10}$$

Therefore, the spectra of the message and of the modulation function are to within the scale factor m, the same. The message may be written in the form (see Equation [7.2.17])

$$x(t) = \frac{\psi_x(t) + \psi_x^*(t)}{2} \tag{7.16.11}$$

This formula shows that the upper sideband of the AM signal is represented by the analytic signal $\psi_x(t)$ of a one-sided spectrum at positive frequencies and the lower sideband by the conjugate analytic signal $\psi_x^*(t)$ of a one-sided spectrum at negative frequencies. The sidebands have the geometric form of two conjugate phasors (see Figure 7.15.3). The instantaneous amplitude of the phasors is

$$A(t) = \frac{m}{2}|\psi_x(t)| = \frac{m}{2}\sqrt{x^2(t) + \left(\hat{x}(t)\right)^2} \tag{7.16.12}$$

($\hat{x}(t) = H[x(t)]$) and the instantaneous angular frequency is

$$\omega_x(t) = \pm \frac{d}{dt} \tan^{-1}\left[\frac{\hat{x}(t)}{x(t)}\right] \tag{7.16.13}$$

Therefore, a single sideband represents a signal with simultaneous amplitude and phase modulation. The multiplication of $\psi_x(t)$ or $\psi_x^*(t)$ with the complex carrier (Fourier shift operator) $e^{j\Omega_0 t}$ yields the high-frequency analytic signals. The upper sideband ($\Phi_0 = 0$) is (with $mA_0 = 2$)

$$\psi_{\text{upper}}(t) = \psi_x(t)e^{j\Omega_0 t} \tag{7.16.14}$$

with the modulation function $\psi_x(t)$, and the lower sideband is

$$\psi(t) = \psi_x^*(t)e^{j\Omega_0 t} \tag{7.16.15}$$

with the conjugate modulation function $\psi_x^*(t)$ The above signals represent the complex form of single side-band (SSB) AM. The real notation of these signals is

$$u_{\text{SSB}}(t) = x(t)\cos(\Omega_0 t) \mp \hat{x}(t)\sin(\Omega_0 t) \tag{7.16.16}$$

with the minus sign for the upper sideband and plus sign for the lower one. The products $x(t)\cos(\Omega_0 t)$ and $\hat{x}(t)\text{in}(\Omega_0 t)$ represent double side-band (DSB) compressed carrier AM signals. Therefore, an SSB modulator may be implemented, as shown in Figure 7.16.1.

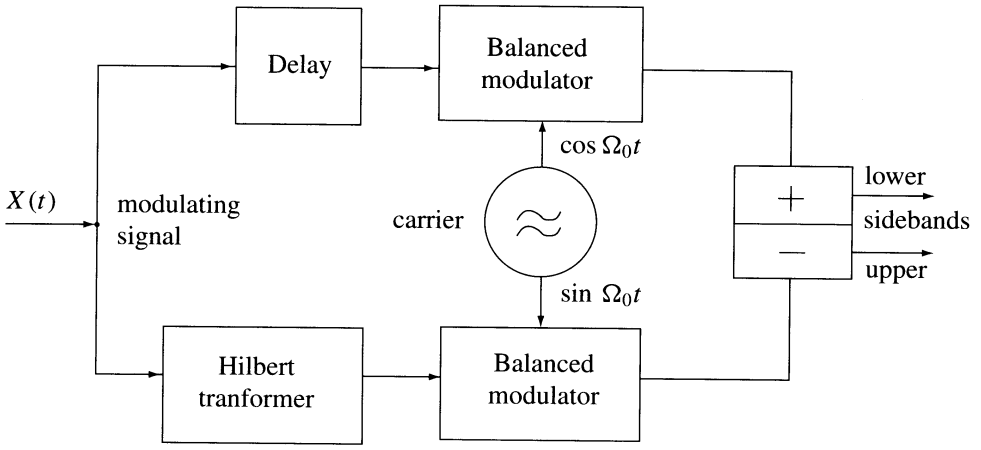

FIGURE 7.16.1 Block diagram of a SSB modulator (phase method) implementing Equation (7.16.16).

The **angle modulation** is represented by the exponential modulation function of the form

$$\gamma(t) = e^{j\varphi[x(t)]} \tag{7.16.17}$$

Therefore, the complex signal representation of the angle modulation has the form

$$\Psi(t) = A_0 e^{j\left[\Omega_0 t + \varphi(t)\right]} \tag{7.16.18}$$

where φ is a function of the modulating signal $x(t)$. In general, this complex signal may be only approximately analytic (see Section 7.15, example 3). In the case of a linear phase modulation, the modulation function has the form

$$\gamma(t) = e^{jmx(t)} \tag{7.16.19}$$

and for the linear frequency modulation

$$\gamma\left(t\right) = e^{jm\int_{-\infty}^{t} x\left(t\right)dt} \tag{7.16.20}$$

The Fourier spectrum of the modulation function is given by the integral

$$\Gamma\left(\omega\right) = \int_{-\infty}^{\infty} e^{j\varphi\left[x\left(t\right)\right]} e^{-j\omega t} dt \tag{7.16.21}$$

If for a specific function $\varphi[x(t)]$ the closed form of this integral does not exist, a numerical integration may be applied. In the simplest case of linear phase modulation with a harmonic modulating signal the modulation function (7.16.19) has the form

$$\gamma\left(t\right) = e^{j\beta\sin\left(\omega_0 t\right)} \tag{7.16.22}$$

where β is the modulation index (in radians). The Fourier series expansion of this complex periodic function has the form:

$$\gamma\left(t\right) = J_0\left(\beta\right) + \sum_{n=1}^{\infty} J_{2n}\left(\beta\right)\cos\left(2n\omega_0 t\right) + \sum_{n=1}^{\infty} J_{2n-1}\left(\beta\right)\sin\left[\left(2n-1\right)\omega_0 t\right] \tag{7.16.23}$$

Using Euler's formulae (see Equations [7.2.19] and [7.2.20]), this modulation function becomes

$$\begin{aligned}\gamma\left(t\right) = J_0\left(\beta\right) &+ \sum_{n=1}^{\infty} J_{2n}\left(\beta\right)\left[\frac{e^{j2n\omega_0 t} + e^{-j2n\omega_0 t}}{2}\right] \\ &+ \sum_{n=1}^{\infty} J_{2n-1}\left(\beta\right)\left[\frac{e^{j\left(2n-1\right)\omega_0 t} - e^{-j\left(2n-1\right)\omega_0 t}}{2}\right]\end{aligned} \tag{7.16.24}$$

Because the exponentials in the time domain are represented by delta functions in the frequency domain $\left(e^{\pm jn\omega_0 t} \overset{F}{\Longleftrightarrow} \delta\left(f \mp n f_0\right)\right)$, the spectrum of the modulation function (zero carrier frequency) has the form shown in Figure 7.16.2 ($\beta = 4$).

Generalized Single Side-Band Modulations

The SSB AM signal defined by Equations (7.16.14) and (7.16.15) is an example of many other possible single side-band modulations. Any kind of modulation of a harmonic carrier is called single side-band modulation if the modulation function is an analytic signal of a one-sided spectrum at positive frequencies for the upper sideband and at negative frequencies for the lower sideband. Therefore, the modulation function should have the form

$$\gamma\left(t\right) = \gamma_x\left(t\right) + j\hat{\gamma}_x\left(t\right) = A\left(t\right)e^{j\phi\left(t\right)} \tag{7.16.25}$$

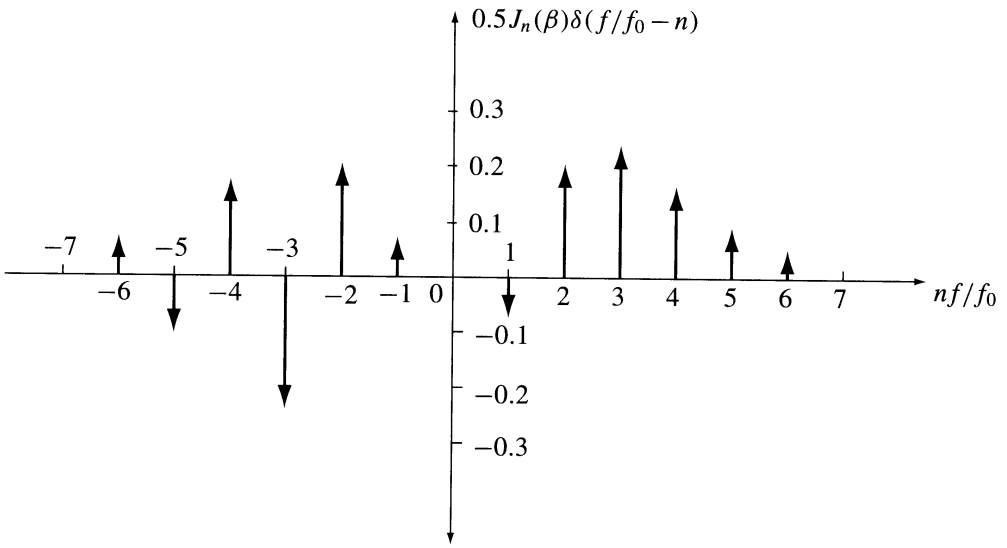

FIGURE 7.16.2 The spectrum of a phase modulated signal translated to zero carrier frequency, i.e., of the modulation function. Phase deviation $\beta = 4$ radians.

where $\gamma_x(t) \overset{H}{\Longleftrightarrow} \hat{\gamma}_x(t)$. Let us use here the notion of the **instantaneous complex phase** defined by Equation (7.15.11) of the form

$$\phi_c(t) = \ln A(t) + j\phi(t) \tag{7.16.26}$$

The modulation function (7.16.25) can be written in the form

$$\gamma(t) = e^{\phi_c(t)} = e^{\ln[A(t)] + j\phi(t)} \tag{7.16.27}$$

that is, the instantaneous amplitude is written in the exponential form

$$A(t) = e^{\ln[A(t)]} \tag{7.16.28}$$

We now put the question: under what conditions are $\gamma(t)$ and simultaneously $\phi_c(t)$ analytic? That is, when is not only the relation (7.16.25), but also the relation

$$\ln A(t) \overset{H}{\Longleftrightarrow} \phi(t) = \hat{\mathrm{LN}}[A(t)] \tag{7.16.29}$$

satisfied? The answer comes from the dual (time domain) version of the **Paley-Wiener criterion**[28]

$$\int_{-\infty}^{\infty} \frac{|\mathrm{Ln}[\mathrm{A}(\mathrm{t})]|}{1+\mathrm{t}^2}\, dt < \infty \tag{7.16.30}$$

which should be satisfied. Let us remember that $A(t)$ is defined as a nonnegative function of time. The Paley-Wiener criterion is equivalent to a requirement that $A(t)$ should not approach zero faster than any exponential function. This is a property of each signal with finite bandwidth that is of any practical signal.

CSSB: Compatible Single Side-Band Modulation

The CSSB signal has the same instantaneous amplitude as the conventional DSB full-carrier AM signal, that is, of the form

$$A(t) = A_o(1 + mx(t)); \quad mx(t) < 1 \tag{7.16.31}$$

and can be demodulated by a conventional linear diode demodulator (but not by a synchronous detector). The one-sided spectrum of the CSSB signal is achieved by a simultaneous specific phase modulation. The analytic modulation function should satisfy the requirement (7.16.29) and has the form

$$\gamma(t) = \left[1 + mx(t)\right] e^{j\hat{\ln}\left[1+mx(t)\right]} \tag{7.16.32}$$

Figure 7.16.3 shows a block diagram of a modulator producing a high-frequency CSSB signal implemented by the use of Equation (7.16.32). This modulation function guarantees the exact cancellation of the undesired sideband. Using digital implementation, the level of the undesired sideband depends only on design. The bandwidth of the nonlinear logarithmic device, the Hilbert filter and phase modulator, should be several times wider than the bandwidth of the input signal. In practice it should be three to four times larger than the baseband. The instantaneous amplitude $A(t)$ should never fall to zero because the logarithm of zero equals minus infinity. Tradeoff is needed between the smallest value of A and the phase deviation.

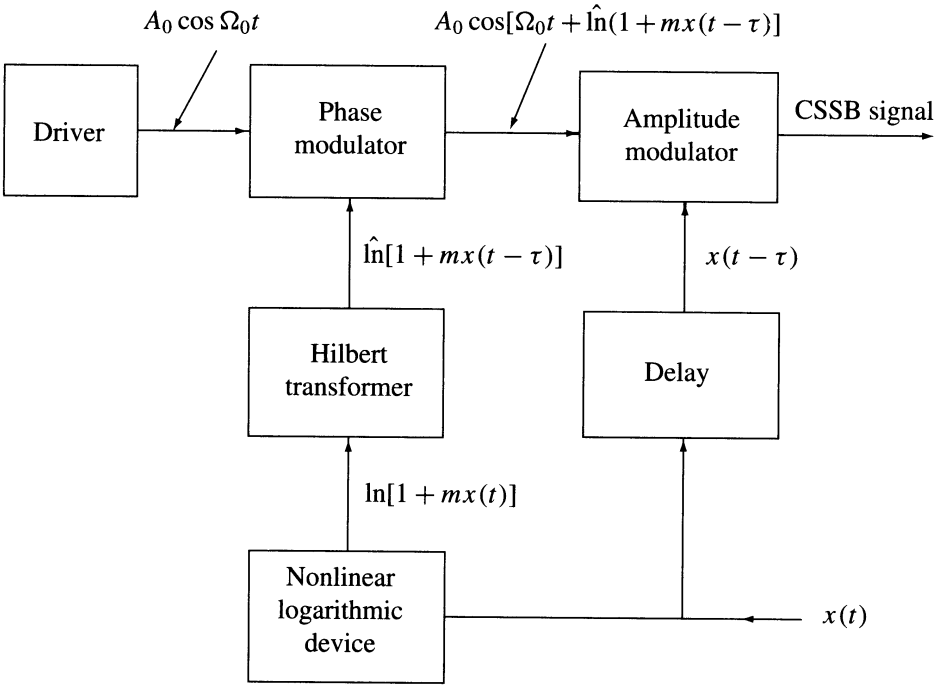

FIGURE 7.16.3 Diagram of the modulator producing the Compatible Single Side-Band AM signal.

Spectrum of the CSSB Signal

It may be a surprise that the **bandwidth** of the one-sided spectrum of the CSSB signal **is limited**. If the spectrum of the modulating signal exists in the interval $-W < f < W$, then the spectrum of the modulation function exists in the interval $0 < f < 2W$. Seemingly, the bandwidths of the CSSB and DSB AM signals

are equal. However, the spectra of many messages such as speech or video signals are nonuniform, with significant terms concentrated at the lower part of the baseband. This enables us to transmit the CSSB signal in a smaller band; for example, from F_0 to $F_0 + W$ instead to $F_0 + 2W$, at the cost of some distortions enforced by the truncation of insignificant terms of the spectrum. Let us investigate the spectra and distortions using the model of a wide-band modulating signal given in the form of the Fourier series.

$$x(t) = \sum_{k=0}^{N} (-1)^k C_{2k+1} \cos\left[(2k+1)\omega_0 t\right]; \quad \omega_0 = 2\pi f_0 \tag{7.16.33}$$

For $C_{2k+1} = 1/(2k + 1)$ this modulating signal is a truncated Fourier series of a square wave. Its bandwidth equals $W = (2N + 1)\, f_0$. The insertion of this signal in Equation (7.16.31) yields a periodic modulation function given by the Fourier series

$$\gamma(t) = \sum_{k=0}^{4N+2} A_k e^{jk\omega_0 t} \tag{7.16.34}$$

The truncation of this series at the term $4N + 2$ is not arbitrary because it will be shown that terms for $k > 4N + 2$ vanish. Therefore, the **bandwidth of** $\gamma(t)$ equals exactly **2W**. To give the evidence, let us insert $x(t)$ given by Equation (7.16.33) in Equation (7.16.32). The square of the instantaneous amplitude of so-defined modulation function is

$$A^2(t) = \left[1 + m \sum_{k=0}^{N} (-1)^k C_{2k+1} \cos\left[(2k+1)\omega_0 t\right]\right]^2 \tag{7.16.35}$$

The highest term of this Fourier series has the harmonic number $4N + 2$. Analogously, the square of the instantaneous amplitude of the modulation function (7.16.34) is

$$A^2(t) = \left[\sum_{k=0}^{4N+2} A_k \cos(k\omega_0 t)\right]^2 + \left[\sum_{k=1}^{4N+2} A_k \sin(k\omega_0 t)\right]^2 \tag{7.16.36}$$

However, the functions (7.16.34) and (7.16.35) should be equal. Therefore, they should have the same coefficients of the Fourier series. The comparison of these coefficients yields a set of $4N + 3$ equations. The solution of these equations yields the coefficients $A_0, A_1, A_2, \ldots, A_{2N+2}$ as functions of the modulation index m and the amplitudes C_{2k+1} of the modulating signal (7.16.31).

Example

1. For the harmonic modulating signal $x(t) = \cos(\omega_0 t)$, $N = 0$, $C_1 = 1$ and $C_{2k+1} = 0$ for $k > 0$. The comparison of the squares of the instantaneous amplitudes yields three equations

$$A_0^2 + A_1^2 + A_2^2 = \left(1 + m^2/2\right) C_1 \tag{7.16.37}$$

$$A_0 A_1 + A_1 A_2 = mC_1 \tag{7.16.38}$$

$$A_0 A_2 = (mC_1)^2/4 \tag{7.16.39}$$

The solution of these equations yields ($C_1 = 1$): The amplitude of the zero frequency carrier

$$A_0 = 0.5 + 0.5\sqrt{1 - m^2} \tag{7.16.40}$$

The amplitude of the first sideband

$$A_1 = m \tag{7.16.41}$$

and the amplitude of the second sideband

$$A_2 = 0.5 - 0.5\sqrt{1 - m^2} \tag{7.16.42}$$

Figure 7.16.4 shows an example of the spectrum of the CSSB signal and Figure 7.16.5, the dependence of the amplitudes on m.

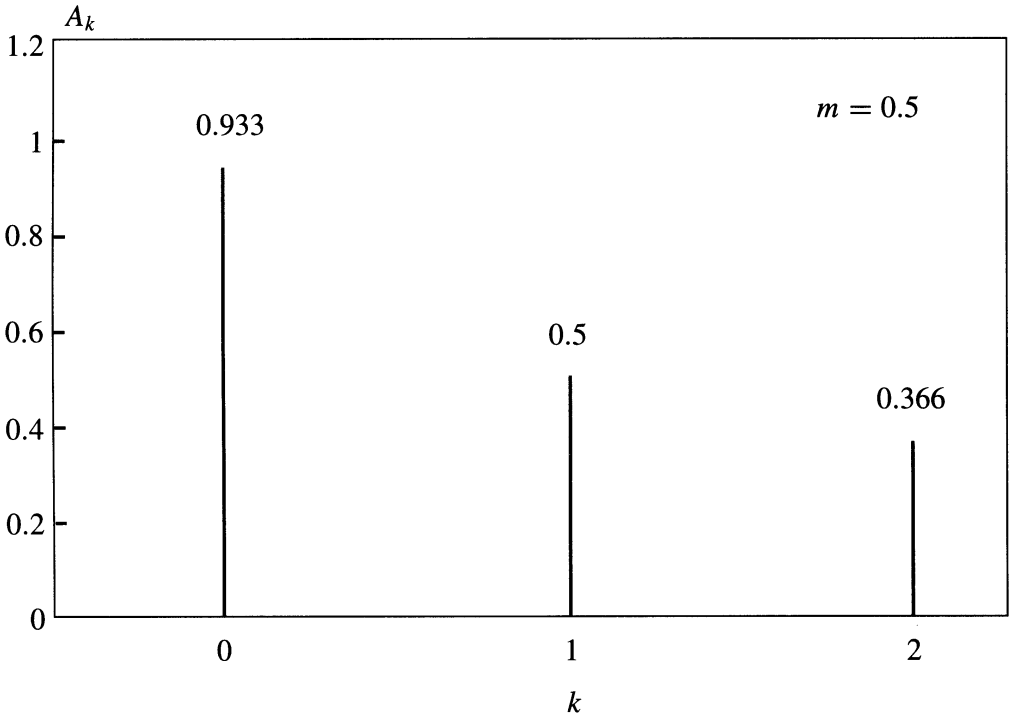

FIGURE 7.16.4 Example of a spectrum of the CSSB AM signal with a cosine envelope.

2. For the modulating signal $x(t) = C_1 \cos(\omega_0 t) - C_3 \cos(3\omega_0 t)$, $N = 1$, and $C_{2k+1} = 0$ for $k > 1$. We get seven equations of the form

$$\sum_{k=0}^{6} A_k^2 = 1 + \frac{m^2}{2}\left(C_1^2 + C_3^2\right) \tag{7.16.43}$$

$$\sum_{k=0}^{5} A_k A_{k+1} = mC_1; \quad \sum_{k=0}^{4} A_k A_{k+2} = \frac{m^2}{2}\left(0.5C_1^2 - C_1 C_3\right) \tag{7.16.44}$$

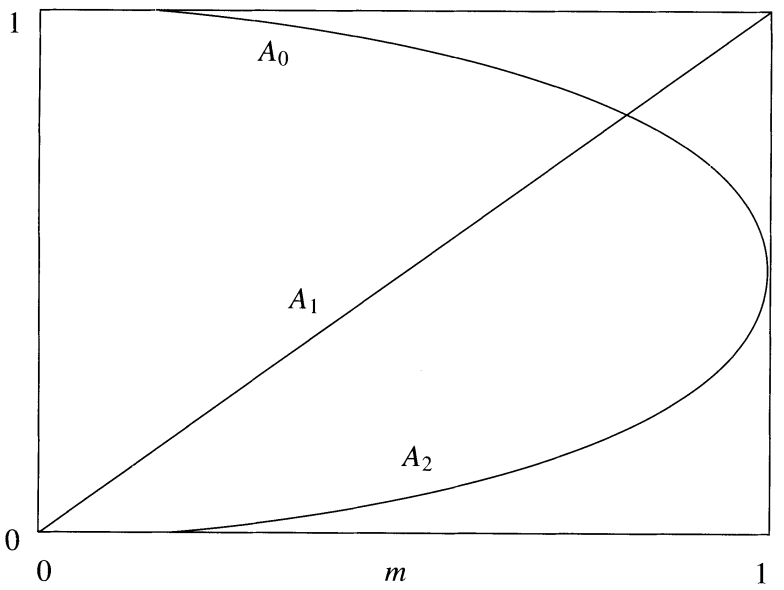

FIGURE 7.16.5 The dependence of the three terms of the spectrum on the modulation index m.

$$\sum_{k=0}^{3} A_k A_{k+3} = -mC_3\,; \quad \sum_{k=0}^{2} A_k A_{k+4} = \frac{-m^2}{2} C_1 C_3 \tag{7.16.45}$$

$$\sum_{k=0}^{1} A_k A_{k+5} = 0\,; \quad \sum_{k=0}^{0} A_k A_{k+6} = \frac{m^2}{4} C_3^2 \tag{7.16.46}$$

The solutions of these equations yield the seven terms of the CSSB signal. In practice it is simpler to find these terms applying any numerical method of determination of the coefficients of the Fourier series expansion of the modulation function (7.16.32). However, the above set of equations gives the evidence that the spectrum has a finite number of terms (example in Figure 7.16.6). The above equations may be used to control the accuracy of numerical calculations. Notice that Equations (7.16.37) and (7.16.43) have the form of power equality equations.

Let us quote three other modulation functions generating CSSB AM signals. The analytic modulation function of the form

$$\gamma(t) = \sqrt{1 + mx(t)}\, e^{j\frac{1}{2}\hat{\ln}\left[1+mx(t)\right]} \tag{7.16.47}$$

uses the square root of the instantaneous amplitude of an AM signal. Its spectrum is exactly one-sided. A squaring demodulator should be applied at the receiver. The phase deviation equals one-half of the phase deviation of the function (7.16.32). Some years ago Kahn implemented a CSSB modulator using the modulation function[17]

$$\gamma(t) = \left[1 + mx(t)\right] e^{j\tan^{-1}\frac{m\hat{x}(t)}{1+mx(t)}} \tag{7.16.48}$$

Similarly Villard (1948) implemented a modulator using another modulation function[40]

$$\gamma(t) = \left(mx(t)\right)e^{jm\hat{x}(t)} \tag{7.16.49}$$

The last two modulation functions are not exactly analytic and their spectra are only approximately one-sided.

CSSB Modulation for Angle Detectors

The modulation function of a single side-band modulation compatible with a linear phase detector has the form

$$\gamma(t) = e^{-\beta\hat{x}(t)+j\beta x(t)} \tag{7.16.50}$$

and the modulation function of a single side-band modulation compatible with a linear frequency demodulator has the form

$$\gamma(t) = e^{-m_f H\left[\int x(t)dt\right]+jm_f\int x(t)dt} \tag{7.16.51}$$

where β and m_f are modulation indexes of phase or frequency modulation (in radians). The above modulation functions are analytic. Therefore, their spectra are exactly one-sided due to the simultaneous amplitude and angle modulation. Notice the exponential amplitude modulation function. For large modulation indexes the required dynamic range of the amplitude modulator is extremely large. An example is the modulating signal $x(t) = \sin(\omega_0 t)$. Here, the instantaneous amplitude has the form $A(t) = \exp[\beta\cos(\omega_0 t)]$ and is shown in Figure 7.16.7. Figure 7.16.8 shows the amplitudes of the one-sided spectrum in dependence of β.

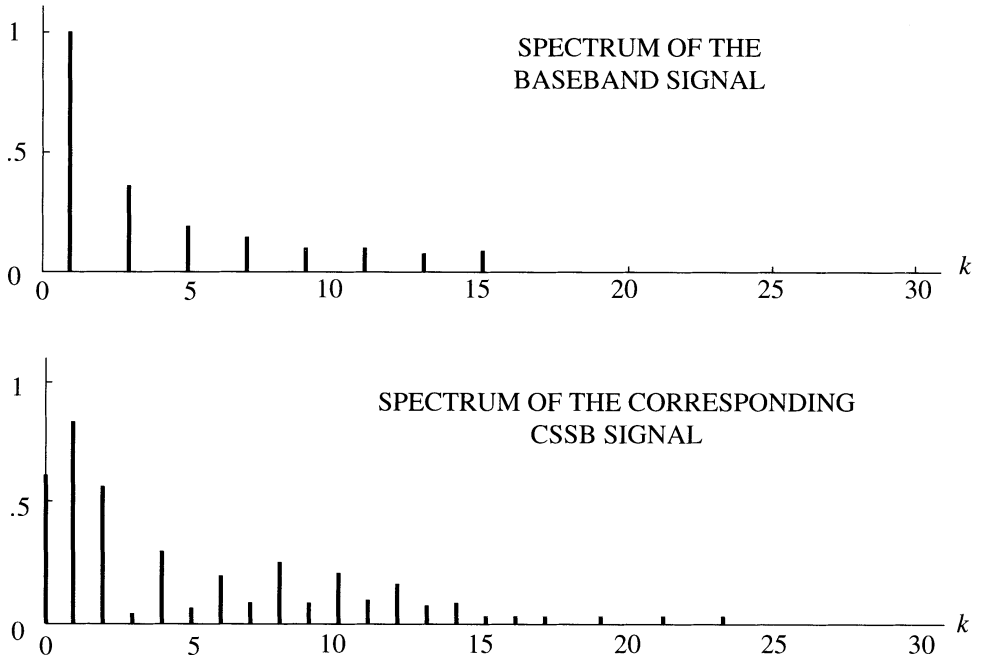

FIGURE 7.16.6 The spectrum of the CSSB AM signal with an envelope given by the Fourier series of a square wave truncated at the fifteenth harmonic number.

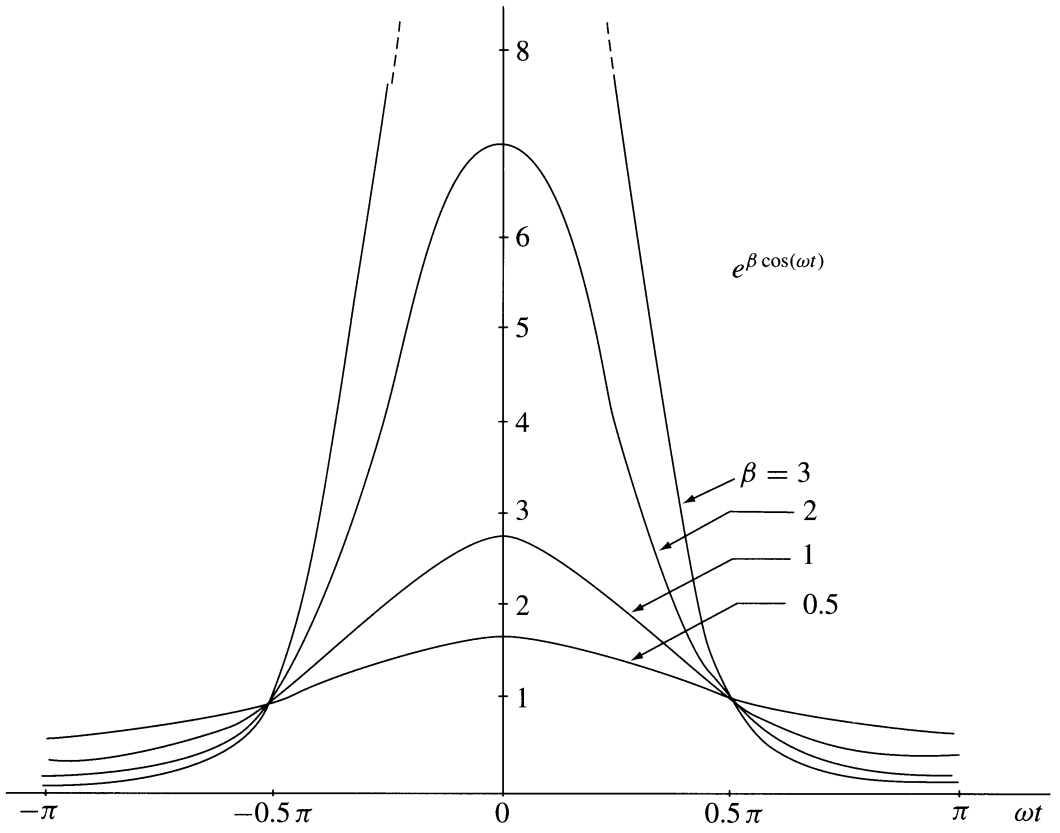

FIGURE 7.16.7 Envelope of the compatible with a linear FM detector single side-band FM signal. β-modulation index in radians.

7.17 Hilbert Transforms in the Theory of Linear Systems: Kramers–Kronig Relations

The notions of **impedance**, **admittance**, and **transfer function** are commonly used to describe the properties of **linear**, **time-invariant** (LTI) systems. If the signal at the input port of the LTI system varies in time as exp $(j\omega t)$, the signal at the output is a sine wave of the same frequency with a different amplitude and phase. In other words, the LTI conserves the waveform of sine signals. A pure sine waveform is a mathematical entity. However, it is easy to generate physical quantities that vary in time practically as $\exp(j\omega t)$. Signal generators producing nearly ideal sine waves are widely used in many applications, including precise measurements of the behavior of circuits and systems. The transfer function of the LTI system is defined as a quotient of the output and input analytic signals

$$H(j\omega) = \frac{\psi_2(t)}{\psi_1(t)} = \frac{A_2 e^{j(\omega t+\varphi_2)}}{A_1 e^{j(\omega t+\varphi_1)}} \tag{7.17.1}$$

This transfer function describes the steady-state, input-output relations. Theoretically, the input sine wave should be applied at the time at minus infinity. In practice, the steady state arrives if the transients die out. The transfer function is time independent because the term $\exp(j\omega t)$ may be deleted from the nominator and denominator of Equation (7.17.1).

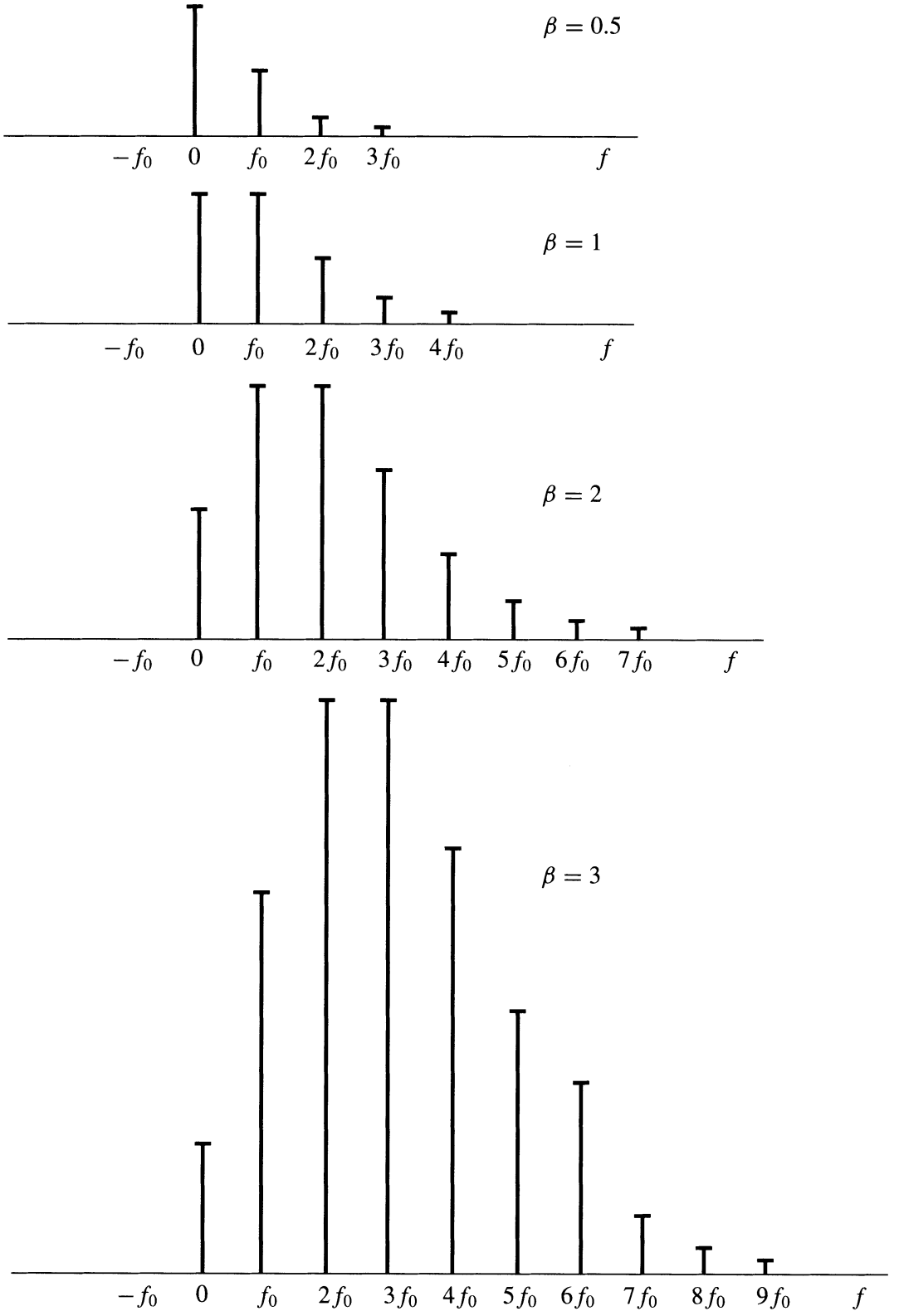

FIGURE 7.16.8 One-sided spectrum of the modulation function of the compatible with a linear detector FM signal.

The frequency domain description by means of the transfer function can be converted into the time-domain description using the Fourier transformation. A response of the LTI system to the delta pulse, i.e., the **impulse response**, is defined by the Fourier pair:

$$h(t) = \delta(t) * h(t) \overset{F}{\Longleftrightarrow} 1H(j\omega) = H(j\omega) \tag{7.17.2}$$

where $\delta(t) \overset{F}{\Longleftrightarrow} \mathbf{1}$.

Causality

All physical systems are causal. Causality implies that any response of a system at the time t, depends only on excitations at earlier times. For this reason, the impulse response of a causal system is one-sided; that is, $h(t) = 0$ for $t < 0$. But one-sided time signals have analytic spectra (see Section 7.3). Therefore, the spectrum of the impulse response given by Equation (7.17.2), and thus the transfer function of a causal system is an analytic function of the complex frequency $s = \alpha + j\omega$. The analytic transfer function

$$H(s) = A(\alpha, \omega) + j\ B(\alpha, \omega) \tag{7.17.3}$$

satisfies the Cauchy-Riemann equations (see Equation [7.2.4])

$$\frac{\partial A}{\partial \alpha} = \frac{\partial B}{\partial \omega}; \quad \frac{\partial A}{\partial \omega} = -\frac{\partial B}{\partial \alpha} \tag{7.17.4}$$

and the real and imaginary parts ($\alpha = 0$) of the transfer function form a Hilbert pair:

$$A(\omega) = \frac{-1}{\pi} P \int_{-\infty}^{\infty} \frac{B(\lambda)}{\lambda - \omega} d\lambda \tag{7.17.5}$$

$$B(\omega) = \frac{1}{\pi} P \int_{-\infty}^{\infty} \frac{A(\lambda)}{\lambda - \omega} d\lambda \tag{7.17.6}$$

A one-sided impulse response can be regarded as a sum of **noncausal** even and odd parts (see Equations [7.3.2] and [7.3.3])

$$h(t) = h_e(t) + h_o(t) \tag{7.17.7}$$

because $h(t)$ is real, we have the following Fourier pairs:

$$h_e(t) = \frac{1}{2}\left[h(t) + h(-t)\right] \overset{F}{\Longleftrightarrow} A(\omega) \tag{7.17.8}$$

$$h_o(t) = \frac{1}{2}\left[h(t) - h(-t)\right] \overset{F}{\Longleftrightarrow} jB(\omega) \tag{7.17.9}$$

The causality of $h(t)$ yields the relations

$$h_e(t) = \text{sgn}(t) h_o(t) \tag{7.17.10}$$

$$h_o(t) = \text{sgn}(t)h_e(t) \tag{7.17.11}$$

These products are the time-domain representation of the convolution integrals (7.17.5) and (7.17.6) (convolution to multiplication theorem).

Physical Realizability of Transfer Functions

The Hilbert relations between real and imaginary parts of transfer functions are valid for physically realizable transfer functions. The terminology "physically realizable" may be misleading because a transfer function given by a closed algebraic form is a mathematical representation of a model of a circuit built using ideal inductances, capacitances, and resistors or amplifiers. Such models are a theoretical, approximate description of physical systems. The physical realizability of a particular transfer function in the sense of circuit (or systems) theory is defined by means of causality. A general question of whether a particular amplitude characteristic can be realized by a causal system (filter) is answered by the Paley-Wiener criterion. Consider a specific magnitude of a transfer function $|H(j\omega)|$ (an even function of ω). It can be realized by means of a causal filter if and only if the integral

$$\int_{-\infty}^{\infty} \frac{\ln\left|H\left(j\omega\right)\right|}{1+\omega^2} d\omega < \infty \tag{7.17.12}$$

is bounded.[28] Then a phase function exists such that the impulse response $h(t)$ is causal. The Paley-Wiener criterion is satisfied only if the support of $|H(j\omega)|$ is unbounded, otherwise $|H(j\omega)|$ would be equal to zero over finite intervals of frequency resulting in infinite values of the logarithm ($\ln|H(j\omega)| = -\infty$).

Minimum Phase Property

Transfer functions satisfying the Paley-Wiener criterion have a general form:

$$H(j\omega) = H_\varphi(j\omega)H_{ap}(j\omega) \tag{7.17.13}$$

where $H_\varphi(j\omega)$ is called a **minimum phase transfer function** and $H_{ap}(j\omega)$ is an all-pass transfer function. The minimum phase transfer function

$$H_\varphi(j\omega) = |H(j\omega)|e^{j\varphi(\omega)} = A_\varphi(\omega) + jB_\varphi(\omega) \tag{7.17.14}$$

has a minimum phase lag $\varphi(\omega)$ for a given magnitude characteristic. The minimum phase transfer function $H_\varphi(s)$ has all the zeros lying in the left half-plane (i.e., $\alpha < 0$) of the s-plane. The minimum phase transfer function is analytic and its real and imaginary parts form a Hilbert pair

$$A_\varphi\left(\omega\right) \overset{\text{H}}{\Longleftrightarrow} -B_\varphi\left(\omega\right) \tag{7.17.15}$$

An important feature of the minimum phase transfer function is that the **propagation function**

$$\gamma(s) = \ln[H(s)] = \beta(\alpha, \omega) + j\varphi(\alpha, \omega) \tag{7.17.16}$$

is analytic in the right half-plane. It is so because all zeros are in the left half-plane and, because we postulate stability, all poles are in the left half-plane, too. Then the real and imaginary part of the propagation function form a Hilbert pair:

$$\varphi(\omega) = \frac{-1}{\pi} P\int_{-\infty}^{\infty} \frac{\beta(\lambda)}{\lambda - \omega} d\lambda = \frac{-1}{\pi} P\int_{-\infty}^{\infty} \frac{\ln|H(j\lambda)|}{\lambda - \omega} d\lambda \tag{7.17.17}$$

$$\beta(\omega) = \frac{1}{\pi} P\int_{-\infty}^{\infty} \frac{\varphi(\lambda)}{\lambda - \omega} \tag{7.17.18}$$

These relations can be converted to take the form of the well-known **Bode phase-integral** theorem:

$$\varphi(\omega_0) = \frac{\pi}{2}\left|\frac{d\beta}{du}\right|_o + \frac{1}{\pi} P\int_{-\infty}^{\infty} \left[\left|\frac{d\beta}{du}\right| - \left|\frac{d\beta}{du}\right|_o\right] \ln\left[\coth|u/2|\right] du \tag{7.17.19}$$

where $u = \ln(\omega/\omega_0)$ is the normalized logarithmic frequency scale, and $d\beta/du$ is the slope of the β-curve in ln-ln scale. The Bode formula shows that for the minimum-phase transfer functions the phase depends on the slope of the β-curve (β is the damping coefficient). The factor $\ln[\coth|u/2|]$ is peaked at $u = 0$ (or $\omega = \omega_0$) and, hence, the phase at a given ω_0 is mostly influenced by the slope $d\beta/du$ in the vicinity of ω_0.

The all-pass part of the **nonminimum phase transfer function** defined by Equation (7.17.13) may be written in the form:

$$H_{ap}(j\omega) = e^{j\psi(\omega)} \tag{7.17.20}$$

Therefore, the total phase function has two terms:

$$\arg[H(j\omega)] = \varphi(\omega) + \psi(\omega) \tag{7.17.21}$$

where $\varphi(\omega)$ is the minimum phase and $\psi(\omega)$ the nonminimum phase part of the total phase.

Amplitude-Phase Relations in DLTI Systems

A discrete, linear, and time-invariant system (DLTI) is characterized by the Z-pair (see also Chapter 6)

$$h(i) \overset{Z}{\Longleftrightarrow} H(z); \quad z = e^{j\psi} \tag{7.17.22}$$

The sequence $h(i)$ ($i = 0, 1, 2, \ldots$) is the impulse response of the system to the excitation by the **Kronecker delta** and $H(z)$ is the one-sided Z transform of the impulse response called the transfer function (or frequency characteristic) of the DLTI system, a function of the **dimensionless** normalized frequency $\psi = 2\pi f/f_s$, where f is the actual frequency and f_s the sampling frequency. For causal systems the impulse response is one-sided ($h(i) = 0$ for $i < 0$). The transfer function $H(e^{j\psi})$ is periodic with the period equal to 2π. This periodic function may be expanded into a Fourier series

$$H(e^{j\psi}) = \sum_{i=-\infty}^{\infty} h(i) e^{-j\psi i} = \sum_{i=0}^{\infty} h(i) e^{-j\psi i} \tag{7.17.23}$$

The Fourier coefficients $h(t)$ are equal to the terms of the impulse response and are given by the Fourier integral:

$$h(i) = \frac{1}{2\pi}\int_{-\pi}^{\pi} H\left(e^{j\psi}\right)e^{j\psi i}d\psi \tag{7.17.24}$$

In general, the transfer function is a complex quantity

$$H(e^{j\psi}) = A(\psi) + jB(\psi) \tag{7.17.25}$$

Analogously to Equation (7.17.7) the causal impulse response $h(i)$ can be regarded as a sum of two noncausal even and odd parts of the form

$$h(i) = h(0) + h_e(i) + h_0(i) \tag{7.17.26}$$

The even part is defined by the equation

$$h_e(i) = 0.5[h(i) + h(-i)]; \quad |i| > 0 \tag{7.17.27}$$

and the odd part by the equation:

$$h_0(i) = 0.5[h(i) - h(-i)] \tag{7.17.28}$$

Let us write the Fourier series (7.17.23) term-by-term. We get

$$H\left(e^{j\psi}\right) = h(0) + \sum_{i=1}^{\infty} h(i)\cos(\psi i) - j\sum_{i=1}^{\infty} h(i)\sin(\psi i) \tag{7.17.29}$$

The comparison of Equations (7.17.25) and (7.17.29) shows that

$$H(\psi) = h(0) + \sum_{i=1}^{\infty} h(i)\cos(\psi i) = h(0) + F^{-1}\left[h_e(i)\right] \tag{7.17.30}$$

and

$$B(\psi) = -\sum_{i=1}^{\infty} h(i)\sin(\psi i) = F^{-1}\left[h_0(i)\right] \tag{7.17.31}$$

and we have a Hilbert pair:

$$A(\psi) \overset{\mathrm{H}}{\Longleftrightarrow} B(\psi) \tag{7.17.32}$$

We used the relations $H[h(0)] = 0$ and $H[\cos(\psi i)] = \sin(\psi i)$. Because $A(\psi)$ and $B(\psi)$ are periodic functions of ψ, we may apply the cotangent form of the Hilbert transform (see Section 7.6).

$$B(\psi) = \frac{1}{2\pi}P\int_{-\pi}^{\pi} A(\Theta)\cot\left[(\Theta - \psi)/2\right]d\Theta \tag{7.17.33}$$

and

$$A(\psi) = h(0) - \frac{1}{2\pi} P\int_{-\pi}^{\pi} B(\Theta)\cot\left[(\Theta - \psi)/2\right] d\Theta \tag{7.17.34}$$

Minimum Phase Property in DLTI Systems

Analogous to Equations (7.17.13) and (7.17.14) the transfer function of the DLTI system may be written in the form:

$$H(z) = H_{\varphi}(z)H_{ap}(z) \tag{7.17.35}$$

where $H_{\varphi}(z)$ satisfies the constraints of a **minimum phase transfer function**; that is, has all the zeros inside the unit circle of the z-plane and $H_{ap}(z)$ is an **all-pass function** consisting of a cascade of factors of the form:

$$H_{ap}(z) = \left[z^{-1} - z_i\right] / \left[1 - z_i^* z^{-1}\right] \tag{7.17.36}$$

The all-pass function has a magnitude of one, hence, $H(z)$ and $H_{\varphi}(z)$ have the same magnitude. $H_{\varphi}(z)$ differs from $H(z)$ in that the zeros of $H(z)$, lying outside the unit circle at points $z = 1/z_i$, are reflected inside the unit circle at $z = z_i^*$. Let us take the complex logarithm of $H_{\varphi}(e^{j\psi})$:

$$\ln[H_{\varphi}(e^{j\psi})] = \ln|H_{\varphi}(e^{j\psi})| + j\ \arg[H_{\varphi}(e^{j\psi})] \tag{7.17.37}$$

and analogous to Equations (7.17.17) and (7.17.18), we have a Hilbert pair

$$\ln\left|H_{\varphi}\left(e^{j\psi}\right)\right| = \ln\left[h(0)\right] - \frac{1}{2\pi} P\int_{-\pi}^{\pi} \arg\left[H_{\varphi}\left(e^{j\Theta}\right)\right]\cot\left[(\Theta - \psi)/2\right] \tag{7.17.38}$$

$$\arg\left[H_{\varphi}\left(e^{j\Theta}\right)\right] = \frac{1}{2\pi} P\int_{-\pi}^{\pi} \log\left|H_{\varphi}\left(e^{j\Theta}\right)\right|\cot\left[(\Theta - \psi)/2\right] d\Theta \tag{7.17.39}$$

It can be proved that the relations (7.17.38) and (78.17.39) are valid for transfer functions with zeros on the unit circle. In general, a stable and causal system has all its poles inside, while its zero may lie outside the unit circle. However, starting from a nonminimum-phase transfer function, a minimum-phase function can be constructed by reflecting those zeros lying outside the unit circle, inside it.

Kramers–Kronig Relations in Linear Macroscopic Continuous Media

The amplitude-phase relations of the circuit theory are known in the macroscopic theory of continuous lossy media as the Kramers–Kronig relations.[18,19] Almost all media display some degree of frequency dependence of some parameters, called **dispersion**. Let us take the example of a linear and isotropic electromagnetic medium. The simplest constitutive macroscopic relations describing this medium are[32]

$$D = \varepsilon\varepsilon_o E = (1 + \chi_e)\varepsilon_o E \tag{7.17.40}$$

$$B = \mu\mu_o H = (1 + \chi_m)\mu_o H \tag{7.17.41}$$

and

$$P = \chi_e \varepsilon_o E \tag{7.17.42}$$

$$M = \chi_m H \tag{7.17.43}$$

where $E[V/m]$ is the electric field vector, $H[A/m]$ is the magnetic field vector, $D[C/m^2]$ is the electric displacement, $B[Wb/m^2]$ is the magnetic induction, $\mu_o = 4\pi\ 10^{-7}[Hy/m]$ the permeability, $\varepsilon_0 = 1/36\pi\ 10^{-9}[F/m]$ the permittivity of free space, and ε, μ, χ_m, and χ_e are dimensionless constants. The vectors P and M are called polarization and magnetization of the medium. If we substitute the electrostatic field vector E with a field varying in time as $\exp(j\omega t)$, then the properties of the medium are described by the frequency-dependent complex susceptibility

$$\chi(j\omega) = \chi'(\omega) - j\chi''(\omega) \tag{7.17.44}$$

where χ' is an even and χ'' an odd function of ω. The imaginary term χ'' represents the conversion of electric energy into heat; that is, losses of the medium. In fact, $\chi(j\omega)$ plays the same role as the transfer function in circuit theory and is defined by the equation:

$$\chi\left(j\omega\right) = \frac{P_m e^{j\left(\omega t+\varphi\right)}}{\varepsilon_o E_m e^{j\omega t}} = \frac{P_m}{\varepsilon_o E_m} e^{j\varphi} \tag{7.17.45}$$

Let us apply Fourier spectral methods to examine Equations (7.17.42) and (7.17.45). We consider a disturbance $E(t)$ given by the Fourier pair

$$E\left(t\right) \overset{F}{\Longleftrightarrow} \mathbf{X}_E\left(j\omega\right) \tag{7.17.46}$$

The response $P(t)$ is represented by the Fourier pair:

$$P\left(t\right) \overset{F}{\Longleftrightarrow} \mathbf{X}_p\left(j\omega\right) \tag{7.17.47}$$

where

$$\mathbf{X}_p(j\omega) = \varepsilon_o \chi\ (j\omega)\mathbf{X}_E(j\omega) \tag{7.17.48}$$

The multiplication-convolution theorem yields the time-domain solution:

$$P\left(t\right) = \varepsilon_o \int_{-\infty}^{\infty} h\left(\tau\right) E\left(t-\tau\right) d\tau \tag{7.17.49}$$

where $h(t)$ is given by the Fourier pair

$$h\left(t\right) \overset{F}{\Longleftrightarrow} \chi\left(j\omega\right) \tag{7.17.50}$$

is the "impulse response" of the medium; that is, the response to the excitation $\delta\ (t\ )$. For any physical medium, the impulse response is causal. This is possible if $\chi\ (j\omega\ )$ is analytic. Therefore, its real and imaginary parts form a Hilbert pair

$$\chi''\left(\omega\right) = -\frac{1}{\pi} P \int_{-\infty}^{\infty} \frac{\chi'\left(\eta\right)}{\eta-\omega} d\eta \tag{7.17.51}$$

$$\chi'(\omega) = \frac{1}{\pi} P \int_{-\infty}^{\infty} \frac{\chi''(\eta)}{\eta - \omega} d\eta \tag{7.17.52}$$

These relations are known as the Kramers–Kronig relations and are a direct consequences of causality. They apply for many media; for example, in optics, the real and imaginary parts of the complex reflection coefficient form a Hilbert pair.

Concept of Signal Delay in Hilbertian Sense

Consider a signal and its Fourier transform:

$$x(t) \overset{F}{\Longleftrightarrow} X(j\omega) \tag{7.17.53}$$

Let us assume that the Fourier spectrum $X(j\omega)$ may be written in the form of a product defined by Equation (7.17.13)

$$X(j\omega) = X_1(j\omega)\, X_2(j\omega) \tag{7.17.54}$$

where $X_1(j\omega)$ fulfills the constraints of a minimum-phase function and $X_2(j\omega)$ is an "all-pass" function of the magnitude equal to one and the phase function $\psi(\omega)$; that is, $X_2(j\omega) = e^{j\psi(\omega)}$. The application of the convolution-multiplication theory yields the convolution

$$x(t) = x_1(t) * x_2(t) \tag{7.17.55}$$

where $x_1(t) \overset{F}{\Longleftrightarrow} X_1(j\omega)$ is defined as a minimum-phase signal satisfying relations (7.17.17) and (7.17.18); that is,

$$\arg\left[X_1(j\omega)\right] \overset{H}{\Longleftrightarrow} \ln\left|X_1(j\omega)\right| \tag{7.17.56}$$

and the signal

$$x_2(t) \overset{F}{\Longleftrightarrow} X_2(j\omega) = e^{j\psi(\omega)} \tag{7.17.57}$$

is defined as the nonminimum-phase part of the signal $x(t)$. Let us formulate the following definitions:

Definition 1
The minimum phase signal $x_1(t)$ has a zero delay in the Hilbert sense.

Definition 2
The delay of the signal relative to the moment $t = 0$ is defined by a specific property of the signal $x_2(t)$. Krylov and Ponomariev[20] used the name "ambiguity function" for $x_2(t)$ and proposed to define the delay by the position of its maximum. Another possibility is to define the delay using the position of the center of gravity of $x_2(t)$.

Examples

1. If the function $x_2(t) = \delta(t)$, the delay equals zero because

$$x(t) = x_1(t) * \delta(t) = x_1(t) \tag{7.17.58}$$

2. If the function $x_2(t) = \delta(t - t_0)$, the delay equals t_0 because

$$x(t) = x_1(t) * \delta(t - t_0) = x_1(t - t_0) \tag{7.17.59}$$

3. Consider a phase-delayed harmonic signal and its Fourier image:

$$\cos\left(\omega_0 t - \varphi_0\right) \overset{F}{\Longleftrightarrow} \pi\delta\left(\omega + \omega_0\right)e^{j\varphi_0} + \pi\delta\left(\omega - \omega_0\right)e^{-j\varphi_0} \tag{7.17.60}$$

or

$$\cos\omega_0 t * \delta\left(t - \frac{\varphi_0}{\omega_0}\right) \overset{F}{\Longleftrightarrow} \pi\left[\delta\left(\omega + \omega_0\right) + \delta\left(\omega - \omega_0\right)\right]e^{-j\varphi_0 \operatorname{sgn}\omega} \tag{7.17.61}$$

Evidently the "ambiguity function" $x_2(t)$ is

$$x_2\left(t\right) = \delta\left(t - \frac{\varphi_0}{\omega_0}\right) \overset{F}{\Longleftrightarrow} e^{-j\varphi_0 \operatorname{sgn}\omega} \tag{7.17.62}$$

and the time delay is, of course, $t_0 = \varphi_0/\omega_0$, as we could expect.

4. Consider the series connection of the first-order low-pass with the transfer function

$$X_1\left(j\omega\right) = \frac{1}{1 + j\omega\tau} \tag{7.17.63}$$

and the first-order all-pass with the phase function of the form

$$\arg\left[X_2\left(j\omega\right)\right] = \tan^{-1}\frac{2\omega\tau}{\left(\omega\tau\right)^2 - 1} \tag{7.17.64}$$

The impulse response of the low-pass is:

$$x_1\left(t\right) = \mathrm{F}^{-1}\left[\frac{1}{1 + j\omega\tau}\right] = 1\left(t\right)e^{-t/\tau} \tag{7.17.65}$$

and satisfies the definition of the minimum-phase signal. The impulse response of the all-pass plays here the role of the "ambiguity function" and has the form:

$$x_2\left(t\right) = \mathrm{F}^{-1}\left[\exp\frac{-2\omega\tau}{\omega^2\tau^2 - 1}\right] = 1\left(t\right)\frac{2}{\tau}e^{-t/\tau} - \delta\left(t\right)$$

We observe that the maximum of $x_2(t)$ is at $t = 0$. However, we expect that the all-pass introduces some delay. In this case it would be advisable to define the delay using the center of gravity of the signal $x_2(t)$.

7.18 Hilbert Transforms in the Theory of Sampling

The generation of a sequence of samples of a continuous signal (sampling) and the recovery of this signal from its samples (interpolation) is a widely used procedure in modern signal processing and communications techniques. Basic and advanced theory of sampling and interpolation is presented in many textbooks. This section presents the role of Hilbert transforms in the theory of sampling and interpolation. Figure 7.18.1, for reference, is the usual means by which the sequence of samples is produced. In general, the sampling pulses may be nonequidistant. However, this section presents the role of Hilbert transforms in the basis **WKS** (Wittaker, Kotielnikow, Shannon) theory of periodic sampling and interpolation.

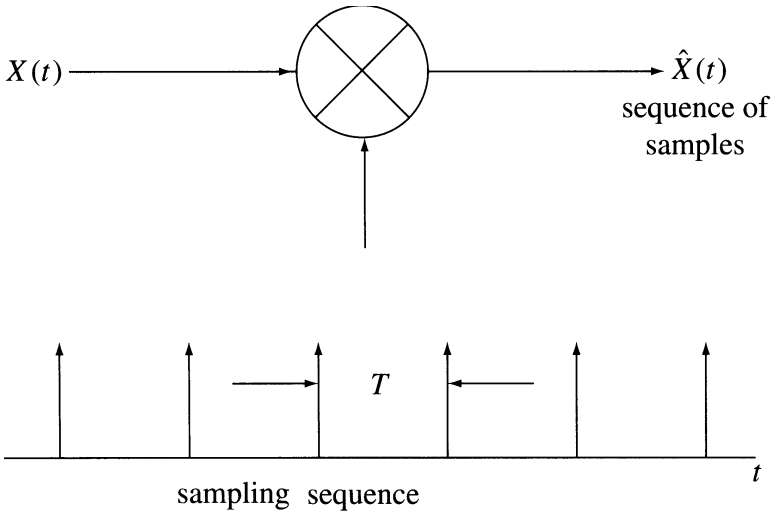

FIGURE 7.18.1 A method of generation of a sequence $\hat{x}(t)$ of samples of the analog signal $x(t)$.

The periodic sequence of sampling pulses may be written in the form (see Equation [7.6.4])

$$p(t) = p_T(t) * \sum_{k=-\infty}^{\infty} \delta(t - kT) \tag{7.18.1}$$

where $p_T(t)$ defines the waveform of the sampling pulse (the generating function of the periodic sequence of pulses) and $f = 1/T$ is the sampling frequency. From the point of view of the presentation of the role of Hilbert transforms in sampling and interpolation, it is sufficient to use the delta sampling sequence inserting $p_T(t) = \delta(t)$. The **delta sampling sequence** is given by the formula (remember that $\delta(t) * \delta(t) = \delta(t)$)

$$p(t) = \sum_{k=-\infty}^{\infty} \delta(t - kT) \tag{7.18.2}$$

For convenience, let us write here the Hilbert transform of this sampling sequence (see Section 7.6, Equation [7.6.18])

$$\sum_{k=-\infty}^{\infty} \delta(t - nT) \overset{\mathrm{H}}{\Longleftrightarrow} \frac{1}{T} \sum_{k=-\infty}^{\infty} \cot\left[(\pi/T)(t - kT)\right] \tag{7.18.3}$$

The Fourier image of the delta sampling sequence is given by another periodic delta sequence

$$\sum_{k=-\infty}^{\infty}\delta\left(t-kT\right)\overset{F}{\Longleftrightarrow}\frac{1}{T}\sum_{k=-\infty}^{\infty}\delta\left(f-k/T\right) \tag{7.18.4}$$

The sampler produces as an output a sequence of samples given by the formula

$$x_s\left(t\right)=\sum_{k=-\infty}^{\infty}x\left(kT\right)\delta\left(t-kT\right) \tag{7.18.5}$$

that is, a sequence of delta functions weighted by the samples of the signal $x(t)$. Let us recall the basic WKS sampling theorem. Consider a signal $x(t)$ and its Fourier image $X(f)$, $\omega = 2\pi f$. If the Fourier image is low-pass band limited, i.e., $|X(jf)| = 0$ for $|f| > W$, then $x(t)$ is completely determined by the sequence of its samples taken at the moments t_k spaced $T = 1/2W$ apart. The sampling frequency $f_s = 2W$ is called the Nyquist rate. The multiplication to convolution theorem yields the spectrum of the sequence of samples

$$X_s\left(jf\right)=X\left(jf\right)*\frac{1}{T}\sum_{k=-\infty}^{\infty}\delta\left(f-k/T\right) \tag{7.18.6}$$

Figure 7.18.2 shows an example of a low-pass band-limited spectrum of a signal $x(t)$ and the well-known three spectra of the sequence of samples: the spectrum of oversampled signal with no aliasing with the sampling frequency $f_s = 1/T > 2W$, the limit case with $f_s = 2W$, and the spectrum of undersampled signal with $f_s < 2W$. Notice that the sequence of samples given by Equation (7.18.5) may be regarded as a model of a signal with pulse amplitude modulation (PAM). The original signal $x(t)$ may be recovered by filtering this PAM signal using the ideal noncausal and physically unrealizable low-pass filter defined by the transfer function

$$Y\left(jf\right)=\begin{cases}1 & \text{for } \left|f\right|<W\\ 0.5 & \text{for } \left|f\right|=W\\ 0 & \text{for } \left|f\right|>W\end{cases} \tag{7.18.7}$$

The noncausal impulse response of this filter is

$$h\left(t\right)=F^{-1}\left[Y\left(jf\right)\right]=2W\frac{\sin\left(2\pi Wt\right)}{2\pi Wt} \tag{7.18.8}$$

and is called the **interpolatory function**. The total response is a sum of responses to succeeding samples giving the well-known **interpolatory expansion** ($f_s = 2W$):

$$x\left(t\right)=\sum_{k=-\infty}^{\infty}x\left[\frac{k}{2W}\right]\frac{\sin\left[2\pi W\left(t-\dfrac{k}{2W}\right)\right]}{2\pi W\left(t-\dfrac{k}{2W}\right)} \tag{7.18.9}$$

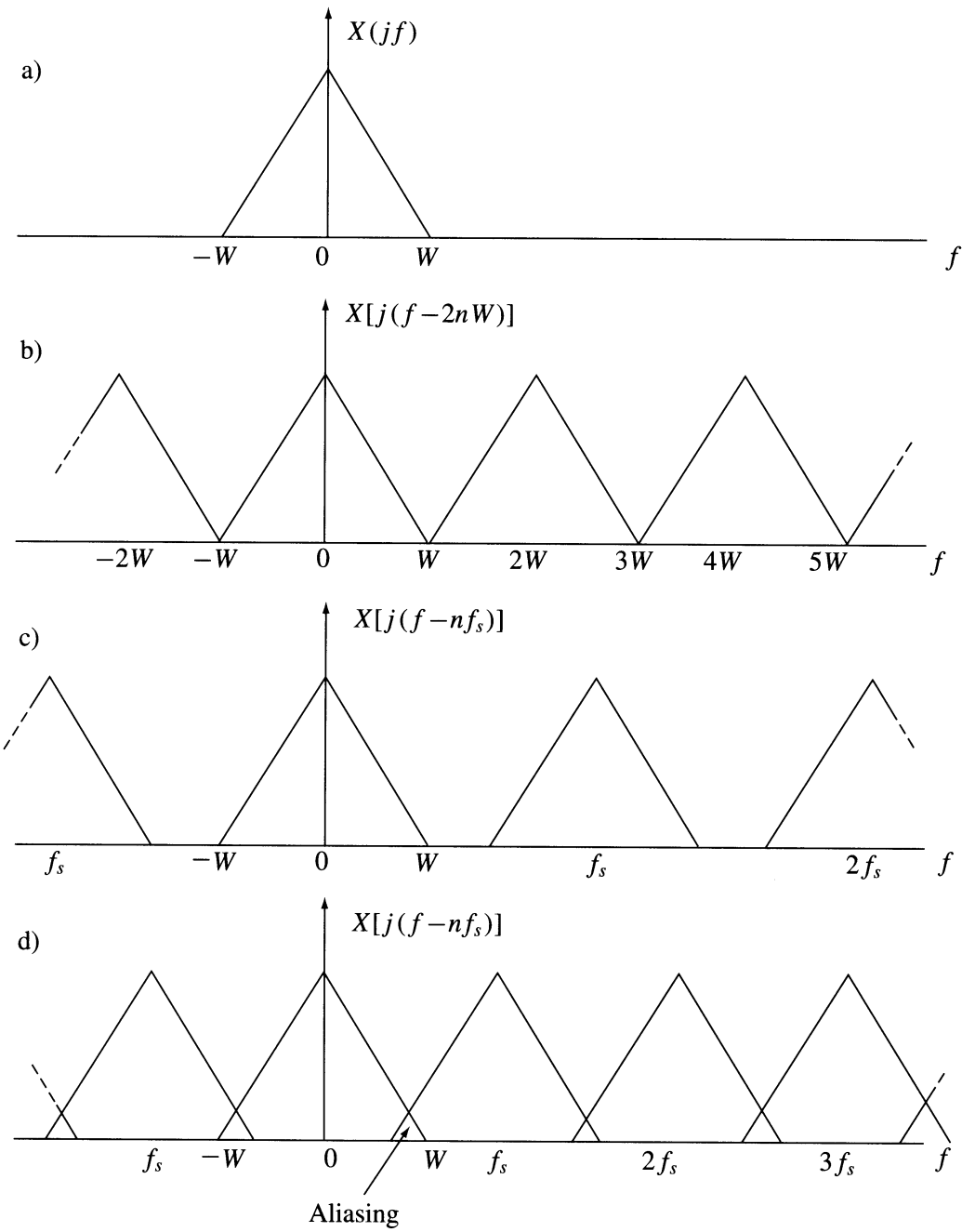

FIGURE 7.18.2 (a) A band-limited low-pass spectrum of a signal, (b) the corresponding spectrum of the sequence of sampled with Nyquist rate of sampling $f_s < 2W$, (c) spectrum by oversampling $f_s > 2W$, and (d) spectrum by undersampling $f_s < 2W$ showing the aliasing of the sidebands.

The summation exactly restores the original signal $x(t)$. In the following text the argument of the interpolatory function will be written using the notation

$$2\alpha\left(t,k\right) = 2\pi W\left(t - \frac{k}{2W}\right) \tag{7.18.10}$$

giving the following form of the interpolation expansion

$$x(t) = \sum_{k=-\infty}^{\infty} x\left(\frac{k}{2W}\right) \frac{\sin[2\alpha(t,k)]}{2\alpha(t,k)} \tag{7.18.11}$$

Notice that the sampling of the function $x(t) = a$ (a constant) yields the formula

$$\sum_{k=-\infty}^{\infty} \frac{\sin[2\alpha(t,k)]}{2\alpha(t,k)} = 1 \tag{7.18.12}$$

This equation may be used to calculate the accuracy of the interpolation due to any truncation of the summation.

The Whittaker's interpolatory function and its Hilbert transform are forming the Hilbert pair

$$\frac{\sin[2\alpha(t,k)]}{2\alpha(t,k)} \overset{\text{H}}{\Longleftrightarrow} \frac{\sin^2[\alpha(t,k)]}{\alpha(t,k)} \tag{7.18.13}$$

Therefore, the interpolatory expansion of the Hilbert transform $H[x(t)] = \hat{x}(t)$, due to the linearity property, is given by the formula

$$\hat{x}(t) = \sum_{k=-\infty}^{\infty} x\left[\frac{k}{2W}\right] \frac{\sin^2[\alpha(t,k)]}{\alpha(t,k)} \tag{7.18.14}$$

This formula may be applied to calculate the Hilbert transforms of low-pass signals using their samples. The transfer function of the low-pass Hilbert filter (transformer) is given by the Fourier transform of the impulse response given by the right-hand side of Equation (7.18.13):

$$\begin{aligned} Y_H(jf) &= F\left[\frac{\sin^2(\alpha,k)}{\alpha(t,k)}\right] \\ &= -j\,\mathrm{sgn}(f)Y(jf) \\ &= \begin{cases} j & \text{for } |f| < W \\ 0 & \text{for } f = 0\,; \quad 0.5 \text{ for } |f| \\ -j & \text{for } |f| < W \end{cases} \end{aligned} \tag{7.18.15}$$

The sampling of the function $x(t) = a$ yields

$$\sum_{k=-\infty}^{\infty} \frac{\sin^2[\alpha(t,k)]}{\alpha(t,k)} = 0 \tag{7.18.16}$$

The expansion of the analytic signal $\psi(t) = x(t) + j\,\hat{x}(t)$ using interpolatory functions has the form

$$\psi(t) = \sum_{k=-\infty}^{\infty} x\left[\frac{k}{2W}\right]\left[\frac{\sin[2\alpha(t,k)]}{2\alpha(t,k)} + j\frac{\sin^2[\alpha(t,k)]}{\alpha(t,k)}\right] \tag{7.18.17}$$

and using trigonometric identities we get the following form of the interpolatory expansion of the analytic signal:

$$\psi(t) = -j\sum_{k=-\infty}^{\infty} x\left[\frac{k}{2W}\right]\frac{e^{j2\alpha(t,k)} - 1}{2\alpha(t,k)} \tag{7.18.18}$$

Band-Pass Filtering of the Low-Pass Sampled Signal

Consider the ideal band-pass with a physically unrealizable transfer function in the form of a "spectral window" as shown in Figure 7.18.3. The impulse response of this filter is

$$h(t) = 2(f_2 - f_1)\frac{\sin[\pi(f_2 - f_1)]}{\pi(f_2 - f_1)t}\cos[\pi(f_1 + f_2)t] \tag{7.18.19}$$

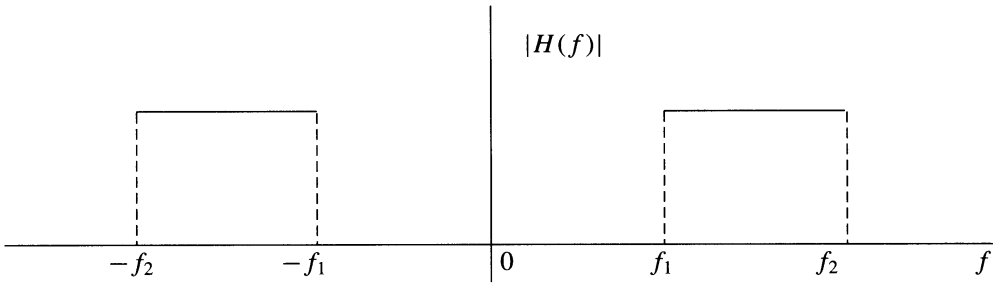

FIGURE 7.18.3 The magnitude of the transfer function of an ideal band-pass.

The insertion $f_1 = W$ and $f_2 = 3W$ yields

$$h(t) = 4W\frac{\sin(2\pi Wt)}{2\pi Wt}\cos(4\pi Wt) \tag{7.18.20}$$

If the sequence of samples of the signal $x(t)$ is applied to the input of this band-pass, the output signal $z(t)$ is given by the interpolatory expansion of the form

$$z(t) = \sum_{k=-\infty}^{\infty}\left\{x(k/(2W))\frac{\sin[2\alpha(t,k)]}{2\alpha(t,k)}\cos[4\alpha(t,k)]\right\} \tag{7.18.21}$$

where $\alpha(t,k)$ is given by Equation (7.18.10). We obtained the compressed-carrier amplitude-modulated signal of the form

$$z(t) = x(t)\cos(4\pi Wt) \tag{7.18.22}$$

with a carrier frequency $2W$. Therefore, the AM-balanced modulator may be implemented using a sampler and a band-pass. Multiplication of the carrier frequency is possible using band-pass filters with $f_1 = 3W$ and $f_2 = 5W$ or $f_1 = 5W$ and $f_2 = 7W$, …. The conclusion is that in principle one may multiply the carrier frequency of AM signals getting undistorted sidebands (envelope). The comparison of Equations (7.18.11) and (7.18.22) enables us to write the signal $z(t)$ in the form:

$$z(t) = \left\{\sum_{k=-\infty}^{\infty} x\left[\frac{k}{2W}\right]\frac{\sin\left[2\alpha(t,k)\right]}{2\alpha(t,k)}\right\}\cos(4\pi Wt) \tag{7.18.23}$$

and because $\cos(4\pi Wt - k2\pi) = \cos(4\pi Wt)$, in the form

$$z(t) = \sum_{k=-\infty}^{\infty} x\left[\frac{k}{2W}\right]\frac{\sin\left[2\alpha(t,k)\right]}{2\alpha(t,k)}\cos(4\pi Wt) \tag{7.18.24}$$

Analogously, a single side-band AM signal may be produced by band-pass filtering of the sequence of samples using a filter with $f_1 = 2W$ and $f_2 = 3W$ (upper sideband). The impulse response of this filter is

$$h(t) = 2W\frac{\sin(\pi Wt)}{\pi Wt}\cos(5\pi Wt) \tag{7.18.25}$$

and the interpolatory expansion is:

$$z_{\mathrm{SSB}}(t) = \sum_{k=-\infty}^{\infty} x\left[\frac{k}{2W}\right]\frac{\sin\left[2\alpha(t,k)\right]}{\alpha(t,k)}\cos\left[5\alpha(t,k)\right] \tag{7.18.26}$$

This SSB signal may be written in the standard form given by Equation (7.16.16) (see Section 7.16)

$$z_{\mathrm{SSB}}(t) = x(t)\cos(4\pi Wt) - \hat{x}(t)\sin(4\pi Wt) \tag{7.18.27}$$

Let us derive the above form starting with Equation (7.18.25). Using the trigonometric identity $\cos(5\alpha) = \cos\alpha\cos(4\alpha) - \sin\alpha\sin(4\alpha)$, Equation (7.18.26) becomes

$$z_{\mathrm{SSB}}(t) = \sum_{k=-\infty}^{\infty} x\left[\frac{k}{2W}\right]\left\{\frac{\sin\left[2\alpha(t,k)\right]}{2\alpha(t,k)}\cos\left[4\alpha(t,k)\right] - \frac{\sin^2\left[\alpha(t,k)\right]}{\alpha(t,k)}\sin\left[4\alpha(t,k)\right]\right\} \tag{7.18.28}$$

It may be shown in the same manner as before that Equations (7.18.27) and (7.18.28) have identical left-hand sides.

Sampling of Band-Pass Signals

Consider a band-pass signal $f(t)$ with the spectrum limited in band $f_1 < |f| < f_2 = f_1 + W$ (see Figure 7.18.4). In general, a so-called second-order sampling should be applied to recover, using interpolation, the signal $f(t)$. However, it may be shown that alternatively, first-order sampling at the rate W may be applied with simultaneous sampling of the signal $f(t)$ and of its Hilbert transform $H[f(t)] = \hat{f}(t)$. The following interpolation formula has to be applied to recover the signal using the sequences of samples $f(k/W)$ and $\hat{f}(k/W)$.

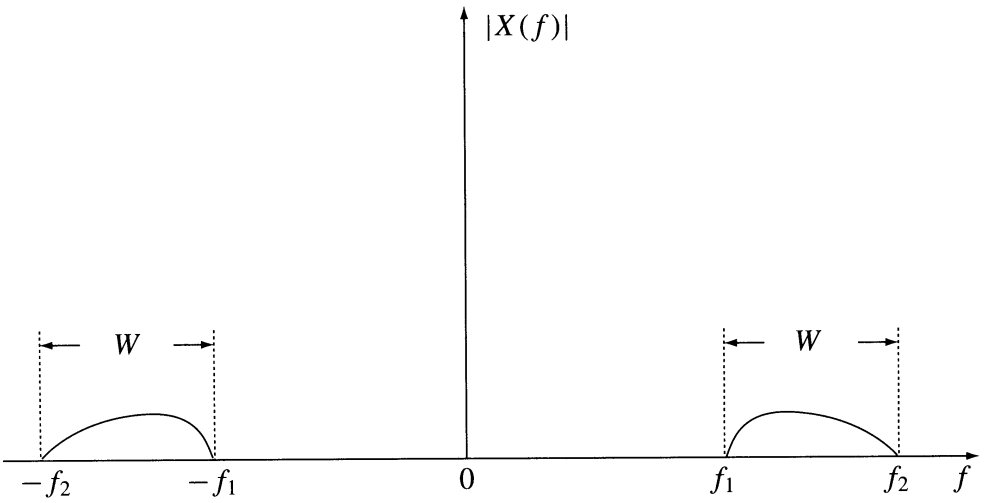

FIGURE 7.18.4 The magnitude of the spectrum of a band-pass signal.

$$f(t) = \sum_{k=-\infty}^{\infty} f\left(\frac{n}{W}\right) s\left(t - \frac{n}{W}\right) + \hat{f}\left(\frac{n}{W}\right) \hat{s}\left(t - \frac{n}{W}\right) \tag{7.18.29}$$

where the interpolating functions are given by the impulse response of the band-pass

$$s(t) = \frac{\sin(\pi W t)}{\pi W t} \cos\left[2\pi\left(f_1 + \frac{W}{2}\right)t\right] \tag{7.18.30}$$

and of a band-pass Hilbert filter (see Section 7.21)

$$\hat{s}(t) = \frac{\sin(\pi W t)}{\pi W t} \sin\left[2\pi\left(f_1 + \frac{W}{2}\right)t\right] \tag{7.18.31}$$

7.19 Definition of Electrical Power in Terms of Hilbert Transforms and Analytic Signals

The problem of efficient energy transmission from the source to the load is of importance in electrical systems. Usually the voltage and current waveforms may be regarded as sinusoidal. However, many loads are nonlinear and, therefore, nonsinusoidal cases should be investigated. In many applications the voltages and currents are nearly periodic, unperiodic, or even random. Therefore, some generalizations of theories developed for periodic cases are needed.

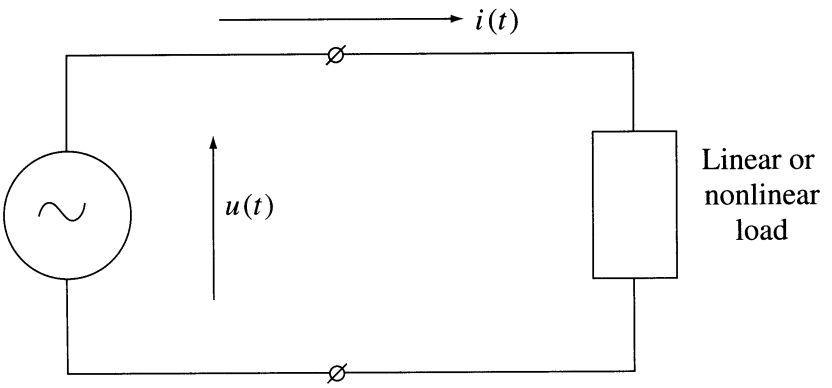

FIGURE 7.19.1 An electrical one-port where $u(t)$ is the instantaneous voltage and $i(t)$ the instantaneous current.

Consider an electrical one-port (linear or nonlinear) as shown in Figure 7.19.1. The **instantaneous power** is defined by the equation:

$$P(t) = u(t)i(t) \tag{7.19.1}$$

where $u(t)$ is the instantaneous voltage across the load and $i(t)$ the instantaneous current in the load. We arbitrarily assign a positive sign to P if the energy $P(t)dt$ is delivered from the source to the load and a negative sign for the opposite direction. The above formal definition of power involves **all limitations** associated with the definition of voltage, current, and the electrical one-port.

Let us introduce the notion of **quadrature instantaneous power** defined by the equation

$$Q(t) = u(t)\hat{i}(t) = -\hat{u}(t)i(t) \tag{7.19.2}$$

where $\hat{u}$ and $\hat{i}$ are Hilbert transforms of the voltage and current waveforms.

Harmonic Waveforms of Voltage and Current

Consider the classical case of a linear load with sine waveforms of $u(t)$ and $i(t)$. We have

$$u(t) = U\cos(\omega t + \varphi_u) \tag{7.19.3}$$

$$i(t) = J\cos(\omega t + \varphi_i) \tag{7.19.4}$$

The instantaneous power is

$$P(t) = U\,J\cos(\omega t + \varphi_u)\cos(\omega t + \varphi_i) \tag{7.19.5}$$

The Fourier series expansion of $P(t)$ is

$$P(t) = 0.5U\,J\cos(\varphi_i - \varphi_u) + 0.5U\,J\,[\cos[2(\omega t + \varphi_i)]\cos(\varphi_i - \varphi_u) - \sin[2(\omega t + \varphi_i)]\sin(\varphi_i - \varphi_u)] \tag{7.19.6}$$

The instantaneous quadrature power is

$$Q(t) = U\,J\cos(\omega t + \varphi_u)\sin(\omega t + \varphi_i) \tag{7.19.7}$$

The Fourier series expansion of $Q(t)$ is

$$Q(t) = 0.5U\,J\,\sin(\varphi_i - \varphi_u) + 0.5U\,J\,[\sin[2(\omega t + \varphi_i)]\,\cos(\varphi_i - \varphi_u) + \cos[2(\omega t + \varphi_i)]\,\sin(\varphi_i - \varphi_u)] \tag{7.19.8}$$

The mean value of $P(t)$ defined by the equation

$$\overline{P} = \frac{1}{T}\int_0^T P(t)\,dt = 0.5U\,J\cos(\varphi_i - \varphi_u); \quad \omega = \frac{2\pi}{T} \tag{7.19.9}$$

is called the **active power** and it is a measure of the unilatral energy transfer from the source to the load. The mean value of the quadrature power $Q(t)$ defined by the equation

$$\overline{Q} = \frac{1}{T}\int_0^T Q(t)\,dt = 0.5U\,J\sin(\varphi_i - \varphi_u) \tag{7.19.10}$$

is called the **reactive power**. The value of the reactive power depends on energy that is delivered periodically back and forth between the source and the load with no net transfer. The waveform of the instantaneous power given by Equation (7.19.6) is shown in Figure 7.19.2 (for convenience $\varphi_u = 0$). The energy transfer from the source to the load is given by the integral

$$E_+ = \frac{1}{\omega}\int_{-\pi/2}^{\pi/2-\varphi_i} U\,I\cos(\omega t)\cos(\omega t + \varphi_i)\,d\omega t = \frac{U\,I}{2\omega}\left[(\pi - \varphi)\cos\varphi + \sin\varphi\right] \tag{7.19.11}$$

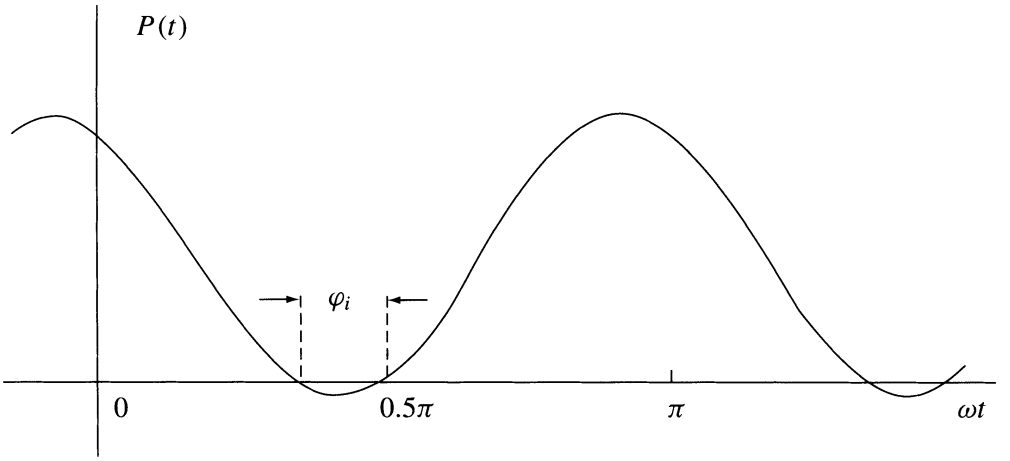

FIGURE 7.19.2 The waveform of the instantaneous power given by Equation (7.19.5).

and the energy transfer from the load to the source during the remaining part of the half-period is

$$E_- = \frac{1}{\omega}\int_{\pi/2-\varphi_i}^{\pi/2} U\,I\cos(\omega t)\cos(\omega t + \varphi_i)\,d\omega t = \frac{U\,I}{2\omega}\left[\varphi\cos\varphi - \sin\varphi\right] \tag{7.19.12}$$

Therefore, the net energy transfer toward the load is

$$E = E_+ - E_- = \frac{U\,I\,T}{4}\cos(\varphi_i) \tag{7.19.13}$$

The division of this energy by $0.5T$ gives the mean value of the power equal to the active power. However, the division of E_- by $0.5T$ yields

$$\overline{P}_- = \frac{2E}{T}\left[\varphi \cos \varphi_i - \sin \varphi_i\right] \tag{7.19.14}$$

and this mean power differs from the reactive power defined by Equation (7.19.10). Therefore, the notions of active and reactive power differ considerably. The active power equals the time-independent or constant term of the instantaneous power given by the Fourier series (7.19.6) while the reactive power equals the amplitude of the quadrature (or sine) term of (7.19.6). Notice that in the Fourier series (7.19.8) the role of both quantities is reversed. Let us recall that the quantity

$$S = 0.5UJ = U_{\mathrm{RMS}}\, J_{\mathrm{RMS}} \tag{7.19.15}$$

is called the **apparent power** and the quantity

$$\rho = \cos\left(\varphi_i - \varphi_u\right) = \frac{\overline{P}}{S} \tag{7.19.16}$$

is called the **power factor**. The power factor may be regarded as a normalized correlation coefficient of the voltage and current signals while $\sin(\varphi_i - \varphi_u) = SQR(1 - \rho^2)$ may be called the anticorrelation coefficient. The quantities S, $\overline{P}$, and $\overline{Q}$ satisfy the relation

$$S^2 = \overline{P}^2 + \overline{Q}^2 \tag{7.19.17}$$

Notion of Complex Power

Consider the analytic (complex) form of the voltage and current harmonic signals defined by Equations (7.19.3) and (7.19.4). We have $\psi_u(t) = U \exp(\omega t + \varphi_u)$ and $\psi_i(t) = J \exp(\omega t + \varphi_i)$. The complex power is defined by the equation:

$$S = \frac{1}{2}\psi_u\left(t\right)\psi^*_i\left(t\right) = 0.5U\, J \exp\left[j\left(\varphi_i - \varphi_u\right)\right] \tag{7.19.18}$$

In the following text, the symbol S will be used to denote the complex power. We have

$$S = P + j\,Q = |S| \exp[j(\varphi_i - \varphi_u)] \tag{7.19.19}$$

The real part of S equals the active power and the imaginary part equals the reactive power. The module of the complex power equals the apparent power and the argument equals the phase angle $\varphi_i - \varphi_u$.

Generalization of the Notion of Power

The above-described well known notions of apparent, active, and reactive power were in the past generalized by several authors for nonsinusoidal cases and later for signals with finite average power. The nonsinusoidal periodic waveforms of $u(t)$ and $i(t)$ may be described in the frequency domain by the Fourier series:

$$u\left(t\right) = U_0 + \sum_{n=1}^{N} U_n \cos\left(n\omega t + \varphi_{un}\right) \tag{7.19.20}$$

$$i(t) = I_0 + \sum_{n=1}^{N} J_n \cos\left(n\omega t + \varphi_{in}\right) \tag{7.19.21}$$

where ω is a constant equal to the fundamental angular frequency, $\omega = 2\pi/T$, and T is the period. Some or even all harmonics of the voltage waveform may not be included in the current waveform and vice versa. The active power may be defined using the same equation (7.19.9) as for sinusoidal waveforms. Inserting Equations (7.19.20) and (7.19.21) into (7.19.9) yields

$$\overline{P} = U_0 J_0 + \sum 0.5 U_n J_n \cos\left(\varphi_{in} - \varphi_{un}\right) \tag{7.19.22}$$

The summation involves terms included in both waveforms. Analogously, the reactive power is defined using Equation (7.19.10):

$$\overline{Q} = \sum 0.5 U_n J_n \sin\left(\varphi_{in} - \varphi_{un}\right) \tag{7.19.23}$$

This definition of the reactive power was proposed in 1927 by Budeanu[6] and is nowadays commonly accepted. It has been sometimes criticized as "lacking of physical meaning." Another definition of reactive power was introduced by Fryze[10] who proposed to resolve the current waveform in two components:

$$i(t) = i_p(t) + i_q(t) \tag{7.19.24}$$

The "in-phase" component is given by the relation

$$i_p(t) = \frac{\frac{1}{T}\int_0^T iu\,dt}{\frac{1}{T}\int_0^T u^2\,dt} u(t) = \frac{\overline{P}}{U_{\text{RMS}}^2} u(t) \tag{7.19.25}$$

U_{RMS} is the root mean square (RMS) value of the voltage. The "quadrature" component is

$$i_q = i - i_p \tag{7.19.26}$$

and satisfies the orthogonality property

$$\int_0^T i_q i_p\,dt = 0 \tag{7.19.27}$$

This orthogonality yields for the RMS values:

$$I_{\text{RMS}}^2 = I_{p,\text{RMS}}^2 + I_{q,\text{RMS}}^2 \tag{7.19.28}$$

The reactive power is defined by the product

$$Q = U_{\text{RMS}}\, I_{q,\text{RMS}} \tag{7.19.29}$$

The comparison of Budeanu's and Fryze's definitions of the reactive power shows how misleading it is to apply the same name, "reactive power," for notions having **different** definitions. Let us illustrate this statement with an example. A source of a cosine voltage is loaded with the ideal diode with a nonlinear characteristic (see Figure 7.19.3)

$$\begin{aligned} i &= Gu \quad \text{if } u > 0 \\ i &= 0 \quad \text{if } u < 0 \end{aligned} \tag{7.19.30}$$

The current has the waveform of a half-wave rectified cosine (see Figure 7.19.3a) and may be resolved into the "in-phase" and "quadrature" components. The Fourier series expansion of the current has the form

$$i(t) = \frac{U}{\pi}\left[1 + \frac{\pi}{2}\cos(\omega t) + \frac{2}{3}\cos(2\omega t) - \frac{2}{15}\cos(4\omega)t + \frac{2}{35}\cos(6\omega t) - \cdots\right] \tag{7.19.31}$$

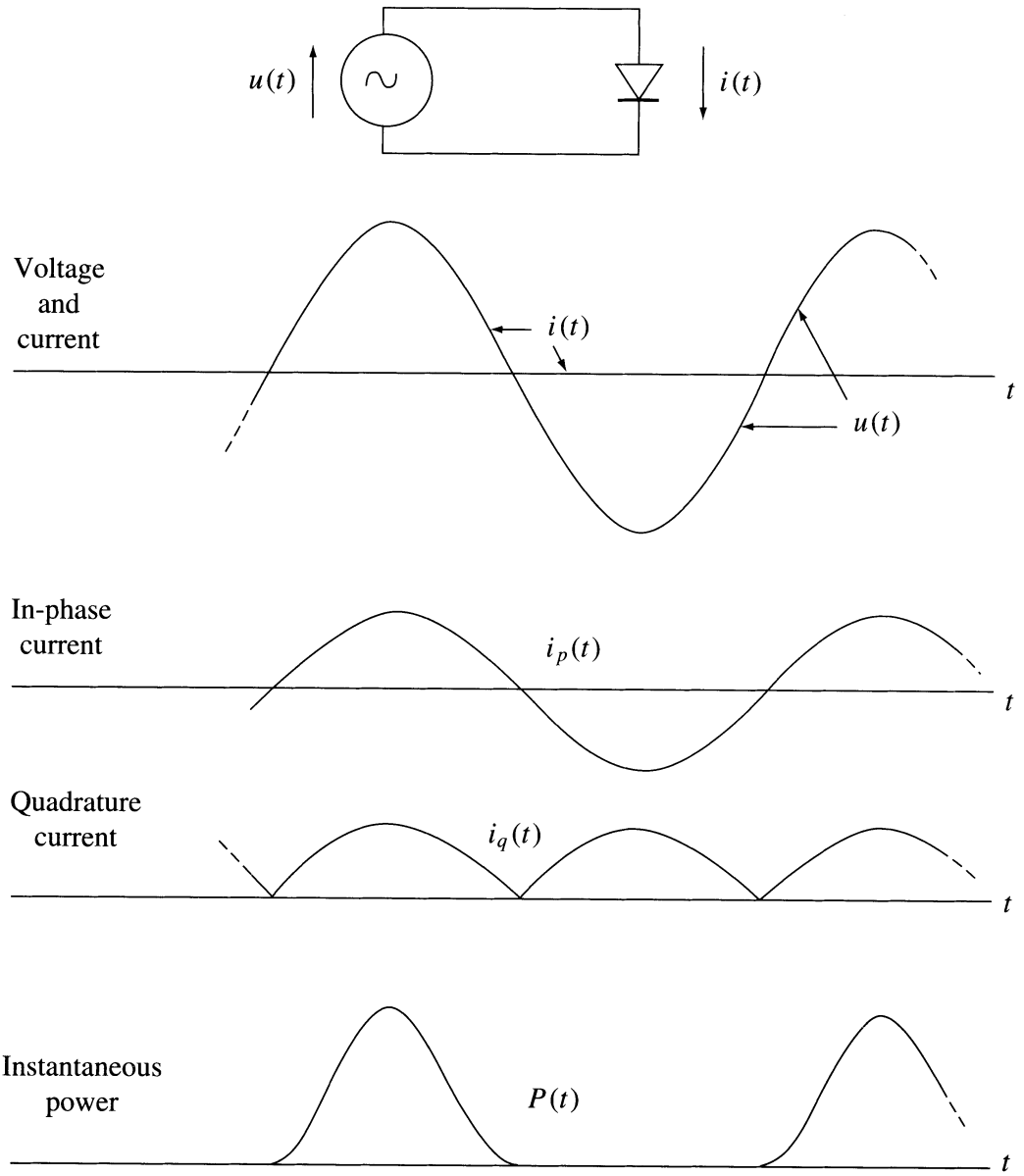

FIGURE 7.19.3 (a) A source of sine voltage loaded with a diode, (b) the voltage and current waveforms, (c) the in-phase component of the current, (d) the quadrature component of the current, and (e) the waveform of the instantaneous power.

The "in-phase" component is

$$i_p(t) = \frac{U}{2}\cos(\omega t) \tag{7.19.32}$$

and the Fourier series of the "quadrature" component (full-wave rectified cosine) is

$$i_q(t) = \frac{U}{\pi}\left[1 + \frac{2}{3}\cos(2\omega t) - \frac{2}{15}\cos(4\omega t) + \frac{2}{35}\cos(6\omega t) - \cdots\right] \tag{7.19.33}$$

The reactive power defined by Equation (7.19.23) equals zero while the reactive power is defined by Equation (7.19.29) equals

$$Q = \frac{U^2}{8} \tag{7.19.34}$$

However, the instantaneous power (Figure 7.19.3) is always positive, so there is no energy oscillating back and forth between the source and load. Therefore, we should expect that the reactive power equals zero. This requirement is satisfied using Budeanu's definition but not Fryze's definition.

Generalization of the Notion of Power for Signals with Finite Average Power

A generalized theory of electric power by use of Hilbert transforms was presented by Nowomiejski.[24] He considered voltages and currents with **finite average power**; that is, finite RMS defined by the equations

$$U_{\text{RMS}} = \sqrt{\lim_{T\Rightarrow\infty}\frac{1}{2T}\int_{-T}^{T} u^2(t)\,dt} \tag{7.19.35}$$

$$I_{\text{RMS}} = \sqrt{\lim_{T\Rightarrow\infty}\frac{1}{2T}\int_{-T}^{T} i^2(t)\,dt} \tag{7.19.36}$$

The apparent power is defined as

$$S = U_{\text{RMS}}\, I_{\text{RMS}} \tag{7.19.37}$$

and the active and reactive powers are defined by means of the relations:

$$\overline{P} = \lim_{T\Rightarrow\infty}\frac{1}{2T}\int_{-T}^{T} u(t)i(t)\,dt \tag{7.19.38}$$

and

$$\overline{Q} = \lim_{T\Rightarrow\infty}\frac{1}{2T}\int_{-T}^{T} u(t)i(t)\,dt \tag{7.19.39}$$

or

$$\overline{Q} = -\lim_{T\Rightarrow\infty}\frac{1}{2T}\int_{-T}^{T}\hat{u}(t)i(t)dt \tag{7.19.40}$$

where ^ indicates the Hilbert transform. Nowomiejski has not explicitly defined the notion of the quadrature power (see Equation [7.19.2]) but in fact the integrand in Equations (7.19.39) and (7.19.40) equals $Q(t)$. However, a new quantity called **distortion power** was defined. Generally, for each value of T the identity

$$\begin{aligned}\int_{-T}^{T}u^2(t)dt\int_{-T}^{T}i^2(t)dt = &\left|\int_{-T}^{T}u(t)i(t)dt\right|^2 \\ &+\int_{-T}^{T}\int_{-T}^{T}\frac{1}{2}\left[u(t)i(\tau)-u(\tau)i(t)\right]^2 dt\,d\tau\end{aligned} \tag{7.19.41}$$

holds true, and because the limit exists

$$S^2 = \left\{\lim_{T\Rightarrow\infty}\frac{1}{2T}\int_{-T}^{T}u^2(t)dt\right\}\left\{\lim_{T\Rightarrow\infty}\frac{1}{2T}\int_{-T}^{T}i^2(t)dt\right\} \tag{7.19.42}$$

the quantity D, called distortion power, may be defined by means of the equation

$$\overline{D} = \sqrt{\lim_{T\Rightarrow\infty}\left[\frac{1}{2T}\right]\int_{-T}^{T}\int_{-T}^{T}\frac{1}{2}\left[u(t)i(\tau)-u(\tau)i(\tau)\right]^2 dt\,d\tau} \tag{7.19.43}$$

Based on Equation (7.19.41) we arrive at

$$S^2 = \overline{P}^2 + \overline{D}^2 \tag{7.19.44}$$

In the case

$$i(t) = \text{const}\ u(t) \tag{7.19.45}$$

the "quadrature" component defined by Equation (7.19.19) equals zero and the distortion power equals zero, too. Otherwise, the distortion power is given by

$$\overline{D} = U\sqrt{\lim_{T\Rightarrow\infty}\frac{1}{2T}\int_{-T}^{T}i_q^2(t)dt} \tag{7.19.46}$$

Let us define a power factor ρ_D using the relation:

$$\rho_D = \frac{\overline{P}}{\overline{P}^2 + \overline{D}^2} \tag{7.19.47}$$

The power factor is a measure of the efficiency of the utilization of the power supplied to the load being equal to unity only, if the distortion power $D = 0$. The cross-correlation of the instantaneous voltage and current waveforms is defined by the integral

$$\rho_{ui}(\tau) = \lim_{T \Rightarrow \infty} \frac{1}{2T} \int_{-T}^{T} u(t) i(t - \tau) dt \tag{7.19.48}$$

This function enables us to introduce the frequency domain interpretations of the above-defined powers. The **cross-power spectrum** $\Theta(\omega)$ is defined by the Fourier pair

$$\rho_{u-i}(\tau) \overset{F}{\Longleftrightarrow} \Theta(\omega) \tag{7.19.49}$$

It may be shown that the active power is given by the integral of the power spectrum

$$\overline{P} = \frac{1}{2\pi} \int_{-\infty}^{\infty} \Theta(\omega) d\omega \tag{7.19.50}$$

In general, $\Theta(\omega)$ is a complex function, but the integral of the odd imaginary part equals zero. The reactive power is given by

$$\overline{Q} = \frac{1}{2\pi j} \int_{-\infty}^{\infty} \operatorname{sgn}(\omega) \Theta(\omega) d\omega \tag{7.19.51}$$

Hence, the **complex power** is

$$S = \overline{P} + j\overline{Q} = \frac{1}{2\pi} \int_{-\infty}^{\infty} \left[1 + \operatorname{sgn}(\omega)\right] \Theta(\omega) d\omega \tag{7.19.52}$$

Because the integrand presents a one-sided complex power spectrum, the complex power is an analytic function and $\overline{P}$ and $\overline{Q}$ form a pair of Hilbert transforms. If at least one of the signals $u(t)$ or $i(t)$ does not contain a constant component, Equation (7.19.52) reduces to the form

$$S = \overline{P} + j\overline{Q} = \frac{1}{\pi} \int_{-\infty}^{\infty} \Theta(\omega) d\omega \tag{7.19.53}$$

Notice that the Wiener-Khinchin relation (7.19.49) holds for stationary and ergodic processes. If the load presents a linear, time-invariant, and strictly stable system defined by the Fourier pair

$$h(t) \overset{F}{\Longleftrightarrow} H(j\omega) \tag{7.19.54}$$

(where $h(t)$ is the impulse response and $H(j\omega)$ is the transfer function) then the autocorrelation function of the voltage and its power spectrum are given by the Fourier pair

$$\rho_{u-u}(\tau) \overset{F}{\Longleftrightarrow} \Phi(\omega) \tag{7.19.55}$$

and the RMS values of the voltage and current have the form

$$U_{\text{RMS}}^2 = \rho_{u-u}(0); \quad I_{\text{RMS}}^2 = \frac{1}{2\pi} \int_{-\infty}^{\infty} \Phi(\omega) \left| H(j\omega) \right|^2 d\omega \tag{7.19.56}$$

and the complex power is given by

$$S = \overline{P} + j\overline{Q} = \frac{1}{\pi}\int_0^\infty \Phi(\omega) H^*(\omega)\, d\omega \tag{7.19.57}$$

7.20 Discrete Hilbert Transformation

The theory and applications of the DHT (Discrete Hilbert Transformation) are closely tied with the principles of digital signal processing.[26,30] Because discrete transforms will be included in another handbook in this series, this section presents only basic concepts. The formulas for the DFT and for the Z-transformation are given to fix the notations because there are various notations (definitions) of the DFT.

For reference, let us recall the Fourier transformations given by Equations (7.1.6) or (7.1.7) and defined using the exponential kernels $\exp(-j2\pi ft)$ and $\exp(j2\pi ft)$, respectively ($\omega = 2\pi f$). In digital signal processing, a time signal $u(t)$ is substituted by a sequence of samples $u(i)$. Therefore, in the DFT the time variable t is replaced by the discrete integer variable i, $0 \le i \le N-1$, where N is the length of the sequence. The discrete signal has the form of a sequence of samples $u(0)$, $u(1)$, $u(2)$, …, $u(N-1)$. The DFT of this sequence is defined by the formula

$$U(k) = \sum_{i=0}^{N-1} u(i) e^{-jw}; \quad w = 2\pi ik/N \tag{7.20.1}$$

where k is a discrete integer frequency variable, $0 \le k \le N-1$. The discrete spectrum is periodic; that is $U(k) = U(k+N) = U(k+2N)\ldots$. The inverse transformation denoted DFT^{-1} has the form

$$u(i) = \frac{1}{N}\sum_{k=0}^{N-1} U(k) e^{jw} \tag{7.20.2}$$

The sequence generated by this inverse transformation is periodic; that is, $u(t) = u(i+N) = u(i+2N) = \ldots$. Usually of interest is the basic period. The comparison of Fourier integrals with the DFT shows that integration is replaced by summation and the exponential kernel $\exp(\pm j\omega t)$ is replaced by $\exp(\pm jw)$. The discrete Fourier pair may be shortened to

$$u(i) \overset{\text{DFT}}{\Longleftrightarrow} U(k) \tag{7.20.3}$$

In general, for real sequences $u(i)$ is the spectral function $U(k)$ is complex, i.e.,

$$U(k) = U_{re}(k) + jU_{im}(k) \tag{7.20.4}$$

The real part is defined by the cosine DFT of the form

$$U_{re}(k) = \sum_{i=0}^{N-1} u(i)\cos(w) \tag{7.20.5}$$

and the imaginary part by the sine DFT of the form

$$U_{im}(k) = -\sum_{i=0}^{N-1} u(i)\sin(w) \tag{7.20.6}$$

A given sequence may be resolved in two parts

$$u(i) = u_e(i) + u_0(i) \tag{7.20.7}$$

where for even values of N the even and odd parts are given by

$$u_e(i) = \frac{u(N/2+i) + u(N/2-i)}{2}; \quad u_o(i) = \frac{u(N/2+i) - u(N/2-i)}{2} \tag{7.20.8}$$

with $N/2 \le i \le N-1$. The cosine transform depends only on $u_e(i)$ and the sine transform on $u_0(i)$. Using the complex form (7.20.4) the inverse DFT may be written in the form

$$u(i) = \frac{1}{N}\sum_{k=0}^{N-1}\left[U_{Re}(k)\cos(w) - U_{im}(k)\sin(w)\right] \tag{7.20.9}$$

The one-sided Z-transformation of the sequence $u(i)$ is defined by the formula (see also Chapter 6)

$$U(z) = \sum_{i=0}^{N-1} u(i) z^{-i} \tag{7.20.10}$$

where the complex frequency variable $z = x + jy$ is continuous differently than the discrete frequencies used in the DFTs. We shall denote the Z-pair by

$$u(i) \overset{Z}{\Longleftrightarrow} U(z) \tag{7.20.11}$$

The discrete one-sided convolution is defined by the equation

$$y(i) = \sum_{m=0}^{N-1} h(i-m)u(m) \tag{7.20.12}$$

and if $h(i) \overset{Z}{\Longleftrightarrow} H(z)$ and $u(i) \overset{Z}{\Longleftrightarrow} U(z)$ then the well-known convolution to multiplication property yields the Z-pair

$$y(i) \overset{Z}{\Longleftrightarrow} H(z)U(z) \tag{7.20.13}$$

Because the DFT is periodic, it is a periodic function of the normalized frequency

$$\psi = 2\pi\, k/N \tag{7.20.14}$$

The basic period equals the interval $0 \le \psi < 2\pi$, the next period is $2\pi \le \psi < 4\pi$, and so forth. The DFT equals the Z-transform for values of z given by

$$z = e^{j\psi}; \qquad \psi = 2\pi k/N \tag{7.20.15}$$

that is, equally spaced on the unit circle of the z-plane (see Figure 7.20.1). The half-period $0 \le \psi < \pi$ (upper half-circle) is classified as positive frequencies and the other half-period, $\pi \le \psi < 2\pi$, as negative

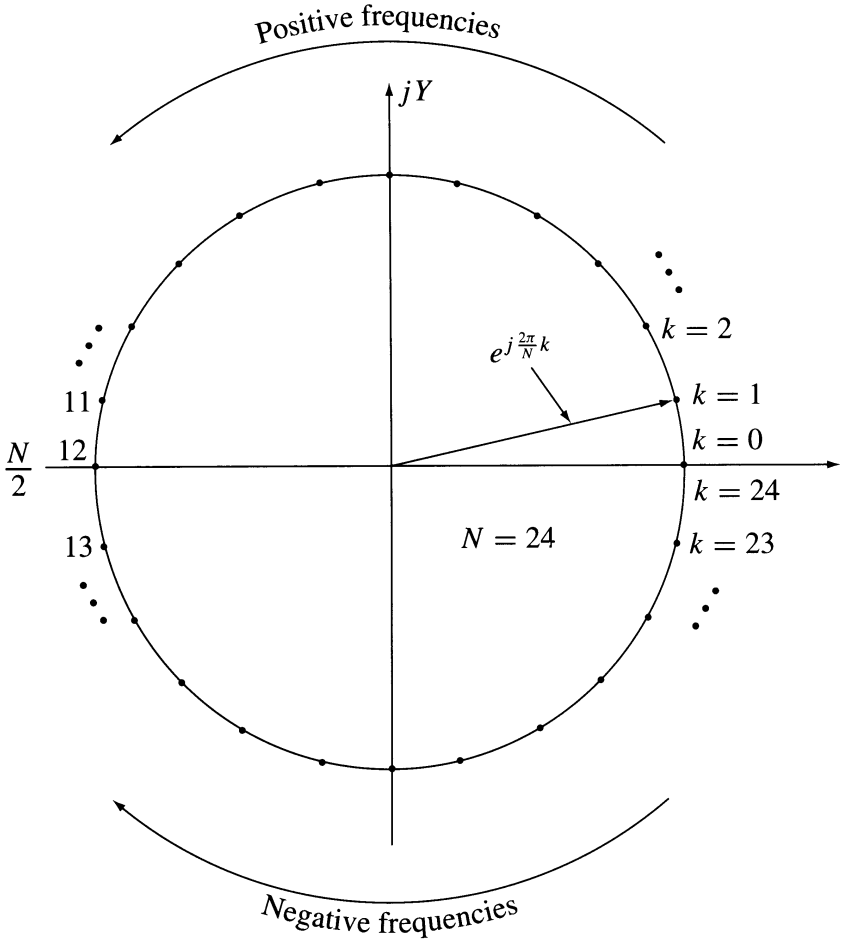

FIGURE 7.20.1 The unit circle in the $z = x + jy$ plane (see Equation (7.20.15), $N = 24$.

frequencies. The insertion of Equation (7.20.15) in (7.20.13) yields the k-domain form of the multiplication to convolution theorem

$$y(i) = u(i) * h(i) \overset{\text{DFT}}{\Longleftrightarrow} U(k)H(k) \tag{7.20.16}$$

The discrete equivalent of the delta pulse is the Kronecker delta sample

$$\delta_K(i) = \begin{cases} 1 & \text{for } i = 0 \\ 0 & \text{for } i \neq 0 \end{cases} \tag{7.20.17}$$

The impulse response of the DLTI system defined as the response to the δ_K sample and the transfer function $H(z)$ of the system are forming a Z-pair

$$h(i) \overset{Z}{\Longleftrightarrow} H(z) \tag{7.20.18}$$

The insertion $z = e^{j\psi}$ ($\psi = 2\pi\ k/N$) yields the relation

$$h(i) \overset{\text{DFT}}{\Longleftrightarrow} H(k) \tag{7.20.19}$$

The transfer function of an ideal discrete Hilbert filer is defined by the equation (N even)[7]

$$H(k)=\begin{cases}-j & \text{for } k=1,2,\ldots,N/2-1\\ 0 & \text{for } k=0,\text{and } N/2\\ j & \text{for } k=N/2+1,N/2+2,\ldots,N-1\end{cases} \tag{7.20.20}$$

This transfer function may be written in the closed form

$$H(k) = -j\ \mathrm{sgn}(N/2 - k)\ \mathrm{sgn}(k) \tag{7.20.21}$$

where

$$\mathrm{sgn}(x)=\begin{cases}1 & \text{for } x>0\\ 0 & \text{for } x=0\\ -1 & \text{for } x<0\end{cases} \tag{7.20.22}$$

The output sequence $v(i)$ of the Hilbert filter by a given input sequence $u(i)$ defines the discrete Hilbert pair

$$u(i)\overset{\text{DHT}}{\Longleftrightarrow}v(i) \tag{7.20.23}$$

The impulse response of the Hilbert filter is given by the inverse DFT of $H(k)$:

$$h(i)=\frac{1}{N}\sum_{k=0}^{N-1}H(k)e^{jw}=\frac{1}{N}\sum_{k=0}^{N-1}-j\mathrm{sgn}(N/2-k)\,\mathrm{sgn}(k)e^{jw}=\frac{1}{N}\sum_{k=0}^{N-1}\sin(w) \tag{7.20.24}$$

($w = 2\pi ik/N$). The closed form of this sum is (see Figure 7.20.2)

$$h(i)=\frac{2}{N}\sin^2(\pi i/2)\cot(\pi i/N)\quad i=0,1,\ldots N-1 \tag{7.20.25}$$

Therefore, the impulse response is given by the samples of the cotangent function (compare with Equation [7.6.27] with the even samples (i = 0, 2, 4, …, N) cancelled by the term $\sin^2(\pi i/2)$. The convolution to multiplication theorem (7.20.16) yields the DHT in the form of the convolution:

$$v(i)=-u(i)\otimes h(i)=-u(i)\otimes\frac{2}{N}\sin^2(\pi i/2)\cot(\pi i/N)\quad i=0,1,\ldots,N-1(\text{Neven}) \tag{7.20.26}$$

where the sign $\otimes$ denotes a so-called circular convolution. This convolution may be written in the form

$$v(i)=\sum_{r=0}^{N-1}h(i-r)u(r) \tag{7.20.27}$$

Concluding, the DHT of a given sequence $u(i)$ may be calculated using the above circular convolution or alternatively via the DFT using the algorithm:

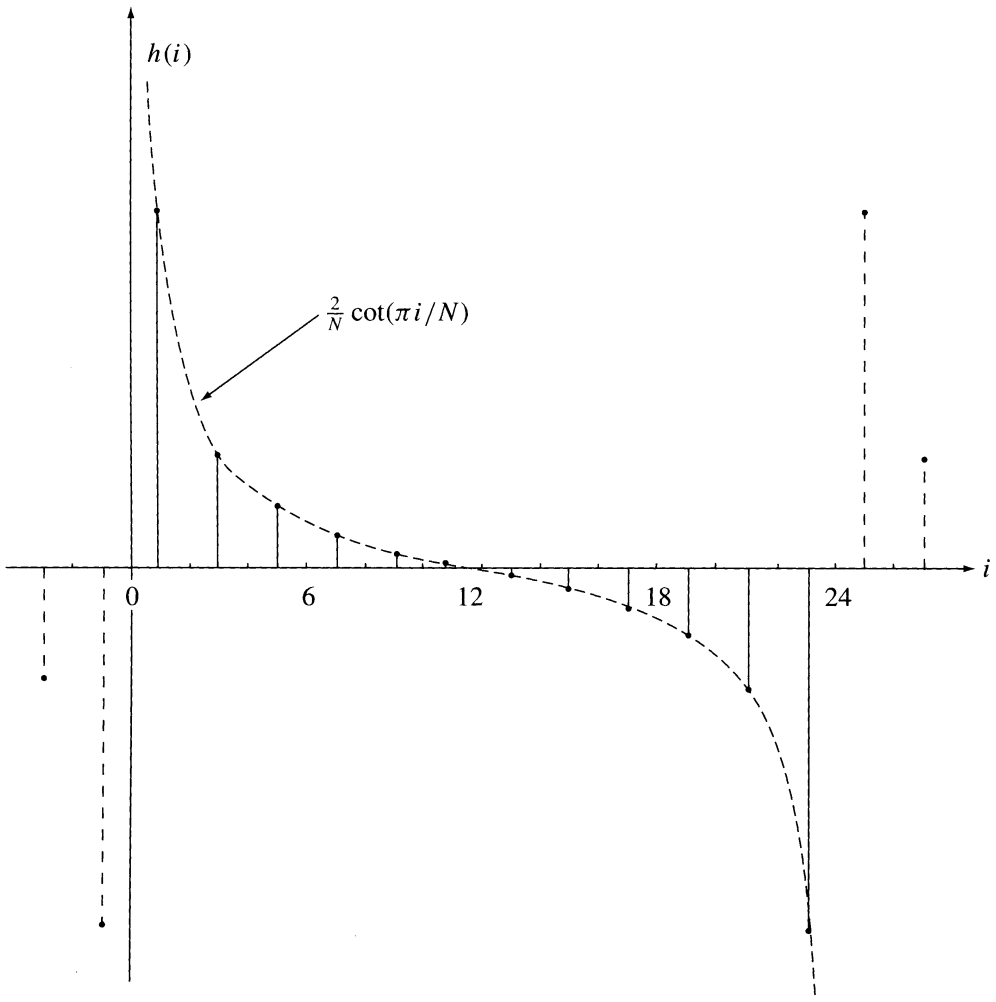

FIGURE 7.20.2 The noncausal impulse response of a Hilbert filter (see Equation 7.20.5)), $N = 24$.

$$u(i) \overset{\text{DFT}}{\Rightarrow} U(k) \Rightarrow V(k) = -j\,\text{sgn}(N/2-k)\,\text{sgn}(k)U(k) \overset{\text{DFT}^{-1}}{\Rightarrow} v(i) \quad i = 0, 1, \ldots, N-1(\text{Neven}) \tag{7.20.28}$$

Both algorithms give exactly the same result. Of course, the convolution algorithm is faster, because it involves only a single summation. However, the DFT may be replaced by the FFT.

The above formulas apply for even values of N. If N is odd, the transfer function of the Hilbert filter has the form

$$H(k) = \begin{cases} -j & \text{for } k = 1, 2, \ldots, (N-1)/2 \\ 0 & \text{for } k = 0 \\ j & \text{for } k = N/2+1, (N+1)/2, \ldots, N-1 \end{cases} \tag{7.20.29}$$

and the impulse response is

$$h(i) = \frac{2}{N}\sum_{k=1}^{(n-1)/2} \sin(2\pi ik/N); \quad i = 0, 1, 2, \ldots, N-1 \tag{7.20.30}$$

or

$$h(i) = \frac{1}{N}\left[1 - \frac{\cos(\pi i)}{\cos(\pi i/N)}\cot(\pi i/N)\right] \tag{7.20.31}$$

Properties of the DFT and DHT Illustrated with Examples

Parseval's Theorem

Consider the discrete Fourier pair $u(i) \overset{\text{DFT}}{\Longleftrightarrow} U(k)$. The discrete form of the Parseval's energy (or power) equality has the form

$$E\left[u(i)\right] = \sum_{i=0}^{N-1}\left|u(i)\right|^2 = \frac{1}{N}\sum_{k=0}^{N-1}\left|U(k)\right|^2 \tag{7.20.32}$$

This equation may be used to check the correctness of calculations of DFTs and DHTs. However, the energies of the sequences $u(i)$ and its DHT, $\upsilon(i)$, may differ, in general,

$$E[u(i)] \neq E[\upsilon(i)] \tag{7.20.33}$$

The explanation is given by Equation (7.20.28). The operator $-j\,\mathrm{sgn}(N/2 - k)\,\mathrm{sgn}(k)$ cancels the spectral terms $U(0)$ and $U(N/2)$. The term $U(0)$ has the form

$$U(0) = \sum_{i=0}^{N-1} u(i) = N u_{\text{DC}} \tag{7.20.34}$$

where u_{DC} is the mean value of the signal sequence $u(i)$, or in electrical terminology, the DC term. The algorithm of DHT cancels this term. Therefore, the sequence $\upsilon(i)$ is defined by the DHT pair

$$u_{\text{AC}}(i) \overset{\text{DHT}}{\Longleftrightarrow} \upsilon(i) \tag{7.20.35}$$

where $u_{\text{AC}}(i) = u(i) - u_{\text{DC}}$ is the alternate current component of the signal sequence (with DC term removed). The energies of the sequences $u_{\text{AC}}(i)$ and $\upsilon(i)$ are given by the equation

$$\sum_{i=1}^{N-1}\left|u_{\text{AC}}(i)\right|^2 = \sum_{i=1}^{N-1}\left|\upsilon(i)\right|^2 + \frac{\left|U(N/2)\right|^2}{N} \tag{7.20.36}$$

that is, the energies differ by the energy of the spectral term $U(N/2)$ and only if this term equals zero are both energies equal.

Example

Consider the signal given by a Kronecker delta $u(0) = \delta_K(i)$ and $u(i) = 0$ for $i \geq 1$, $N = 8$. This sequence and its DFT are shown in Figure 7.20.3a,b. The circular convolution (7.20.26) yields in this case

$$\upsilon(i) = -\delta_K(i) * \frac{1}{4}\sin^2(\pi i/2)\cot(\pi i/N) \tag{7.20.37}$$

that is, the following sequence

i	0	1	2	3	4	5	6	7
$v(i)$	0	$\left[\cot(\pi/8)\right]/4$	0	$\left[\cot(3\pi/8)\right]/4$	0	$-\left[\cot(3\pi/8)\right]/4$	0	$-\left[\cot(3\pi/8)\right]/4$

where $[\cot(\pi/8)]/4 = (\sqrt{2} + 1)/4 = 0.6035\ldots$ and $[\cot(3\pi/8)]/4 = (\sqrt{2} - 1)/4 = 0.1035\ldots$. The sequence $v(i)$ and its DFT are shown in Figure 7.20.3c,d. The DC term defined by Equation (7.20.34) is $u_{DC} = 1/N = 0.125$. For convenience, Figure 7.20.3e,f shows the sequence $u_{AC}(i)$ and its DFT. The energies are: $E[u(i)] = 1$, $E[u_{AC}(i)] = 1 - 1^2/N = 0.875$, $E[v(i)] = 1 - 1^2/N - 1^2/N = 1 - 2/N = 0.75$.

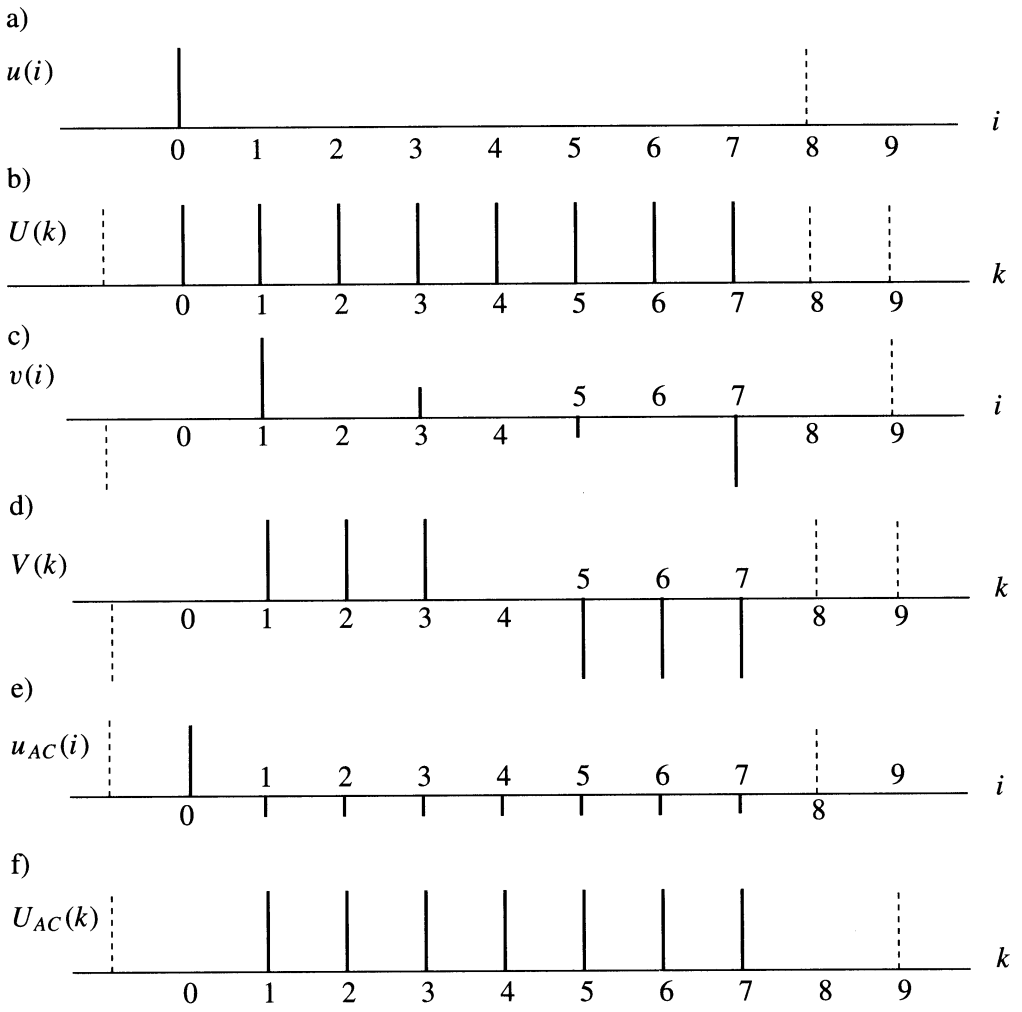

FIGURE 7.20.3 (a) The sequence $u(i)$ consisting of a single sample $\delta_K(i)$, (b) its spectrum $U(k)$ given by the DFT, (c) the samples of the discrete Hilbert transform, (d) the corresponding spectrum $V(k)$, (e) the samples of the AC component of $u(i)$, and (*f*) the corresponding spectrum $U_{AC}(k)$.

Shifting Property

Consider the discrete Fourier pair $u(i) \overset{\text{DFT}}{\Longleftrightarrow} U(k)$. It can be shown that

$$u(i+m) \overset{\text{DFT}}{\Longleftrightarrow} e^{j2\pi mk/N} U(k) \tag{7.20.38}$$

where m is an integer.

Example

The spectrum of Figure 7.20.3b is real with all samples equal to 1. The shifted-by-one interval ($m = 1$) delta pulse and its spectrum are

$$\delta_K(i-m) \overset{\text{DFT}}{\Longleftrightarrow} e^{-j2\pi k/N} \tag{7.20.39}$$

This spectrum is complex and of the form

k	0	1	2	3	4	5	6	7
$U_{re}(k)$	1	$\sqrt{2}/2$	0	$-\sqrt{2}/2$	−1	$-\sqrt{2}/2$	0	$\sqrt{2}/2$
$U_{im}(k)$	0	$-\sqrt{2}/2$	−1	$-\sqrt{2}/2$	0	$\sqrt{2}/2$	1	$\sqrt{2}/2$
$\lvert U(k)\rvert$	1	1	1	1	1	1	1	1

This example shows the general rule that shift changes in phase relations will have no effect on the magnitude of the spectrum.

Linearity

Consider the discrete Fourier pairs $u_1(i) \overset{\text{DFT}}{\Longleftrightarrow} U_1(k)$ and $u_2(i) \overset{\text{DFT}}{\Longleftrightarrow} U_2(k)$. Due to the linearity property the summation of the sequences yields

$$au_1(i) + bu_2(i) \overset{\text{DFT}}{\Longleftrightarrow} aU_1(k) + bU_2(k) \tag{7.20.40}$$

where a and b are constants. The linearity property applies also for the DHTs:

$$au_1(i) + bu_2(i) \overset{\text{DFT}}{\Longleftrightarrow} av_1(i) + bv_2(i) \tag{7.20.41}$$

Example

Consider the sequence of two deltas $u(i) = \delta_K(i) + \delta_K(i-1)$ for $i = 0$ and 1 and $u(i) = 0$ for $1 < i \le N - 1$, $N = 8$. The DFT of this sequence may be obtained by adding to each term of the real part of the spectrum given by Equation (7.20.39) the number 1; that is, the terms of the spectrum of $\delta_K(i)$ (see Figure 7.20.3b). This yields the complex spectrum

k	0	1	2	3	4	5	6	7
$U_{re}(k)$	2	$1+\sqrt{2}/2$	1	$1-\sqrt{2}/2$	0	$1-\sqrt{2}/2$	1	$1+\sqrt{2}/2$
$U_{im}(k)$	0	$-\sqrt{2}/2$	−1	$-\sqrt{2}/2$	0	$\sqrt{2}/2$	1	$\sqrt{2}/2$
$\lvert U(k)\rvert$	2	1.847…	$\sqrt{2}$	0.765…	0	0.765…	$\sqrt{2}$	1.847…

Notice that the term $U(N/2) = U(4)$ equals zero. Therefore, the energies $E[u_{AC}(i)] = E[v(i)] = 2 - 2^2/N = 1.5$ are equal. The DC term $u_{DC} = 2/N = 0.25$.

Example

Consider the sequence

$$u(i) = e^{-0.05\pi\left[(N-1)/2-i\right]^2}; \quad N = 16 \tag{7.20.42}$$

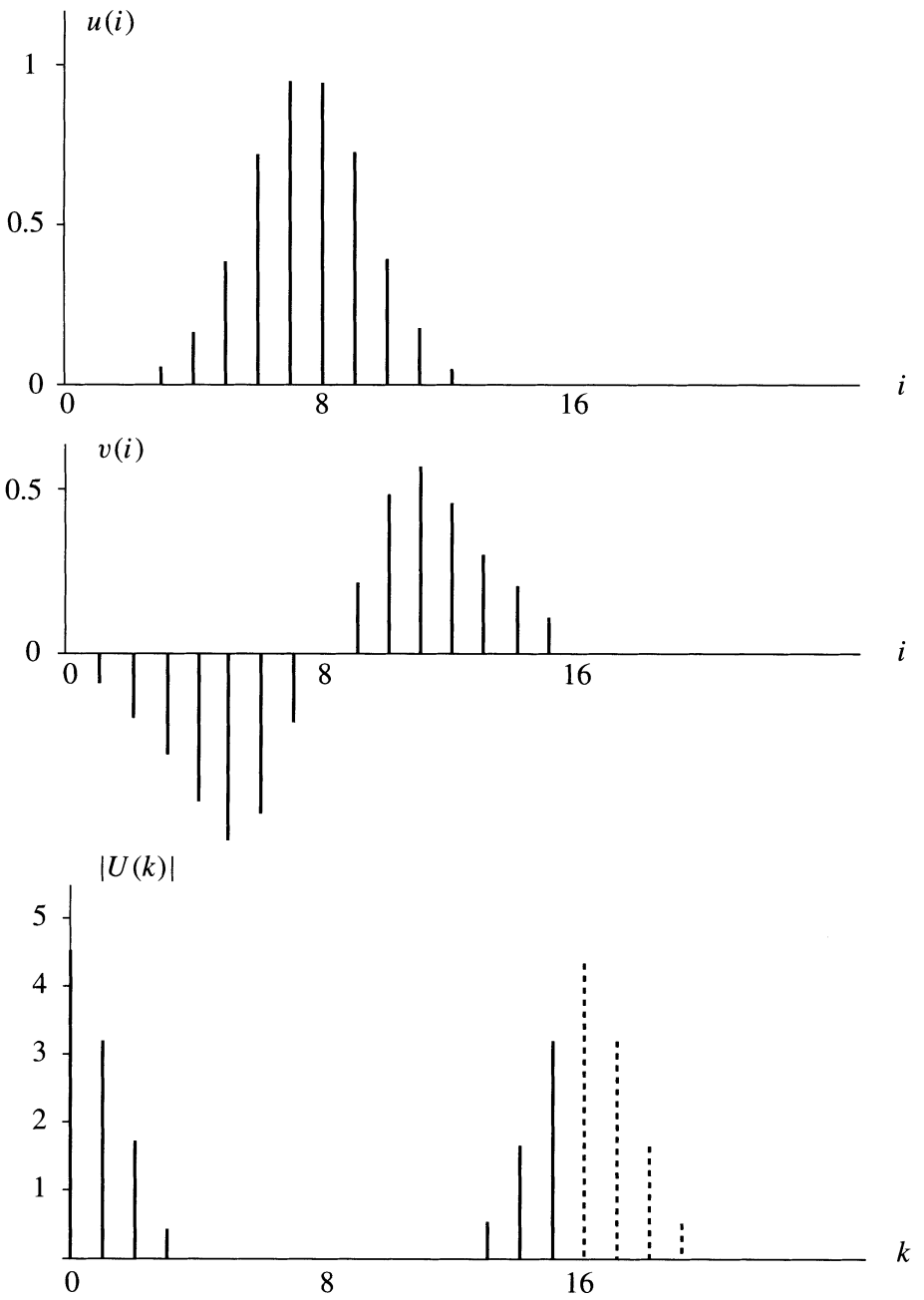

FIGURE 7.20.4 (Top) A sequence of samples of a Gaussian pulse, (middle) the samples of the DHT, and (bottom) the samples of the magnitude of the DFT of the Gaussian pulse.

representing a sampled Gaussian pulse as shown in Figure 7.20.4 (top). Figure 7.20.4 (middle/bottom) shows the DFT of this pulse and the DHT calculated via the DFT. The DC term equals $u_{DC} = 0.2795\ldots$. The energies are: $E[u(i)] = 3.1622\ldots$, $E[u_{AC}(i)] = E[\upsilon(i)] = 1.9122\ldots$, that is, the energy difference is negligible due to the negligible value of the term $U(N/2)$.

Complex Analytic Discrete Sequence

A sequence of complex samples of a signal and its discrete Hilbert transform does not represent an analytic signal in the sense of the definition of the analytic function. However, it is possible to define the analytic sequence of the form of a sequence of samples

$$\psi(i) = u(i) + j\upsilon(i) \tag{7.20.43}$$

where $\upsilon(i)$ is the DHT of $u(i)$. Let us derive the spectrum of the sequence $\psi(i)$. If $u(i) \overset{\text{DFT}}{\Longleftrightarrow} U(k)$, then the spectrum of $\upsilon(i)$ is given by Equation (7.20.28), and due to the linearity property, the spectrum of the complex sequence $\psi(i)$ is

$$\psi(i) \overset{\text{DFT}}{\Longleftrightarrow} U(k) + j\left[-j\,\text{sgn}(N/2-k)\text{sgn}(k)\right]U(k)$$

that is,

$$\psi(i) \overset{\text{DFT}}{\Longleftrightarrow} \left[1 + \text{sgn}(N/2-k)\text{sgn}(k)\right]U(k) \quad k = 0, 1, \ldots, N-1(\text{Neven}) \tag{7.20.44}$$

The spectrum is doubled at positive frequencies and canceled at negative frequencies.

Example

Consider the signals and spectra of Figure 7.20.3. Figure 7.20.5 shows the real spectra of the delta pulse and its DHT and the resulting spectrum of the complex sequence. The terms of the spectrum of $u(i)$ are canceled at negative frequencies and doubled at positive frequencies. The DC term, i.e., $U(0)$, is unaltered. The property that analytic sequences have a one-sided spectrum makes it possible to implement anti-aliasing schemes of sampling.

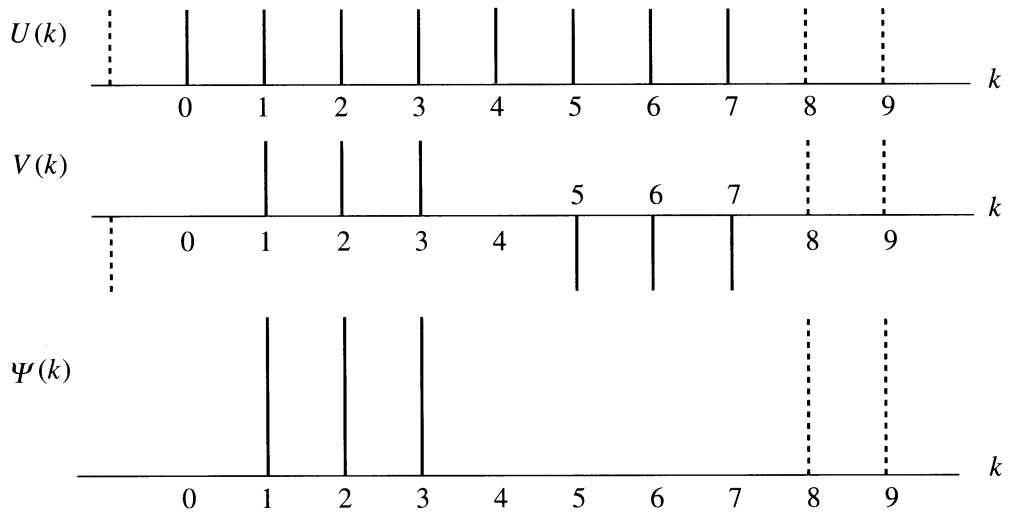

FIGURE 7.20.5 (Top, middle) The spectra $U(k)$ and $V(k)$ of Figure 7.20.3; (bottom) the corresponding spectrum of the analytic sequence.

Bilinear Transformation and the Cotangent Form of Hilbert Transformations

The transfer function of an analog LTI system is defined as the quotient of the output-to-input analytic signals (see Equation [7.17.1]), and if analytical, is an analytic function of the complex frequency $s = \alpha + j\omega$. Similarly, the transfer function of the DLTI system defined by Equation (7.20.18), if analytical, is an analytic function of the complex variable $z = x + jy$. Let us study the problem of a **conformal mapping** of the s-plane into the z-plane by means of the **bilinear transformations** defined by the formulae

$$z = \frac{1+s}{1-s} \tag{7.20.45}$$

and

$$s = \frac{z-1}{z+1} \tag{7.20.46}$$

where s is a normalized complex frequency (normalized $s = s/f_s = s\,\Delta\,t$, where f_s is the sampling frequency and Δt the sampling period). Inserting $s = \alpha + j\omega$ into Equation (7.20.45) and equating the real and imaginary parts yields:

$$x = \frac{1-\alpha^2-\omega^2}{\left(1-\alpha\right)^2+\omega^2}; \quad y = \frac{2\omega}{\left(1-\alpha\right)^2+\omega^2} \tag{7.20.47}$$

These equations are mapping a family of orthogonal lines a = const. and ω = const. of the s-plane into a family of orthogonal circles of the z-plane, as shown in Figure 7.20.6. The magnitude of the variable is $|z| = \mathrm{SQR}(x^2 + y^2)$ giving

$$\left|z\right| = \sqrt{\frac{\left(1+\alpha\right)^2+\omega^2}{\left(1-\alpha\right)^2+\omega^2}} \tag{7.20.48}$$

and the argument

$$\psi = \arg\left(z\right) = \tan^{-1}\left[\frac{2}{1-\alpha^2-\omega^2}\right] \tag{7.20.49}$$

This equation defines the nonlinear dependence between the angular frequency ω and the normalized frequency ψ defined by the representation $z = e^{j\psi}$ (see Equation [7.20.15]). For $s = j\omega$; that is, $\alpha = 0$, Equation (7.20.49) takes the form of a quadratic equation

$$\tan(\psi)\omega^2 + 2\omega - \tan(\psi) = 0 \tag{7.20.50}$$

The roots of this equation are

$$\omega = \tan(\psi/2) \tag{7.20.51}$$

and

$$\omega = -\cot(\psi/2) \tag{7.20.52}$$

Let us use these nonlinear relations to derive a new form of Hilbert transformations. We start with the Hilbert transformation

$$B\left(\omega\right) = -\frac{1}{\pi} P\int_{-\infty}^{\infty} \frac{A\left(\eta\right)}{\eta-\omega} d\eta \tag{7.20.53}$$

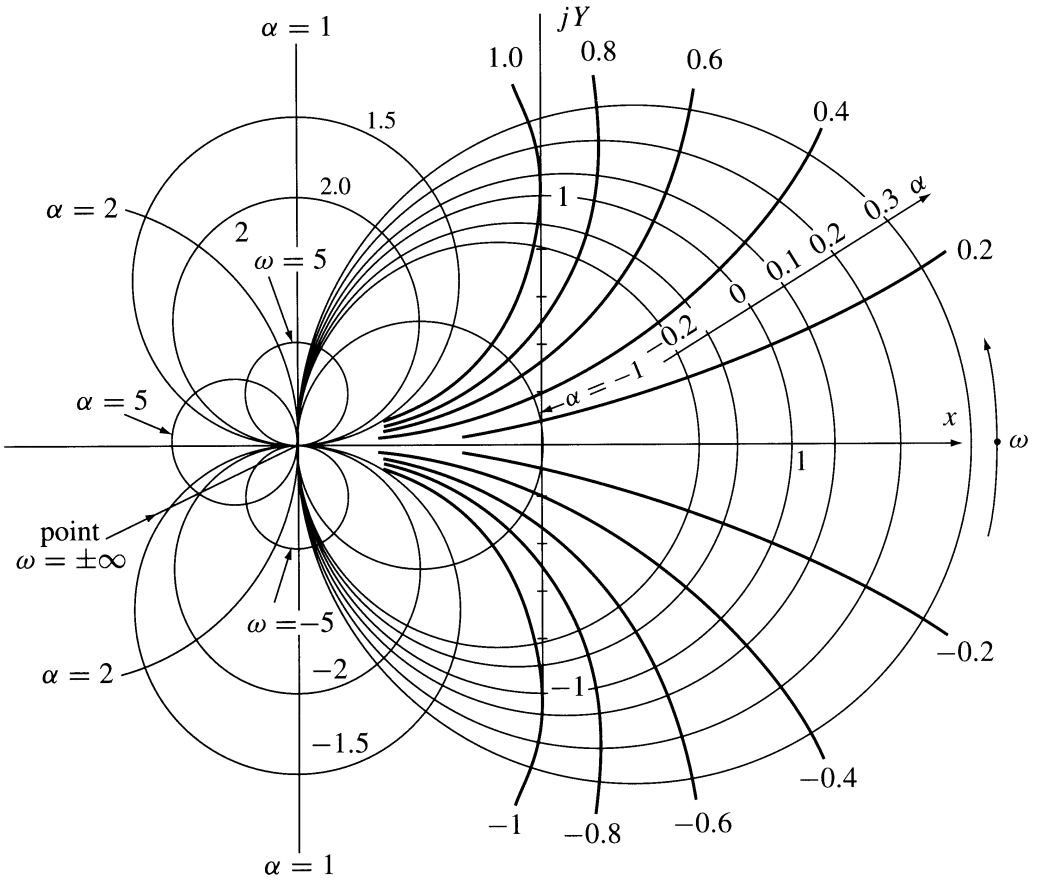

FIGURE 7.20.6 The mapping of the s-plane, $s = \alpha + j\omega$, into the z-plane, $z = x + jy$, defined by Equation (7.20.47).

Let us introduce the notations

$$\eta = \tan(\phi/2); \quad \omega = \tan(\psi/2) \tag{7.20.54}$$

and $d\eta = 0.5[1 + \tan^2(\phi/2)]d\phi$. We get

$$B(\psi) = \frac{1}{\pi} P\int_{-\pi}^{\pi} \frac{A\left[\tan(\phi/2)\right]}{\tan(\phi/2) - \tan(\psi/2)} 0.5\left[1 + \tan^2(\phi/2)\right] d\phi \tag{7.20.55}$$

By means of the trigonometric relation

$$\frac{1 + \tan^2(\phi/2)}{\tan(\phi/2) - \tan(\psi/2)} = \tan(\phi/2) + \cot\left[(\phi - \psi)/2\right] \tag{7.20.56}$$

we get

$$\begin{aligned} B(\psi) = &-\frac{1}{2\pi}\int_{-\pi}^{\pi} A\left[\tan(\phi/2)\right]\tan(\phi/2)\, d\phi \\ &-\frac{1}{2\pi}\int_{-\pi}^{\pi} A\left[\tan(\phi/2)\right]\cot\left[(\phi - \psi)/2\right] d\phi \end{aligned} \tag{7.20.57}$$

If we start with the inverse Hilbert transformation

$$A(\omega) = \frac{1}{\pi} P \int_{-\infty}^{\infty} \frac{B(\eta)}{\eta - \omega} d\eta \tag{7.20.58}$$

the same derivation gives

$$\begin{aligned} A(\psi) &= \frac{1}{2\pi} \int_{-\pi}^{\pi} B\left[\tan(\phi/2)\right] \tan(\phi/2)\, d\phi \\ &+ \frac{1}{2\pi} \int_{-\pi}^{\pi} B\left[\tan(\phi/2)\right] \cot\left[(\phi - \psi)/2\right] d\phi \end{aligned} \tag{7.20.59}$$

The first term of Equation (7.20.57) is a constant depending only on the even part of $A[\tan(\phi/2)]$, while the first term of Equation (7.20.59) depends only on the odd part of $B[\tan(\psi/2)]$.

If we use instead of Equation (7.20.51) the next root defined by Equation (7.20.52), then Hilbert transformations (7.20.57) and (7.20.59) have the alternative form:

$$\begin{aligned} B(\psi) &= \frac{-1}{2\pi} \int_{0}^{2\pi} A\left[-\cot(\phi/2)\right] \cot(\phi/2)\, d\phi \\ &- \frac{1}{2\pi} \int_{0}^{2\pi} A\left[-\cot(\phi/2)\right] \cot\left[(\phi - \psi)/2\right] d\phi \end{aligned} \tag{7.20.60}$$

$$\begin{aligned} A(\psi) &= \frac{1}{2\pi} \int_{0}^{2\pi} B\left[-\cot(\phi/2)\right] \cot(\phi/2)\, d\phi \\ &+ \frac{1}{2\pi} \int_{0}^{2\pi} B\left[-\cot(\phi/2)\right] \cot\left[(\phi - \psi)/2\right] d\phi \end{aligned} \tag{7.20.61}$$

The Hilbert transforms in the cotangent form are periodic functions of the variable ψ.

Example

Consider the square function

$$A(\omega) = \begin{cases} 1 & \text{for } |\omega| < a \\ 0.5 & \text{for } |\omega| = a \\ 0 & \text{for } |\omega| > a \end{cases} \tag{7.20.62}$$

Introducing $\omega = \tan(\psi/2)$ gives

$$A\left[\tan(\psi/2)\right] = \begin{cases} 1 & \text{for } |\psi| < \psi_p = 2\tan^{-1}(a) \\ 0.5 & \text{for } |\psi| = \psi_p \\ 0 & \text{for } |\psi| > \psi_p \end{cases} \tag{7.20.63}$$

The Hilbert transform defined by Equation (7.20.61) is here

$$B(\psi) = -\frac{1}{2\pi}\int_{-\psi_p}^{\psi_p} \tan\left[\frac{\phi}{2}\right] d\phi - \frac{1}{2\pi}\int_{-\psi_p}^{\psi_p} \cot\left[\frac{\phi-\psi}{2}\right] d\phi \tag{7.20.64}$$

The first integral equals zero and the result of the second integration (Cauchy Principal Value (CPV) value) is

$$B(\psi) = \frac{1}{\pi}\ln\left|\frac{\sin\dfrac{\psi_p+\psi}{2}}{\sin\dfrac{\psi_p-\psi}{2}}\right| \tag{7.20.65}$$

Figure 7.20.7 shows $B(\psi)$ for two values of ψ_p: 0.4π and 0.1π corresponding to the normalized frequencies $\omega \cong .726$ and 0.155. The functions $A(\psi)$ and $B(\psi)$ are periodic with the period of 2π.

7.21 Hilbert Transformers (Filters)

The **Hilbert transformer**, also called a **quadrature filter** or wide-band 90° phase shifter, is a device in the form of a linear two-port whose output signal is a Hilbert transform of the input signal. Hilbert transformers find numerous applications, for example, in radar systems, single side-band modulators, speech processing, measurement systems, schemes of sampling band-pass signals, and many other systems. They are implemented as analog or digital filters. The transfer function of the ideal analog Hilbert filter is (see Equation [7.1.10])

$$H(jf) = F[1/(\pi t)] = |H(jf)|e^{j\varphi(f)} = -j\,\mathrm{sgn}(f) \tag{7.21.1}$$

Hence, the transfer function is given by

$$H(jf) = \begin{cases} -j & \text{for } f > 0 \\ 0 & \text{for } f = 0 \\ j & \text{for } f < 0 \end{cases} \tag{7.21.2}$$

The magnitude is $|H(jf)| = 1$ and the phase function is

$$\varphi(f) = \arg[H(jf)] = -(\pi/2)\,\mathrm{sgn}(f) \tag{7.21.3}$$

Notice that the convention with a + sgn by $\varphi(f)$ results in a negative slope of the phase function. The last equation explains the terminology "quadrature filter" or "wide-band 90° phase shifter." The ideal Hilbert filter is noncausal and physically unrealizable. Causality implies the introduction of an infinite delay. In any practical implementation of the Hilbert filter, the output signal is a delayed and more or less distorted Hilbert transform of the input signal. The spectrum of the input signal should be band-limited between the low-frequency edge f_1 and high-frequency edge f_2 of the pass-band. The necessary delay depends only on f_1. Inside the pass-band $W = f_2 - f_1$, it is possible to get an approximate version of the transfer function defined by Equation (7.21.1). Good approximations require sophisticated methods of design and implementations.

Hilbert transformers can be implemented in the form of analog or digital convolvers using the time definition of the Hilbert transforms given by Equations (7.1.3) and (7.1.4) (analog convolutions) or by Equation (7.20.26) (discrete circular convolution). An other implementation uses so-called quadrature filters.

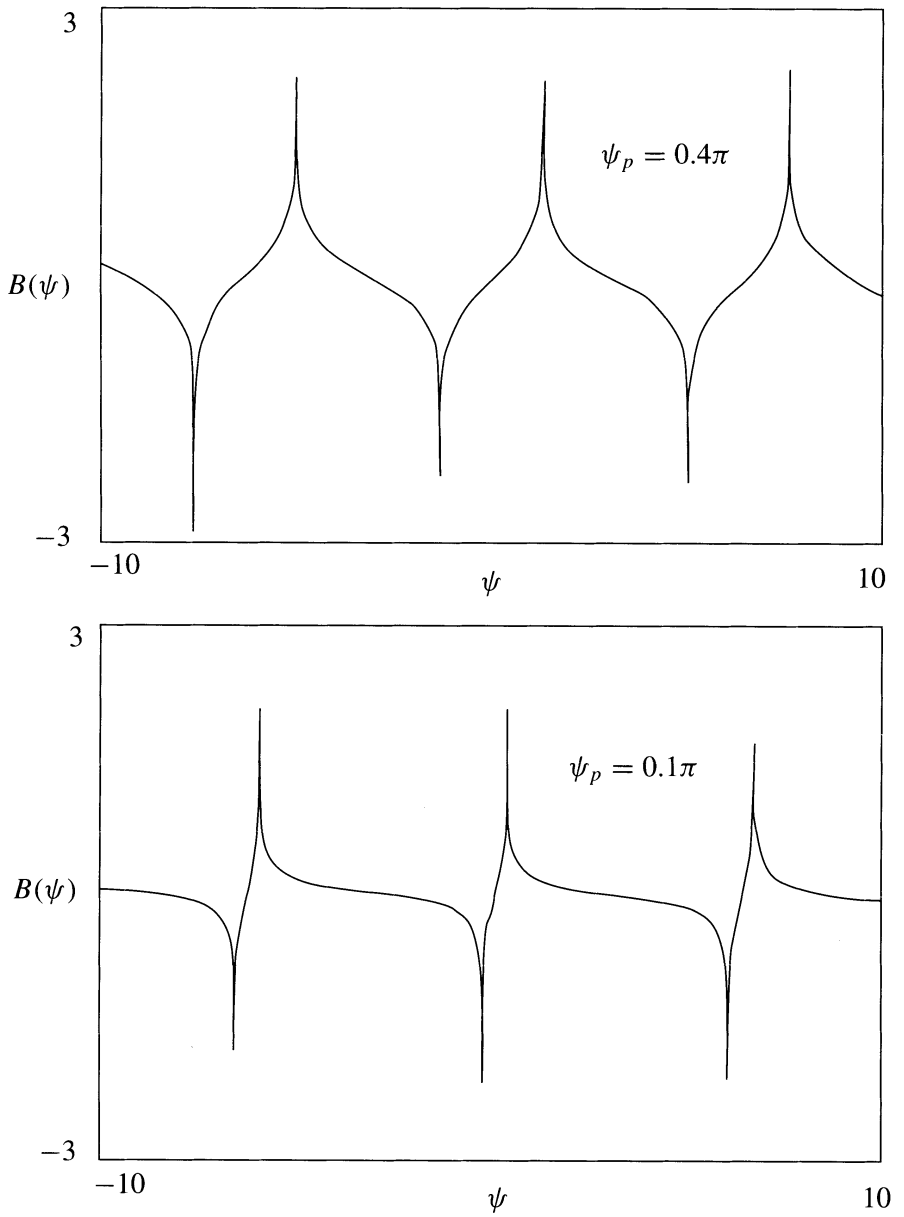

FIGURE 7.20.7 The function $B(\psi)$ given by Equation (7.20.65).

The performance of analog Hilbert transformers depends on design and alignment. Having in mind that ideal alignment is impossible and that even by good initial alignment it is detoriated by aging and various physical changes; for example, temperature, humidity, pressure, vibrations, and others, the use of extremely sophisticated design methods and implementations may be unreasonable. Differently, the performance of digital Hilbert transformers may depend only on design.

Because the magnitude of the transfer function defined by Equation (7.21.2) equals 1, all-pass filters are frequently used in analog and digital implementations of Hilbert transformers.

Phase-Splitter Hilbert Transformers

Analog Hilbert transformers are mostly implemented in the form of a phase splitter consisting of two parallel all-pass filters with a common input port and separated output ports, as shown in Figure 7.21.1. The transfer functions of the all-pass filters are

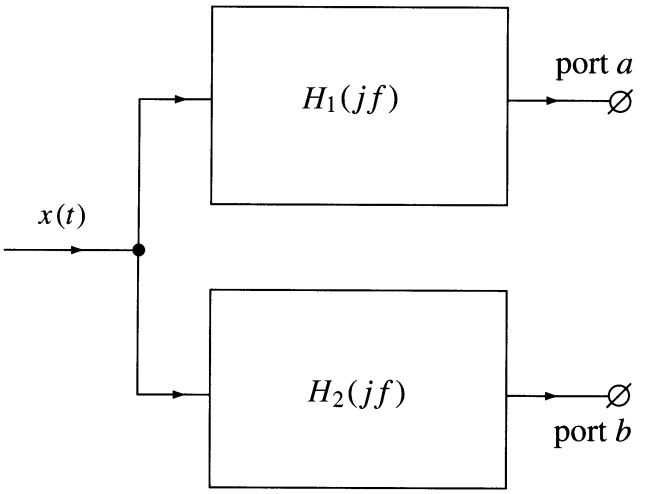

FIGURE 7.21.1 A phase splitter Hilbert transformer, where $H_1(jf)$ and $H_2(jf)$ are all-pass transfer functions.

$$H_1(jf) = e^{j\varphi_1(f)}; \quad H_2(jf) = e^{j\varphi_2} \tag{7.21.4}$$

The magnitude of both functions equals 1. The antisymmetry of the phase functions allows us to consider only the positive frequency part. The phase difference of the harmonic signals at the output ports of the phase splitter should be:

$$\delta(f) = \varphi_1(f) - \varphi_2(f) = -\pi/2; \quad \text{all } f > 0 \tag{7.21.5}$$

The realization of this requirement is possible in a limited frequency band between the low-frequency edge f_1 and the high-frequency edge f_2, as shown in Figures 7.21.6 to 7.21.9. Therefore, the spectrum of the input signal should be band limited between f_1 and f_2. Due to unavoidable amplitude and phase errors, the output signals of the phase splitter approximately are forming a Hilbert pair. The phase functions of the all-pass filters defined by Equation (7.21.4) should be inside the band $W = f_2 - f_1$, approximately linear in the logarithmic frequency scale, but are nonlinear in a linear scale. This nonlinearity introduces phase distortions. Therefore, the output signals are forming a distorted in relation to the input signal Hilbert pair. The distortions can be removed using a suitable phase equalizer connected in series to the input port, as shown in Figure 7.21.2. By proper phase equalization the output signals are forming an undistorted pair of Hilbert transforms.

Analog All-Pass Filters

Hilbert transformers in the form of phase splitters are implemented using all-pass filters. A convenient choice is the all-pass consisting of two complementary filters, a low-pass and a high-pass, as shown in Figure 7.21.3a. The impedance $Z(j\omega) = X(j\omega)$ is a loss-less one-port (pure reactance). The transfer function of this all-pass has the form:

$$H(j\omega) = \frac{R - jX(\omega)}{R + jX(\omega)}; \quad \omega = 2\pi f \tag{7.21.6}$$

The magnitude of this function equals one for all f and the phase function is

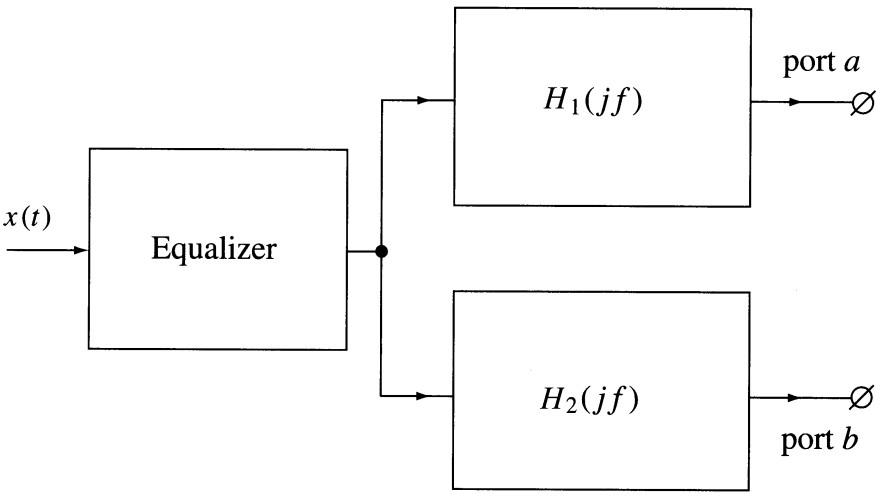

FIGURE 7.21.2 The series connection of a phase equalizer and the Hilbert transformer of Figure 7.21.1.

$$\varphi(\omega) = \arg\left[\left(R - jX(\omega)\right)^2\right] = \tan^{-1}\left[\frac{-2RX(\omega)}{R^2 - X^2(\omega)}\right] \tag{7.21.7}$$

The insertion $X = 1/\omega C$ (see Figure 7.21.3b) yields the phase function of a first-order all-pass

$$\varphi(y) = \tan^{-1}\left[\frac{-2y}{1-y^2}\right]; \quad y = \omega RC = \omega\tau \tag{7.21.8}$$

The insertion $X = \omega L - 1/\omega C$ (see Figure 7.21.3c) yields a phase function of a second-order all-pass

$$\varphi(y) = \tan^{-1}\left[\frac{-2\left(1-y^2\right)qy}{\left(1-y^2\right)^2 - q^2y^2}\right] \tag{7.21.9}$$

where $y = \omega/\omega_r$, $\omega_r = 1/\sqrt{LC}$ and $q = \omega_r RC = R\sqrt{C/L}$. The phase functions defined by Equations (7.21.8) and (7.21.9) are shown in Figure 7.21.4 in linear and logarithmic frequency scales. The second-order function best shows linearity in the logarithmic scale for $q = 4$. Notice that the phase functions are continuous if we remove the phase jumps by π by changing the branch of a multiple-valued $\tan^{-1}$ function, similar to that in Figure 7.15.2. To get a wider frequency range of Hilbert transformers, higher order all-passes have to be applied. But more practical is the use of a series connection of first-order all-passes with appropriate staggering of the individual phase functions. For a given frequency band $W = f_2 - f_1$, optimum staggering yields the smallest value of the RMS phase error. The local value of the phase error is defined as a difference between $\delta(f)$ given by Equation (7.21.5) and $-\pi/2$. Therefore, the local error is

$$\varepsilon(f) = \delta(f) + \pi/2 \tag{7.21.10}$$

The design methods of 90° phase splitters were described by Dome[9] in 1946. Later Darlington,[8] Orchard,[27] Weaver,[38] and Saraga[33] described design methods based on a Chebyshev approximation of a desired phase error. Tables and diagrams of these approximations can be found in Bedrosian.[2]

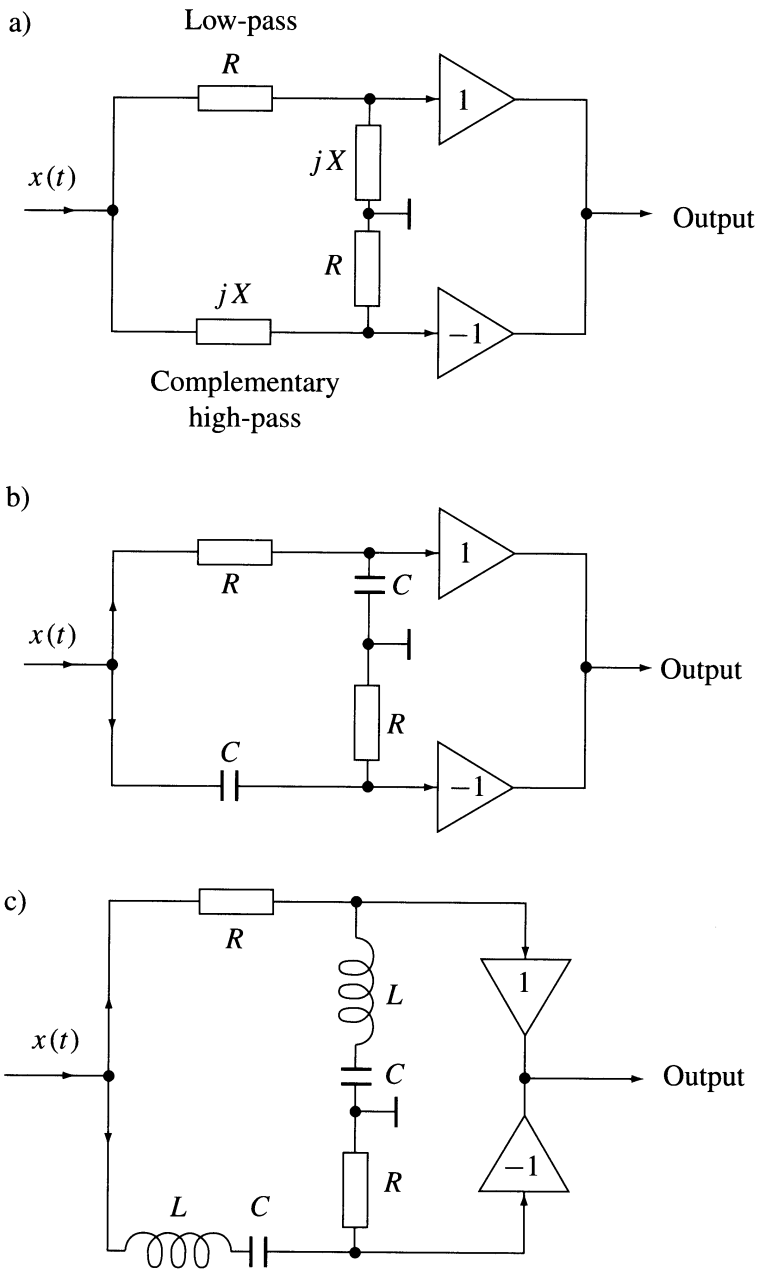

FIGURE 7.21.3 An all-pass consisting of (a) a low-pass and a complementary high-pass, (b) a first-order RC low-pass and complementary CR high-pass, and (c) a second-order RLC low-pass and complementary RLC high-pass.

A Simple Method of Design of Hilbert Phase Splitters

Analog Hilbert transformers are designed using models of a given filter consisting of loss-less capacitors, low-loss inductors, ideal resistors, and ideal operational amplifiers. More accurate models that take into account spurious capacitances, inductances, and other spurious effects are sophisticated and rarely applied at the design stage. The alignment of circuits with an accuracy better than 0.5 to 1% is difficult to achieve. Having in mind the above arguments, the required accuracy of design of the parameters of the phase splitter is limited. Therefore, the simple method of design using a personal computer may be effective in many applications and is presented here.

The method consists of two steps. In the first step, the phase function $\varphi_1(f)$, given by Equation (7.21.4), is linearized in the logarithmic frequency scale. In the second step, the phase function $\varphi_2(f)$ is obtained

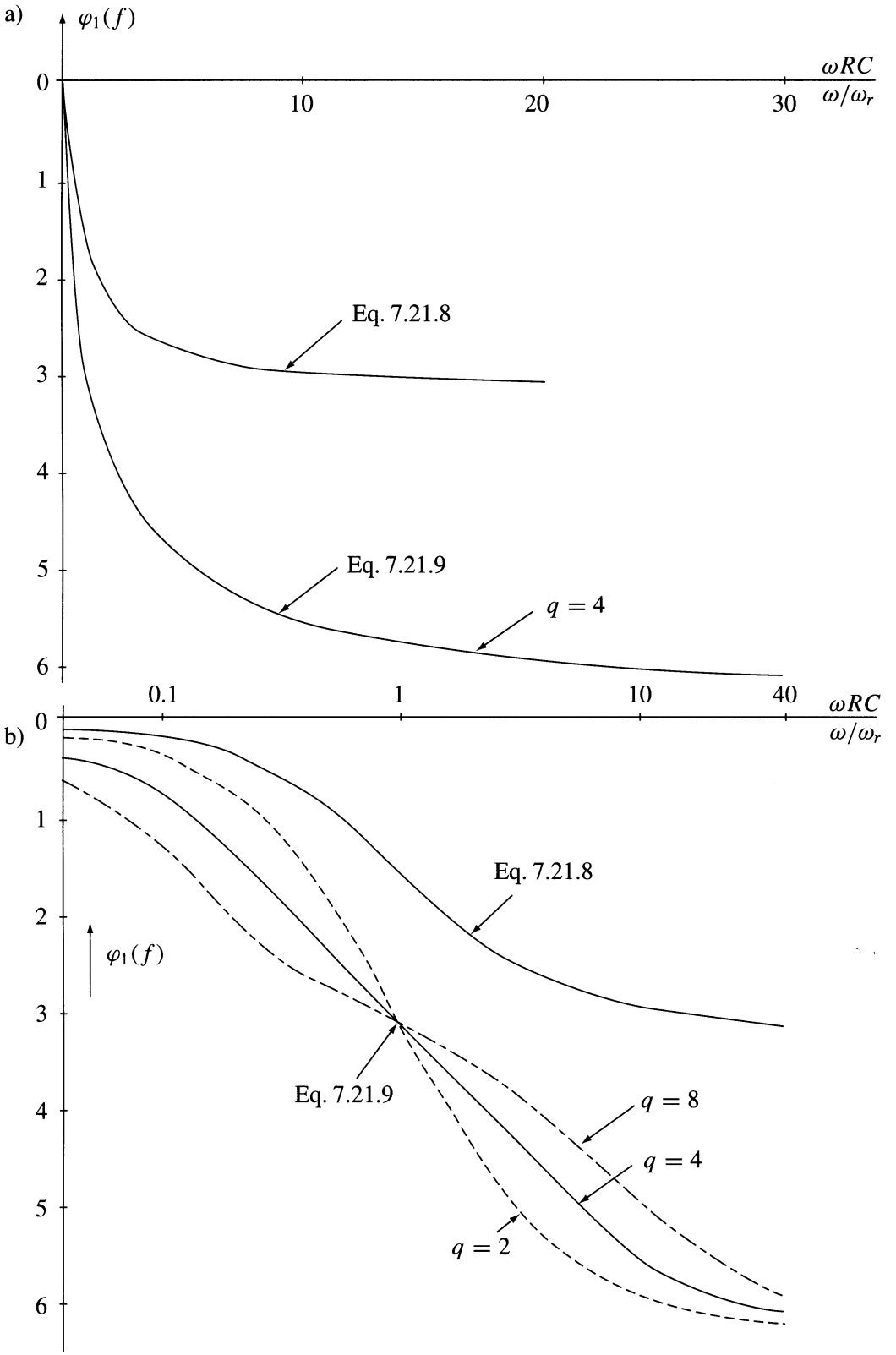

FIGURE 7.21.4 (a) Nonlinear phase functions of the first-order all-pass given by Equation (7.21.8) and the second-order all-pass given by Equation (7.21.9). (b) The same functions in a logarithmic frequency scale. The second-order function shows best linearity for $q = 4$.

by shifting the function $\varphi_1(f)$ in order to get a minimum value of the RMS phase error defined by Equation (7.21.5). The lower and upper frequency edges f_1 and f_2 are chosen as abcissae at which the error function diverges. The method is illustrated by four examples of design of Hilbert transformers given by the circuit models in Figure 7.21.5.

Example

First example: The Hilbert transformer of this example is implemented using two first-order all-pass filters (see Figure 7.21.5a). The phase function of the first filter is (see Equation [7.21.8])

$$\varphi_1(f) = \tan^{-1}\left[\frac{-2y}{y^2-1}\right]; \quad y = 2\pi f RC = 2\pi f \tau \tag{7.21.11}$$

The first step is abandoned because $\varphi_1(f)$ has no degree of freedom for linearization. In the second step we have to find the shift parameter denoted a in the phase function

$$\varphi_2(f) = \tan^{-1}\left[\frac{-2ay}{a^2y^2-1}\right], \quad Y = 2\pi f RC \tag{7.21.12}$$

giving the minimum RMS phase error. The functions $\varphi_1(f)$, $\varphi_2(f)$, and the error function $\varepsilon(f)$ are shown in Figure 7.21.6. Simple computer calculations yield the value of $a = 0.167$ giving the normalized frequency edges $y_1 = 1.75$ and $y_2 = 3, 5$, and the RMS phase error $\varepsilon_{RMS} = 0.012$. The pass-band equals one octave.

Second example: The phase splitter of this example is implemented using two first-order all-pass filters in each chain (see Figure 7.21.5b). The phase function of the first filter is

$$\varphi_1(f) = \tan^{-1}\left[\frac{-2y}{y^2-1}\right] + \tan^{-1}\left[\frac{-2ay}{a^2y^2-1}\right], \quad Y = 2\pi f RC \tag{7.21.13}$$

In the first step, we have to find the shift parameter a to get the best linearity of $\varphi_1(f)$ in the logarithmic scale. Small changes of a introduce a tradeoff between the RMS phase error and the pass-band of the Hilbert transformer. In the second step we have to find the value of the shift parameter b in the phase function

$$\varphi_2(f) = \tan^{-1}\left[\frac{-2by}{b^2y^2-1}\right] + \tan^{-1}\left[\frac{-2aby}{a^2b^2y^2-1}\right], \quad y = 2\pi f R \tag{7.21.14}$$

yielding the minimum of the RMS phase error. Figure 7.21.7 shows an example with $a = 0.08$ and $b = 0.24$ giving the normalized edge frequencies $y_1 = 1.6$ and $y_2 = 30$ ($f_2/f_1 = 18.75$ or more than 4 octaves) with $\varepsilon_{RMS} = 0.016$.

Third example: The phase splitter consists of three first-order all-passes in each chain (see Figure 7.21.5c). The phase functions are

$$\varphi_1(f) = \tan^{-1}\left[\frac{-2y}{y^2-1}\right] + \tan^{-1}\left[\frac{-2ay}{a^2y^2-1}\right] + \tan^{-1}\left[\frac{-2by}{b^2y^2-1}\right] \tag{7.21.15}$$

and

$$\varphi_2(f) = \tan^{-1}\left[\frac{-2cy}{c^2y^2-1}\right] + \tan^{-1}\left[\frac{-2cay}{c^2a^2y^2-1}\right] + \tan^{-1}\left[\frac{-2cby}{c^2b^2y^2-1}\right] \tag{7.21.16}$$

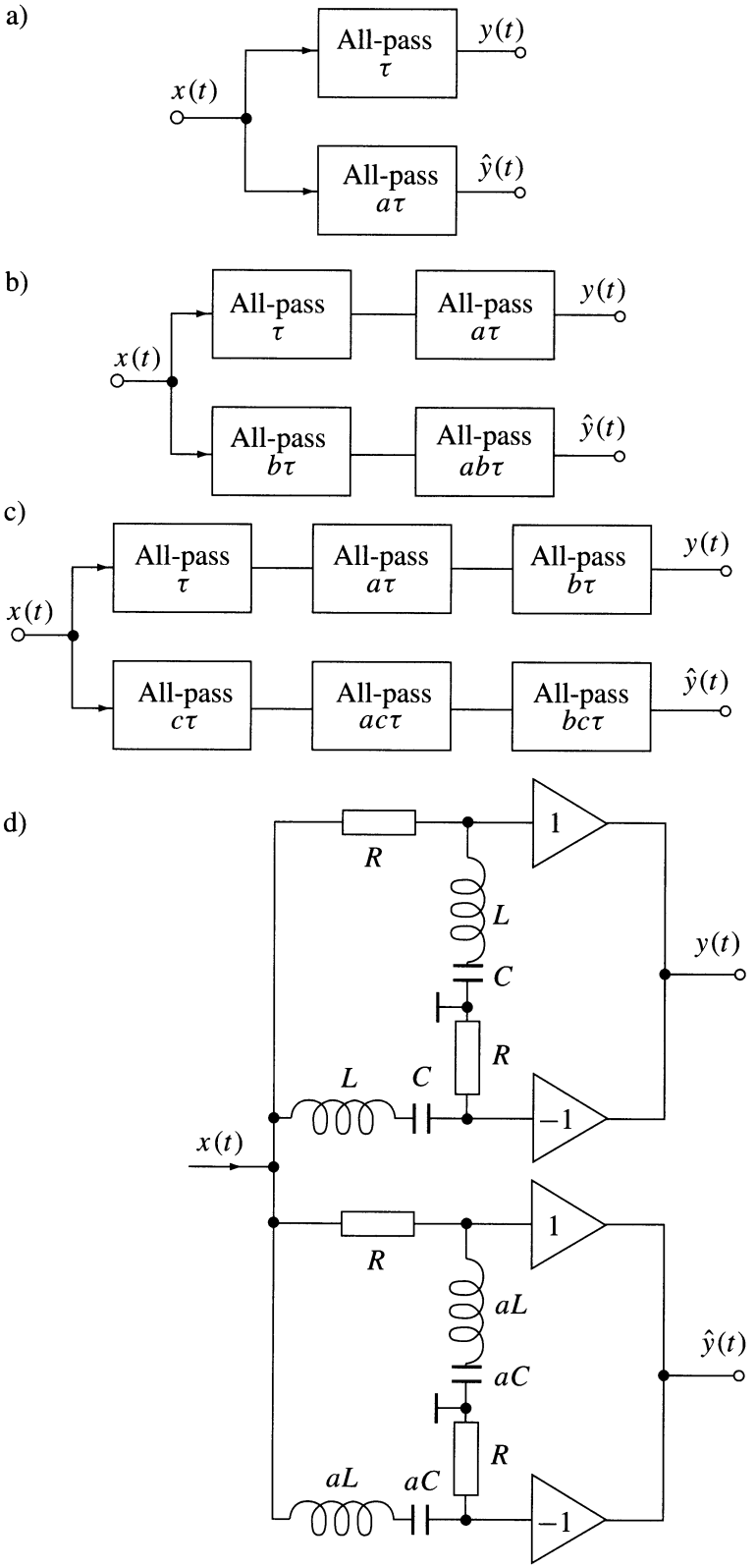

FIGURE 7.21.5 The phase splitter Hilbert transformer using (a) first-order all-pass filters, (b) a series connection of two first-order all-passes, (c) three first-order all-passes, and (d) second-order all-passes.

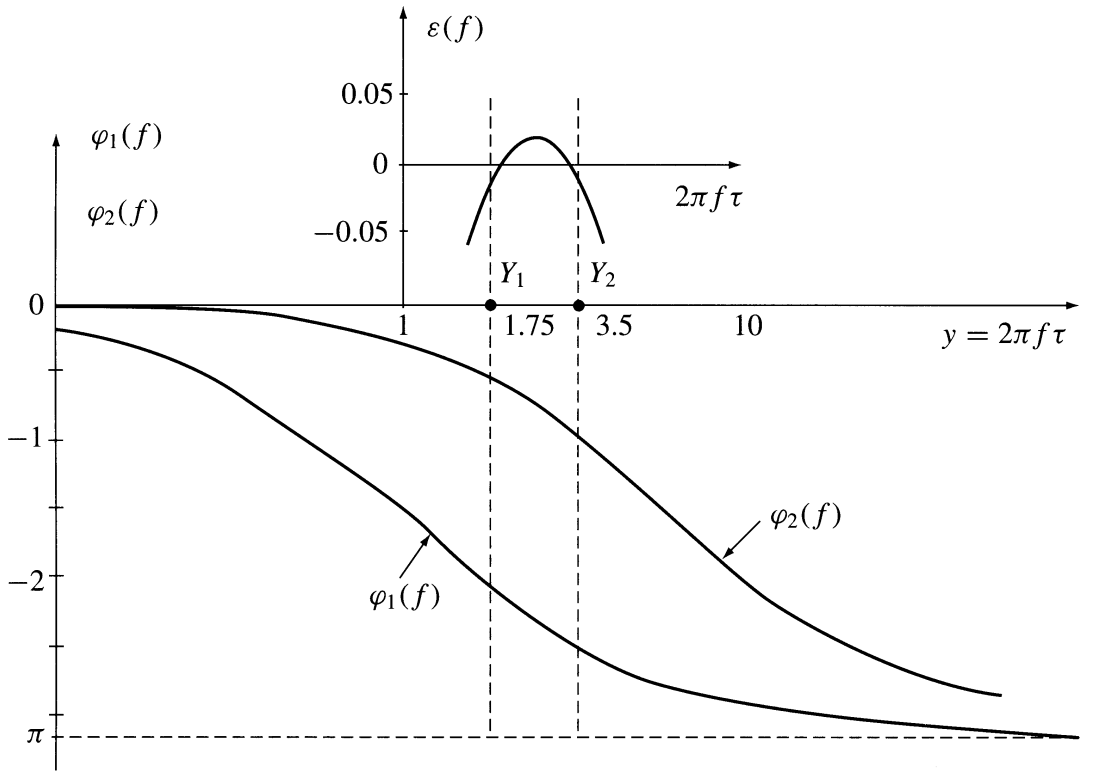

FIGURE 7.21.6 The phase functions and the phase error of the Hilbert transformer of Figure 7.21.5a.

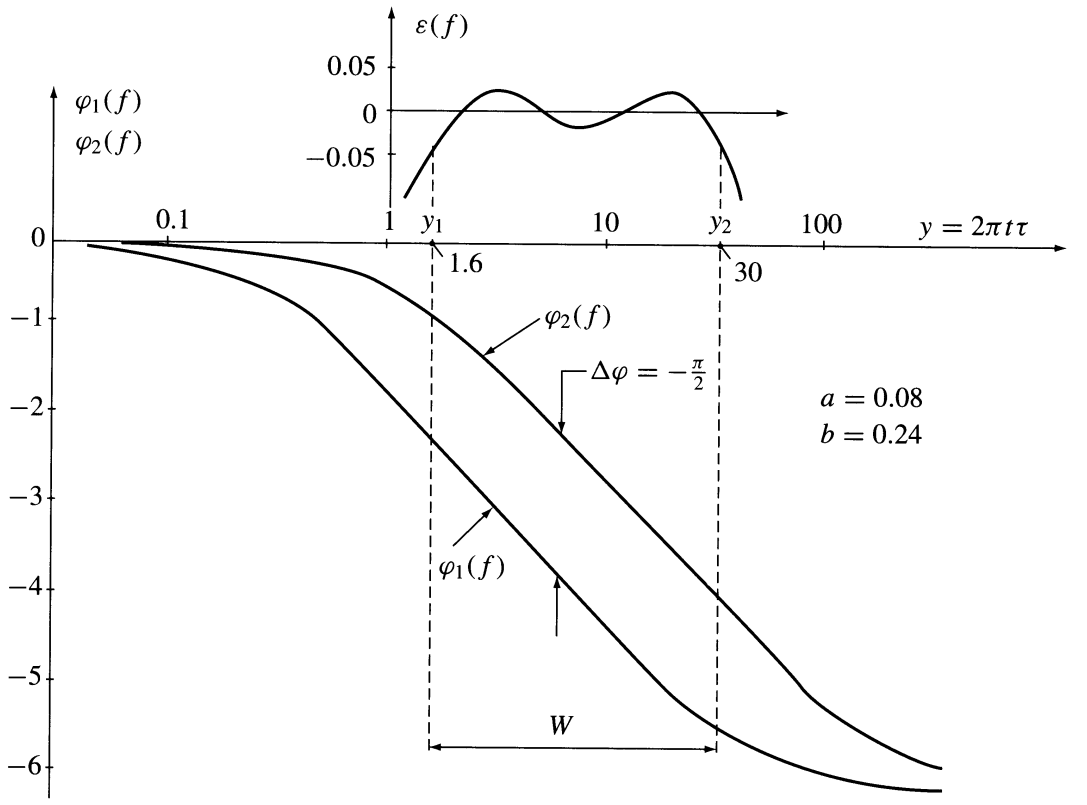

FIGURE 7.21.7 The phase functions and the phase error of the Hilbert transformer of Figure 7.21.5b.

Good linearity of the phase function $\varphi_1(f)$ depend on the shift parameters a and b. The first step yields $a = 0.08$ and $b = 0.008$. In the second step the parameter $c = 0.24$ yields the minimum value of the RMS phase error. Figure 7.21.8 shows the phase functions and the error distribution $\varepsilon(f)$. The RMS phase error is $\varepsilon_{RMS} = 0.025$. The edge frequencies are $y_1 = 1.8$, $y_2 = 300$ giving $f_2/f_1 = 166$ (more than 7 octaves). A smaller phase error may be achieved at the cost of frequency range.

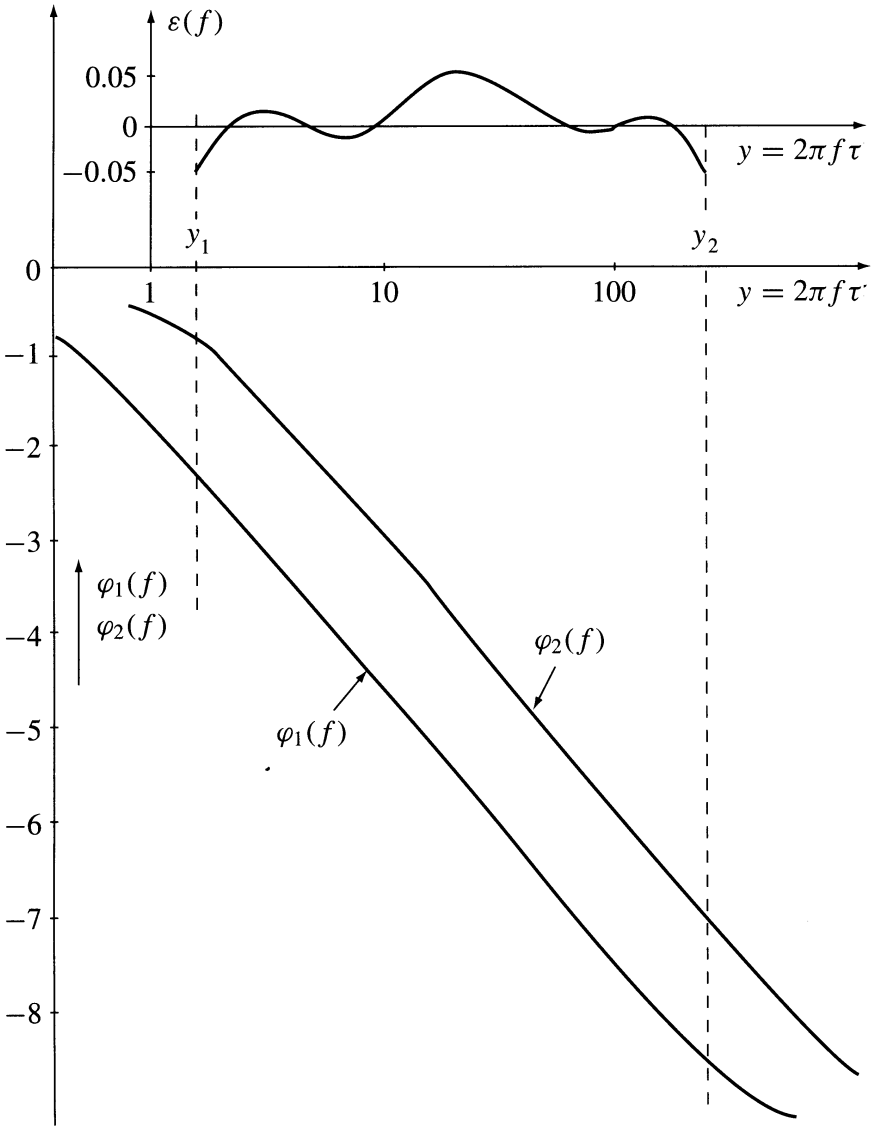

FIGURE 7.21.8 The phase functions and the phase error of the Hilbert transformer of Figure 7.21.5c.

Fourth example: The phase splitter consists of one second-order all-pass in each chain (see Figure 7.21.5d). The phase functions are

$$\varphi_1(f) = \tan^{-1}\left[\frac{2(1-y^2)qy}{(1-y^2)^2 - q^2y^2}\right], \quad Y = 2\pi fRC \tag{7.21.17}$$

$$\varphi_2(f) = \tan^{-1}\left[\frac{2\left(1-a^2y^2\right)qay}{\left(1-a^2y^2\right)^2 - q^2a^2y^2}\right], \quad Y = 2\pi f RC \tag{7.21.18}$$

Good linearity of $\varphi_1(f)$ yields the value $q = 4$ (see Figure 7.21.9). The minimum value of the RMS phase error yields the shift parameter $a = 0.232$. The phase functions and the error distribution are shown in Figure 7.21.4. The edge frequencies are $y_1 = 0.5$ and $y_2 = 9$ giving $f_2/f_1 = 18$ with $\varepsilon_{\text{RMS}} = 0.0186$. The bandwidth is about the same as in the second example with two first order all-passes in each chain.

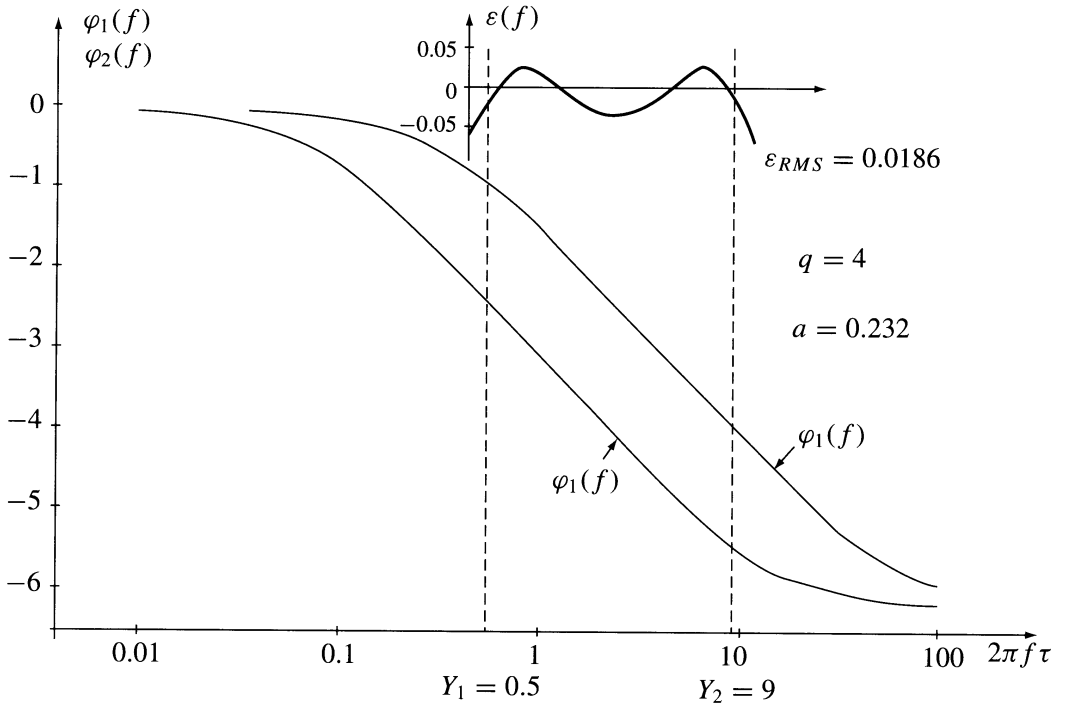

FIGURE 7.21.9 The phase functions and the phase error of the Hilbert transformer of Figure 7.21.5d.

Delay, Phase Distortions, and Equalization

The phase functions of the all-pass filters used to implement the Hilbert transformer are, disregarding the small phase errors, linear in the logarithmic frequency scale, but nonlinear in a linear frequency scale. Let us investigate the phase distortions due to that nonlinearity for the Hilbert filter of the second example. Consider a wide-band test signal given by the Fourier series of a square wave truncated at the seventh harmonic term:

$$x(t) = \frac{4}{\pi}\left[\sin(\omega_1 t) + \frac{1}{3}\sin(3\omega_1 t) + \frac{1}{5}\sin(5\omega_1 t) + \frac{1}{7}\sin(7\omega_1 t)\right] \tag{7.21.19}$$

where $\omega_1 = 2\pi f_1 = 1.75/\tau$ was chosen near the low-frequency edge of the pass-band W. The spectrum of this signal is enclosed inside W. The waveforms of this signal and its Hilbert transform are shown in Figure 7.21.10a. The phase-distorted Hilbert pair at the output ports of the phase splitter is shown in Figure 7.21.10b. The phase distortions can be removed by connecting a phase equalizer in series to the input port, predistorting the input signal (see the waveform of Figure 7.21.10d). The required phase functions of the equalizer may have the form

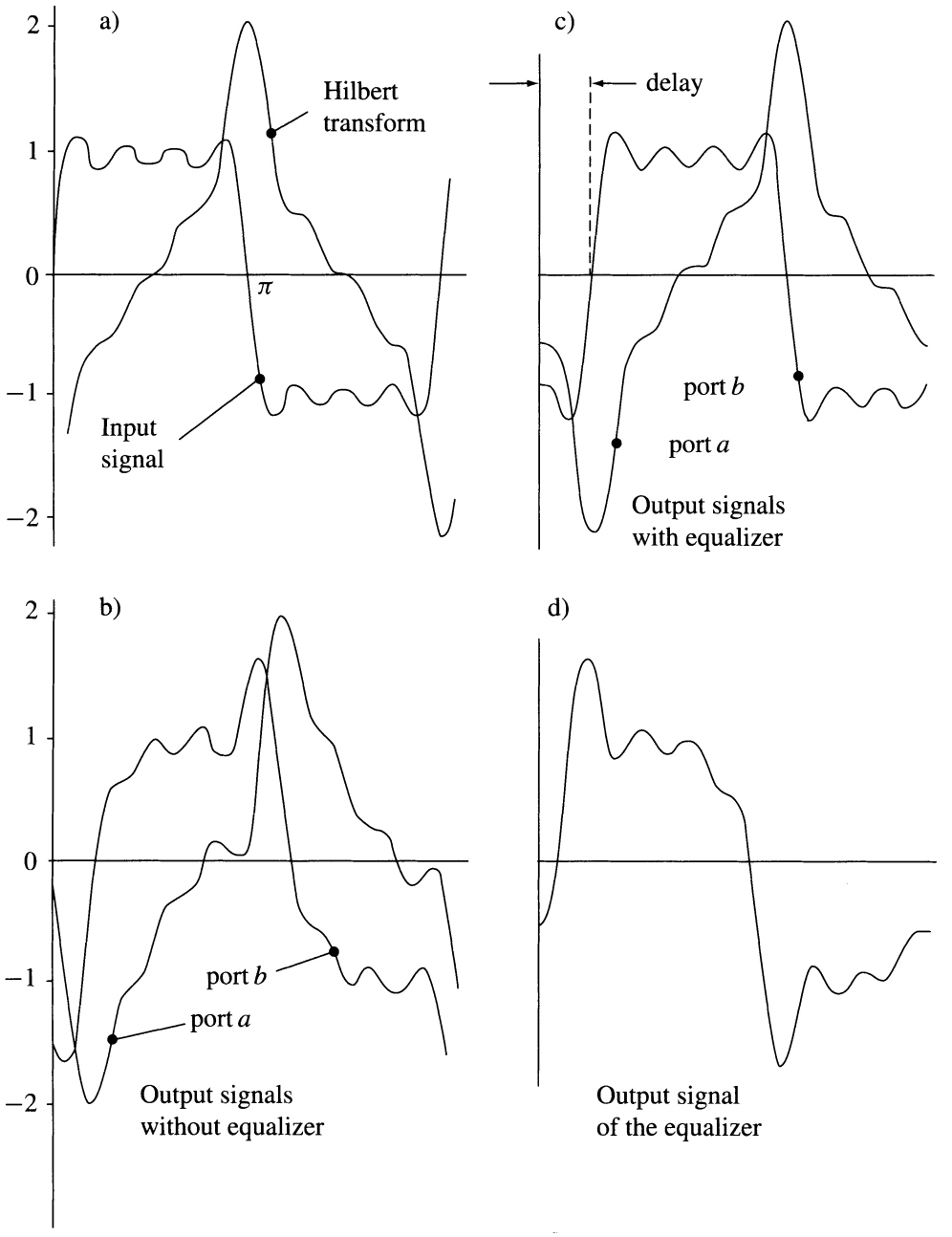

FIGURE 7.21.10 The waveform given by (a) the truncated Fourier series (7.21.15) and of its Hilbert transform, (b) the distorted Hilbert pair at the output with no equalization, (c) the equalized undistorted and delayed Hilbert pair, and (d) the input signal predistorted by the equalizer.

$$\varphi_{\text{equalizer}}(f) = \varphi_L(f) - \varphi_2(f) \tag{7.21.20}$$

where $\varphi_2(f)$ is given by Equation (7.21.14) and

$$\varphi_L(f) = \varphi_2(f_0) + \left.\frac{d\varphi_2(f)}{df}\right|_{f=f_0} (f - f_0) \tag{7.21.21}$$

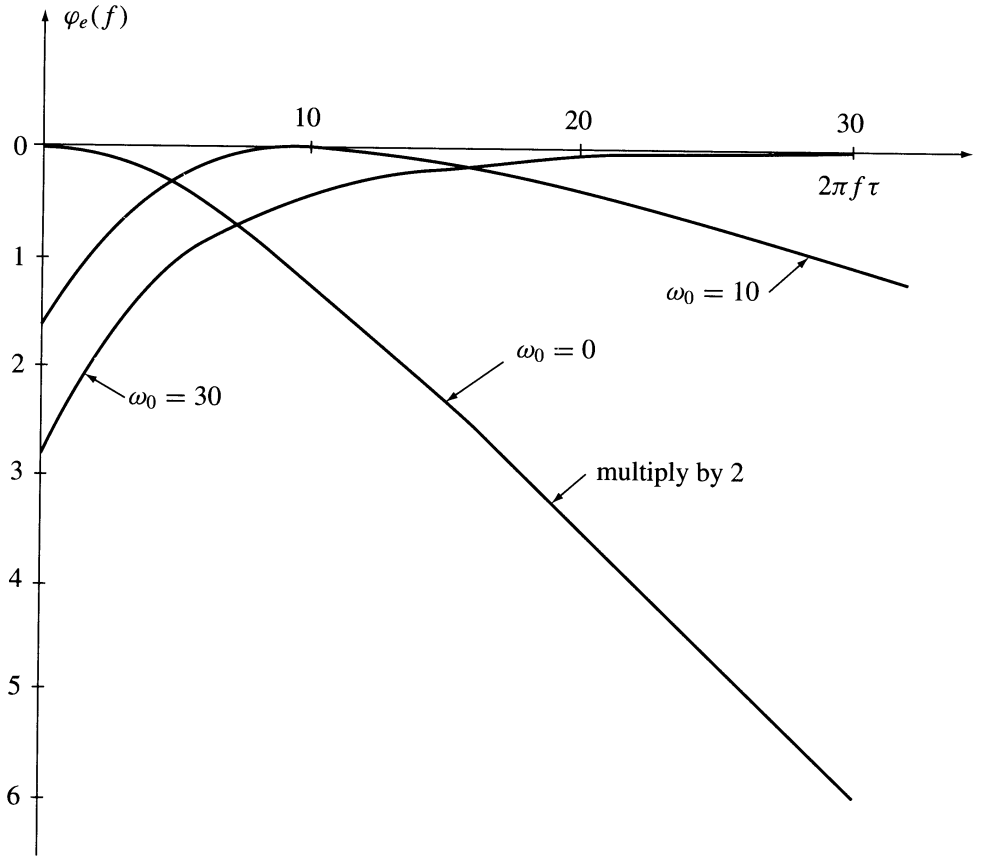

FIGURE 7.21.11 The phase functions of the equalizer given by Equation (7.21.10) for the phase function $\varphi_2(f)$ given by Equation (7.21.14).

is a linear phase function tangential to $\varphi_2(f)$ at $f = f_0$. Figure 7.21.11 shows the phase function of the equalizer for three different values of the abcissae f_0. Figure 7.21.10c shows the delayed and practically undistorted output waveforms of the equalized Hilbert transformer with $f_0 = 0$. **The delay** is given by the slope of the phase function

$$t_0 = \left.\frac{d\varphi_2(f)}{df}\right|_{f_0=0} = -2\tau b(1+a) \tag{7.21.22}$$

giving the delay $t_0 = 0.5065$ sec ($\tau = 1$). Another method of linearization of the phase function is given in Reference 21.

Hilbert Transformers with Tapped Delay-Line Filters

Tapped delay-line filters often referred to as transversal filters may be used as phase equalizers. Such a filter enables the approximation of a given transmittance $H(jf)$ with a desired accuracy. Therefore, a Hilbert filter may be implemented using a tapped delay line,[15,34] (see Figure 7.21.12). If the spectrum of the input signal is band-pass limited such that $X(f) = 0$ for $|f| > W$, then the transfer function of the ideal Hilbert transformer given by Equation 7.21.2 may be truncated at $|f| = W$. The tapped delay-line Hilbert filter may be designed using a periodic repetition of this truncated function, as shown in Figure 7.21.13. The expansion of this function in a Fourier series yields, using truncation, the following approximate form of the transfer function

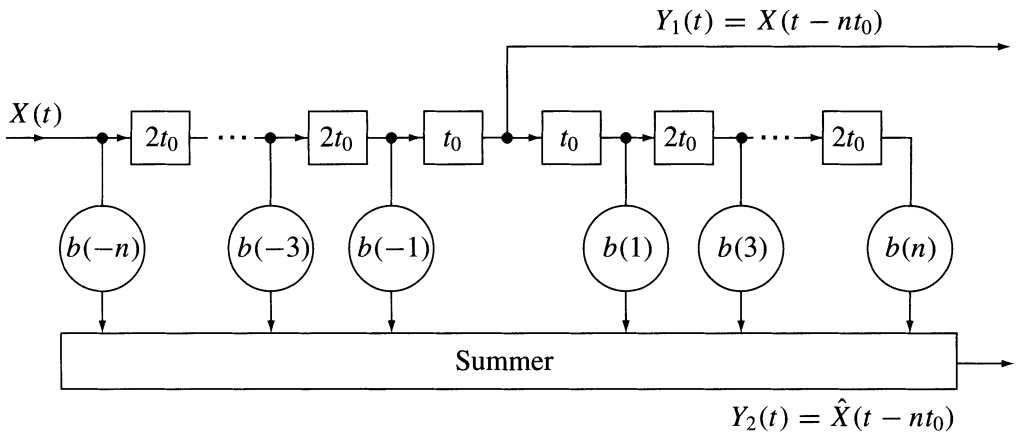

FIGURE 7.21.12 A tapped delay line Hilbert transformer.

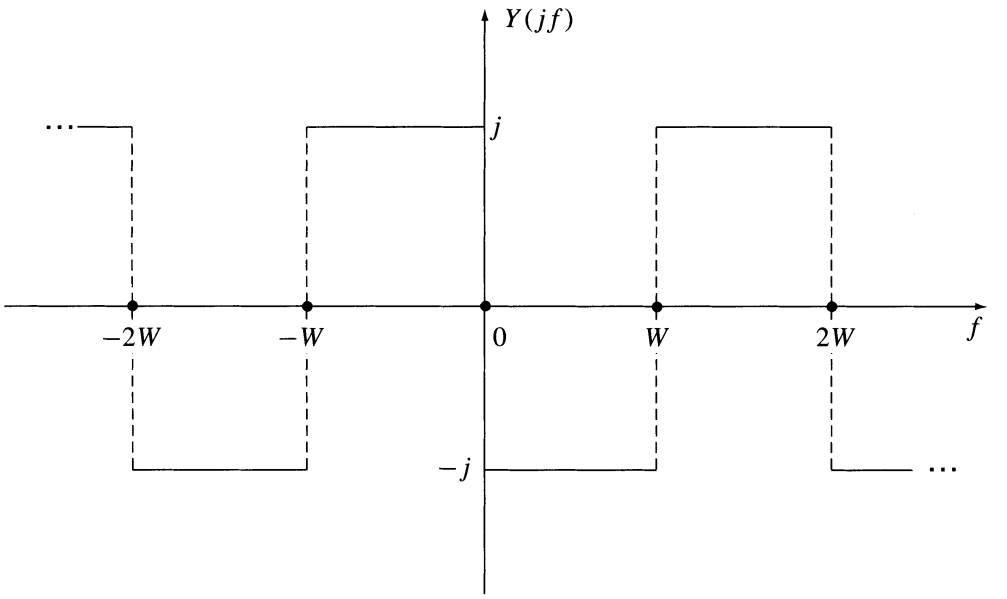

FIGURE 7.21.13 A truncated at ± W and periodically repeated transfer function of an ideal Hilbert transformer (see Equation [7.21.2]).

$$H_N(jf) = 2j \sum_{i=1}^{(N-1)/2} b(i) \sin[i 2\pi f t_0]; \quad t_0 = \frac{1}{2W} \tag{7.21.23}$$

with

$$b(i) = -\frac{2}{\pi i} \sin^2\left[\frac{\pi i}{2}\right] \tag{7.21.24}$$

Different from the implementations of Hilbert transformers with all-pass filters, where the design amplitude equals error zero and the phase error is distributed over the pass-band, here the roles are interchanged. The amplitude error is distributed over the pass-band and there is no phase error (linear phase). The RMS amplitude ripple decreases with the increasing number of tapes of the delay line (increasing

number of coefficients $b(n)$. The transversal Hilbert transformer, disregarding the small distortions due to the amplitude ripple, produces at the output a delayed undistorted signal and its Hilbert transform. However, analog implementations are rarely used in favor of digital implementations in the form of FIR (Finite Impulse Response) Hilbert transformers.

Band-Pass Hilbert Transformers

The transfer function of a band-pass Hilbert transformer may be defined as the frequency-translated transfer function of a low-pass Hilbert transformer. The transfer function of an ideal low-pass with linear phase is given by the formula

$$H_{\mathrm{LP}}(jf) = \Pi[f/(2W)]e^{-j2\pi f\tau} \tag{7.21.25}$$

where τ is the time delay and $\Pi(x)$ has the form

$$\Pi\left(x\right) = \begin{cases} 1 & \text{for } |x| < 0.5 \\ 0.5 & \text{for } |x| = 0.5 \\ 0 & \text{for } |x| > 0.5 \end{cases} \tag{7.21.26}$$

This is illustrated in Figure 7.21.14. The impulse response of this filter is

$$h_{\mathrm{LP}}\left(t\right) = F^{-1}\left[H_{\mathrm{LP}}\left(jf\right)\right] = 2W\frac{\sin X}{X} \tag{7.21.27}$$

where $X = 2\pi W(t-\tau)$. The response, as shown in Figure 21.15 is noncausal, but for large delays τ is nearly causal. The transfer function of the Hilbert transformer derived from Equation (7.21.25) is given by

$$H_{\mathrm{H}}(jf) = H_{\mathrm{LP}}(jf)\,e^{-j\,[0.5\pi\,\mathrm{sgn}(f)\,+\,2\pi f\tau\,]} \tag{7.21.28}$$

as illustrated in Figure 7.21.14a,c. The impulse response of such a Hilbert transformer is

$$h_H\left(t\right) = F^{-1}\left[H_H\left(jf\right)\right] = \frac{1}{\pi\left(t-\tau\right)}\left[1-\cos 2\pi W\left(t-\tau\right)\right] \tag{7.21.29}$$

or

$$h_H\left(t\right) = \frac{2\sin^2\left[\pi W\left(t-\tau\right)\right]}{\pi\left(t-\tau\right)} \tag{7.21.30}$$

This is illustrated in Figure 7.21.15b. If W goes to infinity the mean value of $h_H(t)$ taken over the period $T = 1/W$ approximates the distribution $1/(\pi\,(t-\tau)$. The transfer function of an ideal band-pass filter is given by

$$H_{\mathrm{BP}}\left(jf\right) = \left\{\prod\left[\frac{f+f_0}{2W}\right] + \prod\left[\frac{f-f_0}{2W}\right]\right\}e^{-j2\pi f\tau} \tag{7.21.31}$$

This is illustrated in Figure 7.21.16a,b. The impulse response of this filter is

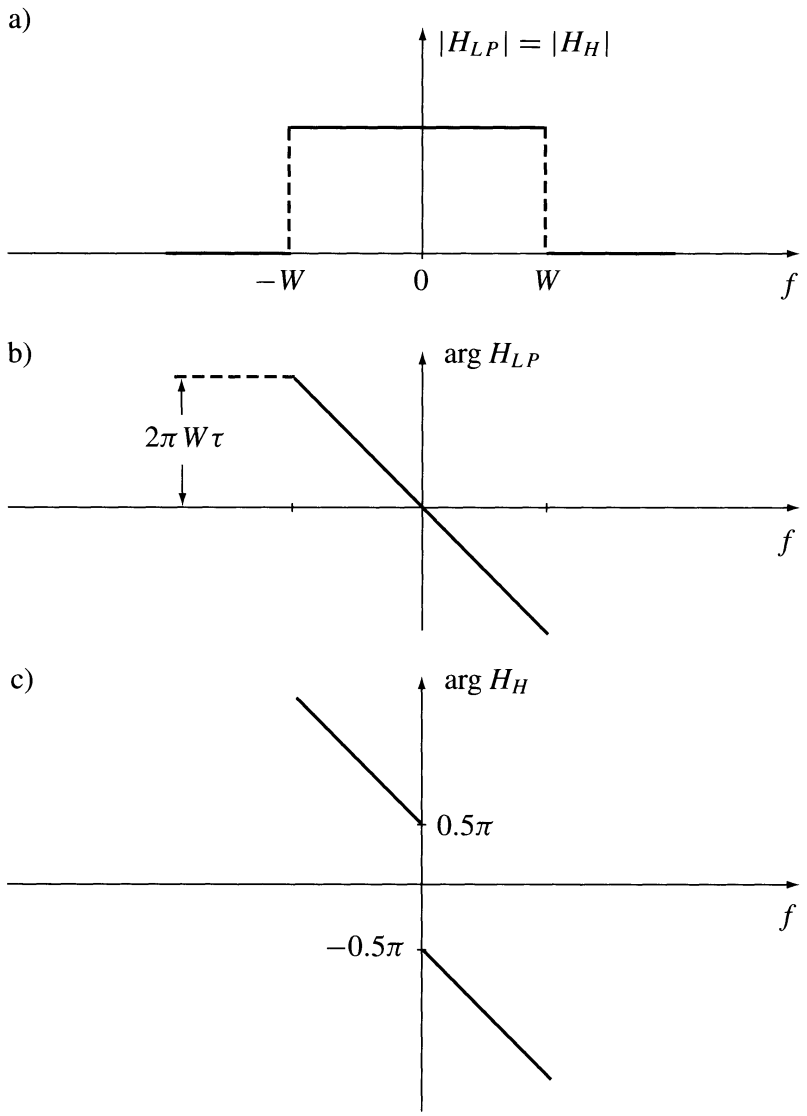

FIGURE 7.21.14 The transfer function of the ideal low-pass: (a) magnitude, (b) linear phase function, and (c) phase function of a Hilbert transformer derived from the low-pass function.

$$h_{\mathrm{BP}}(t) = 2W\frac{\sin X}{X}\cos\left[2\pi f_0(t-\tau)\right] \tag{7.21.32}$$

and is shown in Figure 7.21.17a. The transfer function of an ideal band-pass Hilbert transformer derived from the transfer function (7.21.31) is

$$H_{\mathrm{HBP}}(jf) = H_{\mathrm{BP}}(jf)\ \exp\{-j\ 0.5\pi[\mathrm{sgn}(f+f_0) + \mathrm{sgn}(f-f_0)]\} \tag{7.21.33}$$

This is illustrated in Figure 7.21.16a,c. The impulse response of this Hilbert transformer is

$$h_{\mathrm{HBP}}(t) = \frac{2\sin^2\left[\pi W(t-\tau)\right]}{\pi(t-\tau)}\cos\left[2\pi f_0(t-\tau)\right] \tag{7.21.34}$$

and is shown in Figure 7.21.17b.

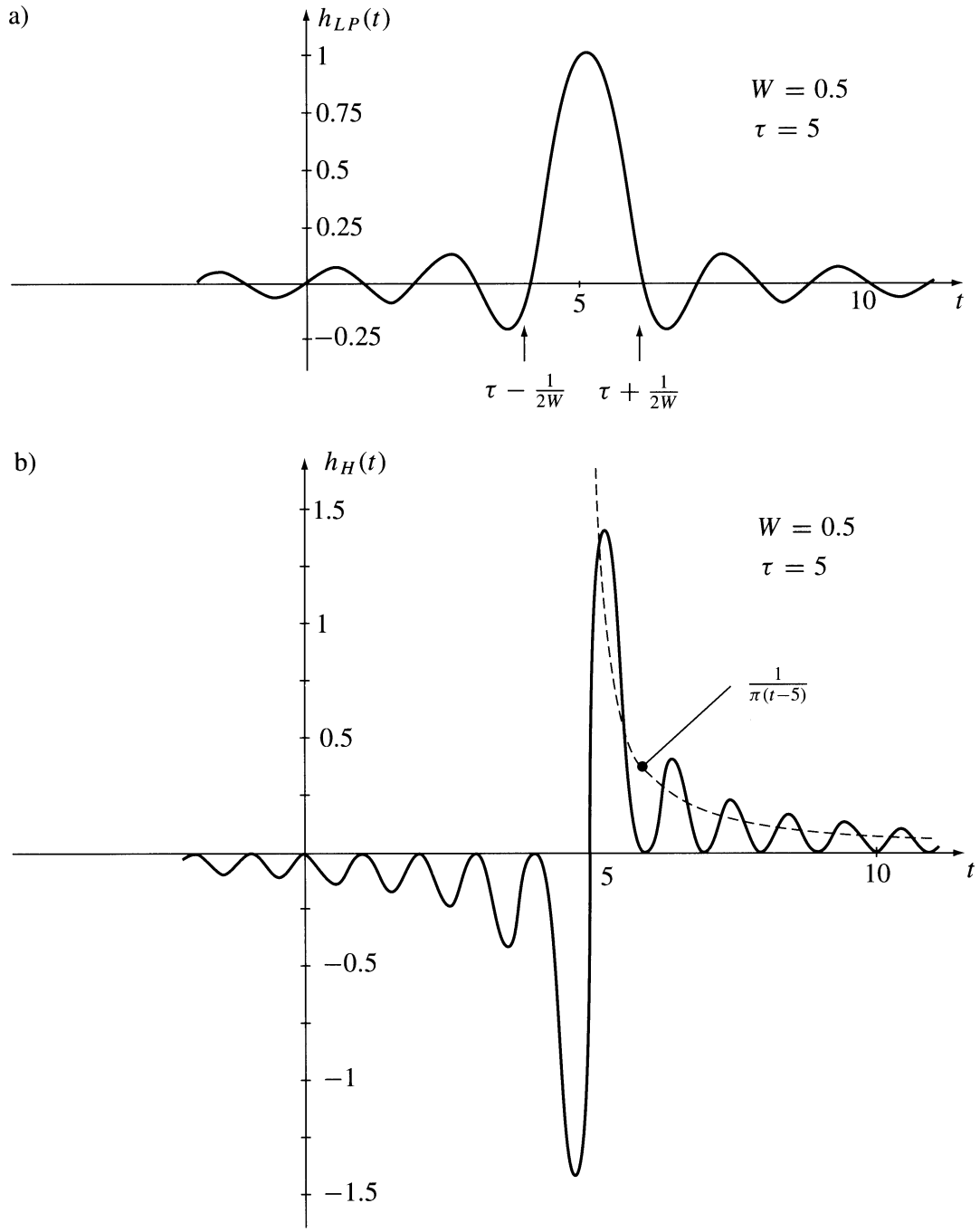

FIGURE 7.21.15 Impulse responses of (a) the low-pass and (b) the corresponding Hilbert transformer. Transfer functions are shown in Figure 7.21.14.

Consider the response of the band-pass Hilbert transformer to a band-pass signal $u_1(t) = x(t)\cos(2\pi f_0 t)$ where $x(t)$ has no spectral terms for $|f| > W$ and $f_0 > W$. This response has the form

$$u_2(t) = \hat{x}(t-\tau)\cos\left[2\pi f_0(t-\tau)\right] \tag{7.21.35}$$

that is, the modulating signal $x(t)$ is replaced by the delayed version of its Hilbert transform. Notice that due to Bedrosian's theorem the Hilbert transform of the input signal (see Section 7.12) has the form

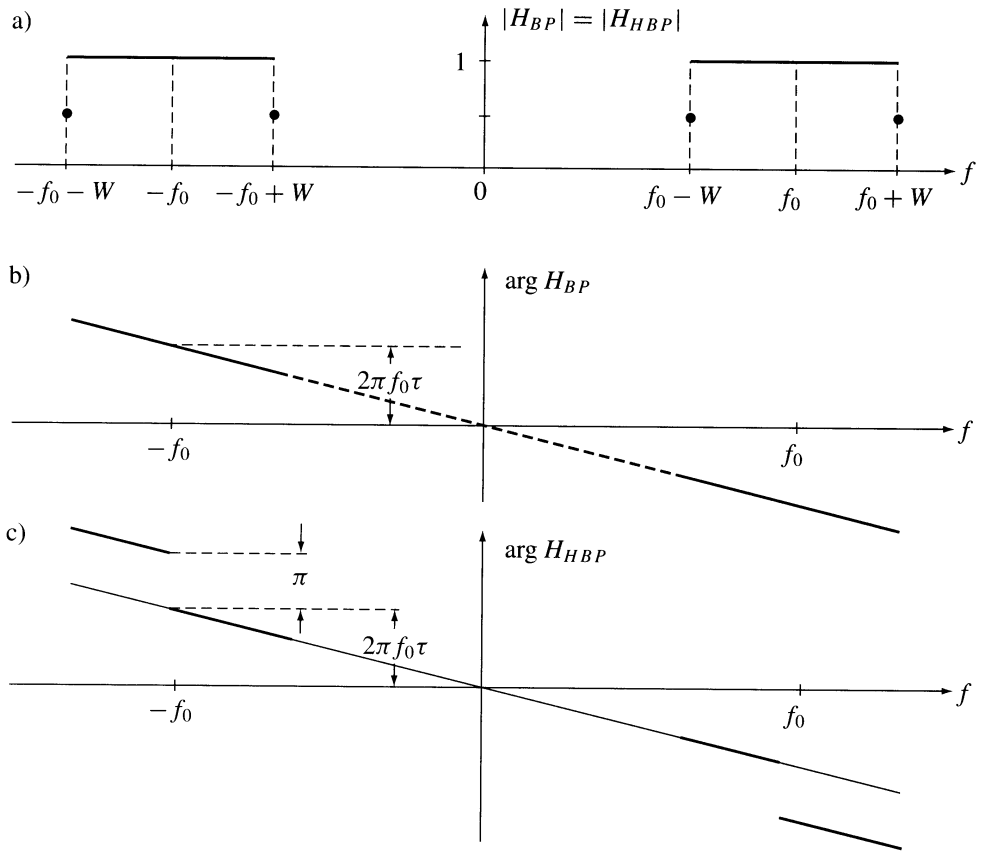

FIGURE 7.21.16 The transfer functions of an ideal band-pass filter and of the corresponding Hilbert transformer: (a) the magnitude, (b) the phase function of the band-pass, and (c) the Hilbert transformer.

$$u_2(t) = x(t - \tau)\ \sin[2\pi\ f_0(t - \tau)] \tag{7.21.36}$$

that is, only the carrier is Hilbert transformed, compared to signal (7.21.35), for which the envelope is transformed. The transfer function of a band-pass producing at the output the Hilbert transform in agreement with Bedrosian's theorem is given by the equation

$$H_{\mathrm{HBP}}(jf) = -j\ \mathrm{sgn}(f)\ H_{\mathrm{BP}}(jf) \tag{7.21.37}$$

where $H_{\mathrm{BP}}(jf)$ is given by Equation (7.21.31) and is shown in Figure 7.21.18.

A possible implementation of a band-pass Hilbert transformer defined by Equation (7.21.31) is shown in Figure 7.21.19. It consists of a linear phase lower side-band band-pass, analogous upper side-band band-pass, and a substractor. Figure 7.21.20 shows the implementation of such a Hilbert transformer by use of a SAW (Surface Acoustic Wave) filter.

Generation of Hilbert Transforms Using SSB Filtering

The Hilbert transform of a given signal may be obtained by band-pass filtering of a double side-band AM signal. The SSB signal has the form (see Section 7.16)

$$u_{\mathrm{SSB}}(t) = x(t)\cos(2\pi F_0 t) \mp \hat{x}(t)\sin(2\pi F_0 t) \tag{7.21.38}$$

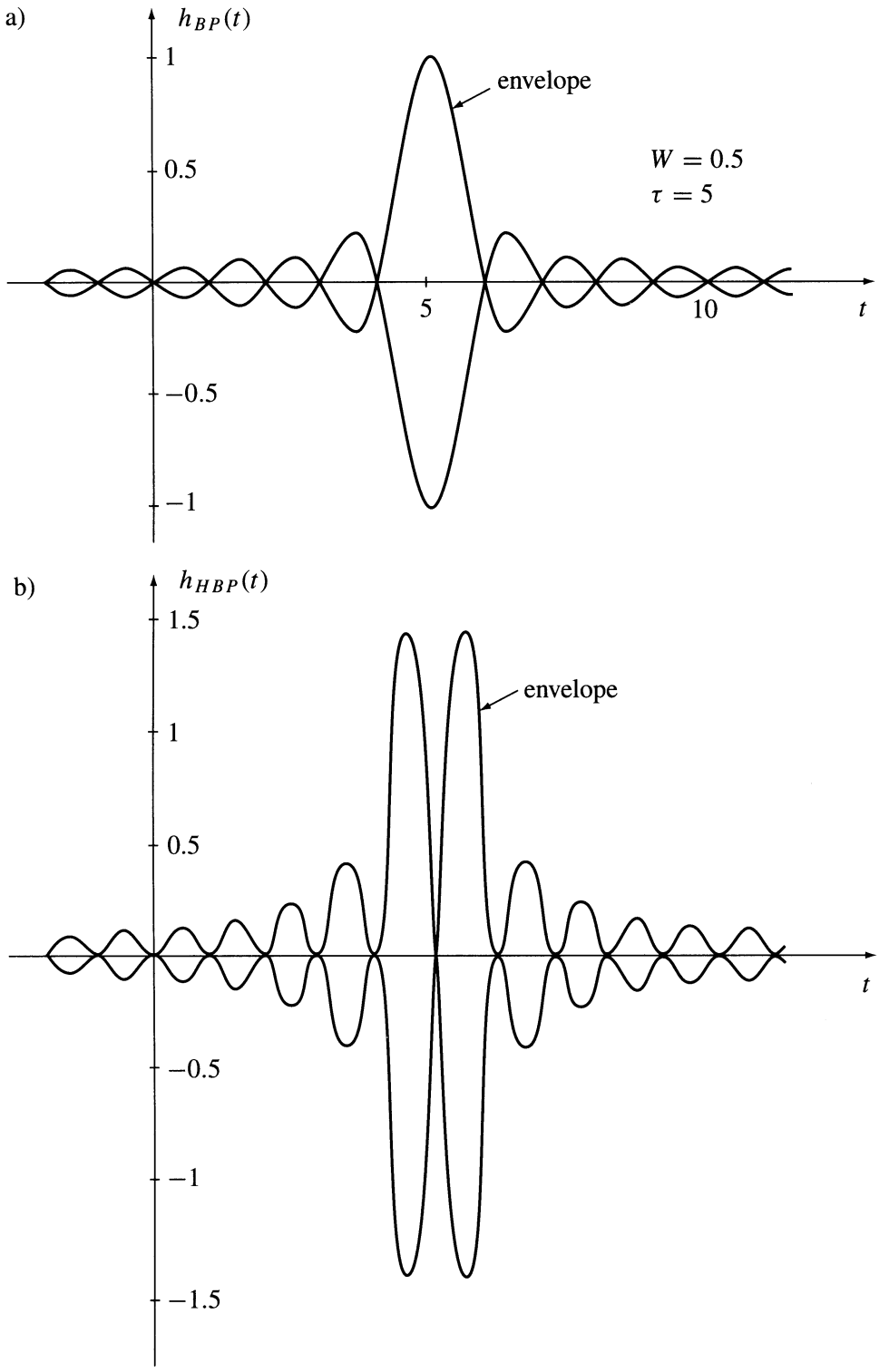

FIGURE 7.21.17 The envelopes of the impulse responses of (a) a band-pass and (b) the Hilbert transformer. Transfer functions are shown in Figure 7.21.16.

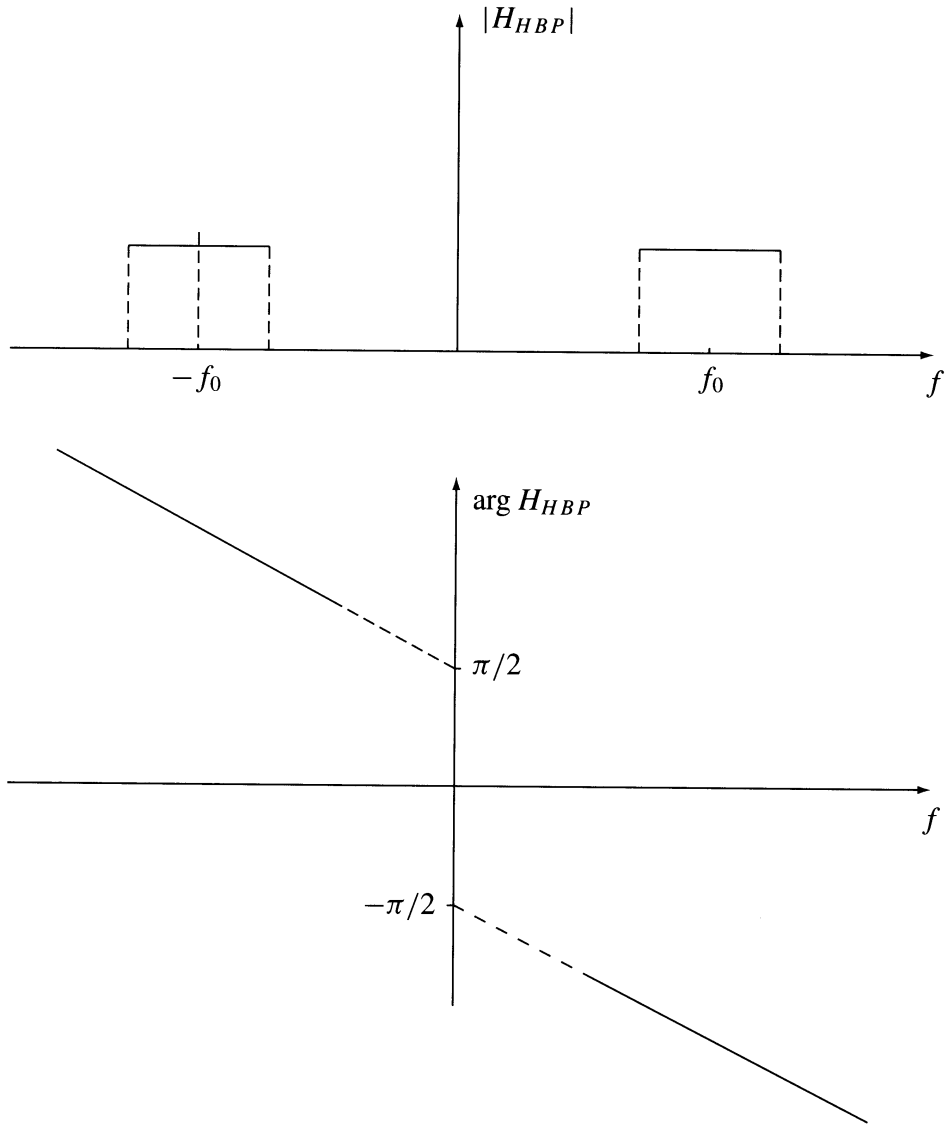

FIGURE 7.21.18 The transfer function of a Hilbert transformer that transforms the carrier signal with no change of the waveform of the envelope.

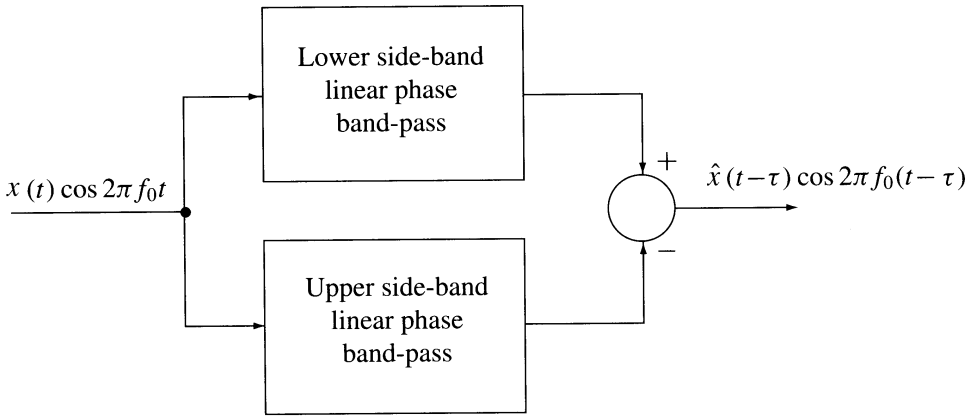

FIGURE 7.21.19 The implementation of the Hilbert transformer of the transfer function defined in Figure 7.21.16 using two band-pass filters.

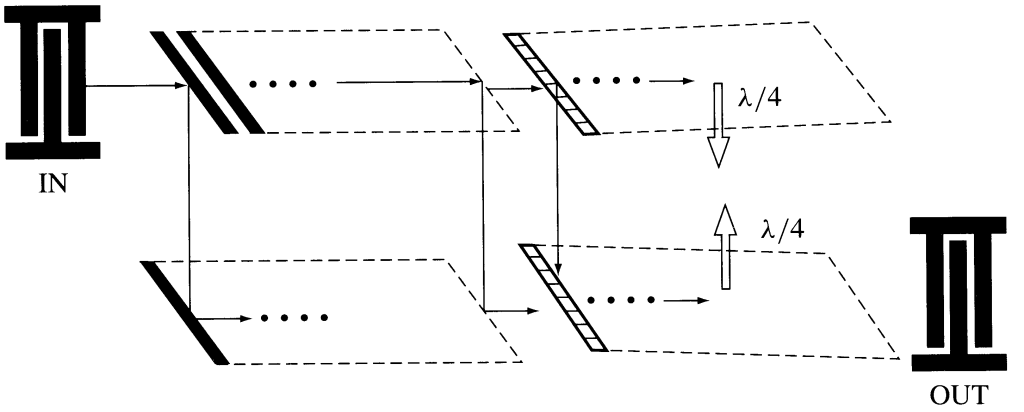

FIGURE 7.21.20 A SAW filter implementing the band-pass Hilbert transformer of Figure 7.21.19.

where F_0 is the carrier frequency. Such a signal can be obtained by band-pass filtering of a double side-band AM signal. A synchronous demodulator using the quadrature carrier $\sin(2\pi F_0 t)$ generates at his output the Hilbert transform $\hat{x}(t)$.

Digital Hilbert Transformers

The ideal discrete-time Hilbert transformer is defined as an all-pass with a pure imaginary transfer function, that is, if

$$H\left(e^{j\psi}\right) = H_r\left(\psi\right) + jH_i\left(\psi\right), \quad \text{then} \quad H_r\left(\psi\right) = 0 \quad \text{all } f \tag{7.21.39}$$

and

$$H\left(e^{j\psi}\right) = jH_i\left(\psi\right) = \begin{cases} -j & 0 < \psi < \pi \\ 0 & \psi = 0, \left|\psi\right| = \pi \\ j & -\pi < \psi < 0 \end{cases} \tag{7.21.40}$$

or in another equivalent notation

$$H(e^{j\psi}) = -j\ \mathrm{sgn}(\sin\psi) = -\mathrm{sgn}(\sin\psi)e^{j\pi/2} = |H(\psi)|e^{j\arg H(\psi)} \tag{7.21.41}$$

The magnitude (see Figure 7.21.21) has the form

$$\left|H\left(\psi\right)\right| = \left|\mathrm{sgn}\left(\sin\psi\right)\right| = \begin{cases} 1, & 0 < \left|\psi\right| < \pi \\ 0, & \psi = 0, \left|\psi\right| = \pi \end{cases} \tag{7.21.42}$$

and the phase function is

$$\arg[H(\psi)] = -(\pi/2)\ \mathrm{sgn}(\sin\psi) \tag{7.21.43}$$

Notice that $\psi = 2\pi f_n$, where $f_n = f/f_s$ is a frequency normalized against the sampling frequency f_s. The basic period has the interval from $-\pi$ to π corresponding to the values of f_n from –0.5 to 0.5. The

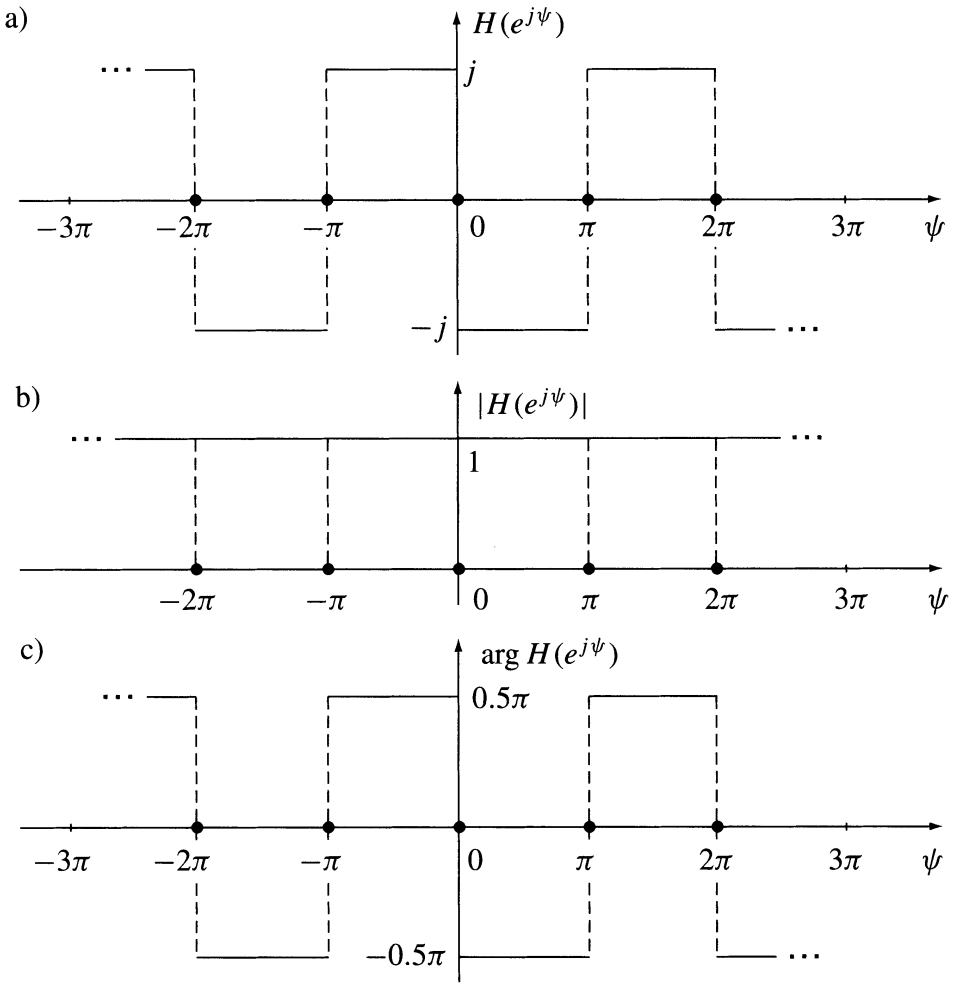

FIGURE 7.21.21 An ideal discrete-time Hilbert transformer's (a) transfer function, (b) magnitude, and (c) phase function.

noncausal infinite range impulse response of the ideal Hilbert transformer has the form of the antisymmetric sequence

$$h(i) = (2/\pi\ i)\ \sin^2(i\pi\ /2) \tag{7.21.44}$$

If one allows the addition of a linear phase term in the ideal frequency response introducing a frequency-independent group delay (in samples), then the transfer function (7.21.40) takes the form

$$H\left(e^{j\psi}\right) = \begin{cases} -je^{-j\psi\tau} & 0 < \psi < \pi \\ 0 & \psi = 0, |\psi| = \pi \\ je^{-j(\psi-2\pi)\tau} & \pi < \psi < 2\pi \end{cases} \tag{7.21.45}$$

and the impulse response takes the form

$$h(i) = (2/\pi)\frac{\sin^2\left[(\pi/2)(i-\tau)\right]}{i-\tau}, \quad i = 0, \pm 1, 2, \ldots \tag{7.21.46}$$

The important feature of the impulse response given by (7.21.44) is that even-numbered samples are exactly zero, and that the samples are antisymmetric, that is,

$$h(i) = -h(-i)\,; \quad i = 0, 1, \ldots \tag{7.21.47}$$

Methods of Design

There are several methods of realizing digital Hilbert transformers. The three basic implementations are

1. The **FIR** (Finite Impulse Response) Hilbert transformer.
2. The **IIR** (Infinite Impulse Response) Hilbert transformer.
3. Digital phase splitter Hilbert transformer.

It is possible to realize a differentiating Hilbert transformer that produces at the output the derivative of the Hilbert transform of the input signal.

FIR Hilbert Transformers[25,31]

The FIR Hilbert transformer is a digital version of the taped delay line Hilbert transformer (see Section 7.21). Its structure is shown in Figure 7.21.22. The string of z^{-1} delays acts as a discrete taped delay line. Such a filter is inherently stable and its impulse response is given by the coefficients (gains) $h(0)$, $h(1)$, $h(2)$, …, $h(i)$, …, $h(N-1)$, that is, has the length of N samples. An example of the impulse response of the FIR Hilbert transformer is shown in Figure 7.21.23b, where for convenience, N is an odd number. This causal impulse response is obtained by a truncation and shifting by $(N-1)/2$ samples of the finite impulse response of the ideal Hilbert transformer in Figure 7.21.23a. The transfer function of the Hilbert filter defined by the causal impulse response (see Equations [7.20.10] and [7.20.11]) is given by the Z-transform

$$H_H(i_1) = \sum_{i_1=0}^{N-1} h_1(i_1)\, z^{-i_1} \tag{7.21.48}$$

where i_1 is the discrete coordinate given in the Equation (7.21.49). The shifted causal impulse response $h_1(i_1)$ and the noncausal impulse $h(i)$ of Figure 7.21.23a satisfy the relation

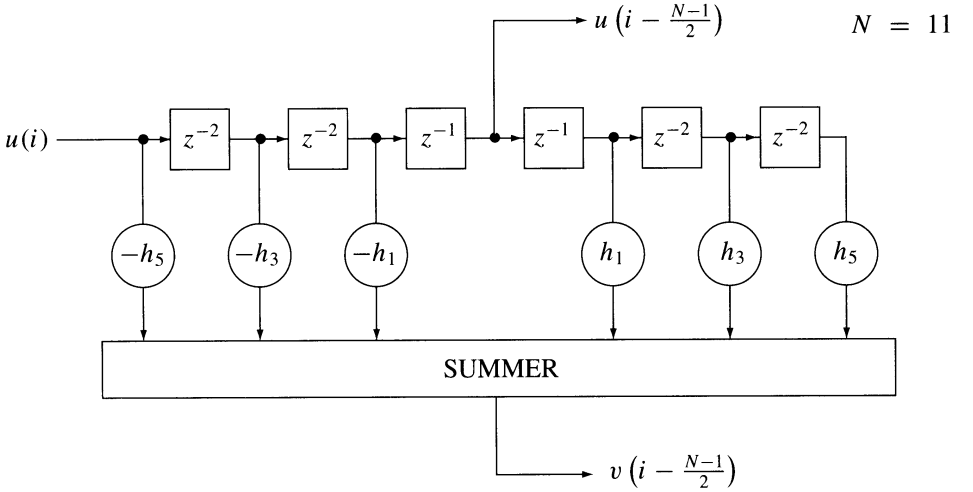

FIGURE 7.21.22 The structure of the FIR Hilbert transformer.

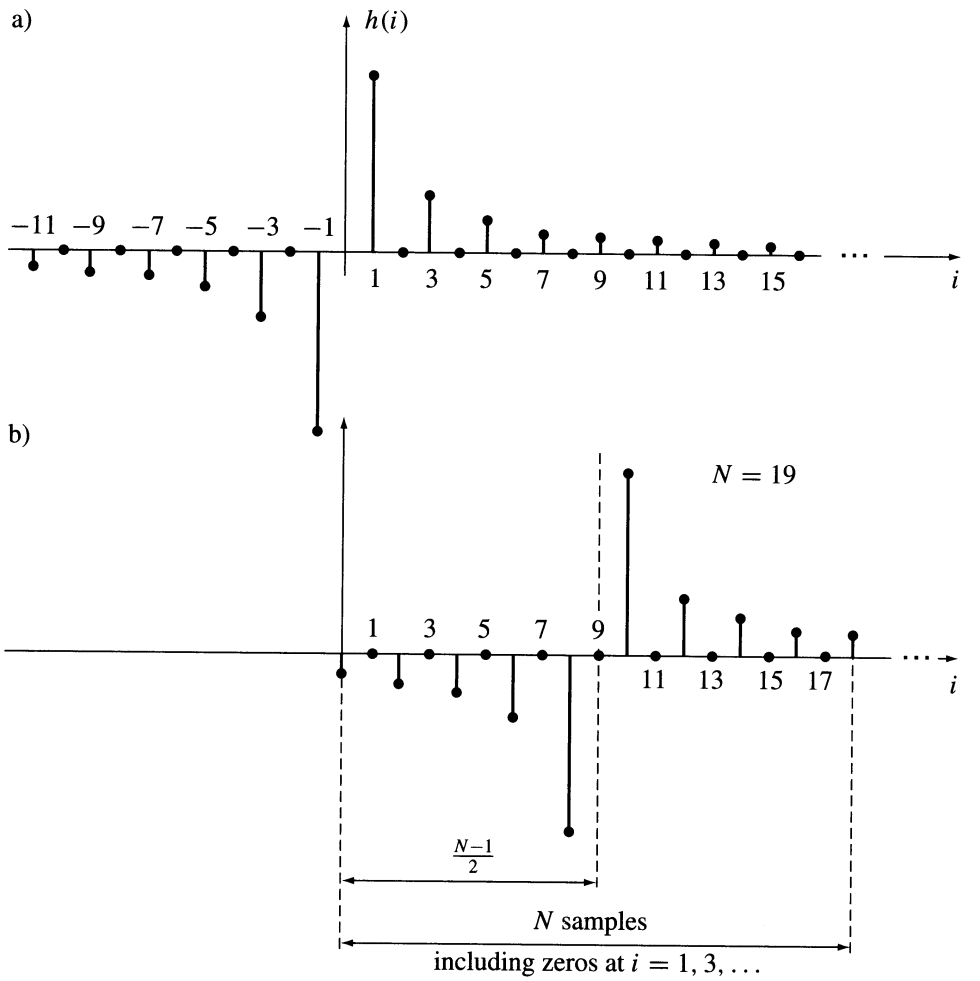

FIGURE 7.21.23 Impulse responses of (a) the ideal discrete time Hilbert transformer (see Equation [7.21.44]) and (b) a FIR Hilbert transformer given by the truncation and shifting of the impulse response shown in (a).

$$h_1\left[i+\left(N-1\right)/2\right]=h\left(i\right),\quad i_1=i+\left(N-1\right)/2,\quad i=\frac{N-1}{2},\ldots,0,\ldots,\frac{N-1}{2} \tag{7.21.49}$$

The insertion of $z = e^{j\psi}$ in Equation (7.21.48) (see Equation [7.20.15]) and using (7.21.49) yields

$$H_H\left(e^{j\psi}\right)=e^{-j\psi\left(N-1\right)/2}\sum_{i=-\left(N-1\right)/2}^{\left(N-1\right)}h\left(i\right)e^{-j\psi i} \tag{7.21.50}$$

Using Euler's formula for the sine function and the relation $h(i) = -h(-i)$, this transfer function takes the form

$$H_H\left(e^{j\psi}\right)=e^{-j\psi\left(N-1\right)/2}\sum_{i=1}^{\left(N-1\right)/2}-j2h\left(i\right)\sin\left(\psi i\right) \tag{7.2.1.51}$$

Because every second sample of the impulse response equals zero, the summation should be written: from $i = 1$ to $(N-1)/2$ step 2. Let us denote this by

$$G\left(e^{j\psi}\right) = -\sum_{i=1}^{(N-1)/2} 2h(i)\sin(\psi i) \tag{7.21.52}$$

This function has the form of a Fourier series and defines the amplitude of the transfer function of the Hilbert transformer (this is not the magnitude because $G(e^{j\psi})$ has positive and negative values). An example is shown in Figure 7.21.24. The normalized dimensionless pass-band of this Hilbert transformer is given by the edge frequencies

$$W_\psi = \psi_2 - \psi_1 = \pi - 2\Delta \tag{7.21.53}$$

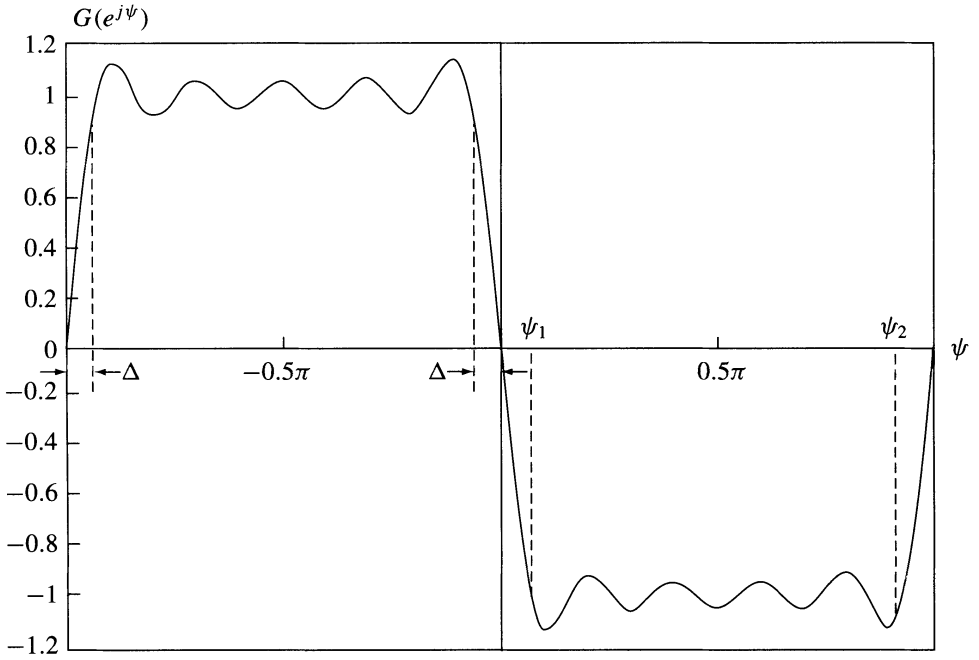

FIGURE 7.21.24 The $G(e^{j\psi})$ function of a FIR Hilbert transformer defined by the Fourier series (7.21.55).

Because $\psi = 2\pi f/f_s$, where f is the frequency in [Hz] and f_s is the sampling frequency, the pass-band in [Hz] is

$$W_f[Hz] = \frac{\pi - 2\Delta}{2\pi} f_s \tag{7.21.54}$$

The pass-band increases and the amplitude δ of the ripple decreases with increasing length N of the impulse response; that is, at the cost of the delay, which equals $(N-1)/2$ samples. The amplitude ripple in the pass-band depends on the coefficients $h(i)$ in the Fourier series (7.21.52). Let us consider three cases:

1. The coefficients $h(i)$ are given by the Fourier series of an odd square periodic function of the form

$$G\left(e^{j\psi}\right) = -\frac{4}{\pi}\left[\sin(\psi i) + \frac{1}{3}\sin(3\psi i) + \frac{1}{5}\sin(5\psi i)\right.$$
$$\left. \cdots + \frac{1}{2i+1}\sin\left[\psi i(N-1)/2\right]\right] \tag{7.21.55}$$

corresponding to the truncation of the Fourier series by a rectangular window. This yields a nonequiripple amplitude distribution with "Gibbs peaks" at the edges of the pass-band, as shown in Figure 7.21.24.

2. The coefficients $h(i)$ in the above Fourier series are changed using an appropriate spectral window function; for example, Blackman, Hamming, or Kaiser windows. This yields a more uniform amplitude ripple.
3. The coefficients $h(i)$ are calculated to obtain an equiripple amplitude distribution in the pass-band in the mini-max or Tchebycheff sense; for example, using the Parks-McClellan algorithm.[22] Figure 7.21.25 shows an example for $N = 19$. The product of N and Δ is given by the asymptotic relation derived by Kaiser[29]

$$N\,\Delta \cong 0.61\,\log_{10}\delta \tag{7.21.56}$$

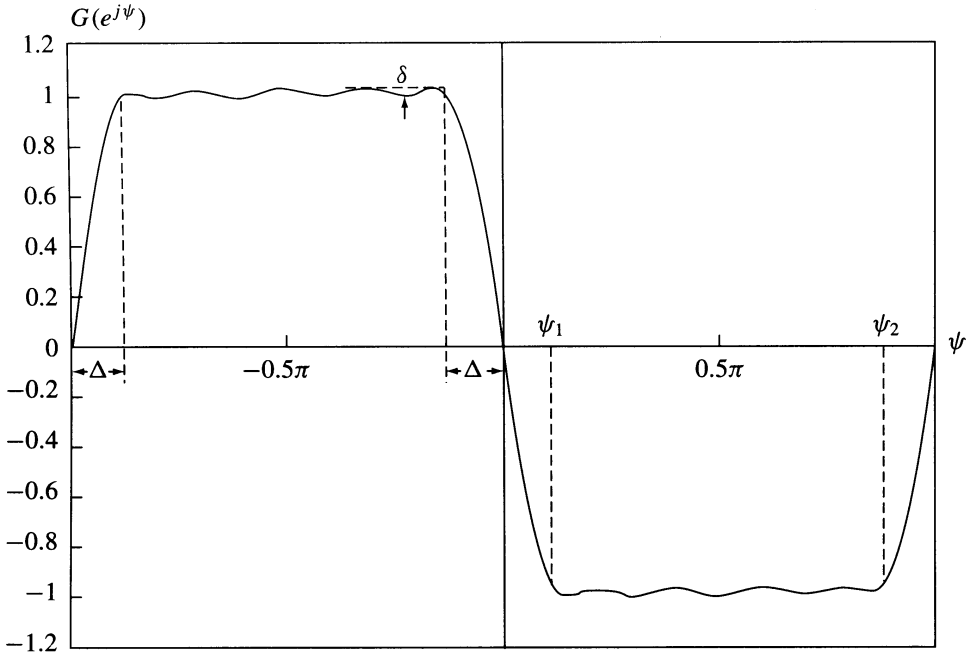

FIGURE 7.21.25 The equiripple $G(e^{j\psi})$ function of a FIR Hilbert transformer designed in the mini-max or Tchebycheff sense.

Concluding, the FIR Hilbert transformer has a linear-phase characteristic and an amplitude ripple in the pass-band depending on design. Odd values of N are preferred. Design with even N is possible but inconvenient because all the impulse response coefficients are nonzero and the frequency response cannot have the required symmetry. A symmetric FIR Hilbert transformer (odd N) may be eventually derived from the corresponding designs of symmetric half-band FIR filters.[16]

Digital Phase Splitters

A digital Hilbert transformer may be implemented in the form of a digital phase splitter as shown in Figure 7.21.26. The transfer functions of the all-pass filters may be derived directly from the analog transfer functions by use of the bilinear frequency transformation (see Section 7.20). Details of the procedure can be found in any textbook on digital filters. All basic properties of the analog implementation are conserved. Without a phase equalizer the output Hilbert pair is distorted in reference to the input signal. Nonlinearity of the bilinear transformation introduces some tradeoffs not present in the analog case.

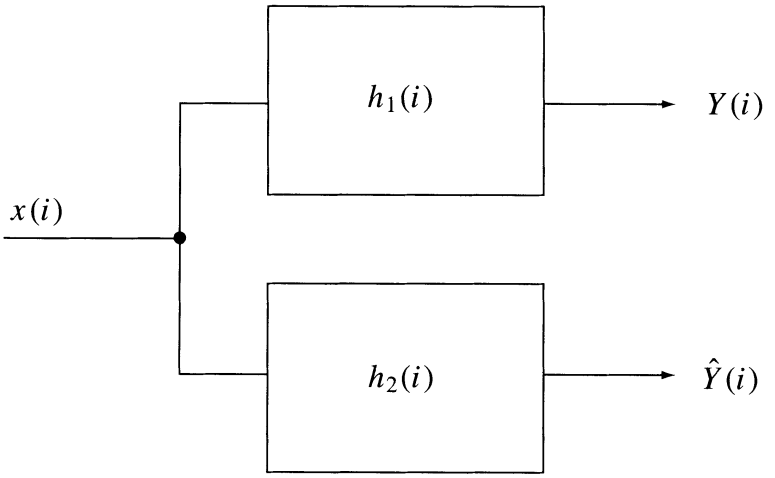

FIGURE 7.21.26 The discrete-time (or digital) version of the phase splitter Hilbert transformer of Figure 7.21.1 .

IIR Hilbert Transformers

IIR Hilbert transformers may be derived using noncausal generalized half-band filters. Generalized half-band filters are derived by modifying the conventional elliptic filter design so that all poles of the half-band filter lie on the imaginary axis. The IIR ideal half-band transfer function proposed by Ansari[1] has the form

$$H_{\mathrm{HB}}(z) = 1 + z^{-1}G(z^2) \tag{7.21.57}$$

where $G(z^2)$ is an all-pass filter with unit magnitude. The ideal example of this transfer function is shown in Figure 7.21.27a. Let us show that the transfer function of an ideal IIR Hilbert transformer is given by

$$H_H(z) = z^{-1}G(-z^2) \tag{7.21.58}$$

This is illustrated step-by-step in Figure 7.21.27. The term

$$F(z) = z^{-1}G(-z^2) \tag{7.21.59}$$

is an all-pass with $F(e^{j\psi})$ shown in Figure 7.21.27b. It has a unit magnitude and a phase function equal to zero in the pass-band and $\pm\pi$ in the stop-band as shown in Figure 7.21.27d. This phase function can be written in the form

$$\Phi(\psi) = 0.5\pi\,[\mathrm{sgn}(\sin(2\psi)) - \mathrm{sgn}(\psi)] \tag{7.21.60}$$

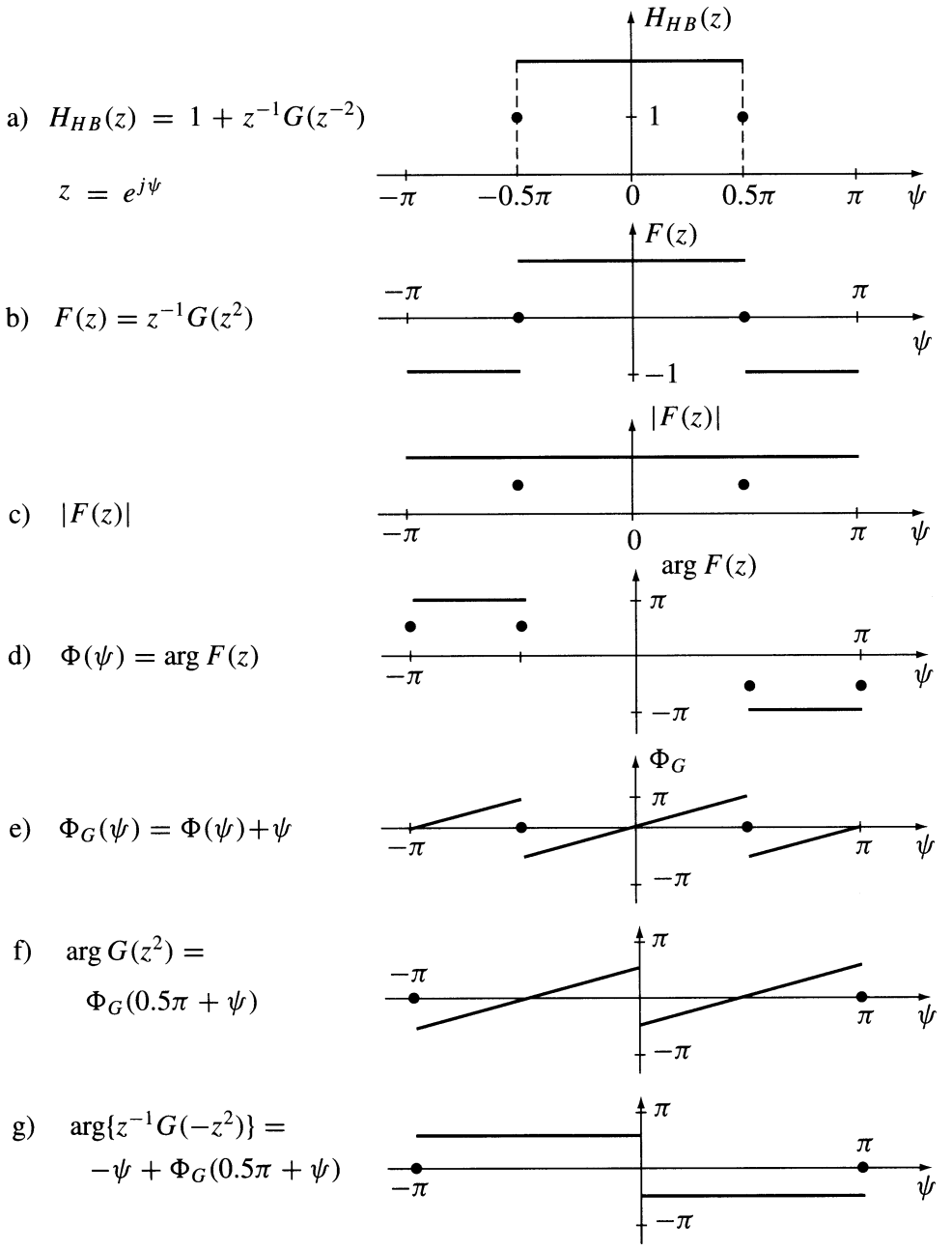

FIGURE 7.21.27 Step-by-step derivation of the IIR transfer function of a Hilbert transformer defined by Equation (7.21.58), starting from the transfer function of the ideal half-band filter given by (7.21.57).

The term $F(z)$ can be written in the form ($z = e^{j\psi}$)

$$F\left(e^{j\psi}\right) = e^{-j\psi} e^{j\Phi_G(\psi)} = e^{j\Phi(\psi)} \tag{7.21.61}$$

where

$$\Phi_G(\psi) = \Phi(\psi) + \psi \tag{7.21.62}$$

This phase function is shown in Figure 7.21.27e. Because $z^2 = e^{j2\psi}$ and $-z^2 = e^{j2(0.5\pi+\psi)}$, we have

$$H_H\left(e^{j\psi}\right) = e^{-j\psi} e^{j\Phi_G\left(0.5\pi+\psi\right)} \tag{7.21.63}$$

The phase function $\Phi_G(0.5\pi + \psi)$ is shown in Figure 7.21.27f and is the same as the phase function of the ideal Hilbert transformer (see Equation [7.21.43]) and finally the phase function of $H_H(z)$ is shown in Figure 7.21.27g.

Differently than FIR transformers, the above IIR Hilbert transformer is designed with an equiripple phase function and exact amplitude. The explicit form of the noncausal transfer function may have the form

$$H\left(z\right) = z^{-1} \sum_{i=1}^{N} \frac{1 - a_i z^2}{z^2 - a_i} \tag{7.21.64}$$

where N is an integer. Let us present an example. Consider the IIR Hilbert transformer with the low-frequency edge $\psi_1 = 0.02\pi$, the high-frequency edge $\psi_2 = 0.98\pi$ ($\Delta = 0.02\pi$), and with the required amplitude of the phase ripple $|\Delta\Phi| \le 0.01\pi$. The following relation between the phase ripple and the stop-band amplitude ripple of the half-band filter was derived[1]

$$\delta = \sin(0.5\Delta\Phi) \tag{7.21.65}$$

Inserting $\Delta\Phi = 0.01\pi$ gives $\delta = 0.0157$. The design procedure described in Reference 1a was applied to find the filter coefficients $a(i)$ giving $a(1) = 5.36078$, $a(2) = 1.2655$, $a(3) = 0.94167$, and $a(4) = 0.53239$. The insertion of the coefficients in Equation (7.21.64) enabled the calculation of the phase function shown in Figure 7.21.28. The phase error has a symmetric distribution around $\Psi = 0.5\pi$, i.e., half of the sampling frequency. The pass-band of this Hilbert transformer covers about 4.5 octaves. The phase ripple in the pass-band may be eliminated using half-band Butterworth IIR filters. For this kind of filter the coefficients $a(i)$ in Equation (7.21.64) are given by a simple formula

$$a_i = \tan^2[\pi i/2N + 1)]; \quad i = 1, 2, \ldots, N \tag{7.21.66}$$

Figure 7.21.29 shows a family of maximum flat phase functions for $N = 2$, 4, and 6. The pass-band depends considerably on the permissible phase error at the edges. The edge frequencies for edge errors 0.1% and 1% are given in the table:

N	2		4		6	
Edge Error	ψ_1	ψ_2	ψ_1	ψ_2	ψ_1	ψ_2
0.1%	0.36	0.64	0.24	0.76	0.165	0.835
1%	0.265	0.735	0.165	0.835	0.115	0.885

The widest pass-band for $N = 6$ and 1% error covers about 3 octaves and the smallest for $N = 2$ and 0.1% only 1 octave. The frequency around which the phase function is maximally flat equals $\psi = 0.5\pi$. It can be shifted by use of a suitable digital-to-digital frequency transformation. The disadvantage of the Butterworth filter is that the ratio of the first to the last coefficient is very large and increases with N.

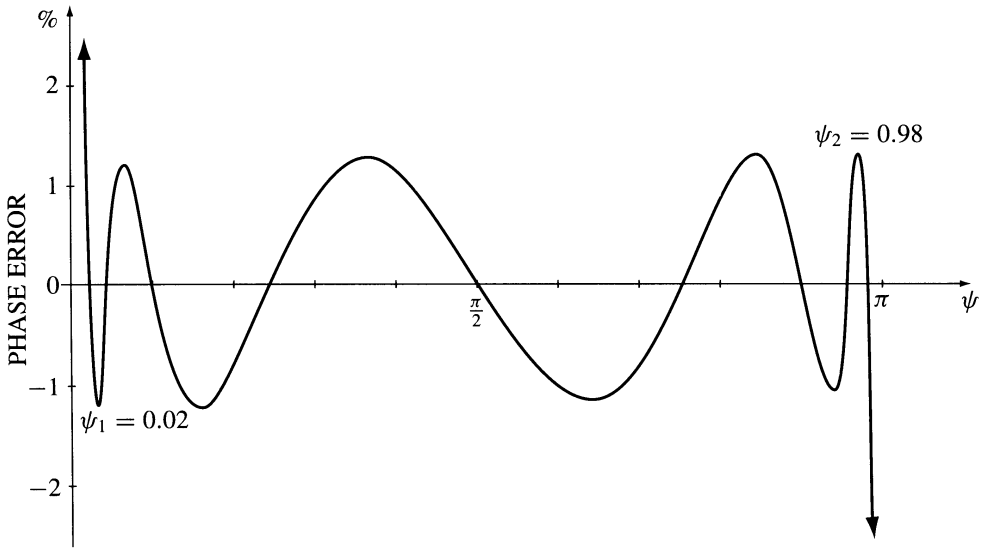

FIGURE 7.21.28 An example of the equiripple phase function of the IIR Hilbert transformer.

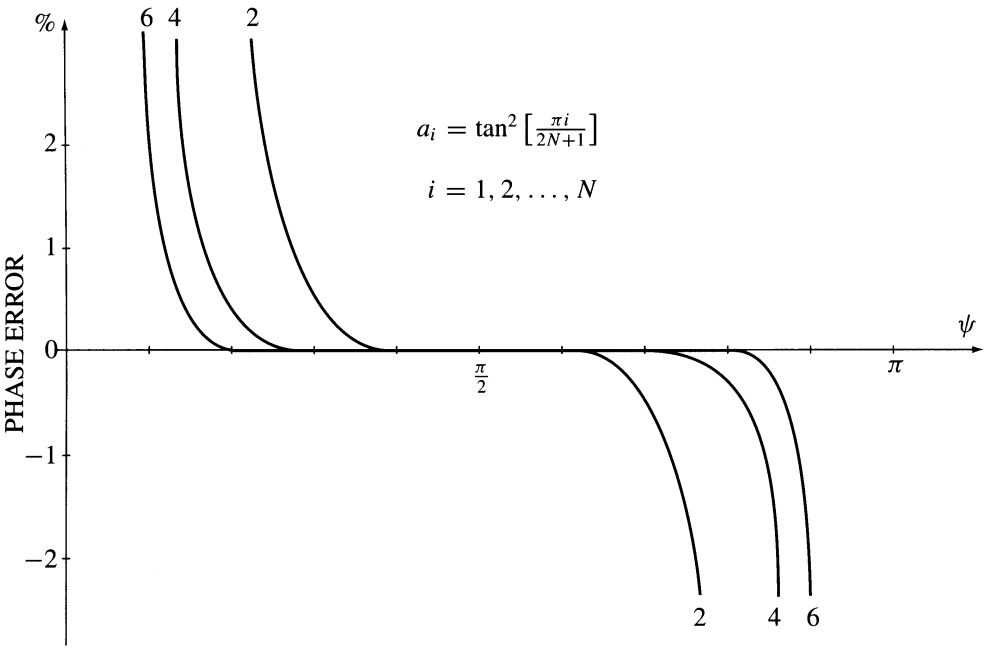

FIGURE 7.21.29 Phase errors of Butterworth IIR Hilbert transformers.

Differentiating Hilbert Transformers

The differentiating Hilbert transformer is defined as a linear system the output of which is the derivative of the Hilbert transform of the input signal. In principle, a differentiating Hilbert transformer may be implemented as a cascade connection of a differentiator and a Hilbert transformer as shown in Figure 7.21.30. However, it may be designed as a specialized FIR filter. Due to the cascade connection, the

transfer function of the differentiating discrete Hilbert transformer is given by the product of the transfer function of the discrete Hilbert transformer given by Equation 7.21.45 and the transfer function of the ideal discrete differentiator of the form[29]

$$H_D\left(e^{j\psi}\right) = \begin{cases} j\psi e^{-j\psi t} & 0 < \psi < \pi \\ 1 & |\psi| = k\pi; \quad k = 0, 1, 2 \\ j(\psi - 2\pi)e^{-j(\psi - 2\pi)\tau} & \pi < \psi < 2\pi \end{cases} \tag{7.21.67}$$

or using the equivalent notation

$$H_{\mathrm{D}}(e^{j\psi}) = [\psi + \mathrm{sgn}(\sin(\psi)) - 1]e^{j[0.5\pi - \psi\tau - \pi\tau(\mathrm{sgn}(\sin(\psi)) - 1)}$$

$$0 < \psi < 2\pi \tag{7.21.68}$$

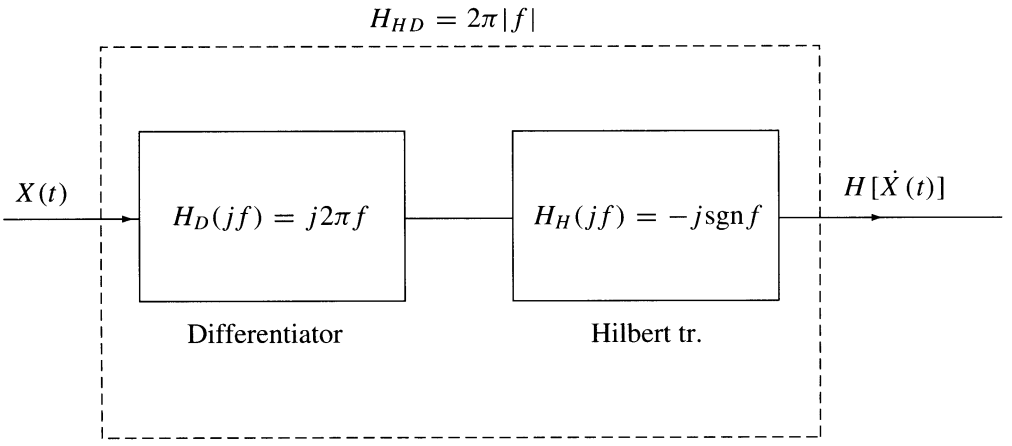

FIGURE 7.21.30 A cascade connection of a Hilbert transformer and a differentiating filter.

The product of both transfer functions may be written in the form

$$H_{\mathrm{HD}}(e^{j\psi}) = [\psi + \pi(\mathrm{sgn}(\sin(\psi)) - 1]\ \mathrm{sgn}(\sin(\psi))e^{-j[2\psi\tau - \pi\tau(\mathrm{sgn}(\sin(\psi)) - 1)} \tag{7.21.69}$$

The magnitude and the phase function of this transfer function of the differentiating Hilbert transformer are shown in Figure 7.21.31. The inverse Fourier transform with ($\tau = 0$) yields the noncausal, even, and of infinite duration impulse response:

$$h_{\mathrm{HD}}(i) = \begin{cases} a(i) = -\left[2\sin^2(0.5\pi i)\right] / (\pi i^2); & i \neq 0 \\ 0.5\pi; & i = 0 \end{cases} \tag{7.21.70}$$

This is illustrated in Figure 7.21.32a. The design method is the same as for the discrete Hilbert filter. The impulse response should be truncated to include N samples and shifted by $\tau = (N - 1)/2$ samples as shown in Figure 7.21.31b. The $G(e^{j\psi})$ function defined by Equation (7.21.52) here takes the form

$$G_{\mathrm{HD}}(e^{j\psi}) = [\psi + \pi(\mathrm{sgn}(\sin(\psi)) - 1]\ \mathrm{sgn}(\sin(\psi)): \quad 0 < \psi < 2\pi \tag{7.21.71}$$

and in this case is equal to the magnitude of the transfer function (see Figure 7.21.31). The truncated Fourier series is

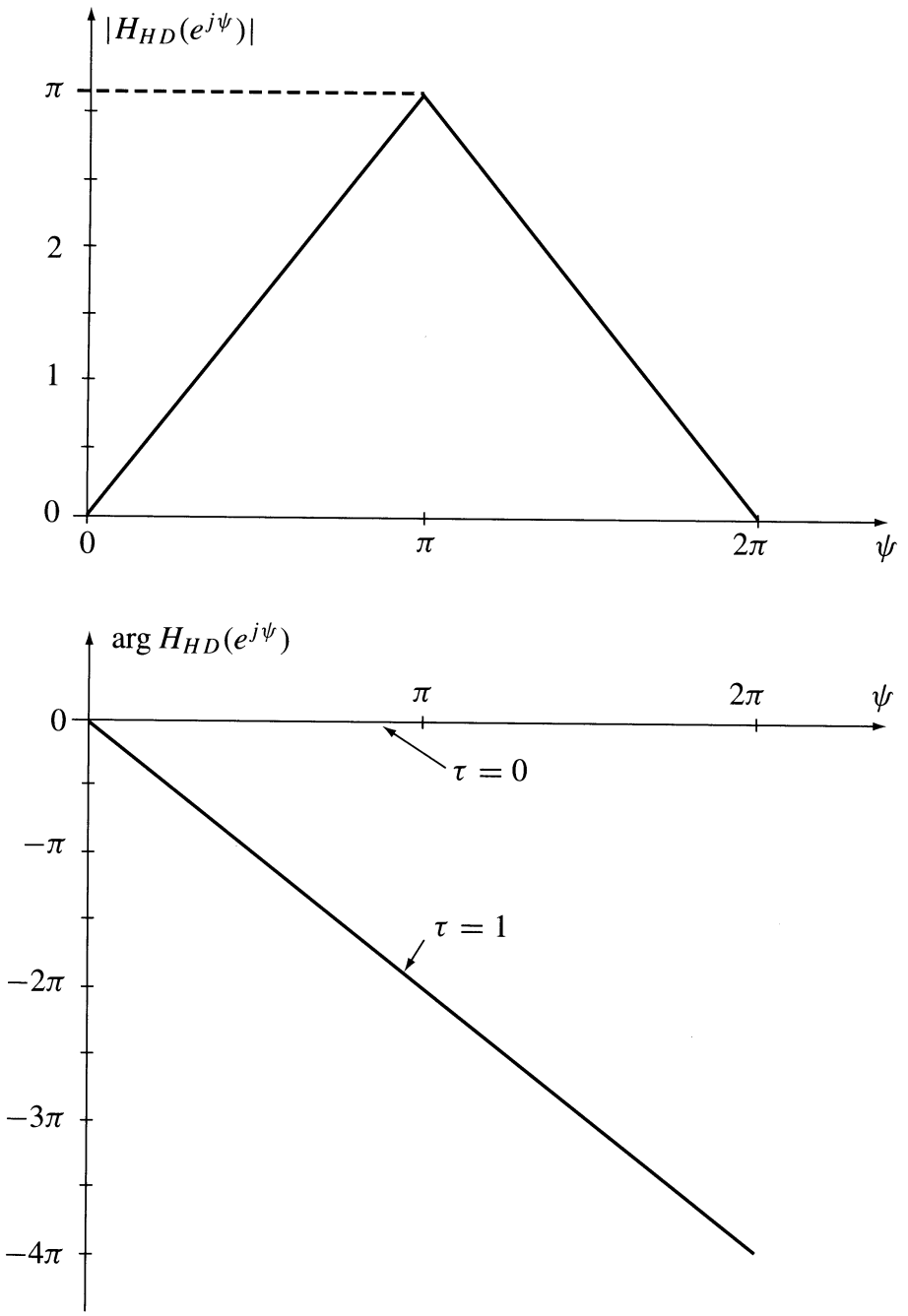

FIGURE 7.21.31 The transfer function of a differentiating Hilbert transformer: (a) magnitude and (b) phase function.

$$G_{\mathrm{HDT}}\left(e^{j\psi}\right) = 0.5\pi - \sum_{i=1}^{(N-1)/2} 2a(i)\cos(\psi i) \tag{7.21.72}$$

Compare this function with the analogous function of the FIR Hilbert transformer (see Equation [7.21.31]). The design methods to get the desired amplitude ripple are the same as described in the three points following Equation (7.21.52). However, the Fourier series given by Equation (7.21.53) takes for the differentiating Hilbert transformer the form

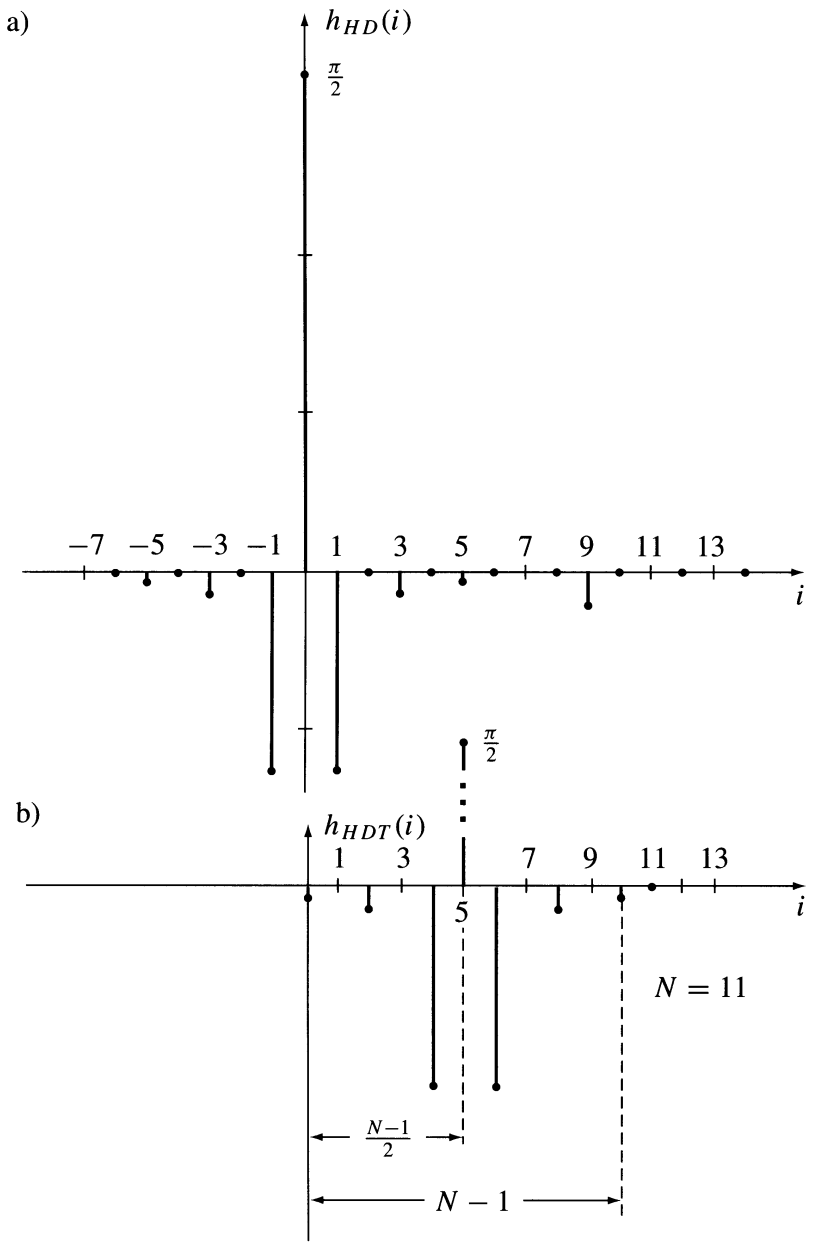

FIGURE 7.21.32 The impulse responses of the differentiating Hilbert transformer: (a) noncausal ideal and (b) truncated and causal.

$$G_{\mathrm{HDT}}\left(e^{j\psi}\right) = \frac{\pi}{2} - \left(\frac{4}{\pi}\right)\left[\cos\psi + \left(\frac{1}{9}\right)\cos 3\psi + \left(\frac{1}{25}\right)\cos 5\psi + \cdots\right] \tag{7.21.73}$$

This Fourier series differs by three important features from the series given by Equation (7.21.53). First, it converges faster (coefficients $1/i^2$ instead $1/i$) and, second, there are no Gibbs peaks at the edges of the pass-band. Third, the function is unipolar with the mean value equal to $\pi/2$. An example of the magnitude designed in the minimax sense is shown in Figure 7.21.33. The coefficients are given in Table 7.21.1.

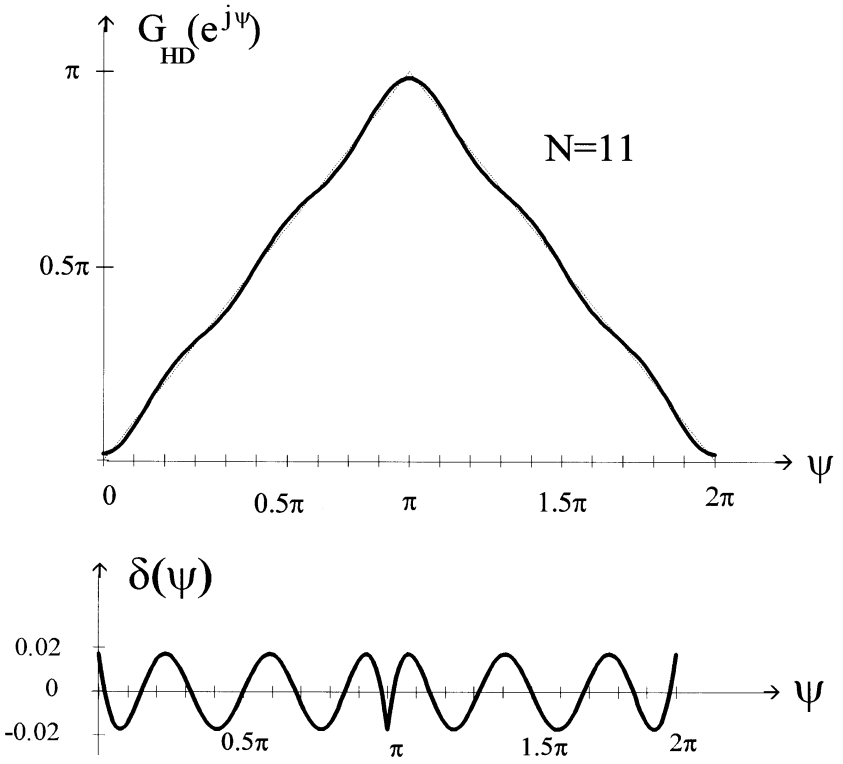

FIGURE 7.21.33 The $G(e^{j\psi})$ function of a FIR differentiating Hilbert transformer.

TABLE 7.21.1

	Pass-Band Edges				
	$\psi_1 = 0$; $N = 7$	$\psi_2 = \pi$ $N = 11$	$N = 19$	$\psi_1 = 0.2\pi$; $N = 11$	$\psi_2 = 0.8\pi^*$ $N = 19$
$a(1)$	0.6426919	0.6388893	0.6373537	0.6068935	0.6184231
$a(3)$	0.0997952	0.07348499	0.0715001	0.0450341	0.05423771
$a(5)$		0.0459263	0.0263422	0.00615878	0.0118350*
$a(7)$			0.0140561		0.00260689
$a(9)$			0.0020769		0.0003889

(Data from a paper of Cizek, 1989, URSI, ISSSE, *corrected by this author.)

7.22 Multidimensional Hilbert Transformations

Multidimensional transformations are applied in modern multidimensional digital signal processing. The theory of complex notation of multidimensional signals uses multidimensional Hilbert transforms. These are the reasons basic definitions and properties of multidimensional Hilbert transformations are presented here. As in the one-dimensional case, the theory of Hilbert transformations is closely tied with multidimensional Fourier transformations.

Let us define the n-dimensional signal $u(\mathbf{x})$ as a function of the n-dimensional variable $\mathbf{x} = \{x_1, x_2, \ldots, x_n\}$, an n-dimensional real column vector. For example, a single frame of a video black-and-white signal may be described by the 2-D signal $u(x_1, x_2)$.

Evenness and Oddness of *N*-Dimensional Signals

Let us remember that the 1-D signal may be resolved in a sum of the even and odd parts (see Equations [7.3.2] and [7.3.3]). Therefore, it has two degrees of freedom concerning evenness or oddness. In general, the n-dimensional real signal $u(\mathbf{x})$ has 2^n degrees of freedom in this respect. For example, a 2-D function may be resolved into a sum of four terms:

$$u(x_2, x_1) = u_{ee}(x_2, x_1) + u_{eo}(x_2, x_1) + u_{oe}(x_2, x_1) + u_{oo}(x_2, x_1) \tag{7.22.1}$$

where the indices "e" and "o" indicate evenness or oddness in respect to the variables x_1 and x_2. Notice that the indices "ee," "eo," "oe," and "oo" are written in the natural order of binary numbers using "e" = 0 (zero) and "o" = 1, i.e., 00, 01, 10, 11. The even-even part is given by

$$u_{ee}\left(x_2, x_1\right) = \frac{u\left(x_2, x_1\right) + u\left(x_2, -x_1\right) + u\left(-x_2, x_1\right) + u\left(-x_2, -x_1\right)}{4} \tag{7.22.2}$$

the even-odd part by

$$u_{eo}\left(x_2, x_1\right) = \frac{u\left(x_2, x_1\right) - u\left(x_2, -x_1\right) + u\left(-x_2, x_1\right) - u\left(-x_2, -x_1\right)}{4} \tag{7.22.3}$$

the odd-even part by

$$u_{oe}\left(x_2, x_1\right) = \frac{u\left(x_2, x_1\right) + u\left(x_2, -x_1\right) - u\left(-x_2, x_1\right) - u\left(-x_2, -x_1\right)}{4} \tag{7.22.4}$$

and the odd-odd part by

$$u_{oo}\left(x_2, x_1\right) = \frac{u\left(x_2, x_1\right) - u\left(x_2, -x_1\right) - u\left(-x_2, x_1\right) + u\left(-x_2, -x_1\right)}{4} \tag{7.22.5}$$

We used a reversed order of the indices, that is, (x_2, x_1) instead of (x_1, x_2) and as before used the order 00, 01, 10, 11. The sign of a given term in the nominators of Equations (7.22.2) to (7.22.5) is equal to the product of the signs of odd indexed variables. If only one variable is odd, as in Equations (7.22.3) or (7.22.4), its sign decides. For example, in Equation (7.22.4) we have $-u(-x_2, x_1)$ and $-u(-x_2, -x_1)$ because only the variable x_2 is odd indexed.

A 3-D function may be resolved into a sum of eight terms

$$u(x_3, x_2, x_1) = u_{eee} + u_{eeo} + u_{eoe} + u_{eoo} + u_{oee} + u_{oeo} + u_{ooe} + u_{ooo} \tag{7.22.6}$$

Using the same rules as above, we get:

$$\begin{aligned} u_{eee}\left(x_3, x_2, x_1\right) = {} & \frac{u\left(x_3, x_2, x_1\right) + u\left(x_3, x_2, -x_1\right) + u\left(x_3, -x_2, x_1\right) + u\left(x_3, -x_2, -x_1\right)}{16} \\ & + \frac{u\left(-x_3, x_2, x_1\right) + u\left(-x_3, x_2, -x_1\right) + u\left(-x_3, -x_2, x_1\right) + u\left(-x_3, -x_2, -x_1\right)}{16} \end{aligned} \tag{7.22.7}$$

$$u_{eeo}(x_3,x_2,x_1)=\frac{u(x_3,x_2,x_1)-u(x_3,x_2,-x_1)+u(x_3,-x_2,x_1)-u(x_3,-x_2,-x_1)}{16}+\frac{u(-x_3,x_2,x_1)-u(-x_3,x_2,-x_1)+u(-x_3,-x_2,x_1)-u(-x_3,-x_2,-x_1)}{16} \tag{7.22.8}$$

$$u_{ooe}(x_3,x_2,x_1)=\frac{u(x_3,x_2,x_1)+u(x_3,x_2,-x_1)-u(x_3,-x_2,x_1)-u(x_3,-x_2,-x_1)}{16}+\frac{-u(-x_3,x_2,x_1)-u(-x_3,x_2,-x_1)+u(-x_3,-x_2,x_1)+u(-x_3,-x_2,-x_1)}{16} \tag{7.22.9}$$

$$u_{ooo}(x_3,x_2,x_1)=\frac{u(x_3,x_2,x_1)-u(x_3,x_2,-x_1)-u(x_3,-x_2,x_1)+u(x_3,-x_2,-x_1)}{16}+\frac{-u(-x_3,x_2,x_1)+u(-x_3,x_2,-x_1)+u(-x_3,-x_2,x_1)-u(-x_3,-x_2,-x_1)}{16} \tag{7.22.10}$$

It is possible to introduce a geometric interpretation of the decomposition of a function into even and odd terms, as shown in Figure 7.22.1, and to define the "distance" between the terms. The distance D is

$$1 > D > n \tag{7.22.11}$$

For example, the distance between f_e and f_o or between f_{eo} and f_{oo} equals 1, between f_{ee} and f_{oo} equals 2.

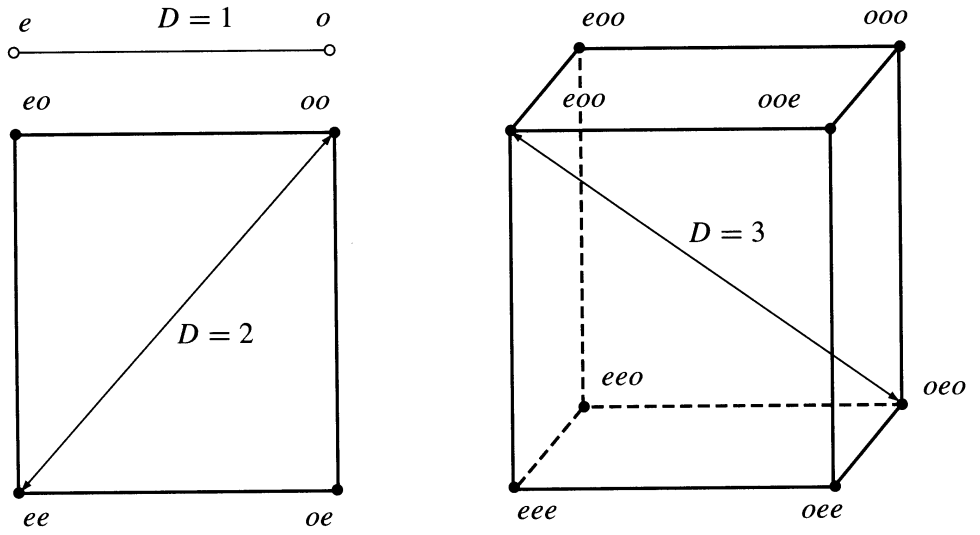

FIGURE 7.22.1 The geometrical interpretation of the "distance" concerning the evenness and oddness of 1-D, 2-D, and 3-D functions.

n-D Hilbert Transformations

The n-dimensional (n-D) Hilbert transformation of the n-dimensional function $u(\mathbf{x})$ is defined by the n-fold integral[37]

$$\upsilon(\mathbf{x}) = H_n\left[u(\mathbf{x})\right] = \frac{1}{\pi^n} P\int_{-\infty}^{\infty}\cdots\int_{-\infty}^{\infty} \frac{u(\mathbf{H})}{\Pi_{k=1}^{n}(x_k - \eta_k)} d\mathbf{H}; \quad \begin{matrix}\mathbf{H} = \{\eta_1, \eta_2, \ldots, \eta_n\} \\ d\mathbf{H} = d\eta_1, d\eta_2, \ldots, d\eta_n\end{matrix} \tag{7.22.12}$$

where P denotes the Cauchy principal value and H_n the operator of the n-D Hilbert transformation. The inverse transformation is

$$u(\mathbf{x}) = H_n^{-1}\left[\upsilon(\mathbf{x})\right] = \frac{(-1)^n}{\pi^n} P\int_{-\infty}^{\infty}\cdots\int_{-\infty}^{\infty} \frac{\upsilon(\mathbf{H})}{\Pi_{k=1}^{n}(x_k - \eta_k)} d\mathbf{H} \tag{7.22.13}$$

The n-dimensional Hilbert pair will be denoted by

$$u(\mathbf{x}) \overset{n-H}{\Longleftrightarrow} \upsilon(\mathbf{x}) \tag{7.22.14}$$

Analogous to the 1-D case, the n-dimensional Hilbert transformation changes the indices of the terms in equations, such as Equations (7.22.1) or (7.22.6), from even to odd and from odd to even. Similar to the 1-D case, the n-D Hilbert transformation may be derived from the n-dimensional Cauchy integral

$$f(z) = \frac{1}{(2\pi i)^n}\int_{\Gamma} \frac{f(\xi)d\xi}{(\xi - \mathbf{z})} \quad \begin{matrix}\mathbf{z} = \{z_1, \ldots z_n\} \\ \xi = \{\xi_1, \ldots \xi_n\}\end{matrix} \tag{7.22.15}$$

where $\Gamma = \partial D_1 \times \cdots \times \partial D_n$ is an n-D surface, being the bound of ∂D, where the region D has the form of the Cartesian product $D = D_1 \times \cdots \times D_n$.

2-*D* Hilbert Transformations

The 2-D Hilbert transformation is given by Equation (7.22.12) with $n = 2$ and has the form[36]

$$\upsilon(\mathbf{x}) = H\left[u(\mathbf{x})\right] = \frac{1}{\pi^2} P\int_{-\infty}^{\infty}\int_{-\infty}^{\infty} \frac{u(\eta_1, \eta_2)}{(x_1 - \eta_1)(x_2 - \eta_2)} d\eta_1 d\eta_2 \tag{7.22.16}$$

and because n is even, the inverse Hilbert transformation has the same form:

$$u(\mathbf{x}) = H\left[\upsilon(\mathbf{x})\right] = \frac{1}{\pi^2} P\int_{-\infty}^{\infty}\int_{-\infty}^{\infty} \frac{\upsilon(\eta_1, \eta_2)}{(x_1 - \eta_1)(x_2 - \eta_2)} d\eta_1 d\eta_2 \tag{7.22.17}$$

The 2-D Hilbert transformation may be written using the convolution notation:

$$\upsilon(x_1, x_2) = u(x_1, x_2) ** \frac{1}{\pi^2 x_1 x_2} \tag{7.22.18}$$

$$u(x_1, x_2) = \upsilon(x_1, x_2) ** \frac{1}{\pi^2 x_1 x_2} \tag{7.22.19}$$

Partial Hilbert Transformations

The partial Hilbert transformation of the n-D function $u(\mathbf{x})$, $\mathbf{x} = \{x_1, x_2, \ldots, x_n\}$ is defined as the Hilbert transformation in respect to a part of the variables. For example, the partial transformation of a 2-D function in respect to x_1 has the form

$$\upsilon_1\left(x_1, x_2\right) = \frac{1}{\pi} P\int_{-\infty}^{\infty} \frac{u\left(\eta_1, x_2\right)}{\left(x_1 - \eta_1\right)} d\eta_1 \tag{7.22.20}$$

and in respect to the variable x_2

$$\upsilon_2\left(x_1, x_2\right) = \frac{1}{\pi} P\int_{-\infty}^{\infty} \frac{u\left(x_1, \eta_2\right)}{\left(x_2 - \eta_2\right)} d\eta_2 \tag{7.22.21}$$

For 3-D functions it is possible to derive three first-order partial Hilbert transforms denoted υ_1, υ_2, υ_3 and three second-order Hilbert transforms denoted υ_{12}, υ_{13}, υ_{23}. For example,

$$\upsilon_1\left(x_1, x_2, x_3\right) = \frac{1}{\pi} P\int_{-\infty}^{\infty} \frac{u\left(\eta_1, x_2, x_3\right)}{\left(x_1 - \eta_1\right)} d\eta_1 \tag{7.22.22}$$

and

$$\upsilon_{12}\left(x_1, x_2, x_3\right) = \frac{1}{\pi^2} P\int_{-\infty}^{\infty}\int_{-\infty}^{\infty} \frac{u\left(\eta_1, \eta_2, x_3\right)}{\left(x_1 - \eta_1\right)\left(x_2 - \eta_2\right)} d\eta_1 d\eta_2 \tag{7.22.23}$$

Spectral Description of *n*-D Hilbert Transformations

The n-dimensional Fourier transformation of $u(\mathbf{x})$ is defined by the n-fold integral

$$U\left(\boldsymbol{\Omega}\right) = F_n\left[u\left(\mathbf{x}\right)\right] = \int_{-\infty}^{\infty} \cdots \int_{-\infty}^{\infty} u\left(\mathbf{x}\right) \exp\left(-j\boldsymbol{\Omega}^{\mathrm{T}}\mathbf{x}\right) d\mathbf{x} \tag{7.22.24}$$

where $\boldsymbol{\Omega} = \{\omega_1, \omega_2, \ldots, \omega_n\}$ is the n-dimensional column vector of Fourier frequencies. The index "T" denotes transpose. Therefore, the **exponential kernel** of the n-D Fourier transformation has the form

$$\exp\left(-j\boldsymbol{\Omega}^{\mathrm{T}}\mathbf{x}\right) = e^{-j\left(\omega_1 x_1 + \omega_2 x_2 + \cdots + \omega_n x_n\right)} \tag{7.22.25}$$

The inverse Fourier transformation is defined by the n-fold integral

$$u\left(\mathbf{x}\right) = F_n^{-1}\left[U\left(\boldsymbol{\Omega}\right)\right] = \int_{-\infty}^{\infty} \cdots \int_{-\infty}^{\infty} U\left(\boldsymbol{\Omega}\right) \exp\left(j\boldsymbol{\Omega}^{\mathrm{T}}\mathbf{x}\right) df_1 df_2 \ldots df_n \tag{7.22.26}$$

where $df_i = d\omega_i / 2\pi$ ($i = 1, 2, \ldots, n$). The n-D Fourier pair may be denoted

$$u\left(\mathbf{x}\right) \overset{n-F}{\Longleftrightarrow} U\left(\boldsymbol{\Omega}\right) \tag{7.22.27}$$

The n-D Fourier image of the Hilbert transform is given by the formula

$$V(\boldsymbol{\Omega}) = F_n\left\{H_n\left[u(\mathbf{x})\right]\right\} = (-j)^n\left[\prod_{k=1}^{n}\operatorname{sgn}(\omega_k)\right]U(\boldsymbol{\Omega}) \tag{7.22.28}$$

Proof

By the definition given by Equation (7.22.24)

$$F_n\left\{H_n\left[u(\mathbf{x})\right]\right\} = \frac{1}{\pi^n}\int_{-\infty}^{\infty}\left\{\int_{-\infty}^{\infty}\frac{U(\mathbf{H})}{\Pi_{k=1}^{n}(x_k-\eta_k)}d\mathbf{H}\right\}\exp\left(-j\boldsymbol{\Omega}^{\mathrm{T}}\mathbf{x}\right)d\mathbf{x} \tag{7.22.29}$$

where $\mathbf{H} = \{\eta_1, \eta_2, \ldots, \eta_n\}$, $d\mathbf{H} = d\eta_1, d\eta_2, \ldots, d\eta_n$ and for convenience the n-fold integrals are denoted by a single integral sign. Formally

$$\begin{aligned} F_n\left\{H_n\left[u(\mathbf{x})\right]\right\} &= \frac{1}{\pi^n}\int_{-\infty}^{\infty}u(\mathbf{H})\,d\mathbf{H}\int_{-\infty}^{\infty}\frac{\exp\left(-j\boldsymbol{\Omega}^{\mathrm{T}}\mathbf{x}\right)}{\Pi_{k=1}^{n}(x_k-\eta_k)}d\mathbf{x} \\ &= \int_{-\infty}^{\infty}u(\mathbf{H})\,d\mathbf{H}\prod_{k=1}^{n}\left(\frac{1}{\pi}\int_{-\infty}^{\infty}\frac{\exp(-j\omega_k x_k)}{x_k-\eta_k}dx_k\right) \end{aligned} \tag{7.22.30}$$

In the one-dimensional case, we have

$$H[\exp(-j\omega\, x)] = j\,\operatorname{sgn}(\omega)\,\exp(-j\omega\, x) \tag{7.22.31}$$

Hence,

$$F_n\left\{H_n\left[u(\mathbf{x})\right]\right\} = (-j)^n\left[\prod_{k=1}^{n}\operatorname{sgn}(\omega_k)\right]\int_{-\infty}^{\infty}u(\mathbf{x})\exp\left(-j\boldsymbol{\Omega}^{\mathrm{T}}\mathbf{x}\right)d\mathbf{x} \tag{7.22.32}$$

and this is equal to Equation (7.22.28).

This equation enables the calculation of the n-D Hilbert transform using the inverse Fourier transform of the spectrum given by the above equation, i.e., using the algorithm

$$u(\mathbf{x}) \overset{n-F}{\Rightarrow} U(\Omega) \Rightarrow V(\Omega) = (-j)^n\left[\prod_{k=1}^{n}\operatorname{sgn}(\omega_k)\right]U(\Omega) \overset{2-F^{-1}}{\Rightarrow} v(\mathbf{x}) \tag{7.22.33}$$

For example, in the 2-D case the Hilbert transform is given by

$$v(x_1, x_2) = \int_{-\infty}^{\infty}\int_{-\infty}^{\infty} -\operatorname{sgn}(\omega_1)\operatorname{sgn}(\omega_2)\,U(\omega_1, \omega_2)e^{j(\omega_1 x_1 + \omega_2 x_2)}df_1 df_2 \tag{7.22.34}$$

($\omega_1 = 2\pi f_1$, $\omega_2 = 2\pi f_2$). This general formula may be simplified, if the signal given by Equation (7.22.1) has only a part of the four terms.

Example[14]

Consider the 2-D Gaussian signal and its Fourier image given by the Fourier pair

$$u(x_1, x_2) = e^{-\pi\left(x_1^2 + x_2^2\right)} \overset{2-F}{\Longleftrightarrow} U(\omega_1, \omega_2) = e^{-\pi\left(f_1^2 + f_2^2\right)} \tag{7.22.35}$$

where $\omega_1 = 2\pi f_1$ and $\omega_2 = 2\pi f_2$. The Fourier image of the Hilbert transform is

$$V(\omega_1, \omega_2) = -\operatorname{sgn}(\omega_1)\operatorname{sgn}(\omega_2) e^{-\pi\left(f_1^2 + f_2^2\right)} \tag{7.22.36}$$

Because this spectral function is real and odd-odd, the 2-D inverse Fourier transformation takes the simplified form

$$v(x_1, x_2) = 4\int_0^\infty \int_0^\infty e^{-\pi\left(f_1^2 + f_2^2\right)} \sin(\omega_1 x_1) \sin(\omega_2 x_2)\, df_1 df_2 \tag{7.22.37}$$

n-D Hilbert Transforms of Separable Functions

The n-dimensional function $u(\mathbf{x})$ is said to be **separable** in the coordinates $\mathbf{x} = \{x_1, x_2, \ldots, x_n\}$ if it is given by the product of 1-D functions

$$u(\mathbf{x}) = f_1(x_1) f_2(x_2) \ldots f_n(x_n) \tag{7.22.38}$$

Let us denote by $g_1(x_1), g_2(x_2), \ldots, g_n(x_n)$ the Hilbert transforms of the terms of this product. Because the Fourier image of a separable function is a separable function of the Fourier coordinates $\Omega = \{\omega_1, \omega_2, \ldots, \omega_n\}$ the inverse Fourier transform is a product of 1-D integrals. Therefore, the Hilbert transform of a separable function has the form

$$v(\mathbf{x}) = g_1(x_1) g_2(x_2) \ldots g_n(x_n) \tag{7.22.39}$$

Analogously, the partial Hilbert transforms of $u(\mathbf{x})$ are separable functions; for example, a first-order partial transform is

$$v_1(\mathbf{x}) = g_1(x_1) f_2(x_2) \ldots f_n(x_n) \tag{7.22.40}$$

and a second order partial transform is

$$v_{12}(\mathbf{x}) = g_1(x_1) g_2(x_2) f_3(x_3) \ldots f_n(x_n) \tag{7.22.41}$$

Examples

1. The 2-D delta pulse is a separable distribution of the form

$$\delta(x_1, x_2) = \delta(x_1)\delta(x_2) \tag{7.22.42}$$

Because $\delta(x_1) \overset{H}{\Longleftrightarrow} 1/(\pi x_1)$ and $\delta(x_2) \overset{H}{\Longleftrightarrow} 1/(\pi x_2)$, the Hilbert transform of the 2-D delta pulse has the form

$$\delta(x_1, x_2) \overset{2\text{-H}}{\Longleftrightarrow} 1/(\pi^2 x_1 x_2) \tag{7.22.43}$$

and the partial transforms are

$$\begin{aligned} \upsilon_1(x_1, x_2) &= \delta(x_2)/(\pi x_1); \\ \upsilon_2(x_1, x_2) &= \delta(x_1)/(\pi x_2) \end{aligned} \tag{7.22.44}$$

2. The 2-D signal has the form

$$u(x_1, x_2) = \Pi_a(x_1)\, \Pi_b(x_2) \tag{7.22.45}$$

The Hilbert transform takes the form (see Table 7.7.1, 4)

$$\upsilon(x_1, x_2) = \frac{1}{\pi^2} \ln\left|\frac{x_1 + a}{x_1 - a}\right| \ln\left|\frac{x_2 + b}{x_2 - b}\right| \tag{7.22.46}$$

and the partial transforms are

$$\begin{aligned} \upsilon_1(x_1, x_2) &= \frac{1}{\pi} \ln\left|\frac{x_1 + a}{x_1 - a}\right| \Pi_b(x_2); \\ \upsilon_2(x_1, x_2) &= \frac{1}{\pi} \Pi_a(x_1) \ln\left|\frac{x_2 + b}{x_2 - b}\right| \end{aligned} \tag{7.22.47}$$

3. Derivation of the Hilbert Transform of a nonseparable function defined by the equation

$$\begin{aligned} u(x_1, x_2) &= \frac{h}{a}\left(a - |x_1| - |x_2|\right); \quad && (x_1, x_2) \in S \\ u(x_1, x_2) &= 0; && (x_1, x_2) \notin S \end{aligned} \tag{7.22.48}$$

The support S is shown in Figure 7.22.2b. This function has the geometric form of a pyramid (Figure 7.22.2a). The Hilbert transform of this function is

$$\begin{aligned} \upsilon(x_1, x_2) = \frac{h}{\pi^2 a} \Bigg\{ & P\int_0^a \int_0^{a - x_2} \frac{a - \eta - \gamma}{(x_1 - \eta)(x_2 - \gamma)}\, d\gamma\, d\eta \\ & + P\int_0^a \int_{-a + x_2}^0 \frac{a - \eta - \gamma}{(x_1 - \eta)(x_2 - \gamma)}\, d\gamma\, d\eta \\ & + P\int_{-a}^0 \int_0^{a + x_2} \frac{a - \eta - \gamma}{(x_1 - \eta)(x_2 - \gamma)}\, d\gamma\, d\eta \\ & + P\int_{-a}^0 \int_{-a - x_2}^0 \frac{a - \eta - \gamma}{(x_1 - \eta)(x_2 - \gamma)}\, d\gamma\, d\eta \Bigg\} \end{aligned} \tag{7.22.49}$$

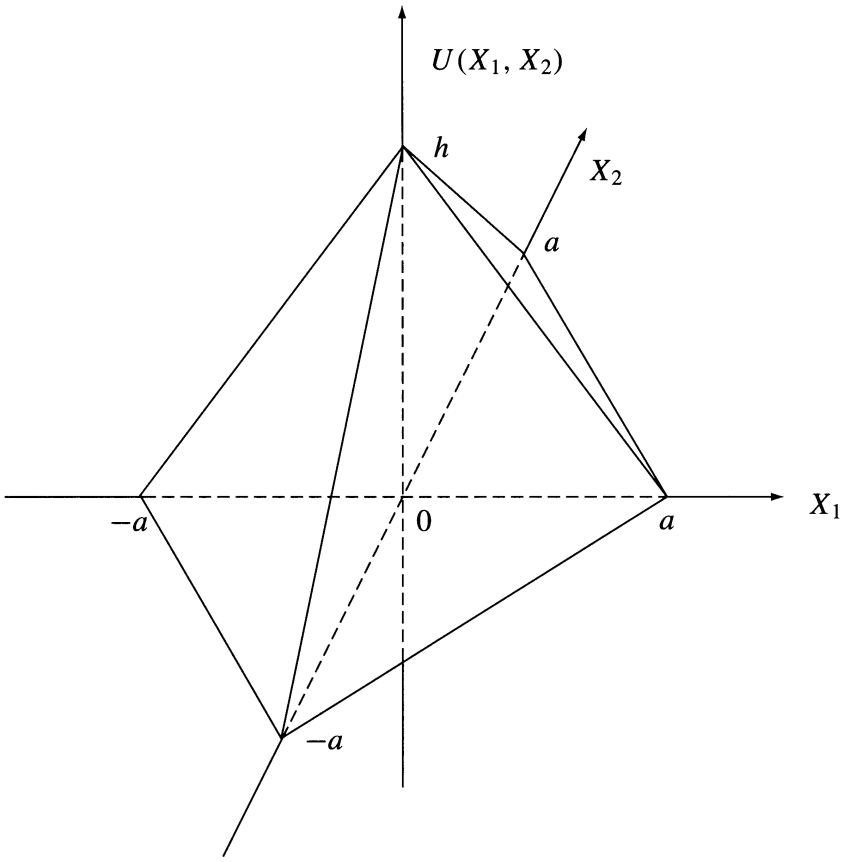

FIGURE 7.22.2a The pyramid pulse.

The integration yields:

$$\upsilon\left(x_1, x_2\right) = \frac{h}{\pi^2 a}\left\{2x_1 \ln\left|x_1\right| \ln\left|\frac{x_2 - a}{x_2 + a}\right|\right.$$
$$+ P\int_0^a \frac{\left(x_1 + \gamma - a\right)\ln\left|x_1 + \gamma - a\right| + \left(x_1 + a - \gamma\right)\ln\left|x_1 + a - \gamma\right|}{x_2 - \gamma} d\gamma \quad (7.22.50)$$
$$\left. + P\int_{-a}^0 \frac{\left(x_1 - a - \gamma\right)\ln\left|x_1 - a - \gamma\right| + \left(a + x_1 + \gamma\right)\ln\left|a + x_1 + \gamma\right|}{x_2 - \gamma} d\gamma \right\}$$

The one-dimensional integrals do not have a closed solution and a numerical integration should be applied. Notice that the support of the Hilbert transform (7.22.50) is infinite, which is different than the finite support of $u(x_1, x_2)$. The partial Hilbert transforms, defined by Equations (7.22.20) and (7.22.21) are

$$\upsilon_1\left(x_1, x_2\right) = \frac{h}{\pi a}\left[-2x_1 \ln\left|x_1\right| + \left(x_1 + x_2 - a\right)\ln\left|x_1 + x_2 - a\right|\right.$$
$$\left. + \left(x_1 + a - x_2\right)\ln\left|x_1 + a - x_2\right|\right] \quad (7.22.51)$$

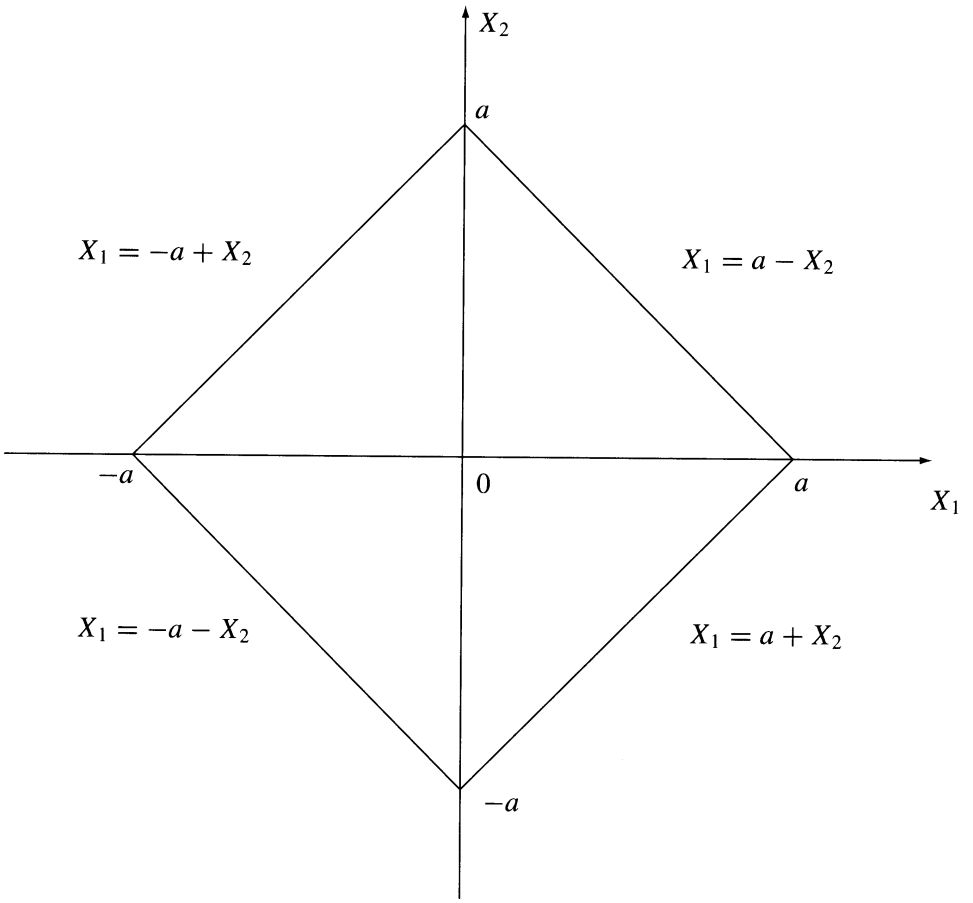

FIGURE 7.22.2b The support of the pyramid pulse.

$$\upsilon_2(x_1, x_2) = \frac{h}{\pi a}\left[-2x_2 \ln|x_2| + (x_2 + x_1 - a)\ln|x_2 + x_1 - a| + (x_2 + a - x_1)\ln|x_2 + a - x_1|\right] \tag{7.22.52}$$

The supports of these functions are shown in Figure 7.22.2c. They are infinite in one dimension and finite in a band $(-a, a)$ in the second dimension.

Properties of 2-D Hilbert Transformations

Selected properties of 2-D Hilbert transformations are summarized in Table 7.22.1.

Orthogonality

The terms of the 1-D Hilbert pair form a pair of orthogonal functions satisfying the condition

$$E = \int u(t)\,\upsilon(t)\,dt = 0 \tag{7.22.53}$$

that is, the **mutual energy** of both signals equals zero. In general, the terms of the 2-D Hilbert pair are not orthogonal; that is, the mutual energy

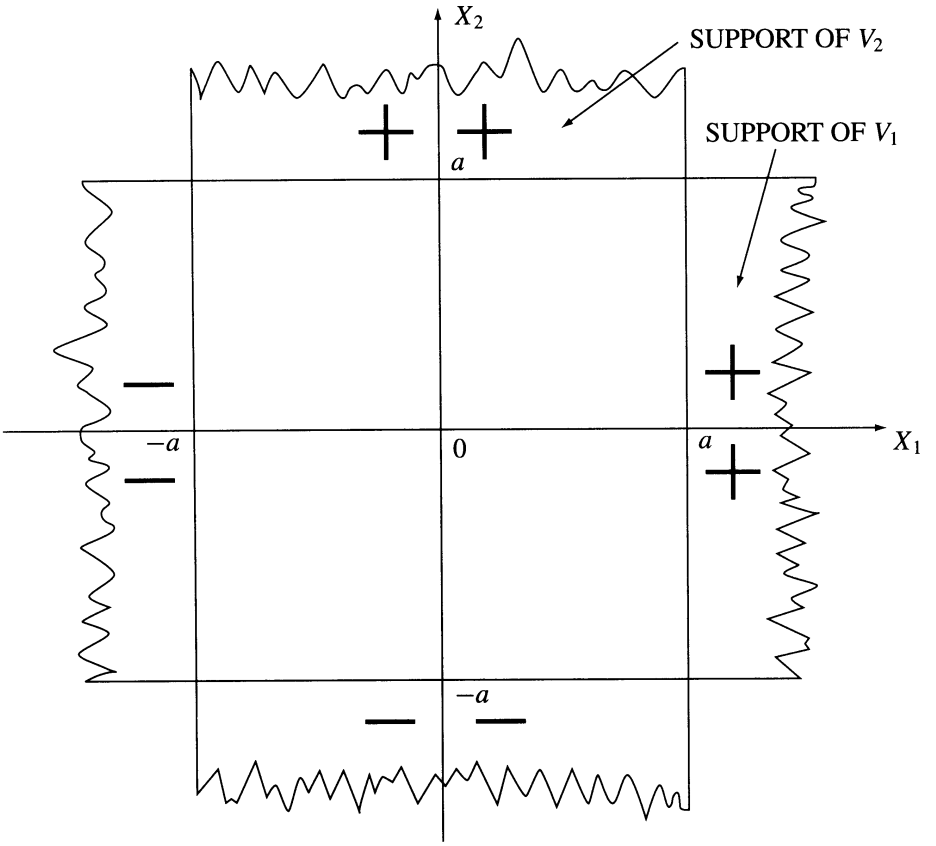

FIGURE 7.22.2c The supports of the partial Hilbert transforms of this pulse.

$$E = \iint u\left(x_1, x_2\right) v\left(x_1, x_2\right) dx\, dx \neq 0 \tag{7.22.54}$$

does not equal zero. However, this integral equals zero for 2-D separable signals and for nonseparable signals with certain symmetry; for example, the pyramid signal defined by Equation (7.22.48). For separable signals the above double integral takes the form of a product of single integrals, each of which equals zero.

Example

Consider the 2-D Gaussian signal of the form[14]

$$\begin{aligned} u\left(x_1, x_2\right) = &\left[2\pi\sigma_1\sigma_2 \mathrm{SQR}\left(1-\rho^2\right)\right]^{-1} \\ &\times \exp\left\{-\left(1-\rho^2\right)^{-1}\left[\left(x_1/\sigma_1\right)^2 + \left(x_2/\sigma_2\right)^2 - 2\rho x_1 x_2/\left(\sigma_1\sigma_1\right)\right]\right\} \end{aligned} \tag{7.22.55}$$

This function is well known in probability theory. It is a separable function if the parameter $\rho = 0$. Otherwise, for $0 < \rho < 1$ it is a nonseparable function. Its Hilbert transform may be calculated using the inverse Fourier transform of the Fourier image, which has the form

$$U\left(\omega_1, \omega_2\right) = \exp\left\{-0.5\left[\sigma_1^2\omega_1^2 + \sigma_2^2\omega_2^2 + 2\rho\sigma_1\sigma_2\omega_1\omega_2\right]\right\} \tag{7.22.56}$$

TABLE 7.22.1

Number	Name	Original Signal or the Inverse Transform	Hilbert Transform
1	notations	$u(x_1, x_2) = H_2^{-1}[v(x_1, x_2)];$	$v(x_1, x_2) = H_2[u(x_1, x_2)]$
2	signal domain definitions	$u(x_1, x_2) = 1/(\pi^2 x_1 x_2) * *v(x_1, x_2);^a$	$v(x_1, x_2) = 1/(\pi^2 x_1 x_2) * *u(x_1, x_2)^b$
3	Fourier spectra	$u(x_1, x_2) \overset{2-F}{\Longleftrightarrow} U(\omega_1, \omega_2) =;$ $-\operatorname{sgn}(\omega_1)\operatorname{sgn}(\omega_2)V(\omega_1, \omega_2)$	$v(x_1, x_2) \overset{2-F}{\Longleftrightarrow} V(\omega_1, \omega_2) =$ $-\operatorname{sgn}(\omega_1)\operatorname{sgn}(\omega_2)U(\omega_1, \omega_2)$
4	linearity	$au_a(x_1, x_2) + bu_b(x_1, x_2);$	$av_a(x_1, x_2) + bv_b(x_1, x_2)$
5	change of symmetry	$u_{ee} + u_{oo} + u_{eo} + u_{oe};^c$	$v_{oo} + v_{ee} - v_{oe} - v_{eo}{}^c$
6	iteration	$v(x_1, x_2) \overset{2-H}{\Rightarrow} u(x_1, x_2)$	
7	energy equality	$\int\int u^2(x_1, x_2)\, dx_1\, dx_2 = \int\int v^2(x_1, x_2)\, dx_1\, dx_2$	
8	product of low-pass and high-pass signals with strongly separated spectra	$u_{LP}(x_1, x_2)$ $u_{HP}(x_1, x_2)$ $H_2(u_{LP}u_{HP})$ =	low-pass signal high-pass signal $u_{LP}[H_2(u_{HP})]$
9	separable functions	$f_1(x_1) \overset{H}{\Longleftrightarrow} g_1(x_1);\ f_2(x_2) \overset{H}{\Longleftrightarrow} g_2(x_2)$	
	Total Hilbert tr.	$u(x_1, x_2) = f_1 f_2$	$v(x_1, x_2) = g_1 g_2$
	Partial Hilbert tr.	$v_1(x_1, x_2) = g_1 f_2$	$v_2(x_1, x_2) = f_1 g_2$

[a] See Eq. (7.22.17)

[b] See Eq. (7.22.16)

[c] indices: e-even, o-odd

Because U is a real function, the inverse Fourier transformation has the simplified form

$$v(x_1, x_2) = \int_{-\infty}^{\infty}\int_{-\infty}^{\infty} -\operatorname{sgn}(\omega_1)\operatorname{sgn}(\omega_2)U(\omega_1, \omega_2)\cos(\omega_1 x_1 + \omega_2 x_2)\, df_1 df_2 \quad (7.22.57)$$

and the partial Hilbert transforms are given by the integrals

$$v_1(x_1, x_2) = \int_{-\infty}^{\infty}\int_{-\infty}^{\infty} -\operatorname{sgn}(\omega_1)U(\omega_1, \omega_2)\sin(\omega_1 x_1 + \omega_2 x_2)\, df_1 df_2 \quad (7.22.58)$$

$$v_2(x_1, x_2) = \int_{-\infty}^{\infty}\int_{-\infty}^{\infty} -\operatorname{sgn}(\omega_2)U(\omega_1, \omega_2)\sin(\omega_1 x_1 + \omega_2 x_2)\, df_1 df_2 \quad (7.22.59)$$

Because these integrals cannot be expressed in the closed form, a numerical integration scheme must be used for their approximation. Figure 7.22.3 shows the equal-value contour lines of the Gaussian function $u(x_1, x_2)$ and the total and partial Hilbert transforms ($\rho = 0.5$, $\sigma_1 = 1$, $\sigma_2 = 2$). The numerical integration yields the value of the mutual energy $E \cong 0.25$ (relative to the signal energy). E equals zero only if $\rho = 0$, i.e., for separable Gaussian signals.

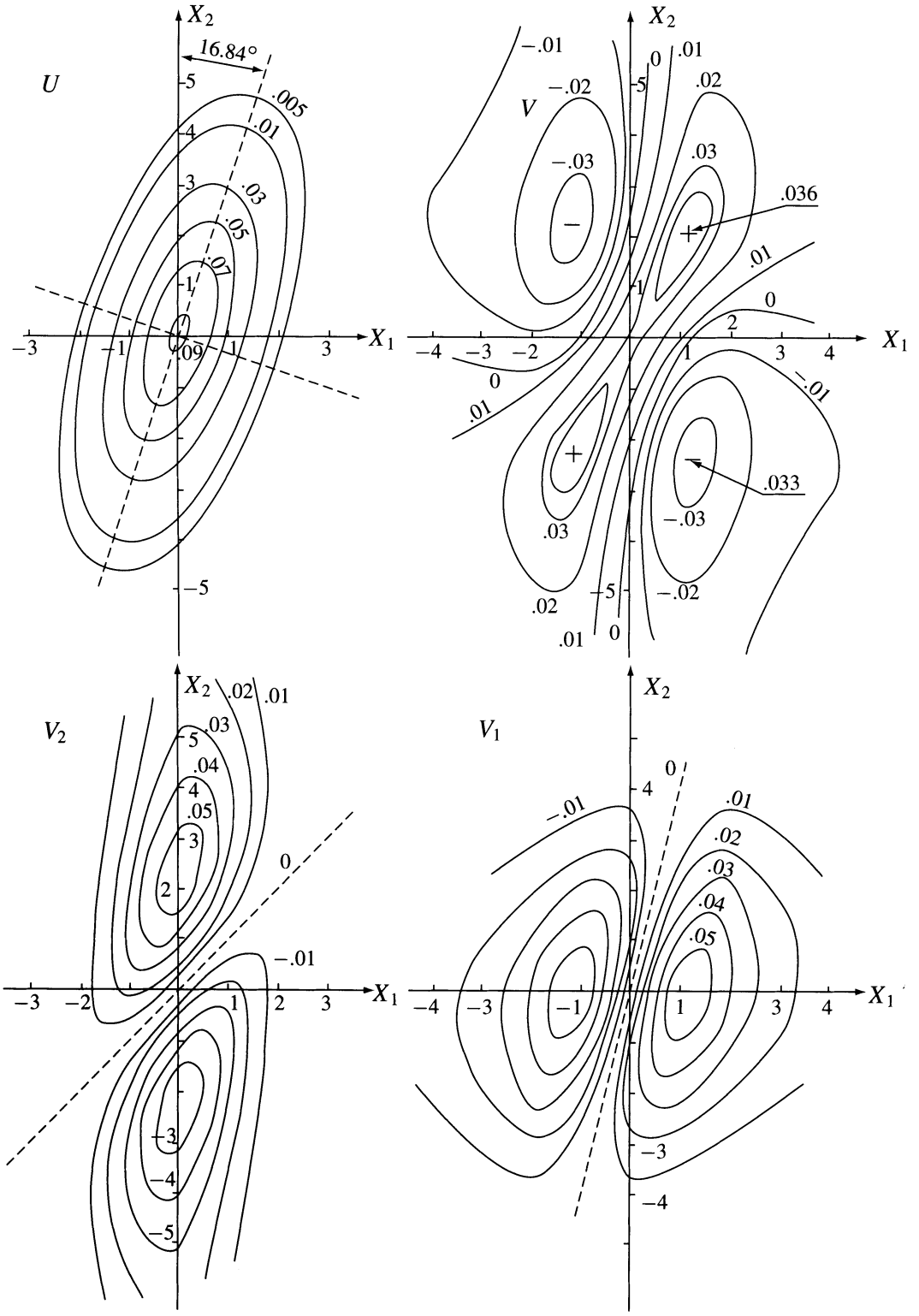

FIGURE 7.22.3 The elliptical equal-value contours of a nonseparable Gaussian function (see Equation [7.22.55]) and of the Hilbert transforms υ, υ_1, and υ_2, where $\rho = 0.5$, $\sigma_1 = 1$, $\sigma_2 = 2$.

Stark's Extension of Bedrosian's Theorem[37]

Bedrosian's theorem defines the Hilbert transform of a product of low-pass and high-pass signals. Stark formulated an extension of this theorem for 2-D signals. A 2-D function $u_{LP}(x_1, x_2) \overset{2\text{–F}}{\Longleftrightarrow} U_{LP}(\omega_1, \omega_2)$ is said to be low-pass with cutoff vector $\Omega_0 = \{\omega_{10}, \omega_{20}\}$ if

$$\max |\omega_1| = \omega_{10} \quad \text{and} \quad \max |\omega_2| = \omega_{20}$$

$$\text{all } \omega_1 \in \text{supp } U_{LP}(\omega_1, \omega_2) \quad \text{all } \omega_2 \in U_{LP}(\omega_1, \omega_2) \tag{7.22.60}$$

where supp U_{LP} denotes the support of the Fourier image; that is, the set of points for which $U_{LP}(\omega_1, \omega_2)$ is not zero. Analogously, the function $U_{HP}(x_1, x_2) \overset{2\text{–F}}{\Longleftrightarrow} U_{HP}(\omega_1, \omega_2)$ is said to be high-pass with cutoff vector $\Omega_0 = \{\omega_{10}, \omega_{20}\}$ if

$$\min |\omega_1| = \omega_{10} \quad \text{and} \quad \min |\omega_2| = \omega_{20}$$

$$\text{all } \omega_1 \in \text{supp } U_{HP}(\omega_1, \omega_2) \quad \text{all } \omega_2 \in U_{HP}(\omega_1, \omega_2) \tag{7.22.61}$$

The signals u_{LP} and u_{HP} are said to be strongly spectrally separable if the conditions (7.22.60) and (7.22.61) are satisfied. We say that the functions U_{LP} and U_{HP} are spectrally disjointed if they have nonoverlapping supports. However, spectral disjointedness may not coincide with strong separability, as shown in Figure 7.22.4. Stark's extension of Bedrosian's theorem has the form

$$H_2[u_{LP}(x_1, x_2)u_{HP}(x_1, x_2)] = u_{LP}(x_1, x_2)H_2[u_{HP}(x_1, x_2)] \tag{7.22.62}$$

that is, only the high-pass term of the product is transformed.

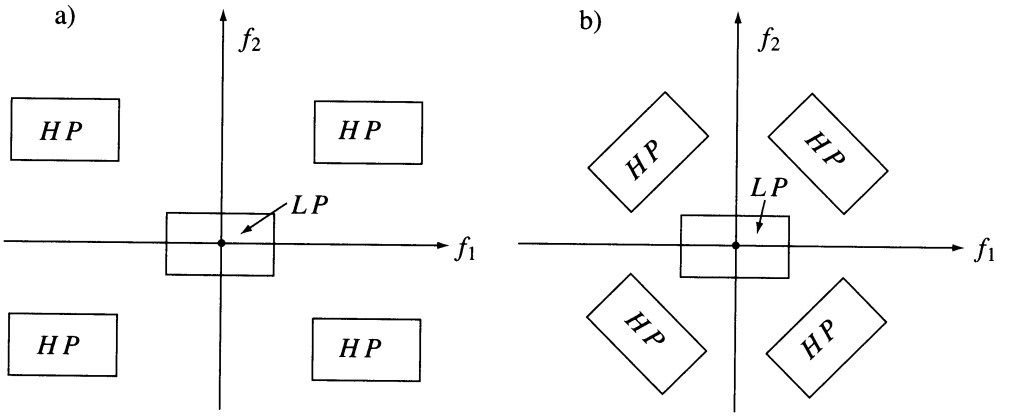

FIGURE 7.22.4 (a) LP is the support of the spectrum of a low-pass signal, HP is the support of the spectrum of a high-pass signal strongly separable from the low-pass. (b) Analogous spectra with spectral disjointedness.

Appendix 7.22

Consider the 2-D signal given by Equation (7.22.1). Its 2-D Fourier transform is

TABLE 7.22.2 2-D Total and Partial Hilbert Transforms

Notations: $u(x_1, x_2)$ — original signal, $v(x_1, x_2)$ — total Hilbert transform, $v_1(x_1, x_2)$ or $v_2(x_1, x_2)$ — partial Hilbert transforms

Number	Name	Original signal, Total, and Partial Hilbert transforms	
1	delta	$u = \delta(x_1, x_2)$	$v = 1/(\pi^2 x_1 x_2)$
		$v_1 = \delta(x_2)/(\pi x_1)$	$v_2 = \delta(x_1)/(\pi x_2)$
2	Gaussian pulse	$u = e^{-\pi(x_1^2+x_2^2)}$	$\omega_1 = 2\pi f_1;\ \omega_2 = 2\pi f_2$
		$v = 4\int_0^\infty \int_0^\infty e^{-\pi(f_1^2+f_2^2)} \sin(\omega_1 x_1)\sin(\omega_2 x_2)\, df_1\, df_2$	
		$v_1 = 4\int_0^\infty \int_0^\infty e^{-\pi(f_1^2+f_2^2)} \sin(\omega_1 x_1)\cos(\omega_2 x_2)\, df_1\, df_2$	
		$v_2 = 4\int_0^\infty \int_0^\infty e^{-\pi(f_1^2+f_2^2)} \cos(\omega_1 x_1)\sin(\omega_2 x_2)\, df_1\, df_2$	
3	Cauchy pulse	$u = \frac{ab}{(a^2+x_1^2)(b^2+x_2^2)}$	$v = \frac{x_1 x_2}{(a^2+x_1^2)(b^2+x_2^2)}$
		$v_1 = \frac{x_1 b}{(a^2+x_1^2)(b^2+x_2^2)}$	$v_2 = \frac{a x_2}{(a^2+x_1^2)(b^2+x_2^2)}$
4	Cube pulse	$u = \Pi_a(x)\Pi_b(x_2)$	$v = \frac{1}{\pi^2}\ln\left\lvert\frac{x_1+a}{x_1-a}\right\rvert \ln\left\lvert\frac{x_2+b}{x_2-b}\right\rvert$
		$v_1 = \frac{1}{\pi}\ln\left\lvert\frac{x_1+a}{x_1-a}\right\rvert \Pi_b(x_2)$	$v_2 = \frac{1}{\pi}\ln\left\lvert\frac{x_2+b}{x_2-b}\right\rvert \Pi_a(x_1)$
5	Sinc pulse	$u = \frac{\sin(ax_1)\sin(bx_2)}{abx_1x_2}$	$v = 4\frac{\sin^2(ax_1/2)\sin^2(bx_2/2)}{abx_1x_2}$
		$v_1 = 2\frac{\sin^2(ax_1/2)\sin(bx_2)}{abx_1x_2}$	$v_2 = 2\frac{\sin(ax_1)\sin^2(bx_2/2)}{abx_1x_2}$
6	nonseparable Gaussian pulse	see Eqs. (7.22.55) to (7.22.59)	
7	pyramid pulse	see Eqs. (7.22.48) to (7.22.52)	
8	2-D periodic signals	see Table 7.22.3	

$$\begin{aligned} U(\omega_1,\omega_2) &= \int_{-\infty}^{\infty}\int_{-\infty}^{\infty} u(x_1,x_2)\, e^{-j(\omega_1 x_1+\omega_2 x_2)}\, dx_1 dx_2 \\ &= U_{\mathrm{Re}} + jU_{\mathrm{Im}} \\ &= U_{ee} - U_{oo} - j(U_{eo}+U_{oe}) \end{aligned} \tag{7.22.63}$$

where

$$U_{ee}(\omega_1,\omega_2) = \int_{-\infty}^{\infty}\int_{-\infty}^{\infty} u_{ee}(x_1,x_2)\cos(\omega_1 x_1)\cos(\omega_2 x_2)\, dx_1 dx_2 \tag{7.22.64}$$

$$U_{oo}(\omega_1,\omega_2) = \int_{-\infty}^{\infty}\int_{-\infty}^{\infty} u_{oo}(x_1,x_2)\sin(\omega_1 x_1)\sin(\omega_2 x_2)\, dx_1 dx_2 \tag{7.22.65}$$

$$U_{oe}(\omega_1,\omega_2) = \int_{-\infty}^{\infty}\int_{-\infty}^{\infty} u_{oe}(x_1,x_2)\sin(\omega_1 x_1)\cos(\omega_2 x_2)\, dx_1 dx_2 \tag{7.22.66}$$

$$U_{eo}(\omega_1,\omega_2) = \int_{-\infty}^{\infty}\int_{-\infty}^{\infty} u_{eo}(x_1,x_2)\cos(\omega_1 x_1)\sin(\omega_2 x_2)\, dx_1 dx_2 \tag{7.22.67}$$

TABLE 7.22.3 2-D Total and Partial Hilbert Transforms of Periodic Functions
Notations: $u(x_1, x_2)$ — original signal, $v(x_1, x_2)$ — total Hilbert transform, $v_1(x_1, x_2)$ or $v_2(x_1, x_2)$ — partial Hilbert transforms

Number	Original signal, total, and partial Hilbert transforms	
1	$u = \cos(\omega_1 x_1)\cos(\omega_2 x_2)$ $v_1 = \sin(\omega_1 x_1)\cos(\omega_2 x_2)$	$v = \sin(\omega_1 x_1)\sin(\omega_2 x_2)$ $v_2 = \cos(\omega_1 x_1)\sin(\omega_2 x_2)$
2	$u = \sin(\omega_1 x_1)\sin(\omega_2 x_2)$ $v_1 = -\cos(\omega_1 x_1)\sin(\omega_2 x_2)$	$v = \cos(\omega_1 x_1)\cos(\omega_2 x_2)$ $v_2 = -\sin(\omega_1 x_1)\cos(\omega_2 x_2)$
3	$u = \cos(\omega_1 x_1 + \omega_2 x_2)$ $v_1 = \sin(\omega_1 x_1 + \omega_2 x_2)$	$v = -\cos(\omega_1 x_1 + \omega_2 x_2)$ $v_2 = \sin(\omega_1 x_1 + \omega_2 x_2)$
4	$u = \sin(\omega_1 x_1 + \omega_2 x_2)$ $v_1 = -\cos(\omega_1 x_1 + \omega_2 x_2)$	$v = -\sin(\omega_1 x_1 + \omega_2 x_2)$ $v_2 = -\cos(\omega_1 x_1 + \omega_2 x_2)$
5	$u = e^{j(\omega_1 x_1 + \omega_2 x_2)}$ $v_1 = -j\,\mathrm{sgn}(\omega_1)e^{j(\omega_1 x_1 + \omega_2 x_2)}$;	$v = -\mathrm{sgn}(\omega_1)\,\mathrm{sgn}(\omega_2)e^{j(\omega_1 x_1 + \omega_2 x_2)}$ $v_2 = -j\,\mathrm{sgn}(\omega_2)e^{j(\omega_1 x_1 + \omega_2 x_2)}$
6	$u = \mathrm{sgn}[\cos(\omega_1 x_1)]\,\mathrm{sgn}[\cos(\omega_2 x_2)]$ (2-D square wave) $v = (4/\pi^2)\ln\lvert\tan(\omega_2 x_1/2 + \pi/4)\rvert\ln\lvert\tan(\omega_1 x_2/2 + \pi/4)\rvert$ $v_1 = (2/\pi)\ln\lvert\tan(\omega_1 x_1/2 + \pi/4)\rvert\,\mathrm{sgn}[\cos(\omega_2 x_2)]$ $v_2 = (2/\pi)\ln\lvert\tan(\omega_2 x_2/2 + \pi/4)\rvert\,\mathrm{sgn}[\cos(\omega_1 x_1)]$	
7	$u = \sum_{n=-\infty}^{\infty}\sum_{m=-\infty}^{\infty}\delta(x_1 - na, x_2 - mb)$ (2-D delta sampling sequence) $v = \frac{1}{ab}\sum_{n=-\infty}^{\infty}\sum_{m=-\infty}^{\infty}\cot[(\pi/a)(x_1 - na)]\cot[(\pi/b)(x_2 - mb)]$ $v_1 = \frac{1}{a}\sum_{n=-\infty}^{\infty}\sum_{m=-\infty}^{\infty}\cot[(\pi/a)(x_1 - na)]\delta(x_2 - mb)$ $v_2 = \frac{1}{b}\sum_{n=-\infty}^{\infty}\sum_{m=-\infty}^{\infty}\cot[(\pi/b)(x_2 - mb)]\delta(x_1 - na)$	

TABLE 7.22.4 n-D Hilbert Transforms of Harmonic Functions

n	Function	Hilbert Transform
1	$\cos(\omega t)$ $\sin(\omega t)$	$\sin(\omega t)$ $-\cos(\omega t)$
2	$\cos(\omega_1 x_1 + \omega_2 x_2)$ $\sin(\omega_1 x_1 + \omega_2 x_2)$	$-\cos(\omega_1 x_1 + \omega_2 x_2)$ $-\sin(\omega_1 x_1 + \omega_2 x_2)$
3	$\cos(\omega_1 x_1 + \omega_2 x_2 + \omega_3 x_3)$ $\sin(\omega_1 x_1 + \omega_2 x_2 + \omega_3 x_3)$	$-\sin(\omega_1 x_1 + \omega_2 x_2 + \omega_3 x_3)$ $\cos(\omega_1 x_1 + \omega_2 x_2 + \omega_3 x_3)$
4	$\cos(\omega_1 x_1 + \omega_2 x_2 + \omega_3 x_3 + \omega_4 x_4)$ $\sin(\omega_1 x_1 + \omega_2 x_2 + \omega_3 x_3 + \omega_4 x_4)$	$\cos(\omega_1 x_1 + \omega_2 x_2 + \omega_3 x_3 + \omega_4 x_4)$ $\sin(\omega_1 x_1 + \omega_2 x_2 + \omega_3 x_3 + \omega_4 x_4)$
1	$e^{j\omega t}$	$-j\,\mathrm{sgn}(\omega)e^{j\omega t}$
2	$e^{j(\omega_1 x_1 + \omega_2 x_2)}$	$-\mathrm{sgn}(\omega_1)\,\mathrm{sgn}(\omega_2)e^{j(\omega_1 x_1 + \omega_2 x_2)}$
3	$e^{j(\omega_1 x_1 + \omega_2 x_2 + \omega_3 x_3)}$	$-j\,\mathrm{sgn}(\omega_1)\,\mathrm{sgn}(\omega_2)\,\mathrm{sgn}(\omega_3)e^{j(\omega_1 x_1 + \omega_2 x_2 + \omega_3 x_3)}$
4	$e^{j(\omega_1 x_1 + \omega_2 x_2 + \omega_3 x_3 + \omega_4 x_4)}$	$\mathrm{sgn}(\omega_1)\,\mathrm{sgn}(\omega_2)\,\mathrm{sgn}(\omega_3)\,\mathrm{sgn}(\omega_4)e^{j(\omega_1 x_1 + \omega_2 x_2 + \omega_3 x_3 + \omega_4 x_4)}$

Using computer programs for numerical integration, the insertion in these integrals of $u(x_1, x_2)$ instead of u_{ee}, u_{oo}, … does not change the result because the trigonometric kernels are selecting the right terms themselves. Because the Fourier image of the Hilbert transform is

$$V(\omega_1, \omega_2) = -\mathrm{sgn}(\omega_1)\,\mathrm{sgn}(\omega_2)\left[U_{ee} - U_{oo} - j\left(U_{oe} + U_{eo}\right)\right] \tag{7.22.68}$$

the inverse Fourier transform yields the Hilbert transform

$$\upsilon(x_1, x_2) = \upsilon_{ee} + \upsilon_{oo} + \upsilon_{oe} + \upsilon_{eo} \tag{7.22.69}$$

where due to the symmetry conditions, the terms of u may be given by one-sided integrals

$$V_{ee}(x_1, x_2) = 4\int_0^\infty \int_0^\infty U_{ee}(\omega_1, \omega_2)\cos(\omega_1 x_1)\cos(\omega_2 x_2)\, df_1 df_2 \tag{7.22.70}$$

$$V_{oo}(x_1, x_2) = 4\int_0^\infty \int_0^\infty U_{oo}(\omega_1, \omega_2)\sin(\omega_1 x_1)\sin(\omega_2 x_2)\, df_1 df_2 \tag{7.22.71}$$

$$V_{oe}(x_1, x_2) = 4\int_0^\infty \int_0^\infty U_{oe}(\omega_1, \omega_2)\sin(\omega_1 x_1)\cos(\omega_2 x_2)\, df_1 df_2 \tag{7.22.72}$$

$$V_{eo}(x_1, x_2) = 4\int_0^\infty \int_0^\infty U_{eo}(\omega_1, \omega_2)\cos(\omega_1 x_1)\sin(\omega_2 x_2)\, df_1 df_2 \tag{7.22.73}$$

Two-Dimensional Hilbert Transformers

The transfer function of the ideal "noncausal" 2-D Hilbert transformer is given by a product of 1-D transfer functions (see Equations [7.21.11] to [7.21.13]). Therefore,

$$H_{2\text{-}H}(f_1, f_2) = \left[-j\,\mathrm{sgn}(f_1)\right]\left[-j\,\mathrm{sgn}(f_2)\right] = \left|H_{2\text{-}H}\right| e^{j\Phi(f_1, f_2)} \tag{7.22.74}$$

The magnitude equals 1 and the phase function is

$$\Phi(f_1, f_2) = -\frac{\pi}{2}\mathrm{sgn}(f_1) - \frac{\pi}{2}\mathrm{sgn}(f_2) \tag{7.22.75}$$

7.23 Multidimensional Complex Signals

Short Historical Review

The complex notation of harmonic signals in the form of Euler's equation $e^{j\omega t} = \cos(\omega t) + j\sin(\omega t)$ was introduced to electrical engineering at the end of the 19th century (E. Kennedy and C. Steinmetz) and soon proliferated to many science and engineering disciplines. Restating the equation in the form $\cos(\omega t) = 0.5(e^{j\omega t} + e^{-j\omega t})$ introduces the concept of **negative frequencies**, commonly used in modern Fourier spectral analysis. In 1946, Gabor[11] introduced the extension of the complex notation of time signals in the form of the **analytic signal** $\psi(t) = u(t) + j\upsilon(t)$ where $\upsilon(t)$ is the Hilbert transform of $u(t)$ (see Section 7.3). It has the unique feature that its Fourier transform is one-sided. In 1964 this author[12] used the analytic signal to define the notion of the instantaneous complex frequency. This section presents how the complex notation of signals and the notion of the analytic signal can be **generalized** for multidimensional signals. This generalization has been recently developed by this author.[13]

Definition of the Multidimensional Complex Signal

Let us remember that no definition is "true" or "false." However, it is very desirable that a definition of the n-dimensional complex signal satisfy certain requirements. The basic requirement is the **compatibility**

with the 1-D case, i.e., with the definition of the analytic signal. Many other requirements may be formulated, such as usefulness in applications. The definition of the multidimensional complex signal introduced in Reference 13 is based on the frequency domain description of the multidimensional signals given by the Fourier pair

$$u(\mathbf{x}) \overset{n-F}{\Longleftrightarrow} U(\boldsymbol{\Omega}) \tag{7.23.1}$$

where $\mathbf{x} = \{x_1, x_2, \ldots, x_n\}$ and $\Omega = \{\omega_1, \omega_2, \ldots, \omega_n\}$ are n-dimensional real column vectors (see Section 7.22). Let us remember that the **kernels** of the n-D Fourier transformations are: in 1-D $e^{\pm j\omega t}$, in 2-D $e^{\pm j(\omega_1 x_1 + \omega_2 x_2)}$, in 3-D $e^{\pm j(\omega_1 x_1 + \omega_2 x_2 + \omega_3 x_3)}$, and in n-D $e^{\pm j(\omega_1 x_1 + \cdots + \omega_n x_n)}$. These kernels have the form of complex signals of a constant amplitude $A = 1$ and **linear phase** in respect to the variables $x_1, x_2, \ldots, x_n$. Therefore, a compatible definition of a multidimensional complex signal should define n-dimensional complex harmonic signals in the form of the above kernels of the n-D Fourier transformation. Because the 1-D complex analytic signal has a one-sided spectrum at positive frequencies, let us define the n-dimensional complex signal using the inverse Fourier transform of its spectrum cancelled at all **orthants** of the Fourier frequencies space except in the first orthant. In 1-D this space has two **half-axes**, in 2-D four **quadrants**, in 3-D eight **octants**, and in general 2^n **orthants**. Mathematicians denote the orthant with all the axis of positive sign by R^+. Therefore, the n-D complex signal is defined by the Fourier pair

$$\psi(\mathbf{x}) \overset{n-F}{\Longleftrightarrow} \Gamma(\boldsymbol{\Omega}) = 2^n \mathbf{1}(\boldsymbol{\Omega}) U(\boldsymbol{\Omega}) \tag{7.23.2}$$

The cancellation of the spectrum in all but the first orthant is achieved by multiplication of the n-D Fourier image by the n-**D unit step function** (or distribution) $\mathbf{1}(\Omega)$ defined by the formula ($\Omega = \{\omega_1, \omega_2, \ldots, \omega_n\}$)

$$\mathbf{1}(\boldsymbol{\Omega}) = \begin{cases} 1 & \text{all } \omega > 0 \\ 0.5 & \text{all } \omega = 0 \\ 0 & \text{all } \omega < 0 \end{cases} \tag{7.23.3}$$

The numerical factor 2^n is used to normalize the energy of the complex signal. The n-D unit step may be written in the form of a product of 1-D unit steps; that is, given by the formula

$$\mathbf{1}(\Omega) = \mathbf{1}(\omega_1) \otimes \mathbf{1}(\omega_2) \otimes \cdots \otimes 1(\omega_n) \tag{7.23.4}$$

where $\otimes$ denotes a **tensor product** of distributions. In the following text we will suppress the symbol $\otimes$ because here it has a pure formal meaning. The 1-D unit step may be written in the form $\mathbf{1}(\omega) = 0.5[1 + \text{sgn}(\omega)]$ (see Equation [7.3.16]). The insertion of this form in Equation (7.23.4) yields

$$\mathbf{1}(\Omega) = [0.5\ \text{sgn}(\omega_1)][0.5 + 0.5\ \text{sgn}(\omega_2)] \ldots [0.5 + 0.5\ \text{sgn}(\omega_n)] \tag{7.23.5}$$

The application of the convolution to multiplication theorem of Fourier analysis to the spectrum $\Gamma(\Omega)$ defined by Equation (7.23.2) yields the signal domain definition of the n-D complex signal in the form of the n-fold convolution

$$\psi(\mathbf{x}) = \psi_\delta(\mathbf{x}) * \cdots * u(\mathbf{x}) \tag{7.23.6}$$

where the signal $\psi_\delta(\mathbf{x})$ is given by the inverse Fourier transform of the unit step; that is,

TABLE 7.23.1 The n-D Complex Signals and Its Fourier Spectra

n-D	Complex Signal	Fourier Image	
1-D	$\psi_1 = u + jv$	$\Gamma(\omega) = [1 + \text{sgn}(\omega)]U(\omega)$	(7.23.9)
2-D	$\psi_1 = u - v + j(v_1 + v_2)$	$\Gamma(\omega_1, \omega_2) = U(\omega_1, \omega_2)$ $\times [1 + \text{sgn}(\omega_1) + \text{sgn}(\omega_2) + \text{sgn}(\omega_1)\,\text{sgn}(\omega_2)]$	(7.23.10)
3-D	$\psi_1 = u - v_{12} - v_{13} - v_{23} +$ $j(v_1 + v_2 + v_3 - v)$	$\Gamma(\omega_1, \omega_2, \omega_1) = U(\omega_1, \omega_2, \omega_3)$ $\times [1 + \text{sgn}(\omega_1) + \text{sgn}(\omega_2) + \text{sgn}(\omega_3)$ $+ \text{sgn}(\omega_1)\,\text{sgn}(\omega_2) + \text{sgn}(\omega_1)\,\text{sgn}(\omega_3)$ $+ \text{sgn}(\omega_2)\,\text{sgn}(\omega_3) + \text{sgn}(\omega_1)\,\text{sgn}(\omega_2)\,\text{sgn}(\omega_3)]$	(7.23.11)
	⋮	⋮	
n-D	$\psi_1 = F^{-1}[\Gamma(\boldsymbol{\Omega})]$	$\Gamma(\boldsymbol{\Omega}) = 2^n \mathbf{1}(\boldsymbol{\Omega})U(\boldsymbol{\Omega})$	(7.23.12)

u is the original signal, v is its total Hilbert transform, v_1, v_2, v_3 are the first-order partial Hilbert transforms, v_{12}, v_{13}, v_{23} are the second-order partial Hilbert transforms. For notational ease, the dependence of $u, v, v_1, \ldots$ on $x_1, x_2, x_3, \ldots$ is omitted. The index 1 in ψ_1 indicates a complex signal with a single orthant spectrum in the first orthant (in R^+).

$$\psi_\delta(\mathbf{x}) \overset{n-F}{\Longleftrightarrow} 2^n \mathbf{1}(\boldsymbol{\Omega}) \tag{7.23.7}$$

The n-D delta pulse (distribution) $\delta(\mathbf{x}) = \delta(x_1)\delta(x_2)\ldots\delta(x_n)$ may be defined by the inverse Fourier transform of the spectrum $U(\boldsymbol{\Omega}) = \mathbf{1}$, i.e., by the Fourier pair

$$\delta(\mathbf{x}) \overset{n-F}{\Longleftrightarrow} \mathbf{1} \tag{7.23.8}$$

Therefore, the signal $\psi_\delta(\mathbf{x})$ defines the ***n*-D complex delta distribution** (see the 1-D case, Section 7.5, Equation [7.5.7] and a more detailed description in the next part of this section). Notice that Equations (7.23.2) and (7.23.6) uniquely define the n-D complex signal due to the uniqueness theorem of the Fourier analysis.

To get the structure of the n-D complex signal $\psi(\mathbf{x})$ let us insert in the spectrum $\Gamma(\Omega)$ defined by Equation (7.23.2) the developed form of the multiple product given by Equation (7.23.5), as shown in Table 7.23.1. The real part of the complex signals ψ_1 in Table 7.23.1 corresponds to the spectral terms obtained by multiplication of $\Gamma(\Omega)$ by 1, $\text{sgn}(\omega_1)\,\text{sgn}(\omega_2)$, …, $\text{sgn}(\omega_1)\,\text{sgn}(\omega_2)\,\text{sgn}\,(\omega_3)\,\text{sgn}(\omega_4)$, …; that is, by a product of an even number of signum functions, and the imaginary part by $\text{sgn}(\omega_1)$, …, $\text{sgn}(\omega_1)\,\text{sgn}(\omega_2)\,\text{sgn}(\omega_3)$, …; that is, by a product of an odd number of signum functions.

Example

Consider the 2-D harmonic signal $u = \cos(\omega_1 x_1)\cos(\omega_2 x_2)$. The Hilbert transforms are (see Table 7.22.3) $v = \sin(\omega_1 x_1)\sin(\omega_2 x_2)$, $v_1 = \sin(\omega_1 x_1)\cos(\omega_2 x_2)$, $v_2 = \cos(\omega_1 x_1)\sin(\omega_2 x_2)$. The insertion of u, v, v_1, and v_2 into Equation (7.23.10) yields the complex signal

$$\psi_1(x_1, x_2) = \cos(\omega_1 x_1)\cos(\omega_2 x_2) - \sin(\omega_1 x_1)\cos(\omega_2 x_2) + j[\sin(\omega_1 x_1)\cos(\omega_2 x_2) + \cos(\omega_1 x_1)\cos(\omega_2 x_2)] \tag{7.23.13}$$

The application of standard trigonometric relations yields

$$\omega_1(x_1, x_2) = e^{j(\omega_1 x_1 + \omega_2 x_2)} \tag{7.23.14}$$

Notice that the real part of this signal equals $u - v = \cos(\omega_1 x_1 + \omega_2 x_2)$ and is not equal to u. The n-D generalization of the above signal is $u(\mathbf{x}) = \cos(\omega_1 x_1) \cos(\omega_2 x_2) \ldots \cos(\omega_2 x_2)$, yielding the complex signal

$$\psi(\mathbf{x}) = e^{j(\omega_1 x_1 + \omega_2 x_2 + \cdots \omega_n x_n)} \tag{7.23.15}$$

This formula gives evidence that the important requirement of compatibility of the definition of a multidimensional complex signal with the 1-D case is satisfied by complex signals with single orthant spectra.

Example

Consider the 2-D delta pulse distribution $\delta(x_1, x_2) = \delta(x_1)\delta(x_2)$. The Hilbert transforms are given in Table 7.23.2 and Equation (7.23.10) yields the following form of the 2-D complex delta distribution

$$\psi_\delta(x_1, x_2) = \delta(x_1, x_2) - 1/(\pi^2 x_1 x_2) + j[\delta(x_2)/(\pi x_1) + \delta(x_1)/(\pi x_2)] \tag{7.23.16}$$

The insertion in Equation (7.23.11) of the appropriate Hilbert transforms of the 3-D delta pulse $\delta(x_1, x_2, x_3)$ yields the following form of the 3-D complex delta distribution

$$\begin{aligned}\psi_\delta(x_1, x_2, x_3) = \delta(x_1, x_2, x_3) - \frac{\delta(x_3)}{\pi^2 x_1 x_2} - \frac{\delta(x_2)}{\pi^2 x_1 x_3} - \frac{\delta(x_1)}{\pi^2 x_2 x_3} \\ + j\left(\frac{\delta(x_2, x_3)}{\pi x_1} + \frac{\delta(x_1, x_3)}{\pi x_2} + \frac{\delta(x_1, x_2)}{\pi x_2} - \frac{1}{\pi^3 x_1 x_2 x_3}\right)\end{aligned} \tag{7.23.17}$$

Conjugate 2-D Complex Signals

The 2-D complex signal defined by Equation (7.23.10) has the single quadrant spectrum in the first quadrant. Let us define 2-D complex signals with single quadrant spectra in successive quadrants. The accepted numeration of the quadrants is shown in Figure 7.23.1. The so-defined complex signals and their spectra are shown in Table 7.23.2.

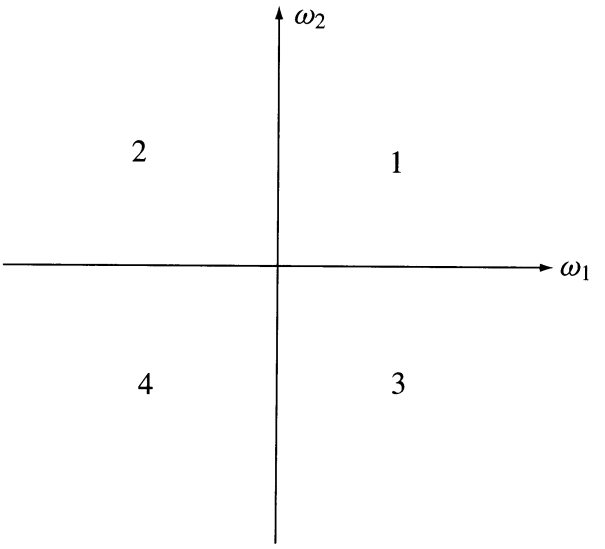

FIGURE 7.23.1 The numeration of quadrants (see Appendix)

TABLE 7.23.2 2-D Complex Signals with Single-Quadrant Spectra in Successive Quadrants of the Fourier Frequency Plane (ω_1, ω_2)

Quadrant	Complex Signal	Fourier Image
1	$\psi_1 = u - v + j(v_1 + v_2)$	$\Gamma_1(\omega_1, \omega_2) = 4\,\mathbf{1}(\omega_1, \omega_2)U(\omega_1, \omega_2) = U[1 + \text{sgn}(\omega_1) + \text{sgn}(\omega_2) + \text{sgn}(\omega_1)\,\text{sgn}(\omega_2)]$
2	$\psi_2 = u + v - j(v_1 - v_2)$	$\Gamma_2(\omega_1, \omega_2) = 4\,\mathbf{1}(-\omega_1, \omega_2)U(\omega_1, \omega_2) = U[1 - \text{sgn}(\omega_1) + \text{sgn}(\omega_2) - \text{sgn}(\omega_1)\,\text{sgn}(\omega_2)]$
3	$\psi_3 = u + v + j(v_1 - v_2)$	$\Gamma_3(\omega_1, \omega_2) = 4\,\mathbf{1}(\omega_1, -\omega_2)U(\omega_1, \omega_2) = U[1 + \text{sgn}(\omega_1) - \text{sgn}(\omega_2) - \text{sgn}(\omega_1)\,\text{sgn}(\omega_2)]$
4	$\psi_4 = u - v - j(v_1 + v_2)$	$\Gamma_4(\omega_1, \omega_2) = 4\,\mathbf{1}(-\omega_1, -\omega_2)U(\omega_1, \omega_2) = U[1 - \text{sgn}(\omega_1) - \text{sgn}(\omega_2) + \text{sgn}(\omega_1)\,\text{sgn}(\omega_2)]$
Two pairs of conjugate signals: $\psi_1 = \psi_4^*$ and $\psi_3 = \psi_2^*$		

Notations: See Table 7.23.1.

Local (or "Instantaneous") Amplitudes, Phases, and Complex Frequencies

Let us write the complex signals of Table 7.23.2 in polar coordinates:

$$\psi_1(x_1, x_2) = \psi_4^*(x_1, x_2) = A_1(x_1, x_2)\, e^{j\Phi_1(x_1, x_2)} \tag{7.23.18}$$

$$\psi_3(x_1, x_2) = \psi_2^*(x_1, x_2) = A_2(x_1, x_2)\, e^{j\Phi_2(x_1, x_2)} \tag{7.23.19}$$

This representation defines the **local** (or "instantaneous") **amplitudes**

$$A_1(x_1, x_2) = \text{SQR}\,\{[u(x_1, x_2) - v(x_1, x_2)]^2 + [v_1(x_1, x_2) + v_2(x_1, x_2)]^2\} \tag{7.23.20}$$

$$A_2(x_1, x_2) = \text{SQR}\,\{[u(x_1, x_2) + v(x_1, x_2)]^2 + [v_1(x_1, x_2) - v_2(x_1, x_2)]^2\} \tag{7.23.21}$$

and the **local** (or "instantaneous") **phases**

$$\Phi_1(x_1, x_2) = \tan^{-1} \frac{v_1(x_1, x_2) + v_2(x_1, x_2)}{u(x_1, x_2) - v(x_1, x_2)} \tag{7.23.22}$$

$$\Phi_2(x_1, x_2) = \tan^{-1} \frac{v_1(x_1, x_2) - v_2(x_1, x_2)}{u(x_1, x_2) + v(x_1, x_2)} \tag{7.23.23}$$

of the real signal $u(x_1, x_2)$. Analogous to the 1-D case (see Section 7.15, Equation [7.15.12]) let us define the **complex phases**

$$\Phi_{1c}(x_1, x_2) = \text{Ln}\ \psi_1(x_1, x_2) \tag{7.23.24}$$

$$\Phi_{2c}(x_1, x_2) = \text{Ln}\ \psi_3(x_1, x_2) \tag{7.23.25}$$

and the **partial** instantaneous complex frequencies

$$s_{1x_1}(x_1, x_2) = \frac{\partial \Phi_{1c}(x_1, x_2)}{\partial x_1} = \alpha_{1x_1}(x_1, x_2) + j\omega_{1x_1}(x_1, x_2) \tag{7.23.26}$$

$$s_{1x_2}(x_1, x_2) = \frac{\partial \Phi_{1c}(x_1, x_2)}{\partial x_2} = \alpha_{1x_2}(x_1, x_2) + j\omega_{1x_2}(x_1, x_2) \tag{7.23.27}$$

$$s_{2x_1}(x_1, x_2) = \frac{\partial \Phi_{2c}(x_1, x_2)}{\partial x_1} = \alpha_{2x_1}(x_1, x_2) + j\omega_{2x_1}(x_1, x_2) \tag{7.23.28}$$

$$s_{2x_2}(x_1, x_2) = \frac{\partial \Phi_{2c}(x_1, x_2)}{\partial x_2} = \alpha_{2x_2}(x_1, x_2) + j\omega_{2x_2}(x_1, x_2) \tag{7.23.29}$$

In Equations (7.23.26) and (7.23.28) x_2 is a parameter and the complex frequencies are defined along the lines parallel to the x_1 axis. Similarly, Equations (7.23.27) and (7.23.29) define complex frequencies parallel to the x_2 axis.

For separable 2-D signals (see Equation [7.22.38]), the amplitudes A_1 and A_2 defined by Equations (7.23.20) and (7.23.21) are equal and given by the formula

$$A(x_1, x_2) = \mathrm{SQR}\left[u^2 + \upsilon^2 + \upsilon_1^2 + \upsilon_2^2\right] \tag{7.23.30}$$

and the phases (7.23.22) and (7.23.23) are

$$\Phi_1(x_1, x_2) = \varphi_1(x_1) + \varphi_2(x_2) \tag{7.23.31}$$

$$\Phi_2(x_1, x_2) = \varphi_1(x_1) - \varphi_2(x_2) \tag{7.23.32}$$

where $\varphi_1 = \tan^{-1}(g_1/f_1)$ (see Equation [7.22.38]). The complex frequencies have, for separable signals, the simplified form

$$s_{1x_1} = s_{2x_1} = \alpha_1 + j\omega_1 \tag{7.23.33}$$

$$s_{1x_2} = s_{2x_2}^* = \alpha_2 + j\omega_2 \tag{7.23.34}$$

Example

Consider the 2-D signal of the form

$$u(x_1, x_2) = \frac{\sin(ax_1)\sin(bx_2)}{abx_1x_2} \tag{7.23.35}$$

The insertion of this signal and its Hilbert transforms υ, υ_1, and υ_2 (see Table 7.22.2) in Equation (7.23.30) using certain trigonometric relations yields

$$A(x_1, x_2) = \left|\frac{1 - \cos(ax_1)}{\sin(ax_1)}\right| \left|\frac{1 - \cos(bx_2)}{\sin(bx_2)}\right| \tag{7.23.36}$$

The phase functions (7.23.31) and (7.23.32) take the form

$$\Phi_1\left(x_1, x_2\right) = \tan^{-1}\frac{1-\cos\left(a x_1\right)}{\sin\left(a x_1\right)} + \tan^{-1}\frac{1-\cos\left(b x_2\right)}{\sin\left(b x_2\right)} = \frac{a}{2}x_1 + \frac{b}{2}x_2 \tag{7.23.37}$$

$$\Phi_2\left(x_1, x_2\right) = \tan^{-1}\frac{1-\cos\left(a x_1\right)}{\sin\left(a x_1\right)} - \tan^{-1}\frac{1-\cos\left(b x_2\right)}{\sin\left(b x_2\right)} = \frac{a}{2}x_1 - \frac{b}{2}x_2 \tag{7.23.38}$$

The local partial angular frequencies defined by the imaginary parts of (7.23.33) and (7.23.34) are $\omega_1 = a/2$ and $\omega_2 = b/2$. The local amplitude (7.23.36) is a product of local amplitudes of the separable terms of the signal (7.23.35), and the phase is a sum (or difference) of phases of these terms. The phase functions in this example are linear (a constant slope if we remove the jumps of the multibranch $\tan^{-1}$ function), giving constant values of the angular frequencies.

Relations Between Real and Complex Notation

In one dimension, we have the following well-known relations:

$$u\left(t\right) = \frac{\psi\left(t\right) + \psi^*\left(t\right)}{2}; \quad \upsilon\left(t\right) = \frac{\psi\left(t\right) - \psi^*\left(t\right)}{2j} \tag{7.23.39}$$

In two dimensions, the corresponding relations become (see Table 7.23.2)

$$u\left(x_1, x_2\right) = \frac{\psi_1 + \psi_2 + \psi_3 + \psi_4}{4} \tag{7.23.40}$$

$$\upsilon\left(x_1, x_2\right) = \frac{\psi_1 - \psi_2 + \psi_3 - \psi_4}{4} \tag{7.23.41}$$

$$\upsilon_1\left(x_1, x_2\right) = \frac{\psi_1 - \psi_2 + \psi_3 - \psi_4}{4j} \tag{7.23.42}$$

$$\upsilon_2\left(x_1, x_2\right) = \frac{\psi_1 + \psi_2 - \psi_3 - \psi_4}{4j} \tag{7.23.43}$$

Using the relations $\psi_1 = \psi_4^*$ and $\psi_3 = \psi_2^*$, the real part of the complex signal ψ_1 takes the form

$$u - \upsilon = 0.5\left(\psi_1 + \psi_4\right) = 0.5\left(\psi_1 + \psi_1^*\right) \tag{7.23.44}$$

and the real part of ψ_3 is

$$u + \upsilon = 0.5\left(\psi_2 + \psi_3\right) = 0.5\left(\psi_2 + \psi_2^*\right) \tag{7.23.45}$$

Notice that the spectra of these two signals exist in two quadrants of the Fourier frequency plane. The insertion of the polar representations (7.23.18) and (7.23.19) into (7.23.44) and (7.23.45) yield

$$u - v = A_1 \cos(\Phi_1) \tag{7.23.46}$$

$$u + v = A_2 \cos(\Phi_2) \tag{7.23.47}$$

The summation (or substraction) yields the following relations

$$u(x_1, x_2) = \frac{A_1 \cos(\Phi_1) + A_2 \cos(\Phi_2)}{2} \tag{7.23.48}$$

$$v(x_1, x_2) = \frac{A_2 \cos(\Phi_2) - A_1 \cos(\Phi_1)}{2} \tag{7.23.49}$$

and analogous derivation yields

$$v_1(x_1, x_2) = \frac{A_1 \sin(\Phi_1) + A_2 \sin(\Phi_2)}{2} \tag{7.23.50}$$

$$v_2(x_1, x_2) = \frac{A_2 \sin(\Phi_2) - A_1 \sin(\Phi_1)}{2} \tag{7.23.51}$$

For separable signals, these relations have the simplified form

$$u(x_1, x_2) = A \cos[\varphi_1(x_1)] \cos(\varphi_2(x_2)] \tag{7.23.52}$$

$$v(x_1, x_2) = A \sin[\varphi_1(x_1)] \sin[\varphi_2(x_2)] \tag{7.23.53}$$

$$v_1(x_1, x_2) = A \sin[\varphi_1(x_1)] \cos[\varphi_2(x_2)] \tag{7.23.54}$$

$$v_2(x_1, x_2) = A \cos[\varphi_1(x_1)] \sin[\varphi_2(x_2)] \tag{7.23.55}$$

In three dimensions the number of octants equals eight and the relation between the real and complex notation becomes (we applied the method of numeration of octants given in Appendix 7.23.1),

$$u(x_1, x_2, x_3) = \frac{\psi_1 + \psi_2 + \psi_3 + \psi_4 + \psi_5 + \psi_6 + \psi_7 + \psi_8}{8} \tag{7.23.56}$$

Using the relations $\psi_1 = \psi_8^* = A_1 e^{j\Phi_1}$, $\psi_2 = \psi_7^* = A_2 e^{j\Phi_2}$, $\psi_3 = \psi_6^* = A_3 e^{j\Phi_3}$, and $\psi_4 = \psi_5^* = A_4 e^{j\Phi_4}$, the above formula takes the form

$$(x_1, x_2, x_3) = \frac{A_1 \cos(\Phi_1) + A_2 \cos(\Phi_2) + A_3 \cos(\Phi_3) + A_4 \cos(\Phi_4)}{8} \tag{7.23.57}$$

For separate signals all amplitudes are equal and the phase functions are

$$\Phi_1(x_1, x_2, x_3) = \varphi_1(x_1) + \varphi_2(x_2) + \varphi_3(x_3) \tag{7.23.58}$$

$$\Phi_2(x_1, x_2, x_3) = -\varphi_1(x_1) + \varphi_2(x_2) + \varphi_3(x_3) \tag{7.23.59}$$

$$\Phi_3(x_1, x_2, x_3) = \varphi_1(x_1) - \varphi_2(x_2) + \varphi_3(x_3) \tag{7.23.60}$$

$$\Phi_4(x_1, x_2, x_3) = -\varphi_1(x_1) - \varphi_2(x_2) + \varphi_3(x_3) \tag{7.23.61}$$

The insertion of these phase functions in Equation (7.23.57) yields

$$u(x_1, x_2, x_3) = A \cos[\varphi_1(x_1)] \cos[\varphi_2(x_2)] \cos[\varphi_3(x_3)] \tag{7.23.62}$$

Similar formulae for u, u_1, and u_2 may be easily derived or written directly by comparison with the 2-D case. In general, for the n-D separable signal of the form $u(\mathbf{x}) = \Pi_{k=1}^{n} a_k f(x_k)$ this formula takes the form $u(\mathbf{x}) = A \Pi_{k=1}^{n} \cos[\varphi(x_k)]$, where $A = \Pi_{k=1}^{n} a_k$. If all a_k's are equal to a, then $A = a^n$ or $a = \sqrt[n]{A}$.

Example

Consider again the signal $u(x_1, x_2) = \cos(\omega_{10}x_1) \cos(\omega_{20}x_2)$ of the previous example. The four complex signals of Table 7.23.2 and their spectra are

Quadrant	Complex Signal	Fourier Image
1	$\psi_1 = e^{j(\omega_{10}x_1 + \omega_{20}x_2)}$	$\delta(\omega_1 - \omega_{10}, \omega_2 - \omega_{20})$
2	$\psi_2 = e^{j(-\omega_{10}x_1 + \omega_{20}x_2)}$	$\delta(\omega_1 + \omega_{10}, \omega_2 - \omega_{20})$
3	$\psi_3 = e^{j(\omega_{10}x_1 - \omega_{20}x_2)}$	$\delta(\omega_1 - \omega_{10}, \omega_2 + \omega_{20})$
4	$\psi_1 = e^{j(-\omega_{10}x_1 - \omega_{20}x_2)}$	$\delta(\omega_1 + \omega_{10}, \omega_2 + \omega_{20})$

The spectrum of the signal u is shown in Figure 7.23.2. The insertion of these functions in Equations (7.23.40) to (7.23.51) gives the verifications of these relations.

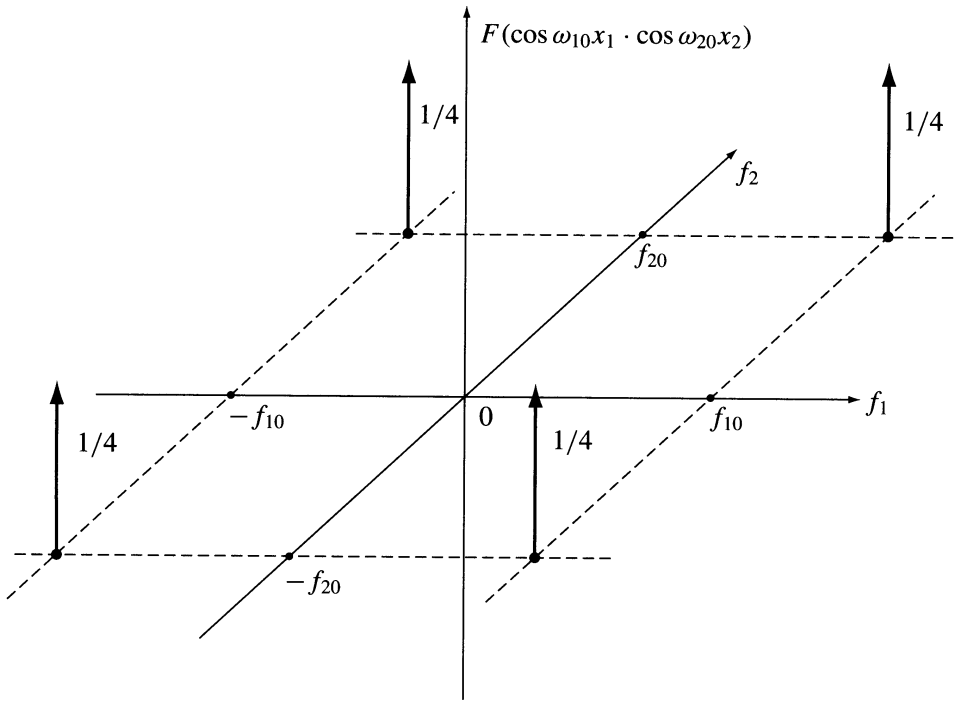

FIGURE 7.23.2 The Fourier spectrum of the 2-D harmonic signal $u(x_1, x_2) = \cos(\omega_{10}x_1) \cos(\omega_{20}x_2)$.

2-D Modulation Theory

The 1-D modulated signal has the complex representation in the form of a product of the **modulation function** and the complex harmonic carrier (see Section 7.16, Equation [7.16.6]). From the formal point of view, the concept of the modulation function can be extended to multidimensional modulating signals with multidimensional harmonic carriers. The n-D complex harmonic carrier has the form

$$\Psi_c(\mathbf{x}) = A_0 e^{j(\omega_{10}x_1+\varphi_1+\omega_{20}x_2+\varphi_2+\cdots+\omega_{n0}x_n+\varphi_n)} \tag{7.23.63}$$

We define the n-D modulated signal in the form of a product

$$\psi(\mathbf{x}) = \gamma(\mathbf{x})\psi_c(\mathbf{x}) \tag{7.23.64}$$

where $\gamma(\mathbf{x}) = f[u(\mathbf{x})]$ is called the n-**D modulation function** and $f[u(\mathbf{x})]$ is a function of the n-D message $u(\mathbf{x})$. As in the 1-D case, the function f defines a specific type of modulation. The 2-D modulated signal has the form

$$\Psi(x_1, x_2) = \gamma(x_1, x_2)A_0 e^{j(\omega_{10}x_1+\omega_{20}x_2)} \tag{7.23.65}$$

where for convenience, the phases $\varphi_1 = \varphi_2 = 0$.

Example

Consider a 2-D low-pass message and its Fourier image

$$u(x_1, x_2) \overset{2-F}{\Longleftrightarrow} U(j\omega_1, \quad j\omega_2) \tag{7.23.66}$$

with the base-band spectrum band limited such that $U(j\omega_1, j\omega_2) = 0$ for $|\omega_1| > a$ and $|\omega_2| > b$. The modulation function of the 2-D suppressed carrier amplitude modulation is

$$\gamma_{\text{AM}}(x_1, x_2) = mu(x_1, x_2) \tag{7.23.67}$$

Figure 7.23.3 shows the spectra of the base-band signal u and of the modulated signal.

The 2-D equivalent of the 1-D SSB modulation is the **single quadrant modulation** (**SQM**). The modulation function is given by the inverse Fourier transform of the base-band single quadrant spectrum

$$\begin{aligned}\gamma_{\text{SQM}}(x_1, x_2) &= F^{-1}\,[\mathbf{41}(\omega_1, \omega_2)\; U(\omega_1, \omega_2)] \\ &= u(x_1, x_2) - \upsilon(x_1, x_2) + j[\upsilon_1(x_1, x_2) + \upsilon_2(x_1, x_2)]\end{aligned} \tag{7.23.68}$$

that is, in the form of the complex signal (7.23.10) in Table 7.23.1. The insertion of this modulation function in Equation (7.23.55) yields the complex SQM signal

$$\Psi_{\text{SQM}}(x_1, x_2) = \left\{u(x_1, x_2) - \upsilon(x_1, x_2) + j\left[\upsilon_1(x_1, x_2) + \upsilon_2(x_1, x_2)\right]\right\} A_0 e^{j(\omega_{10}x_1+\omega_{20}x_2)} \tag{7.23.69}$$

and its real notation is

$$\begin{aligned}u_{\text{SQM}}(x_1, x_2) = {} & u\cos(\omega_{10}x_1)\cos(\omega_{20}x_2) + \upsilon\sin(\omega_{10}x_1)\sin(\omega_{20}x_2) + \\ & - \upsilon_1\sin(\omega_{10}x_1)\cos(\omega_{20}x_2) - \upsilon_2\cos(\omega_{10}x_1)\sin(\omega_{20}x_2)\end{aligned} \tag{7.23.70}$$

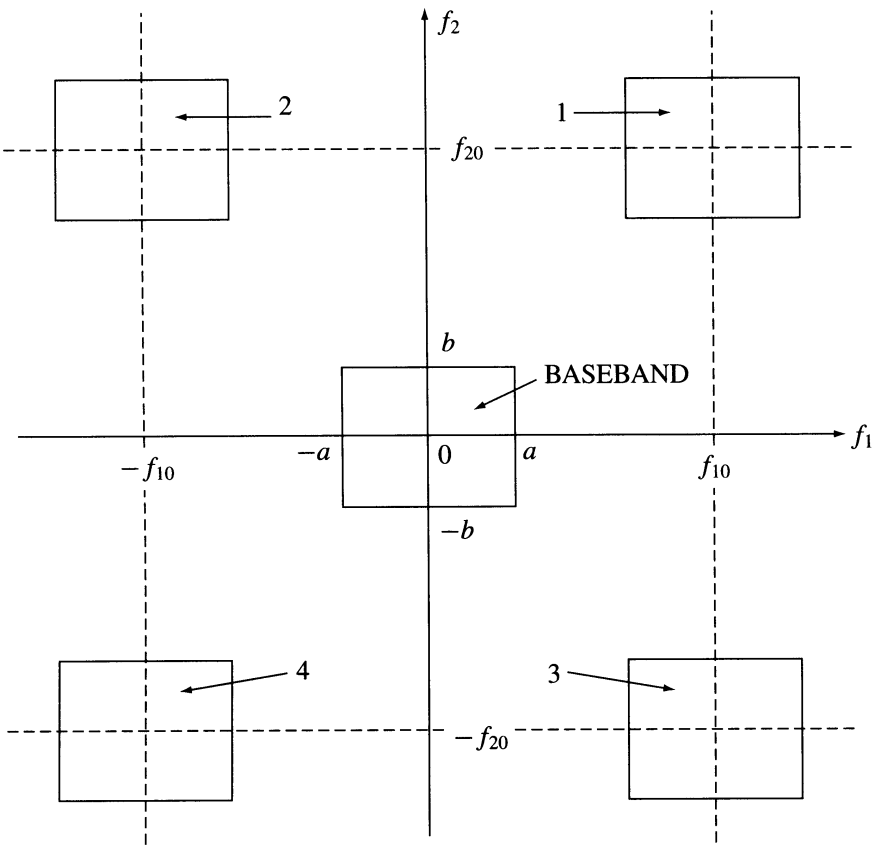

FIGURE 7.23.3 The supports of the spectrum of a 2-D carrier with 2-D amplitude modulation.

Figure 7.23.4 shows the supports of the spectra of γ_{SQM}, Ψ_{SQM}, and u_{SQM}.

7.23.1 Appendix: A Method of Labeling Orthants

The applied numbering method of successive orthants is the following: we assign the binary number zero to a plus sign and the binary number 1 to a minus sign of the variable ω. For example, the unit step function $\mathbf{1}(\omega_4, -\omega_3, -\omega_2, \omega_1)$ corresponds to the binary number 0110. If the decimal-coded binary number is a, we assign to the given orthant the decimal number $l = a + 1$. So, we have in four dimensions:

$l = a + 1$	Binary	Sign of the Ω Axis			
		ω_4	ω_3	ω_2	ω_1
1	0000	+	+	+	+
2	0001	+	+	+	–
3	0010	+	+	–	+
4	0011	+	+	–	–
16	1111	–	–	–	–

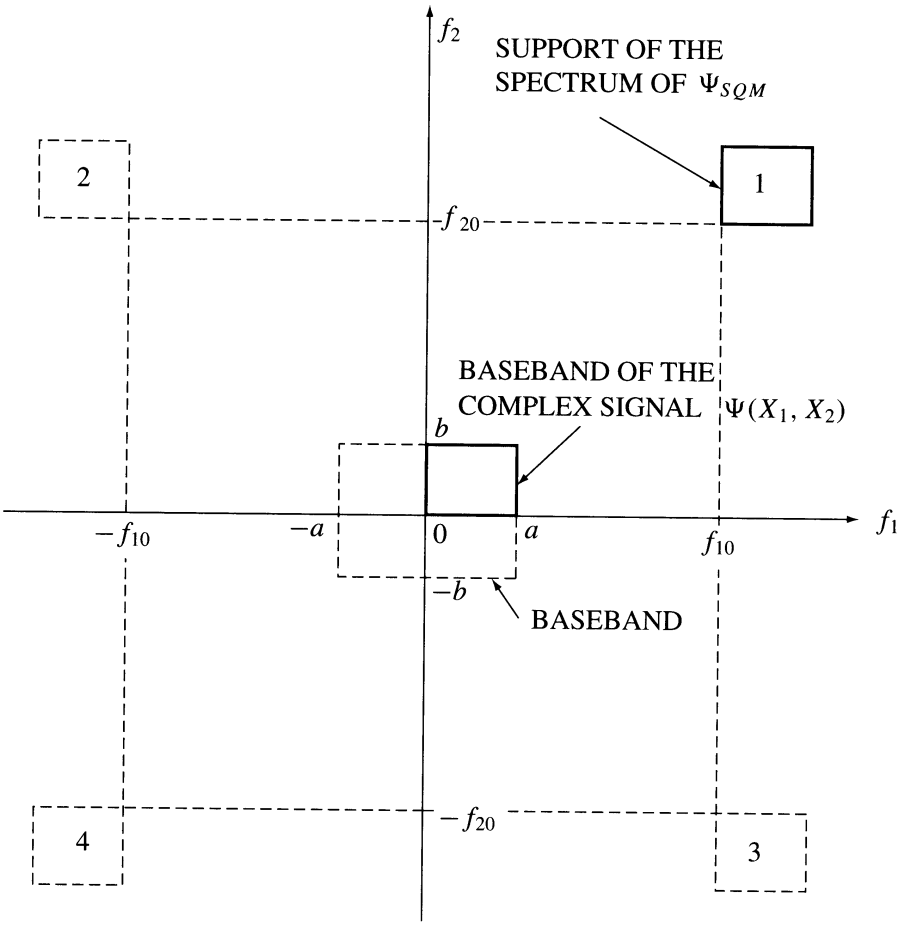

FIGURE 7.23.4 The supports of the spectrum of a 2-D signal with Single Quadrant Modulation (SQM).

References

1. Ansari, R. IIR discrete-time Hilbert transformers, *IEEE Trans. ASSP*, vol. ASSP-35, No. 8, Aug. 1987, pp. 1116–1119.

1a. Ansari, R. Elliptic filter design for generalized half-band filters. vol. ASSP-33, Oct. 1985, pp. 1146–1150.

2. Bedrosian, S. D. Normalised design of 90° phase-difference networks. *Trans. of the Inst. Radio Engrs.* CT-7, 1960, pp. 128–136.

3. Bedrosian, E. The analytic signal representation of modulated waveforms. *Proc. IEEE*, vol. 50, No. 10, Oct. 1962, pp. 2071–2076.

4. Bedrosian, E. A product theorem for Hilbert transforms. *Proc. IEEE* (*Lett.*), vol. 51, No. 5, May 1963, pp. 868–869.

5. Bedrosian, E. and Stark, H. Comments on "An extension of the Hilbert transform product theorem," *Proc. IEEE*, vol. 60, Feb. 1972, pp. 228–229.

6. Budeanu, C. Reactive and fictitious powers, *Romanian National Inst. Publ.*, No. 2, 1927, Bucharest, Romanian.

7. Cižek, V. Discrete Hilbert transform. *IEEE Trans,* vol. AU-18, No. 4, Dec. 1970, pp. 340–343.

8. Darlington, S. Realization of a constant phase difference. *Bell Syst. Tech. J.*, 29, 1950, pp. 94–104.

9. Dome, R. B. Wide-band phase shift networks. *Electronics*, 19, Dec. 1946, pp. 112–115.

10. Fryze, S., Wirk–und Blind–und Scheinleistung in Elektrischen Stromkreisen mit nichtsinusoidalenformigen Verlauf von Strom und Spannung. *Elektrotech. Z.,* 53 (25), 1932, pp. 696–599, (Active, reactive, and apparent power in electrical circuits with nonsinusoidals currents and voltages).
11. Gabor, D. Theory of communications. *J. Inst. EE,* Pt. III, vol. 93, Nov. 1946, pp. 429–457.
12. Hahn, S. L. Complex variable frequency electric circuit theory. *Proc. IEEE* (*Lett.*), vol. 52, no. 6, June 1964, pp. 735–736.
13. Hahn, S. L. Multidimensional complex signals with single-orthant spectra. *Proc. IEEE,* vol. 80, no. 8, Aug. 1992, pp. 1287–1300.
14. Hahn, S. L. Amplitudes, phases and complex frequencies of 2-D Gaussian signals, *Bulletin of the Polish Acad. Sci.,* vol. 40, no. 3, 1992, pp. 289–311.
15. Herman, O. Transversalfilter zur Hilbert-Transformation. *Arch. Elektr. Übertr.,* 23, Heft 12, 1969, pp. 581–587, (Transversal filters as Hilbert transformers).
16. Jackson, L. B. On the relationship between digital Hilbert transformers and certain low-pass filters. *IEEE Trans. ASSP,* vol. 23, no. 8, Aug. 1975, pp. 381–383.
17. Kahn, L. R. Compatible single sideband. *Proc. IRE,* vol. 49, Oct. 1961, pp. 1503–1527.
18. Kramers, H. A. *Phys. Z.,* 30, 1929, p. 522.
19. Kronig, R. de L. *J. Opt. Soc. Amer.,* vol. 12, 1926, p. 547.
20. Krylov, W. W. and Ponomariev, D. M. Definition of the signal delay in linear two-ports using the Hilbert transform (in Russian). *Radiotechnika i Elektronika,* no. 5, 1980, pp. 204–206.
21. Klyagin, L. Ye. Linearization of the phase characteristics of wide-band phase shifters (translated from Russian). *Telecomm. Radio Eng.,* Part 2 (USA) 1967, pp. 82–87.
22. McClellan, J. H. A computer program for designing optimum FIR linear phase digital filters. *IEEE Trans.,* vol. AU-21, no. 6, Dec. 1973, pp. 506–526.
23. Mikusinski, J. The elementary theory of distributions. *Rozprawy Matematyczne XII,* Warsaw: PWN, 1957.
24. Nowomiejski, Z. Generalized theory of electric power, *Archiv. f. Elektrotechnik,* vol. 63, 1981, pp. 177–182, 1972, pp. 1361–1362.
25. Nuttal, A. and Bedrosian, E. On the quadrature approximation of the Hilbert transform of modulated signals. *Proc. IEEE* (*Lett.*), vol. 54, Oct. 1966, pp. 1458–1459.
26. Oppenheim, A. V. and Schafer, R. W. *Digital Signal Processing*. New Jersey: Prentice-Hall, 1975.
27. Orchard, H. J. The synthesis of RC networks to have prescribed transfer functions. *Proc. IRE,* vol. 39, April 1951, pp. 428–432.
28. Paley, E.A.C. and Wiener, N. Fourier transforms in the complex domain. *Amer. Math. Soc. Colloqium Pub.,* 19, New York, 1934.
29. Rabiner, L. R. and Schafer, R. W. On the behaviour of minimax FIR digital Hilbert transformers. *Bell Syst. Tech. J.,* vol. 53, no. 2, Feb. 1974, pp. 363–390, and On the behaviour of minimax relative error FIR differentiators, pp. 333–362.
30. Rabiner, L. R. and Gold, B. *Theory and Applications of Digital Signal Processing*. New Jersey: Prentice-Hall, 1975.
31. Rabiner, L. R. et al. FIR digital filter design techniques using weighted Chebyshev approximation. *Proc. IEEE,* vol. 63, no. 4, Apr. 1975, pp. 585–610.
32. Robinson, F.N.H. *Macroscopic Electromagnetism*, Pergamon Press, Oxford, 1973.
33. Saraga, W. The design of wide-band two-phase networks, *Proc. Inst. Electron. Engrs.*, 38, 1950, pp. 754–770.
34. Schneider, W. Quadraturfilter nach der methode der angezapften Laufzeitketten. *Telefunken-Ztg.,* 40, 1967 (Quadrature filter using the method of a tapped-delay line).
35. Schwartz, L. *Methodes mathematique pour les science physique*. Paris: Hermann, 1965.
36. Stark, H. and Tuteur, F. B. Modern electrical communications. *Theory and Systems*. New Jersey: Prentice-Hall, 1979.

37. Stark, H. An extension of the Hilbert transform product theorem, *Proc. IEEE*, vol. 59, no. 9, Sept. 1971, pp. 1359–1360.
38. Weaver, D. K. Design of RC wide-band 90-degree phase difference networks. *Proc. IRE*, vol. 42, April 1954, pp. 671–676.
39. Weinberger, H. F. *Partial Differential Equations with Complex Variables and Transform Methods*. New York: Blaisdell Publishing Co., 1965.
40. Villard, O. G., Jr. Composite amplitude and phase modulation. *Electronics*, 21, Nov. 1948, pp. 86–89.
41. Carson, J. R. and Fry, C. F., Variable frequency electric circuit theory with application to the theory of frequency modulation, *Bell Syst. Techn. J.*, vol. 6, no. 4, 1954, pp. 513–530.